Universitat Autònoma
de Barcelona

IMMUNOANALYTICAL STRATEGIES BASED ON MAGNETIC CARRIERS FOR FOOD SAFETY

PhD Thesis

TAMARA LAUBE CHAVEZ

Supervisors: María Isabel Pividori Gurgo and Salvador Alegret i Sanromà

PROGRAMA DE DOCTORAT DE QUÍMICA
Departament de Química
Facultat de Ciències

2013

Memòria presentada per aspirar al Grau de Doctor per Tamara Laube Chavez

Tamara Laube Chavez

Vist i plau

Dr. Salvador Alegret i Sanromà	**Dra. María Isabel Pividori Gurgo**
Catedràtic de Química Analítica	**Professora Titular d'Universitat**

Bellaterra (Cerdanyola del Vallès), Novembre de 2013

The present dissertation has been carried out thanks to the PhD fellowship provided by *the Comissionat per a Universitats i Recerca del DIUE de la Generalitat de Catalunya i del Fons Social Europeu* and the following financial support:

Ministry of Science and Innovation (MEC), Madrid
Projects: *“Biorreconocimiento mejorado en biosensores de afinidad para biotecnología. Aplicaciones medioambientales y agroalimentarias”* (BIO2007-63300) and *“Fagosensórica. Sistemas analíticos biosensores basados en nanopartículas fágicas”* (BIO2010-17566).

DURSI, Generalitat de Catalunya
Project: “*Grup de Sensors i Biosensors, Grupo de investigación consolidado*” (2009-SGR00323).

Grup de Sensors i Biosensors
Unitat de Química Analítica
Departament de Química
Universitat Autònoma de Barcelona
Edifici Cn, 08193 Bellaterra

AGRADECIMIENTOS

Hace ya unos cuantos años atrás, en un congreso de biosensores al otro lado del mundo, conocí a los que más adelante serían mis directores de Tesis, Salvador Alegret e Isabel Pividori. Luego de resultarme muy interesante los temas que presentaban y conversar durante largo rato, comenzó a dar vueltas la posibilidad de hacer un doctorado. Y esa idea fue tomando forma, hasta que un año después finalmente decidí cruzar el océano y comenzar una nueva aventura… y de eso ya va a ser casi 6 años.

En primer lugar quiero agradecer a mis directores, Salvador e Isabel, por la oportunidad que me habéis dado de llevar adelante este desafío tan lejos de casa, por el apoyo que he tenido y la confianza que habéis puesto en mí. Realmente ha sido una experiencia muy enriquecedora y me llevo muy buenos recuerdos, además de todo lo aprendido tanto a nivel profesional, como personal. Os agradezco también la oportunidad que me habéis dado de asistir a tantos cursos y congresos que ampliaron aún más mi aprendizaje, principalmente con la posibilidad de participar en la Bioanalytical Nanotechnology School, que nos llevó a Filipinas y México. A Manel, Arben, Alfredo, Susana, gracias por todo lo compartido en esos viajes y aprendido junto a vosotros.

También quiero agradecer a todos los que han colaborado con este trabajo del Grup de Microbiologia Molecular del Departament de Genètica i Microbiologia de la Universitat Autònoma de Barcelona: Montserrat Llagostera, Pilar Cortés, Joan Colom, Denis Spricigo, Susana Escribano, muchas gracias por todo!

Por otro lado, quiero dar las gracias también al Servei de Microscopia de la Universidad Autónoma de Barcelona por la excelente asistencia técnica, que me ha permitido obtener muy buenas "fotos" de mi trabajo. En especial gracias Alex, por tu gran disponibilidad siempre que fue necesario, y por las risas y buena onda, que hacen el trabajo mucho más agradable.

Y ahora pasemos a las personas que me acompañaron en el día a día, pasando a ser mi segunda familia y haciéndome sentir como en casa durante todo este tiempo….

Susy, contigo he coincidido en todo el camino desde el primer día y el primer café, hasta el cierre de esta etapa… me encantó haber compartido tantas cosas contigo en estos años. Has sido siempre una excelente compañía en este camino y una gran *amiga. Anabel, me alegra haber coincidido contigo en mis comienzos y que la amistad haya continuado durante todos estos años. Sandra, Sole, Delfina, Anna, estoy muy contenta de tenerlas también como amigas y de todos los momentos compartidos tanto dentro del laboratorio, como fuera haciendo cafés, jugando al futbol, yendo de excursión, de fiesta, o lo que sea… Rey, it was a great pleasure to meet you; we miss you in the lab. Jose, nunca pierdas esa buena onda y alegría. Alejandra, contigo no he coincidido tanto, pero te deseo todo lo mejor en el doctorado. A los que han estado de estancia: Vane, Michelle Brugnera y Castilho, Thalita, Paula, Paulo, Willian, me alegra mucho haberlos conocido y compartido también buenos momentos con vosotros.*

Y que voy a decir de mis amigos de las plantas de más arriba… Marta, Joan, Cata, gracias por estar siempre ahí y por todos los momentos compartidos. Dentro de poco estaremos los 4 repartidos por el mundo pero estoy segura que seguiremos siempre juntos a pesar de la distancia física que nos separe y ojalá podamos irnos reencontrando cada tanto en Cataluña, Bélgica, Chile, Argentina o donde sea!

Gracias también al grupo futbolero: Mon, Olga, Ana Mari, Marta, Pilar, Sandra, Silvia, Sole, Susy, Cata, Amàlia, Amanda, David, Julio, Nuria, Ari, Elena… NOSOTRAS AHÍ!!! Me he divertido mucho todos estos años y me ha encantado compartir con vosotros entrenos, risas y nuestros días del chocolate!

No puedo dejar de mencionar también a nuestro gabinete psicológico: Marta, Anabel, Susy, gracias por estar ahí… nuestras sesiones de catarsis, cenitas y momentos compartidos siempre devuelven la alegría.

Tampoco quiero olvidarme de toda la gente que hay por la planta con las que uno va compartiendo charlas y sonrisas: Xavi, Cristina, Ferdia, Andrea, Julio, Berta, Kharla, Pedro, Oriol, Sara, Eva, Raquel, Angélica, Fran, Uri, Julia, Elena, Vanessa, Anna, y todos los que han pasado por aquí en estos años....

Por otro lado también quiero dar las gracias a mis amigos voleyboleros que me han acompañado en muchos de mis tiempos libres y también me han dado ánimos en momentos de estrés: Sara, Oscar, Xavi, Made, Dori, Ferrán x 2, Montse, Ricard, Carlos, Iara, Sebas…

Finalmente, quiero agradecer a mis amigos del otro lado del charco que han estado ahí a pesar de la distancia. A mis padres, mi hermana, Mamama y mi familia por todo el apoyo y cariño que me dan siempre. Y por supuesto muchas gracias a tí, Pablo, por estar a mi lado, dándome ánimos y todo el amor siempre… las cosas resultan mucho más fáciles compartiéndolas contigo!

A mis padres y a Denise, por el apoyo incondicional,
más allá de cualquier océano de distancia
y a Pablo, por ser el mejor acompañante en mi camino.

TABLE OF CONTENT

ABBREVIATIONS AND SYMBOLS……………………………………………………………………..i

SUMMARY………………………………………………………………………………………….vii

1. INTRODUCTION 1

1.1 AGENTS AFFECTING FOOD SAFETY 3
  1.1.1 Food allergens. Gliadin and celiac disease 5
  1.1.2 Microbiological contamination in food. *Salmonella* and salmonellosis 10
1.2 AN OVERVIEW OF THE DETECTION METHODS FOR FOOD SAFETY 12
  1.2.1 Gold standard methods for food safety 12
  1.2.2 Rapid methods for food safety 13
1.3 IMMUNOCHEMICAL METHODS 14
  1.3.1 Antibodies as bioanalytical reagent... 15
    1.3.1.1 Antibody production... 16
    1.3.1.2 The antibody-antigen recognition 18
  1.3.2 Labeling of immunological reagents.. 19
    1.3.2.1 Enzymatic labeling.. 21
    1.3.2.2 Biotin tagging for indirect enzymatic labeling 22
  1.3.3 Immunological techniques... 24
    1.3.3.1 Immunoassays based on enzymatic labeling... 25
    1.3.3.2 Enzyme linked immunosorbent assay (ELISA) 26
1.4 BIOSENSING METHODS 28
  1.4.1 Biosensor classification 32
  1.4.2 Electrochemical biosensors 33
    1.4.2.1 Electrochemical immunosensor design.. 35
    1.4.2.2 Amperometric detection 37
    1.4.2.3 Electrochemical transducing materials 40
1.5 INTEGRATION OF MICRO AND NANOMATERIALS IN BIOSENSORS AND BIOASSAYS 41
  1.5.1 Integration of magnetic particles in bioanalytical procedures 44
  1.5.2 Integration of bacteriophages and virus-like nanoparticles in bioanalytical methods 48
1.6 GLIADIN IN GLUTEN-FREE FOODSTUFF. AN OVERVIEW OF THE DETECTION METHODS.. 51
  1.6.1. Proteomic and genomic detection methods... 52
  1.6.2 Immunochemical-based and biosensing detection methods 54
1.7 PATHOGENIC BACTERIA. AN OVERVIEW OF THE DETECTION METHODS 60

1.7.1 Conventional culture-based methods 60
1.7.2 Rapid methods for food pathogen detection 62
1.7.3 Bacteriophages for bacteria detection... 67
1.8 REFERENCES 72

2. AIMS OF RESEARCH AND DISSERTATION OUTLINE 87

3. CONSTRUCTION AND CHARACTERIZATION OF MAGNETO GRAPHITE-EPOXY COMPOSITE ELECTRODES 89

3.1 INTRODUCTION 91
3.2 AIM OF THE CHAPTER 92
3.3 EXPERIMENTAL SECTION 92
3.3.1 Materials 92
3.3.2 Construction of the magneto electrodes based on graphite-epoxy composite (m-GEC) 94
3.3.3 Characterization of the m-GEC electrodes by cyclic voltammetry 95
3.4 RESULTS AND DISCUSSION 97
3.4.1 Characterization of the m-GEC electrodes by cyclic voltammetry 97
3.5 CONCLUSIONS 100
3.6 REFERENCES 100

4. INTEGRATION OF MAGNETIC MICRO AND NANOPARTICLES INTO COMPETITIVE IMMUNOASSAYS FOR THE DETECTION OF GLIADIN IN GLUTEN-FREE FOODSTUFF . 101

4.1 INTRODUCTION 103
4.2 AIM OF THE CHAPTER 104
4.3 EXPERIMENTAL SECTION 105
4.3.1 Materials 105
4.3.1.1 Chemicals and biochemicals 105
4.3.1.2 Instrumentation 106
4.3.2 Gliadin binding on magnetic micro and nanoparticles and coupling efficiency 108
4.3.2.1 Preparation of the gliadin stock solution 108
4.3.2.2 Immobilization of gliadin to tosylactivated magnetic microparticles 108
4.3.2.3 Immobilization of gliadin to carboxyl-activated magnetic nanoparticles 109
4.3.2.4 Coupling efficiency study 110
4.3.3 Epitope orientation and nonspecific adsorption study 110
4.3.4 Competitive magneto immunoassay for the optical detection of gliadin 111
4.3.5 Study of the matrix effect and gliadin extraction procedure from foodstuff 114
4.3.6 Competitive electrochemical magneto immunosensor for gliadin detection 115

4.3.7 Accuracy study in foodstuff 117

4.4 RESULTS AND DISCUSSION 117

4.4.1 Gliadin binding on magnetic micro and nanoparticles and coupling efficiency 117

4.4.2 Epitope orientation and nonspecific adsorption study 119

4.4.3 Competitive magneto immunoassay for the optical detection of gliadin 121

4.4.3.1 Immunoassay optimization using the gliadin-MP 121

4.4.3.2 Immunoassay optimization using the gliadin-nMP 125

4.4.4 Study of the matrix effect and gliadin extraction procedure from foodstuff 127

4.4.5 Competitive electrochemical magneto immunosensor for gliadin detection 130

4.4.6 Accuracy study in foodstuff 134

4.5 CONCLUSIONS 135

4.6 REFERENCES 136

5. DEVELOPMENT AND CHARACTERIZATION OF BIOTINYLATED BACTERIOPHAGES FOR THE DETECTION OF PATHOGENIC BACTERIA 139

5.1 INTRODUCTION 141

5.2 AIM OF THE CHAPTER 142

5.3 EXPERIMENTAL SECTION 142

5.3.1 Materials 142

5.3.1.1 Bacterial strain and bacteriophage lysate preparation 144

5.3.1.2 Bacteriophage purification 145

5.3.1.3 Purity control of phage lysate by electrochemical magneto immunosensing .. 146

5.3.1.4 Safety considerations 147

5.3.2 Bacteriophages biotinylation 148

5.3.3 Immunomagnetic separation and biotin-P22 tagging for the optical and electrochemical detection of *Salmonella* 150

5.3.4 Characterization by gel electrophoresis 152

5.3.5 Fluorometric assay for the evaluation of the degree of labeling 152

5.3.6 Confocal Fluorescence Microscopy 153

5.3.7 Transmission Electron Microscopy (TEM) 154

5.4 RESULTS AND DISCUSSION 154

5.4.1 Bacteriophage purification 154

5.4.2 Characterization of phage biotinylation 156

5.4.3 Characterization of the biotin-P22 phages by gel electrophoresis 161

5.4.4 Fluorometric assay for the evaluation of the degree of labeling 162

5.4.5 Characterization of biotin-P22 phagotagging by fluorescence confocal microscopy 164

5.4.6 Phagotagging magneto immunoassay for the optical and electrochemical detection of *Salmonella* 165

5.4.7 P22 bacteriophages as scaffold for the conjugation of gold nanoparticles 166
5.5 CONCLUSIONS 167
5.6 REFERENCES 168

6. BIOTINYLATED BACTERIOPHAGE AS NANOTAG FOR THE SENSITIVE DETECTION OF PATHOGENIC BACTERIA 171

6.1 INTRODUCTION 173
6.2 AIM OF THE CHAPTER 174
6.3 EXPERIMENTAL SECTION 175
  6.3.1 Materials 175
  6.3.2 Evaluation of the immunomagnetic separation and phagotagging of the bacteria by microscopy techniques 177
  6.3.3 Optimization of the phagotagging magneto immunoassay 177
  6.3.4 Evaluation of different strategies for the electrochemical magneto immunosensor based on phage tagging 179
  6.3.5 Magneto immunoassay with optical detection vs. electrochemical magneto immunosensor based on phage tagging for the detection of *Salmonella* in milk 179
  6.3.6 Specificity study 179
6.4 RESULTS AND DISCUSSION 181
  6.4.1 Evaluation of the immunomagnetic separation and phagotagging of the bacteria by microscopy techniques 181
    6.4.1.1 SEM analysis 181
    6.4.1.2 Confocal microscopy 181
  6.4.2 Optimization of the phagotagging magneto immunoassay 183
    6.4.2.1 Study of the conditions for the immunomagnetic separation 183
    6.4.2.2 Optimization of the concentration for the biotin-P22 and Strep-HRP 184
    6.4.2.3 Study of the phagotagging procedure 186
  6.4.3 Evaluation of different strategies for the electrochemical magneto immunosensor based on phage tagging 188
  6.4.4 Magneto immunoassay with optical detection vs. electrochemical magneto immunosensor based on phage tagging for the detection of *Salmonella* in milk 190
  6.4.5 Specificity study 195
6.5 CONCLUSIONS 196
6.6 REFERENCES 198

7. BIOTINYLATED BACTERIOPHAGES ON STREPTAVIDIN MAGNETIC PARTICLES FOR PHAGOMAGNETIC SEPARATION AND DETECTION OF PATHOGENIC BACTERIA 201

7.1 INTRODUCTION 203
7.2 AIM OF THE CHAPTER 204

7.3 EXPERIMENTAL SECTION 204
  7.3.1 Materials 204
  7.3.2 Evaluation of the optimal conditions for the phagomagnetic immunoassay based on biotin-P22 205
  7.3.3 Study of the capturing of biotin-P22 on the Strep-MP 206
  7.3.4 Evaluation of the biotin-P22 phagomagnetic separation of *Salmonella* by SEM and conventional culture method 207
  7.3.5 Biotin-P22 phagomagnetic immunoassay for the optical detection of *Salmonella* in milk 208
  7.3.6 Specificity study 208
7.4 RESULTS AND DISCUSSION 210
  7.4.1 Evaluation of the optimal conditions for the phagomagnetic immunoassay based on biotin-P22 210
  7.4.2 Study of the capturing of biotin-P22 on the Strep-MP 213
  7.4.3 Evaluation of the biotin-P22 phagomagnetic separation of Salmonella by SEM and conventional culture method 215
  7.4.4 Biotin-P22 phagomagnetic immunoassay for the optical detection of *Salmonella* in milk 217
  7.4.5 Specificity study 224
7.5 CONCLUSIONS 225
7.6 REFERENCES 226

8. BACTERIOPHAGE COVALENT IMMOBILIZATION ON MAGNETIC MICRO AND NANOPARTICLES FOR PHAGOMAGNETIC SEPARATION AND DETECTION OF PATHOGENIC BACTERIA 227

8.1 INTRODUCTION 229
8.2 AIM OF THE CHAPTER 230
8.3 EXPERIMENTAL SECTION 231
  8.3.1 Materials 231
  8.3.2 Covalent immobilization of bacteriophages on magnetic micro and nanocarriers 232
    8.3.2.1 Immobilization on tosylactivated magnetic particles 232
    8.3.2.2 Immobilization on carboxyl-modified magnetic nanoparticles 234
    8.3.2.3 Coupling efficiency and phage/particle ratio studies 234
  8.3.3 Evaluation of phage infectivity and biorecognition towards *Salmonella* of the immobilized P22 phages 234
  8.3.4 Comparison of the performance of both magnetic nano and microcarriers 235
    8.3.4.1 Phagomagnetic immunoassay with optical detection for Salmonella in milk 235
    8.3.4.2 Specificity study 237
  8.3.5 Evaluation of the phagomagnetic separation (PMS) of *Salmonella* by conventional culture methods and confocal microscopy 237

8.3.6 Phagomagnetic electrochemical immunosensor for the detection of *Salmonella* in milk 238
8.3.7 Pre-enrichment studies for the detection of *Salmonella* in contaminated milk 238

8.4 RESULTS AND DISCUSSION 239
8.4.1 Covalent immobilization of bacteriophages on magnetic micro and nanocarriers .. 239
8.4.2 Evaluation of phage infectivity and biorecognition towards *Salmonella* of the immobilized P22 phages 241
8.4.3 Comparison of the performance of both magnetic nano and microcarriers 243
8.4.3.1 Phagomagnetic immunoassay with optical detection for Salmonella in milk .. 243
8.4.3.2 Specificity study 249
8.4.4 Evaluation of the phagomagnetic separation (PMS) of *Salmonella* by conventional culture methods and confocal microscopy 250
8.4.5 Phagomagnetic electrochemical immunosensor for the detection of *Salmonella* in milk 252
8.4.6 Pre-enrichment studies for the detection of *Salmonella* in contaminated milk 255
8.5 CONCLUSIONS 258
8.6 REFERENCES 259

9. GENERAL CONCLUSIONS AND FUTURE PERSPECTIVES 261

PUBLICATIONS 269

ABBREVIATIONS AND SYMBOLS

ABBREVIATIONS AND SYMBOLS

§	Section
λ	Wavelength
a.u.	Absorbance units
µA	Microamper
mV	Milivolt

Ab	Antibody
Abs	Absorbance
Ag	Antigen
antiGliadin-HRP	Anti-gliadin antibody labeled with HRP
antiIgG-HRP	Anti-IgG antibody labeled with HRP (secondary antibody)
AP	Alkaline phophatase
Au-NPs	Gold nanoparticles
BSA	Bovine serum albumin
CFU	Colony-forming units
Da	Dalton (g mol^{-1})
DMSO	Dimethyl sulfoxide
CV%	Coefficient of variation
Cy5	Cyanine 5 dye
DNA	Deoxyribonucleic acid
DOL	Degree of labeling
E	Potential
EDC	Dimethylaminopropyl)-*N′*-ethylcarbodiimide hydrochloride
EIA	Enzymatic immunoassay
ELISA	Enzyme linked immunosorbent assay
EU	European Union
FAO	Food and Agricultural Organization
Fab	Antigen binding fragment of an antibody
Fc	Fragment crystallizable region of an antibody (tail region)
FDA	Food and Drug Administration
FRET	Fluorescence resonance energy transfer
GEC	Graphite-epoxy composite
HACCP	Hazard Analysis and Critical Control Points
HPLC	High performance liquid chromatography
HQ	Hydroquinone
HRP	Horseradish peroxidase

I	Intensity current
IC50	Concentration required for obtaining 50 % of the maximal signal
i.d.	Internal diameter
IgG	Immunoglobulin G
IMS	Immunomagnetic separation
ISFET	Ion-sensitive field-effect transistor
kDa	Kilodalton
LB	Luria-Bertani broth
LOD	Limit of detection
LOQ	Limit of quantification
LPS	Lipopolysaccharides
MALDI-TOF	Matrix-Assisted Laser Desorption/Ionization time of flight
m-GEC	Magneto graphite-epoxy composite
moAb	Monoclonal antibody
MP	Magnetic particles
MS	Mass spectrometry
n	Number of replicates
nm	Nanometer
nMP	Magnetic nanoparticles
NP	Nanoparticles
OD	Optical density
o.d.	Outer diameter
pAb	Polyclonal antibody
pa	Anodic peak
PBS	Phosphate buffered saline
PBST	Phosphate buffered saline with Tween 20
pc	Cathodic peak
PCR	Polymerase chain reaction
PEG	Polyethylene glycol
PFU	Plaque-forming units
PMS	Phagomagnetic separation
ppm	Parts per million (mg kg^{-1})
QCM	Quartz crystal microbalance
QD	Quantum dot
rpm	Revolutions per minute
S/B	Signal to background ratio
SDS	Sodium dodecyl sulphate
SEM	Scanning electron microscopy
SPR	Surface Plasmon Resonance
Strep	Streptavidin

Sulfo-NHS	*N*-hydroxysulfosuccinimide
TEM	Transmission electron microscopy
TMB	3,3’,5,5’- tetrametylbenzidine
TSP	Tailspike protein
tTG	Tissue transglutaminase
v/v	Volume-to-volume ratio
w/v	Weight-to-volume ratio
WHO	World Health Organization

SUMMARY

SUMMARY

Food allergens and food contaminants represent an important health problem worldwide. Tracking and tracing of allergen-free food production chains has become important due to consumer-safety concerns and to fulfill international labeling regulations. On the other hand, the detection of contaminants as pathogenic bacteria is an area of prime interest for food safety since infectious diseases spreading every day through food are a life-threatening problem for millions of people around the world. Food safety can only be ensured through the enforcement of quality-control systems throughout the entire food chain from the incoming raw materials until the final consumer. In this context, the availability of rapid, reliable and highly sensitive methods is mandatory for their use as an “alarm” to rapidly detect potential contaminants and take an immediate action. Therefore, great efforts are directed towards the development of simple, selective and cost-efficient methodologies for the on-site detection of different target analytes in complex food samples.

This dissertation addresses a comprehensive study and assessment of novel and rapid immunoanalytical strategies in different formats by the integration of micro and nanoparticles as well as hybrid bionanoparticles for food safety. Two analytes of different sizes and characteristics (single and multivalence targets) affecting food safety, were selected as a model: the small proteic allergen gliadin and the food-borne pathogen *Salmonella*.

Different immunoassay formats were assessed (competitive and sandwich, direct and indirect) taking advantage of the outstanding features of magnetic micro and nanoparticles as solid support. The results obtained with the novel strategies were evaluated by a dual detection through optical and electrochemical readouts, using magneto immunoassays or magneto immunosensing approaches, respectively. In all cases the signals were obtained by a horseradish peroxidase (HRP) conjugate as the enzymatic optical and electrochemical reporter and the matrix effect and analytical performance were evaluated using spiked food samples.

Regarding the integration of magnetic particles in the detection of food allergens such as gliadin, a competitive approach was developed to detect not only the native protein, but also the small gliadin fragments, being thus valid for both non-treated and hydrolyzed foodstuff. For the first time, the toxic protein fraction of gluten, gliadin, was successfully immobilized in an oriented way by covalent binding on tosylactivated

magnetic particles as well as carboxyl-activated nanoparticles. Excellent detection limits (in the order of μg L^{-1}) were achieved, much lower than the EC recommendation of 20 mg kg^{-1} for gluten-free food. Furthermore the matrix effect, as well as the performance of the assays was successfully evaluated using spiked gluten-free foodstuffs, such as skimmed milk and gluten-free beer, obtaining excellent recovery values.

The integration of bionanomaterials as bacteriophages into the immunoassays was also explored, using P22 bacteriophage as a model to detect *Salmonella.* Bacteriophages possess features such as specificity and rapid growth, which make them ideal agents for the rapid detection of bacteria. Their high stability in a range of harsh conditions including pH, temperature and even in the presence of nucleases or proteolytic enzymes makes them suitable for in situ monitoring of food and environmental contaminants. In addition, they allow an animal-free production (in contrast to antibodies) providing a large amount of viral coating proteins with a big surface for further chemical modification.

Hybrid bionanoparticles were designed and evaluated by i) immobilizing the bacteriophages on magnetic micro and nanoparticles and ii) modifying the phage capsid proteins with biotin tags. Moreover, the highly biotinylated bacteriophages were applied for bacterial tagging when coupled to fluorescent, optical or electrochemical streptavidin-conjugated reporters, as well as for bacteria capturing when attached to streptavidin-modified magnetic particles. The novel hybrid bionanoparticles were extensively characterized through a wide range of techniques, such as microbiological culturing methods, electrophoresis, confocal fluorescence microscopy, scanning electron microscopy and transmission electron microscopy. In all cases, non-competitive approaches were developed by integrating the bacteriophages both for the biorecognition as well as for the tagging of *Salmonella* Thyphimurium. All the developed immunoanalytical strategies were able to considerably reduce the time of the bacteria detection from the 3-5 days required in the conventional microbiology techniques, to as low as 2-4 h. In addition, outstanding limits of detection were achieved, being able to detect below 10^2 CFU mL^{-1} of *Salmonella* in milk samples, and as low as 1 CFU in 25 mL after 6 h pre-enrichment.

Finally, when comparing the performance of the optical and electrochemical readouts, better sensitivity and lower matrix effect were achieved with the electrochemical detection. This fact can be ascribed to the advantageous features provided by the use of magnetic particles coupled to the improved electrochemical properties of the graphite-epoxy composite electrodes developed and highly studied in our research group. Furthermore it should be also pointed out that biosensing devices are promising tools for food safety applications due to their rapid and on-site testing capability as well as the compatibility with miniaturization and mass fabrication technologies.

CHAPTER 1

INTRODUCTION

1.1 AGENTS AFFECTING FOOD SAFETY

Food borne diseases represent currently one of the major public health problems and economic burden worldwide. A 2003 World Health Organization (WHO) report concluded that, only in the USA, there are around 76 million cases annually resulting in 325000 hospitalizations, 5000 deaths, and a total medical cost of $37.1 billion.[1,2]

The concept of food safety involves all aspects guaranteeing the production, handling, storage and commercialization of food in ways that avoid potentially health risks to the final consumer.[3] The tracks within this line of thought are to keep safety between industry and market and then between market and consumer.

The contamination of food may occur at any stage in the process from food production to consumption, i.e. from “farm to fork”, and the most common clinical presentation takes the form of gastrointestinal symptoms. However, such diseases can also have neurological, gynecological, immunological and other symptoms, and even multi-organ failure or cancer may result from the ingestion of contaminated foodstuffs, thus representing a considerable burden of disability as well as mortality.[4]

Food contaminants can be classified according to their nature and origin in basically three types: biological, chemical and physical hazards. Examples of biological hazards are: disease-causing bacteria, viruses, parasites, molds, yeasts, and naturally occurring toxins; while between the chemical types are: pesticides, toxic metals, veterinary drug residues, machine oils, cleansers and cleaning solutions and sanitizers. Finally the physical hazards are objects which are not a part of food, never was meant to be food, but somehow got into the food, as for example: pieces of glass or metal, toothpicks, cigarette butts, pebbles, hair, staples, jewelry.[5] Most of the harmful agents found in foodstuff result from natural environmental contamination that can accidentally enter during the food growth, cultivation, preparation or storage, but some of them are additives intentionally added during the production process, which can be hazardous when present in excess.[6] While additives control was the main concern in the past, today the greatest problems are consequence of microbiological contamination, which caused many outbreaks in recent years, followed by pesticides and drug residues.[7] On the other hand, food allergies and intolerances although affecting only a part of the population, also represent an important health problem related to food in industrialized countries.

All the aforementioned food related problems create high distrust in the consumers. Therefore, the European Commission and regulatory agencies as WHO, FAO (Food and Agricultural Organization) and FDA (US Food and Drug Administration), established food safety as one of the main subjects. Hence, the promotion of new active policies in the food field related to legislation up-dating, reinforcement of control points and increase in scientific advising is carried out in order to ensure the consumer health protection. As an example, the WHO and FAO established in 1963 the Codex Alimentarius Commission, currently consisting of 185 member countries and the EU, with the aim to develop international food regulations to protect the health of the consumers and ensure fair practices in the food trade. In 2003 WHO and FAO published the Codex Alimentarius, or the food code, which is a collection of internationally recognized standards, codes of practice, guidelines and other recommendations relating to foods, whether processed semi-processed or raw, and food production, covering matters such as food labeling, food hygiene, food additives and safety of modern biotechnology processes.[8]

During the past decades, food control was performed by just analyzing the finished products, instead of monitoring every stage involved in their production. However, in that case the cause of contamination could never be identified, which lead to perceive the importance of the establishment of control programs throughout the whole production chain, from the first manufacture in the farm, through the subsequent processing steps and until the final sale. Food quality and safety can only be ensured through the application of quality control systems throughout the entire food chain and many methodological programs like good agricultural, good veterinary practices, good manufacturing and good hygiene practices have been created. Therefore, the Hazard Analysis and Critical Control Points (HACCP) program is accepted worldwide as one of the most efficient preventive programs for public health protection in the food sector. HACCP consists of a systematic approach for the control of potential hazards in a food operation, considering all stages in the food production from the raw materials until the final consumer, and aims to identify problems before they occur and design measurements to reduce these risks to a safe level.[3] Although HACCP programs are specific for each production process, it can be basically divided into seven main principles: i) conduct a hazard analysis, ii) identify critical control points, to prevent, eliminate or reduce potential hazard entering in the food supply, iii) establish critical limits for each critical point, iv) establish critical control point monitoring requirements, v) establish corrective actions, vi) establish procedures for ensuring the HACCP system is working as intended, and vii) establish record keeping procedures, documenting all the aforementioned principles.[9] The seven HACCP principles are included in the international standard ISO 22000 FSMS 2005. This standard is a complete food safety and quality management system incorporating the elements of prerequisite programs (GMP & SSOP), HACCP and the quality management system, which together form an organization's Total Quality Management system.

With the implementation of these HACCP programs, the demand for rapid, sensitive and selective detection methods considerably increased, motivating the development of new techniques for the analysis of different analytes in few hours or even minutes to take the appropriate correcting measures in the shortest time possible. In the case of allergens, reliable detection and quantification methods are also necessary in order to ensure compliance with food labeling and to improve consumer protection. However, the detection in food products can be very difficult, as the contaminating compounds or allergens are often present only in trace amounts and could be masked by the food matrix.[10]

In the next sections, a brief description of the food related targets used as a model in the strategies developed in this dissertation is presented, as well as an overview of the related diseases that they produce. Afterwards, short summaries of the gold standard and rapid methods available for food safety are also introduced.

1.1.1 Food allergens. Gliadin and celiac disease

According to several European and American authors, food allergies affect up to 2-4 % of the adult population and up to 8 % of children,[11–13] although the perceived prevalence of food induced symptoms may be as high as 22 % of the general population.[14] Food allergens can be defined as those substances in foods that can trigger an immune response in allergic individuals. In IgE-mediated food allergies, the allergens are usually naturally occurring, and often abundant, proteins found in a particular food.[15] A special mention should be given to celiac disease, in which, although not classified as an allergy, a similar immunological reaction occurs, being the response at least partly mediated by IgA and cytolytic T cells.[16] In highly sensitized individuals, the intake of minute amounts of allergens can provoke digestive disorders (emesis, diarrhea), respiratory symptoms (rhinitis, asthma), circulatory symptoms (edema, hypotension), and skin reactions (urticaria, atopic dermatitis/eczema) and for some allergic persons, contact with a specific food allergen can even provoke life-threatening reactions (anaphylactic shock), which have been increasing more and more in recent years. [11–13]

Since no cure for food allergic patients is available to date, these individuals must strictly avoid the offending compounds in their diet. Total avoidance is sometimes difficult, as processed food usually contains a wide variety of ingredients including potential allergens. Moreover, sensitive individuals may also be inadvertently exposed to allergenic proteins by consumption of food products supposed to be free of a certain allergen, as food products can be contaminated with 'foreign' food constituents during processing, shipping and storage, for instance by carry-over due to inadequate cleaning of shared processing equipment, or by reuse (rework) of allergen-containing products.[10]

For the allergic consumer it is particularly important to have full information about potential allergens contained in a food product, which lead thus to the creation of proposals intending that all ingredients intentionally added have to be included in the label to ensure that consumers with allergies can identify any allergenic ingredients that may be present in a foodstuff.[17]

Celiac disease, also known as celiac sprue or gluten-sensitive enteropathy, is an autoimmune disorder that affects possibly 1:100 people in Northern Europe and North America[18,19]. The disease was firstly described in a lecture by Samuel Gee in 1887, but the first accurate description of the celiac lesion was provided by Paulley et al in 1954 who examined full-thickness biopsy specimens taken at laparotomy from a patient with celiac disease. The illness results from damage to the upper small intestinal mucosa due to an inappropriate immune response to a cereal protein, which can cause atrophy of intestinal villi and affects the normal absorption of many nutrients leading to development of anemia, osteoporosis or other complications.[20,21]

'Gluten' is the generic term used for the protein fraction of cereal grains that causes celiac disease, being present in wheat, barley and rye. It contains hundreds of protein components, which are unique in terms of their amino acid compositions, as they are characterized by high contents of glutamine and proline and by low contents of amino acids with charged side groups. Traditionally, gluten proteins have been divided into roughly equal fractions according to their solubility in alcohol–water solutions of gluten (e.g. 60 % ethanol): the soluble gliadins (or other related prolamins like hordeins and secalins) and the insoluble glutenins.[22] The first ones, monomers with molecular masses between 30 and 70 kDa, are responsible in triggering the immune system for the production of autoantibodies.[18]

Celiac disease can be diagnosed at any age. However, it appears most commonly in early childhood (between 9 and 24 months) or in the third or fourth decade of life.

Clinical presentation depends on age, sensitivity to gluten, and the amount of gluten ingested in the diet, as well as other unknown factors. Although, it is a disorder that primarily affects the small bowel, the symptoms can range from classic gastrointestinal symptoms, such as diarrhea and abdominal distension, which are more common in infants and young children, to nonspecific gastrointestinal symptoms and extraintestinal manifestations, typical of older age groups. Moreover, some individuals may have no symptoms at all and can be termed as having *silent celiac disease*, which results in a substantial number of undiagnosed cases in the general population, possibly 10 times as many as actually have been diagnosed.[21,23] Patients with celiac disease tend to have other chronic diseases in which the immune system attacks their own cells and tissues, including type-1 diabetes, autoimmune thyroid disease, autoimmune liver disease, rheumatoid arthritis, Addison's disease, and Sjögren's syndrome. Autoantibody production is an important feature of all these autoimmune disorders, signifying a breakdown of immune tolerance to self-antigens.[24]

There is a strong genetic predisposition to celiac disease, with the major risk being attributed to the specific genetic markers known as human leukocyte antigen (HLA)–DQ2 and HLA–DQ8 that are present in affected individuals.[25] However, although the presence of these HLA proteins is necessary for developing celiac disease, it is not enough since about 30 % of the healthy population possess them.[26]

The ability to generate an immune response to gluten depends on the presentation of gluten peptides to T-cells. These peptides, containing around 15 % of proline and 35 % glutamine, are resistant to digestion by gastric and pancreatic enzymes accumulating thus in the intestine, where they reach the epithelial cell membrane passing into the cytosol.[23,27] The further deamidation of the glutamine residues of the peptides by tissue transglutaminase (tTG), an ubiquitous connective tissue enzyme, creates epitopes with increased immunestimulatory potential.[20] When tTG crosslinks with gliadin, the gliadin–tTG complex is taken up by B-cells that express tTG-specific immunoglobulins on their membrane. As a result of this uptake, the gluten–tTG complex is degraded intracellularly and the gluten peptides bind to the HLA DQ2 and DQ8 and are expressed on the cell surface. In celiac patients, gluten-specific T cells recognize this HLA DQ-peptide complex, resulting in the production of tTG specific antibodies and anti-gliadin antibodies causing an inflammatory immune response, responsible for the damage to the small intestine.[18,28]

A specific 33-mer peptide of the α2-gliadin (residues 57-89) was shown to be highly resistant to digestive proteases, containing six T-cell identified epitopes, and being thus the principal contributor for gluten toxicity in genetically susceptible individuals. Analysis with LC-MS and MS revealed that, although the deamidation pattern of LQLQPFPQPQLPYPQPQLPYPQPQLPYPQPQPF was complex, mono-deamidated products at the underlined Gln (Q) residue accumulated with time. Regiospecific deamidation of immunogenic gliadin peptides by tTGase increases their affinity for HLA DQ2 as well as the potency with which they activate patient-derived gluten-specific T cells.[29] Another celiac disease causing 26-mer peptide from γ-gliadin (FLQPQQPFPQQPQQPYPQQPQQPFPQ) was later identified and 21 celiac-specific gluten epitopes were reported up to 2006.[30] Further DQ2 restricted α- and γ-gliadin epitopes were characterized, and their location was established to be in distinct proline-rich clusters of the gliadin protein. Toxic peptides were shown to always contain one of the four following motifs: PSQQ, QQQP, QQPY, or QPYP, although they must be surrounded by other amino acids to cause toxicity.[31]

As celiac disease is a life-long disease, if untreated it is associated with significant morbidity and increased mortality, largely owing to the development of enteropathy-associated intestinal lymphoma. The pathologic changes and symptoms resolve when gluten is excluded from the diet, being thus the strict adherence to a diet free of gluten the only treatment known until now. However, a diet completely free of gluten is very difficult to maintain since gluten is a very common component in human diet, being perhaps after sugar the second most widespread food component in western civilization. Moreover, cross-contamination to naturally gluten-free foodstuff (such as oat) is also very common, which makes that besides the quality control of gluten-containing products, the assessment of gluten in foodstuff that can be contaminated with native or heated proteins from wheat, barley, and rye is also important. In addition, the fact that about 10 % of gluten seems to be made up of potentially toxic gliadin peptides makes extremely important to evaluate the content of these peptides in food.[32,33]

As a result, to increase food safety for celiac patients, gluten has been included in food regulations and labeling in order to prevent harmful effects of gluten-containing food or food components.[34,35] However, the individual variation and clinical heterogeneity occurring in celiac patients created serious problems when establishing the threshold values that should be allowed in gluten-free foodstuff and disagreement exists between and within countries.[27] Therefore as part of the Food Allergen Labeling and Consumer Protection Act of 2004, the US Food and Drug Administration (FDA) defined in 2008 that foods labeled with the term gluten-free, may not exceed gluten contents of 20 mg gluten/kg of food (ppm). One year later, the European Union (EU) enacted Commission Regulation 41/2009 that defines the term “gluten-free” for labeling purposes allowing affected consumers to identify those products that are safe to consume. The European Regulation, which is based on Codex Standard 118, also set a limit of 20 mg/kg product as a threshold, below which the gluten-free label in food products is allowed.[36,37] Furthermore, the category “very low gluten” foods was introduced, in line with the stipulations made by Codex Standard 118-1979. These foods should not contain gluten from wheat, barley, and rye at a level equal to or higher than 100 mg/kg of food.[31] A wide range of commercial gluten-free products are currently available from supermarkets and also on FP10 prescription.[20] Finally, the Association of European Coeliac Societies (AOECS) is a non-profit organization that currently spans 34 countries in Europe and has the right to issue licenses under the newly introduced European Licensing System (ELS) giving producers of gluten-free products the right to use the internationally accepted crossed grain symbol, shown in Figure 1.1, A. This year the AOECS established that in order to certify the validity of the symbol and guarantee the gluten control of the product, it should be accompanied by a registration number, indicating a content below 20 mg/kg of gluten. Moreover, one of the following expressions should be added if necessary: “OATS” if contents of this pure cereal are present, “100” if the product contains until 100 mg/ kg gluten and “100/OATS” if both aforementioned statements occur simultaneously. Some other examples of gluten-free labeling certified by regulatory associations are shown in Figure 1.1, B.

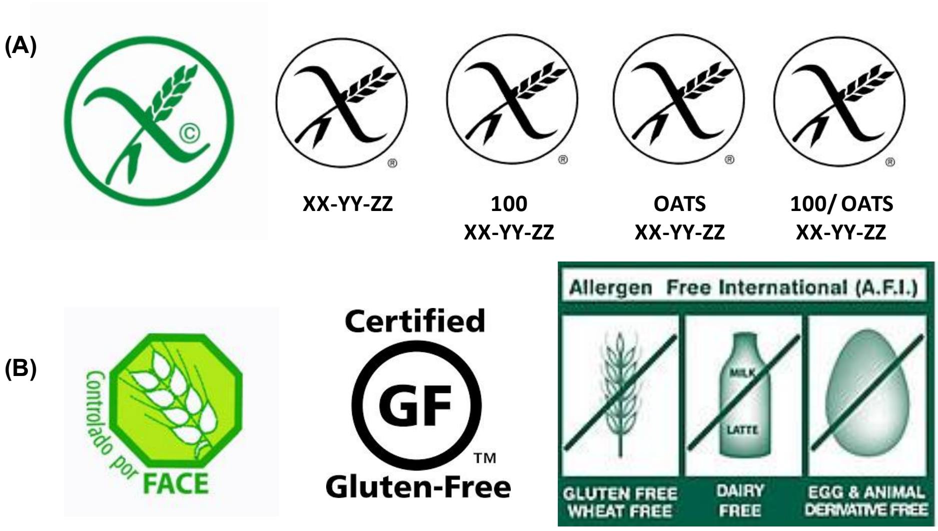

Figure 1.1 Some examples of certified gluten-free labels. (A) International accepted symbol (green) and their variations validated by the AOECS. (B) Trademarks certified by FACE (*Federación de Asociaciones de Celíacos de España*), Gluten Free Organization (supported by the AOAC) and Allergen free International.

1.1.2 Microbiological contamination in food. *Salmonella* and salmonellosis

Bacteria that cause foodborne diseases occur worldwide, being the principal responsible for the majority of foodborne outbreaks *Salmonella* spp., *Listeria monocytogenes*, and some strains of *Escherichia* coli and *Campylobacter*. Some other strains that can also be found in food are *Staphylococcus aureus*, *Clostridium perfrigens* and *Bacillus cereus*. All these pathogens can rapidly multiply in a humid and warm environment and also in protein-rich foodstuff such as meat, fish, seafood, milk, eggs among others. While some infectious microorganisms can be multiplied in the digestive tract and cause disease through cellular invasion or toxin production, other produce enterotoxins in food during their growth and metabolism.[38,39]

Over the past decades, most European countries and the United States have reported a sharp rise in the incidence of disease due to *Salmonella*. This increase, especially the emergence of more virulent isolates, emphasized the need to control this pathogen in the food supply. *Salmonella* are facultative, gram-negative, motile, non-spore forming bacilli, able to live in anaerobic media, belonging to the enterobacteriaceae family. They grow at temperatures between 8 and 45 ºC in a pH range of 4-9 and are resistant to drying, being able to survive in dust and dirt for years. The genus *Salmonella* has been classically divided into three species: *S. Typhi*, *S. cholerae-suis* and *S. enterica*, and can be further catalogued by their antigenicity in over 2300 serotypes, which can be identified by highly specific O (somatic) and H (flagellar) antigens.[40]

Salmonella enterica serovar Typhimurium is one of the most frequently documented serovars associated with human infections since 1997 (CDC 2007). This serotype causes not as severe illnesses as other species like *S. Thypi*, but is the most common agent causing foodborne infections. Its toxicity is due to an outer membrane consisting largely of lipopolysaccharides (LPS) which protect the bacteria from the environment. The LPS is made up of an O-antigen, a polysaccharide core, and lipid A, which connects it to the outer membrane. Lipid A is made up of two phosphorylated glucosamines which are attached to fatty acids. These phosphate groups determine bacterial toxicity. Animals carry an enzyme that specifically removes these phosphate groups in an attempt to protect themselves from these pathogens. The O-antigen, being on the outermost part of the LPS complex is responsible for the host immune response. *S.* Typhimurium has the ability to undergo acetylation of this O-antigen, which changes its conformation, and makes it difficult for antibodies to recognize.[41]

Salmonella is widely distributed in nature, being humans and animals their primary reservoirs. They live in the intestinal tract of humans and other animals, including birds and can pass from the feces of humans and animals to other people or other animals. The illness provoked by this bacterium is called Salmonellosis, a gastroenteritis that can affect humans and other mammals. Salmonellosis in humans occurs in a variety of forms, presenting a broad clinical spectrum. Typically, the incubation period is between 6 and 72 h following ingestion of contaminated food or water and the most common symptoms are abdominal pain, diarrhea (occasionally with mucous or blood), nausea, vomiting, chills, headache and fever. In uncomplicated cases, the acute stage usually resolves within 48 h, but in some cases can be more protracted, persisting until 10-14 days. In most cases the recovery is achieved without treatment, but in some people like infants, elderly (>60 years) and immune-compromised persons, hospitalization can be needed and the infection can spread to the blood stream causing bacteremia, and then to other body sites, leading even to death. However, fatalities rarely exceed 1 % of the affected population and are limited almost entirely to the aforementioned kind of patients.

Many factors have contributed to recent food emergencies and to the increase of *Salmonella* in food supply. Some examples are the increasing complexity of the food production chain because of mass production and the modern large-scale and intensified farming practices that confine many animals or fowl in close quarters. *Salmonella* inadvertently introduced into a herd or flock quickly spreads since the confined conditions expose stock to contaminated feed and water through contact with infected animals and animal feces. Moreover, healthy animals may carry pathogens that cause disease in humans and animals may be infected from feed, from other animals, or from the environment.[40,42] Contaminated foods are often of animal origin, such as meat, poultry, eggs, milk and dairy products, seafood, but also other foods, including vegetables and spices can become contaminated. Infectious doses are highly dependent upon the strain, the health and age of the infected host, but are estimated to be as low as 15-20 CFUs [43]. These low limits of detection are a great challenge, and therefore in order to minimize the affect of food borne illness it is essential to develop sensitive, simple, inexpensive, and reliable tests that can be performed in the context of hazard analysis and critical control point principles.[44] In 1997, a pathogen reduction and HACCP plan for *Salmonella* has been implemented in several large meat and poultry plants in the United States.[40] The inspection of food for the presence of *Salmonella* has become routine all over the world.

1.2 AN OVERVIEW OF THE DETECTION METHODS FOR FOOD SAFETY

The monitoring of food allergens and contaminants often requires very challenging limits of detection and has to be supported by strict analytical quality-control standards, so that the analysis produces unequivocal, precise, and accurate data. Moreover, an analytical method to be used in the determination of food related targets should accomplish an adequate specificity, sensitivity, accuracy, and precision at the relevant contaminant concentration and in the appropriate food matrixes. Therefore, different (bio)analytical methods should be available in order to provide two kinds of information: i) the one required for the rapid decision-making, and ii) the one obtained after the analysis with a validated technique, which confirms the results, normally based on classical standard methods carried out inside the laboratory.

With the high demand for rapid, sensitive, simple, low cost and on-site testing, conventional laboratory methods that provide detailed qualitative and quantitative information about samples are increasingly replaced by rapid-response analytical tools providing a binary yes /no response which indicate whether the target analytes are present above or below a pre-set concentration threshold. These methods are called screening systems and are intended for the high-throughput and low cost analysis of samples, providing a reliable response with minimized preliminary operations, allowing an immediate action to take the appropriate correcting measures. However, it should be pointed out that positive samples sometimes require further confirmation by the use of a conventional alternative.[45–47]

In the next sections (§§ 1.2.1 and 1.2.2), the confirmatory or gold standard techniques, as well as the screening and rapid methods for food safety are briefly introduced. A further and detailed discussion of the state of the art about the methodologies used for the targets selected in this dissertation as a model of food contaminants will be found in §§ 1.6 and 1.7.

1.2.1 Gold standard methods for food safety

In the case of the analysis of chemical contaminants and additives, such as pesticides, toxic metals, veterinary drug residues, flavorings and colors, or food allergens, some quantitative analytical methods commonly applied result from the coupling of chromatographic separation techniques, such as gas chromatography, HPLC, ion chromatography and capillary electrophoresis, with different kinds of detectors based on UV-Vis light absorption or fluorescence, mass spectrometry (MS), light scattering (ELSD), refractometry (RI detectors), conductivity, electrometry or flame ionization. Other methods applied in food control are flow injection analysis (FIA), atomic absorption (AAS), inductively-coupled plasma atomic emission spectrometry (ICP-AES), near infrared spectroscopy (NIR) and Fourier-Transformed infrared spectroscopy, between others. Although most of these techniques are characterized by high selectivity and specificity, good precision and accuracy, as well as low limits of detection and the possibility to make multi-analyte evaluations, they are labor-intensive, costly, required specialized personnel and in some cases are also time-consuming.[48,49]

On the other hand, the classical method for the detection of food-borne pathogens employs culture-dependent techniques based on plate counting, which consist in the enumeration of the colonies that appear after the incubation on a solid culture media (as explained in more detail in § 1.7.1). Special selective and differential media can be used to count specific organisms, which simultaneously contain inhibitors for others, and chromogenic or fluorogenic substrates can be added yielding brightly colored or fluorescent products as a result of the action of different specific bacterial enzymes or metabolites. The use of these selective media and chromogenes, combine the enumeration, detection and identification steps thereby eliminating the need of subculture media and further biochemical tests.[50] Bacterial culturing is a very sensitive method and quite cost-effective, but has the main drawback of being time-consuming, since some days (2-5) are required to obtain final results.

1.2.2 Rapid methods for food safety

The study of new simple methods continued moving forward since the development of rapid, reliable and decentralized methods is mandatory to improve consumer protection. Between the emergent methods, the most important and highly studied were the following two: i) molecular methods operating in the DNA level based principally on the polymerase chain reaction (PCR) and its quantitative and highly accurate variant real-time PCR, and ii) protein-based methods usually involving immunochemical detection.

Currently, the Enzyme-Linked Immunosorbent Assay (ELISA) is one of the most commonly used immunological techniques in laboratories of the food industry and official food control agencies due to its high precision, simple handling and good potential for standardization.[17] Other suitable candidates to cover the demands of

HACCP programs are the biosensors), due to their high sensitivity, selectivity, low cost, besides the fact that they allow the rapid and on-field detection of a wide range of analytes in complex samples, requiring in general minimal sample pretreatment and reduced detection times. In particular immunosensors (§ 1.4.2.1), result promising alternatives to the existent immunochemical assays.[51]

In the following sections (§§ 1.3 and 1.4) the last strategies, namely immunoassays and biosensing approaches, are further discussed since these are the methodologies designed and developed in this dissertation.

1.3 IMMUNOCHEMICAL METHODS

Immunochemical methods, which have been used for decades in clinical chemistry as rapid, simple and reliable tools of screening analysis, have gradually spread in recent years to veterinary medicine, agriculture and other areas including environmental and food contaminants analysis.[52] They allow the identification and quantification of trace amounts of different compounds based on immunological principles, in particular, on the highly specific interaction between the analyte (antigen) and its specific antibody. These methods offer a number of advantages, such as high specificity and sensitivity, rapidity and the possibility of the simultaneous analysis of a great number of samples.[53]

The detection of an antigen requires the production of specific antibodies, its isolation and in many cases also some final purification step. Advances in polyclonal and monoclonal antibodies production have stimulated this technology, since nowadays a wide range of antibodies are available against almost all the important food residue compounds, which can be commercially acquired at reasonably low cost.[54] Because antibody affinity and specificity determine primarily the analytical capability of the immunochemical method, the properties of the antibodies represent an important innovative factor in developing an analytical system. Antibodies “made to measure” are required for both the detection of a single molecule or the simultaneous screening of a group of closely structurally related substances.[52] As an example, to determine sulfanylamide drugs, one should perform a number of specific analyses for determining each particular sulfanylamide or a class-specific analysis by which one can determine the total of closely related compounds.[55] Therefore, the immunological methods can be designed for the detection of one component or as a method of total index (class-specific), depending on the immunogen used for the antiserum production.

One of the most important differences between the chromatographic and immunochemical methods of analysis is in their specificity. Chromatographic methods are used to determine several closely related substances in one sample, and developers face the problem of reducing the number of peaks in the chromatogram, that is, the number of substances to be determined; this is attained using fine sample preparation. In contrast, immunochemical methods are most often used to determine only one substance for which antibodies have been isolated.[53] Moreover, immunological techniques require little or no sample cleanup, without the need of expensive instrumentation and are more suitable for on-field analysis in contrast to the classic instrumental method previously described.

1.3.1 Antibodies as bioanalytical reagent

Antibodies are glycoproteins belonging to the immunoglobulin (Ig) family present in a soluble form in blood and lymph with the main role of identifying and neutralizing foreign agents (such as bacteria and viruses). They are produced by lymphocytic B cells and are responsible for the immunological memory after the elimination of the agent for a future improved response. Five different antibody isotypes are known in mammals, which differ in their biological properties, functional locations and ability to deal with different antigens: IgA, IgG, IgM, IgE, and IgD (rare), from which the IgG group is the most abundant in blood serum (80 %).[56,57]

An antibody (Ab) molecule consists of two pairs of identical polypeptide chains, called light and heavy chains, joined by disulphide bonds. The Figure 1.2 shows the typical IgG structure. Both types of chains present variable domains on the amino-terminus of the protein and constant regions on the carboxyl end. The variable regions make up the antigen (Ag) recognition and binding site, giving the antibody specificity. The amino acid sequence of this region is highly variable, and this contributes to the broad recognition power of the antibody to a wide range of target molecules. When digested with the proteolytic enzyme papain, a mammalian antibody molecule yields two identical 50 kDa Fab fragments (antigen binding fragment) and one 50 kDa Fc fragment (crystallizable fragment).[58,59] The Fab fragment binds to antigen molecules, while the Fc fragment ensures that each antibody generates an appropriate immune response for a given antigen, by binding to a specific class of Fc receptors (located on many mammalian cells) and other immune molecules, mediating different physiological effects related with the different antibody functions.

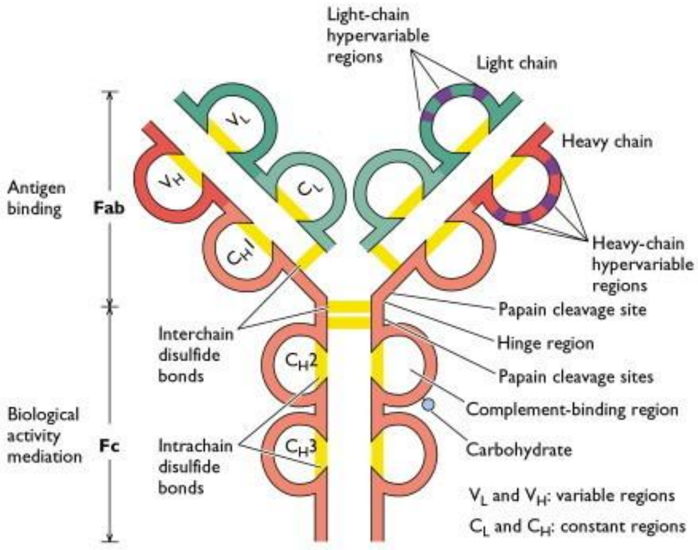
Light-chain hypervariable regions
Light chain
Heavy chain
Antigen binding
Fab
V_L
V_H
C_L
C_H1
Heavy-chain hypervariable regions
Papain cleavage site
Interchain disulfide bonds
Hinge region
C_H2
Papain cleavage sites
Complement-binding region
Biological activity mediation
Fc
Intrachain disulfide bonds
C_H3
Carbohydrate
V_L and V_H: variable regions
C_L and C_H: constant regions

Figure 1.2 Schematic representation of an IgG antibody, showing the variable and constant regions of the heavy and light chains which form their typical structure, consisting of two antigen binding fragments (Fab) and a constant fragment (Fc).

Foreign molecules that activate an immune response in an organism are called immunogens, and usually have a high molecular weight (>10 kDa) and high structural complexity. Besides, if the substance is able to induce the generation of antibodies it is called antigen. If antibodies production against small molecules (< 10 kDa) is required, as for example in the case of toxins, hormones or other compounds, they have to be attached to a larger molecule, such as a protein, which should be strange for the organism but also should not elicit an immune response by itself. In this case, the small molecule is called hapten and the conjugated macromolecule, carrier. Once the body has generated antibodies to an hapten-carrier adduct, the hapten may also be able to bind to the antibody, but it will usually not initiate an immune response.[58]

An immunogen, antigenic molecule or hapten-carrier adduct, inoculated in a host receptor organism is able to trigger an immune response that allows obtaining the specific antibodies as analytical reagent, which present specific binding sites, able to strongly react with the primary compound.

1.3.1.1 Antibody production

The production of a target-specific, high performance antibody depends on the proper strategy in selecting and delivering the antigenic molecules such as small peptides or polypeptides as immunogens. Therefore the successful antibody production depends on the careful planning and implementation with respect to several important steps and considerations: i) synthesize or purify the target antigen (e.g. peptide or hapten); ii) choose an appropriate immunogenic carrier protein; iii) conjugate the antigen and carrier protein to create the immunogen; iv) immunize animals using appropriate schedule and adjuvant formula; and v) screen serum (or hybridoma for antibody titer and isotype (also called antibody characterization).[60]

Polyclonal antibodies (pAb) are produced by using traditional immunization procedures, being rabbits, goats and sheep the most common animals used in the production. The assortment of antibodies present in a pAb preparation may consist of different classes and subclasses produced by the response of many different B lymphocytes, and they may recognize multiple antigens or multiple epitopes located on the same antigen. A certain drawback of the method lies in the fact that it is not possible to produce identical antibody specificity even in two animals of the same species. Moreover, polyclonal antibodies present sometimes cross-reactivity problems reacting with other nonspecific proteins and their supply is limited by the animal dead.[61,62]

These problems have been solved with the production of monoclonal antibodies (moAb), introduced by Kohler and Milstein in 1975 through the discovery of hybridoma technology. In contrast to polyclonal, monoclonal antibodies are synthesized by a population of identical B cells and recognize only a specific epitope on an antigen. During moAb production, the B-lymphocytes are collected from the spleen of immunized mice, rats, or rabbits and fused with myeloma cells (Sp2/0, NS1), producing the hybrid cells, called hybridoma. The hybrid cells are then screened to determine which ones produce antibodies of the desired specificity and the selected clone can be infinitely proliferated by cell culturing in a flask or grown in the peritoneal cavity of a mouse.[63,64] Although the processing of monoclonal antibodies is more complex and expensive, an unlimited production of identical and highly specific antibodies can be achieved. However, the wide spreading is limited by low predictability of the hybridoma technology result.

The type of antibodies (pAb *vs.* moAb) to be used depends on the specific application. If a high specificity is required, monoclonal antibodies are normally preferred. Nevertheless, polyclonal antibodies although their lower specificity, provide a higher sensitivity to the assays and were also found to be superior to monoclonal antibodies in capturing and concentrating target molecules, as in the case of immunomagnetic or immunobead-based captures. Furthermore, polyclonal antibodies are also preferred for the production of secondary antibodies.[62,65]

In some cases difficulties with the antigen isolation and purification arise and thus, the native proteins cannot be used to generate the desired antibodies. As a result, several other strategies like the use of synthetic peptides, recombinant DNA technology, and phage display were introduced as alternative methods for antibody production.[66,67]

In the last decade, molecular biology has generated fundamental changes in antibody production. Preparation of recombinant antibody fragments with novel binding properties was a primary goal by cloning antibody genes through a recombinant DNA technology. The major improvement of recombinant antibodies over polyclonal or monoclonal antibodies is that they are produced by bacteria culturing, which offer a stable genetic source. Furthermore, screening is less time–consuming, the bacteria can be genetically manipulated directing mutagenesis to that part of gene which determines the structure and affinity of antibody binding site and the recombinant antibodies can be produced in abundance in a relatively short period of time.[68] Moreover, large phage libraries expressing antibody fragments on the surface of individual phage particles were used for preparation of recombinant antibodies. The systems enable separation of individual phage particles and subsequent selection of phage antibodies from a large number of expressed phage particles.[69,70]

1.3.1.2 The antibody-antigen recognition

Antigens induce the production of antibodies against different regions in their structure and the antibody-antigen interaction occurs thus between some aminoacidic residues from the antibody (paratope) and a small complementary region in the antigen (epitope). The recognition ability depends on the aminoacidic sequence variability of the Fab region of the antibody. The binding pocket of an antibody can accommodate from 6 to 10 amino acids and the highly specific recognition of the antigen is based on multiple reversible non-covalent interactions: hydrogen bonds, electrostatic interactions, van der Waals forces, and hydrophobic interactions. All of them are weaker than covalent binding, but the total addition of all these forces have a significant effect and define the strong antibody affinity to its specific antigen.

The measure of the strength of the binding is called affinity, and it is usually expressed in terms of the concentration of an antibody-antigen complex measured at equilibrium. The thermodynamic balance of the antigen-antibody binding can be represented by the equation shown in Figure 1.3. This balance is generally highly shifted to the right, with K_a values in a range between 10^8- 10^{10} M^{-1}.[57,58]

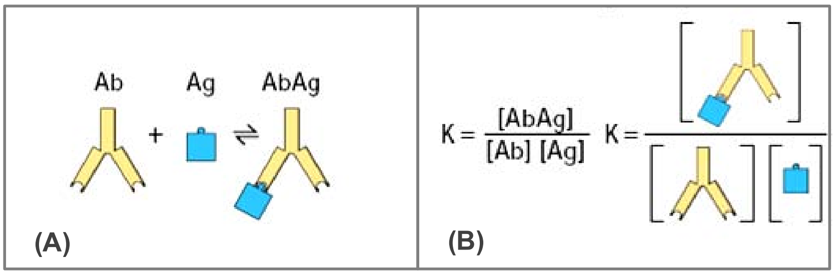

Figure 1.3 The reversible antigen-antibody reaction is outlined in (A), while the calculation of the equilibrium constant or antibody affinity (K) is shown in (B).

The affinity is inversely proportional to the distance between the groups participating in the interaction. In order to minimize the distance and increase the antigen-antibody affinity accordingly, epitope and paratope structures should be complementary. Small changes in the antigen structure (such as a single amino acid) can affect the strength of the interaction causing an abrupt decrease in the affinity. High-affinity antibodies can bind more antigen in a shorter period of time than low-affinity ones, and they form more stable complexes. Hence, high-affinity antibodies are usually preferred in immunochemical techniques.[1]

Some antibodies show cross-reactivity to similar epitopes on other molecules. This makes the immunochemical method less specific but at the same time more applicable to situations where the target is a class of structurally related molecules.[71]

1.3.2 Labeling of immunological reagents

Although in some cases the antibody-antigen complexes result in a visible precipitate, in most immunochemical assays the attachment of antibody to antigen can be visualized only by labeling the antibody or antigen with a marker that can be qualitatively and sometimes quantitatively detected. Thus antibodies or antigens can be labeled with a radioactive isotope for use in radioimmunoassay, fluorochromes that emit visible fluorescence for use in immunohistochemistry, nanoparticles that give electron dense labels for microscopy techniques, or enzymes that give a colored product for enzymatic immunoassays (EIA). Table 1.1 summarizes some of the commonly used labels in immunochemical methods.[72]

Table 1.1 Common labels used for the detection of the antibody-antigen reaction in immunochemical techniques.

Label	Examples	Main use
Fluorochromes	Fluorescein	Immunohisto/ cytochemistry; flow cytometry; fluorimetric assays
	Rhodamine	Immunohisto/ cytochemistry; flow cytometry
	Phycoerythrin, Texas Red, 7-Amino-4-methylcoumarin 3-acetate (AMCA), BODIPY derivatives, Cascade Blue	Flow cytometry
Radioisotope	^{125}I	Competitive and non-competitive RIA
Enzymes	Alkaline phosphatase (AP)	Immunohistochemistry; EIA; immunoblotting
	B-Galactosidase	As above
	Horseradish peroxidase (HRP)	As above; immunoelectron microscopy
	Glucose oxidase	Immunohistochemistry
	Urease	EIA
Electron dense	Gold nanoparticles	Immunoelectron microscopy
	Ferritin	As above

A variation of enzyme labeling involves coupling of a reactive molecule such as biotin to the antibody or antigen. The signal is then indirect detected when an enzyme-conjugated (strept)avidin is added to the system as secondary label. The potential for more than one labeled (strept)avidin to become attached to each antibody through multiple biotinylation sites tends to multiply the signal and hence, provides an increase in the assay sensitivity over biomolecules directly labeled with a detectable tag. This fact provides the amplification needed for the detection of analytes at low concentrations. [73]

In the next sections (§§ 1.3.2.1 and 1.3.2.2) the enzymatic labeling and biotin tagging are explained in more detail since these are two kinds of labeling used in this work.

1.3.2.1 Enzymatic labeling

Enzymes offer the advantages of long shelf life, high sensitivity, and the possibility of direct visualization. They offer several advantages over fluorescently labeled and radiolabeled substances, such as their stability. The most often used enzymes are alkaline phosphatase (AP) or horseradish peroxidase (HRP), but other enzymes like glucose oxidase and β-galactosidase are also applied, and depending on the detection strategy the enzyme can be coupled to the antigen or antibody. A comparison of the properties of AP and HRP is shown in Table 1.2.[74]

Table 1.2 Comparison of horseradish peroxidase and alkaline phosphatase physical properties.

	Horseradish Peroxidase	Alkaline Phosphatase
Size	40 kDa	140 kDa
Price	Relatively inexpensive	Relatively expensive
Stability (storage)	Stable at < 0ºC	Unstable at < 0ºC
Number of substrates	Many	Few
Kinetics	Rapid	Slower
pH optimum	5-7	8-10

The most used conjugation techniques are: i) maleimide activation of the enzyme for reaction with free sulfhydryl groups on the protein previously generated by disulfide bonds reduction, ii) periodate activation in which polysaccharide residues in a glycoprotein are oxidized to aldehyde groups for the subsequent conjugation with amine- or hydrazine-containing molecules, and iii) glutaraldehyde cross-linking based on the reaction of the aldehyde moeties formed on both ends of glutaraldehyde under reducing conditions that couple with amines of the proteins, and 4) carboxylic groups activation by reacting with a carbodiimide and *N*-hydroxy succinimide (NHS). In all cases a high antigen binding activity or epitope availability should be retained after the conjugation of the antibody or antigen, respectively. [54,75]

On the other hand, the applied enzymes should contain surface functional groups that can be used to form conjugates without affecting its catalytic activity or compromising the biorecognition event. Moreover, the enzymes should be stable in the sample matrix and show a high catalytic constant, and it is also desirable that they are readily available in a purified and soluble form at a reasonable cost.[76] Finally, it is recommendable to remove the excess of non-conjugated enzyme in order to lower as much as possible the background signals improving thus the signal to noise ratios.

1.3.2.2 Biotin tagging for indirect enzymatic labeling

The biotin-(strept)avidin binding has become a wide used technique in many biological applications allowing the tagging, identification and immobilization of different biomolecules.[77–79] The protein streptavidin is isolated from *Streptomyces avidinii*, while avidin is a glycosylated positively charged protein obtained from egg white. Although their low sequence homology (around 35 %), both have the same tertiary and quaternary structure and are able to bind until four biotin molecules approximately with the same affinity. The extraordinary affinity of avidin for biotin is one of the strongest known non-covalent interactions of a protein and ligand ($Ka=10^{15}\,M^{-1}$) and allows biotin-containing molecules in a complex mixture to be discretely bound with avidin conjugates. The bond formation is very rapid, and once formed, it is unaffected by extremes in pH, temperature, organic solvents and other denaturing agents, which is very interesting for the application in bioanalytical techniques.[80,81]

Besides the strong affinity for avidin, biotin exhibits two characteristics that make the molecule ideal for labeling proteins and macromolecules. First, biotin is comparatively smaller than globular proteins, which minimizes any significant interference in many proteins and allows multiple biotin molecules to be conjugated to a single protein for maximum detection by avidin. Second, as shown in Figure 1.4, biotin has a valeric acid side chain that is easily derivatized and conjugated to reactive moieties and chemical structures without affecting its avidin-binding function. This feature allows many useful biotinylation reagents to be created.

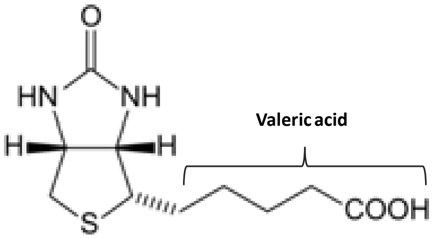

Figure 1.4 Biotin structure showing the bicyclic biotin ring on which the avidin-binding occurs and the valeric acid side chain with its carboxylic reactive group suitable for further chemical reactions.

Common to all the biotinylation reagents is the presence of the bicyclic biotin ring at one end of the structure and a reactive group at the other end that can be used to couple with other molecules. Depending on the reactive group present on the biotinylation reagent, specific functional groups may be modified to create an affinity tag capable of binding avidin (or streptavidin) derivatives. Amine, carboxylate, sulfhydryl, and carbohydrate groups can be specifically targeted for biotinylation through the appropriate choice of the reactive biotin compound. Careful choice of the correct biotinylation reagent can result in directed modification away from active centers or binding sites, and thus preserve the activity of the modified molecule. The distance between the reactive moiety and the biotin molecule can also be adjusted using spacer arms of different lengths to increase the availability of biotin for avidin binding, increase the solubility of the reagent or to make the biotinylation reversible. The more recent biotin compounds use PEG spacers, which offer significant advantages over the more traditional aliphatic compounds because the pronounced water solubility of the PEG cross-linker can prevent aggregation of biotinylated molecules. Biotinylated antibodies are particularly susceptible to aggregation and loss of antigen binding ability if they are modified using hydrophobic biotin compounds. The PEG-based biotin reagents show better solubility and longer stability than their corresponding aliphatic biotinylation compounds of equivalent size.[75]

In addition to the signal amplification provided by the use of the biotin-(strept)avidin detection system (Figure 1.5, A), the signal intensity can be further amplified using the avidin-biotin complex method in which the multiple binding sites of avidin are used to increase the number of enzyme molecules at the target biotinylated antibodies. In this approaches, biotinylated peroxidase is pre-incubated with avidin, forming large complexes between the tetravalent avidin and the enzyme conjugated with multiple biotin molecules as shown in Figure 1.5, B. These large lattice-like complexes with biotin-binding capability can be attracted to the sites of biotin-labeled antibody already bound to the target antigen, producing thus an increase in signal intensity and sensitivity.[82,83]

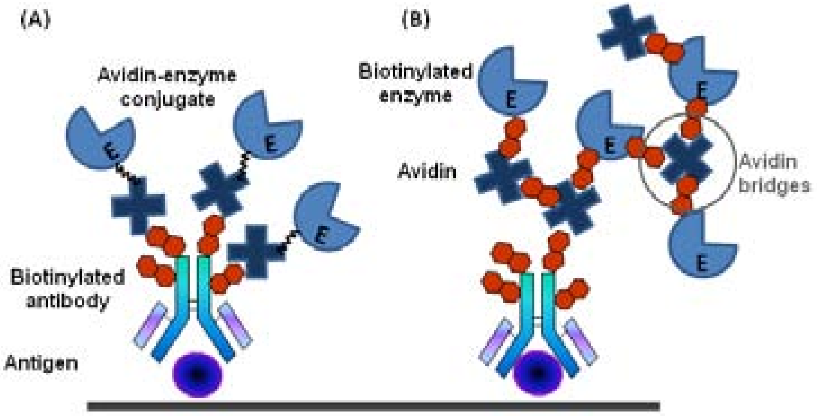

Figure 1.5 Schematic representation of different biotin-streptavidin based approaches, showing in (A) the basic indirect detection system and in (B) the signal amplification obtained after adding the multivalent avidin and biotinylated enzyme, forming huge amplification complexes.

1.3.3 Immunological techniques

The first classical immunological methods were based on the formation of antigen-antibody complexes in solution using unlabeled reagents and the subsequent detection was based on precipitation or agglutination which could be visually detected or through absorbance or light scattering measurements. Some examples of these methods are the precipitin test (based on immunodiffusion or counter-immunoelectrophoresis), complement fixation, hemagglutination, particle agglutination, immunoturbidimetric and light-scattering assays. In all cases, the agglutination was normally amplified by attaching the antigens or antibodies to different kinds of particles (such as polystyrene beads, erythrocytes or latex beads) and depending on the goal, conglomerates formation or inhibition could be detected.[84,85] However, all these techniques were not sensitive enough, could lead to wrong results due to the presence of interfering species and were mostly just applicable for the analysis of high molecular weight molecules. As a result, they were later replaced by faster and more sensitive immunoassays.

The development of radioimmunoassay (RIA), developed in the 1960s by Yalow and Berson (who received the Nobel Prize in medicine in 1977), provided many improvements to the immunochemical methods. In this technique either the antigen or the antibody molecules were labeled with gamma-radioactive isotopes, allowing the monitoring of the antigen-antibody complex formation. Moreover, in some cases even a secondary radiolabeled antibody (against the primary antibody) can be used. As a result, the technique is simple, very sensitive and highly specific, and can be used for the analysis of both antigens and haptens. However, it has the drawbacks of the high cost of reagents and equipments, the high risks associated to the use of radioisotopes, which require a license and trained personnel for their manipulation, the low stability of the labeled reagents and the management of radioactive residuals disposal. All these facts limited its widespread use and led to the replacement of this method by other kind of immunoassays, using non-radioactive labeled markers coupled to colorimetric, luminescence or fluorescence-based detection. Some examples of these techniques were: immunofluorescence assays, fluorescence polarization assays, time- resolved fluorescence immunoassays, chemiluminescence immunoassays and the most widely used enzymatic immunoassays (EIA), which will be more deeply analyzed in the next section.[54,65,71]

1.3.3.1 Immunoassays based on enzymatic labeling

In EIA, enzyme molecules are used as a marker for the detection of the immunocomplex formation. The catalytic features of the enzymes provide an amplification of the signal resulting from the complex formation, improving the sensibility when compared to the RIA technique and eliminating the limitations related to the use of radioisotopes. Furthermore, enzymes offer the advantages of long shelf life, high sensitivity and the possibility of direct visualization or spectrophotometric detection without the need for expensive and sophisticated equipment. When the appropriate substrate is added, the enzyme catalyzes the production of a colored or fluorescent end-product, which can be visualized and quantified. On the other hand, some disadvantages include multiple assay steps, the possibility of interference from endogenous enzymes and some hazardous substrates.

Depending on whether or not the immunocomplex is separated from the free immunoreagents, the EIA can be classified in homogeneous or heterogeneous. In the first type the enzymatic activity is modulated by the formation of the immunocomplex and no washing steps are needed for the separation. An example of this technique is the Enzyme Multiplied Immunoassay (EMIT), applied in some cases for drug or hormones detection in clinical diagnosis. On the other hand, the heterogeneous systems involve the immobilization (covalent or non-covalent) of either antigen or antibody to a solid support and the separation of the excess non-reacted immunoreagents by washing steps. The term Enzyme-Linked Immunosorbent Assay (ELISA) is used for this type of assays and they can be performed using different solid supports, such as microtiter plates, cellulose, nylon membranes/tubes, nitrocellulose membranes, or different kinds of particles, as for example magnetic particles.[54,58]

The most widely applied supports for immunoassays are the 96-well microtiter plates. Technical advances led to automated pipetting devices, multichannel pipettes, and microtiter plate readers and washers, and in the 1980s fully automated test instruments were manufactured by Boehringer-Mannheim and Abbott, among others. Such automated systems have come to stay in laboratories allowing the simultaneous detection of a great number of samples in a short time and at reasonably low cost.[86]

1.3.3.2 Enzyme linked immunosorbent assay (ELISA)

ELISA can be performed in two different formats, depending on the location of antigen or the antibody on the solid surface and on which immunoreagent is labeled:

Sandwich or non-competitive ELISA. In this case, the antigen-specific capture antibodies are immobilized on the solid support, so that if the target is present in the sample, it will bind to the antibodies. Unbound sample is removed by washing, and a second antibody specific for the antigen is added, which is conjugated to an enzyme, to give the color reaction after the addition of substrate. The amount of color is thus directly proportional to the amount of antigen present in the original sample. A requirement for a successful sandwich assay is the multivalence of the antigen, which should be large enough to contain different epitopes for at least 2 antibodies. In cases where the analyte is a small molecule, like some toxins or pesticides, a competitive immunoassay can be used.

Competitive ELISA. In a competitive ELISA format, a structural mimic of the antigen is coated on the solid support, which is usually an antigen conjugated to a protein through a specific conjugation technique. The sample together with the antigen-specific antibody is then incubated in the wells, at which stage, the antigen in the sample is competing with the immobilized antigen for the limited amount of antibody in solution. Another variation of the direct format can also be performed if the specific antibody is immobilized and a labeled antigen competes with the antigen in the sample. However, the first strategy has the advantage that lesser antibody amount is needed and previous labeling of the antigen or hapten-carrier complex is not required. In all cases, after substrate addition a color is formed, which intensity is inversely proportional to the amount of antigen in the solution. The more antigens in the sample, the less labeled immunoreagent will be bound to the surface and the lighter the color. In the competitive immunoassays the antigen can be either an hapten with just one epitope or a macromolecule (divalent or multivalent).[54,71]

Both immunoassay formats can be either direct as previously explained or indirect, depending on which antibody is conjugated to the enzyme label.

Direct and Indirect formats. In the indirect immunoassays, the specific antibody towards the target antigen is unlabeled, and hence, a secondary antibody against the first one conjugated to the enzyme and called secondary antibody, is added. The sensitivity of the indirect format is often better than the direct immunoassay, due to the fact that more than one labeled secondary antibody can bind to each primary specific antibody amplifying thus the signal. Moreover, it also provides versatility due to the fact that the same labeled antibody can be used for different targets in different detection kits, without the need to label every specific antibody. However, the indirect detection presents the drawback that an additional incubation step is needed, requiring thus longer assay times. The different immunoassay types are detailed outlined in Figure 1.6.

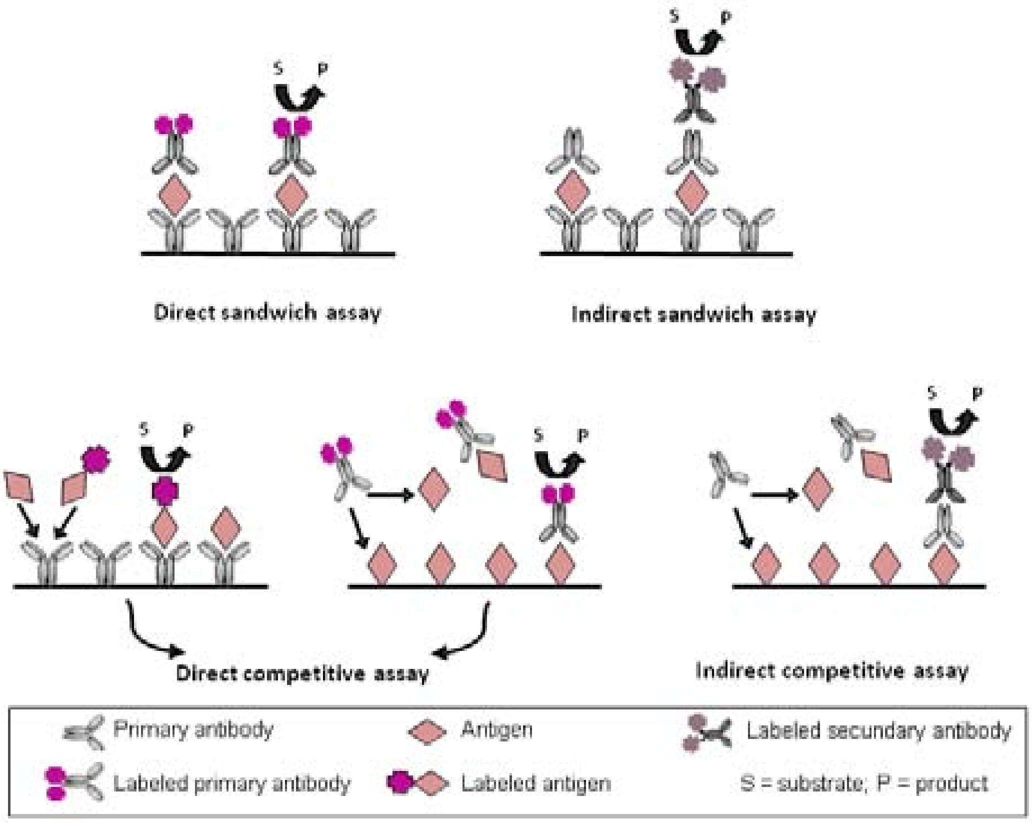
S
P
Direct sandwich assay
Indirect sandwich assay
Direct competitive assay
Indirect competitive assay
Primary antibody
Antigen
Labeled secundary antibody
Labeled primary antibody
Labeled antigen
S = substrate; P = product

Figure 1.6 Schematic representation of the different immunoassay formats (sandwich and competitive, direct and indirect).

Beside the immunoassay format, another important issue to consider is the nonspecific binding, which involves the adsorption of conjugated enzyme or other labels used in an immunoassay to materials other than the analyte.[76] This phenomenon, which increases the background signal, is one of the major limiting factors for obtaining good detection limits and therefore including procedures that minimize nonspecific binding in the immunoassay is critical. With plastic surfaces, such as polystyrene used to make microtiter wells and particles, hydrophobic interactions usually dominate the adsorption processes.[87] The adsorption is entropically driven and can usually be minimized by physically coating the exposed areas of the reaction vessel through surface treatments such as a mixture of a protein blocker as bovine serum albumin and a nonionic detergent like Tween 20.[88] These kind of detergents and proteins can also be added to the buffers to block further nonspecific adsorption with particle-based immunoassays.[89] Other commonly used blockers are polyethylene glycol, gelatin and casein,[90,91] and proprietary blended commercial products. Moreover, sulfonate ion-pairing reagents have been found to reduce the nonspecific adsorption on positively charged surfaces.[87]

A number of quick screening test based on the ELISA principle have been developed against different targets in food and clinical diagnostic. For example, some microplate ELISAs can be performed in around 20 min with good sensitivity. Other approaches involve the antibody immobilization on a paper disc or other membrane mounted either in a plastic card, plastic cup or on the top of a plastic tube. In the lateral flow immunoassay or dipstick test, a capture antibody is immobilized onto a surface of porous membrane (nitrocellulose, nylon, Teflon) in a predefined position and a sample passes along the membrane. The detector reagent, typically coupled to a latex or colloidal metal particle, is deposited into a conjugate pad. When a sample is added to the conjugate pad, the detector reagent is solubilized and begins to move with the sample flow front up the membrane strip. As the sample passes over the zone to which the capture reagent has been immobilized, the analyte detector reagent complex is trapped, and a color develops in proportion to the analyte present in the sample. Substrates leading to the formation of water-insoluble chromogenic products are used in these assays. As a result, most of these screening tests are easy to perform and take just 10 to 15 min, providing in general semi-quantitative information about certain cut-off concentrations for the target substance. Many assay kits are currently commercially available, although being in general less sensitive than the ELISA based assays.[71,92]

1.4 BIOSENSING METHODS

The term biosensor appeared in the scientific literature at the end of the 1970s, although the concept and even the commercialization started before. Leland Charles Clark Jr. is considered as the pioneer of the biosensor research. In 1956 he published his first paper on the electrode to measure oxygen concentration in blood.[93] Some years later, Clark and Lyons developed the first biosensor for glucose analysis consisting of glucose oxidase enzymes entrapped at a Clark oxygen electrode using a dialysis membrane, in which the decrease in the measured oxygen concentration was proportional to the glucose concentration.[94] Clark's ideas turned out to be commercial reality in 1975 with the fruitful re-launch (first launch 1973) of the Yellow Springs Instrument Company's glucose analyzer based on the amperometric detection of hydrogen peroxide. Finally the term biosensor started to be used in 1977, after the development of the first device using living microorganisms immobilized on the surface of an ammonium sensitive electrode. From then on, the design and development of biosensors has continued growing for analytical applications in different fields.[95] As an example, in 1984 Turner and his colleagues published a paper on the use of ferrocene and its derivatives as immobilized mediators for use with oxidoreductases in the fabrication of low-cost enzyme electrodes. This formed the basis for the screen-printed enzyme electrodes launched by MediSense, Cambridge, USA in 1987 with a pen-sized meter for home blood-glucose monitoring. The electronics were redesigned into popular credit-card and computer mouse style formats and MediSense's sales showed exponential growth reaching US $175 million by 1996.[96]

According to the IUPAC (International Union of Pure and Applied Chemistry), a biosensor can be defined as a self-contained integrated device which is capable of providing specific quantitative or semi-quantitative analytical information using a biological recognition element (biochemical or biomimetic receptor) which is either integrated within or in intimate contact with a physicochemical transducer.[97,98]

In other words, biosensors are small analytical devices that detect low concentrations of the target compound through a biological reaction, converting the biorecognition event into quantifiable signals. They usually generate a continuous electric signal, which is proportional to the amount of the specific analyte or group of analytes reacting at the transducer surface. The scheme of a biosensor is shown in Figure 1.7. Different biorecognition elements can be used (enzymes, nucleic acids, antibodies or antigens, cell receptors, tissues, whole cells, etc), which can be integrated within, coupled to or immobilized on the surface of the transducer, and the detection principle is based on their specific interaction with the target analyte, which provides the selectivity to the device.[99–101]

The procedure used for the immobilization of the biorecognition element on the transducer surface is a crucial step in the biosensor development, since it should not affect the activity of the biological material allowing the correct analyte recognition, while simultaneously not disturbing the sensitivity of the transducer element. The most applied immobilization techniques are: i) physical adsorption (in which binding forces are mainly due to hydrogen bonds, ionic interactions and Van der Waals forces), ii) microencapsulation behind different kinds of membranes, iii) entrapment in polymeric gels, iv) cross-linking using bifunctional or multifunctional reagents (such as glutaraldeyhde), and v) covalent binding through functional groups which are not essential for the biological activity.[101–103] Another type of immobilization (only compatible with electrochemical transducers), which does not need a separate modification step since the biological element becomes already integrated on the transducer material is: vi) bulk modification of the electrode material with the biomolecules by the formation of a biocomposite e.g. in carbon paste or graphite epoxy resin.[104,105]

As a result of the biological interaction between the biorecognition element and the analyte a primary signal is produced, which consist in the variation of one or more physical or chemical properties (pH, electron transfer, temperature, potential, mass, optical properties, between others). This primary signal is detected by the transducer and transformed in a secondary electronic output, as previously explained, which can be easily processed as outlined in Figure 1.7.[106,107]

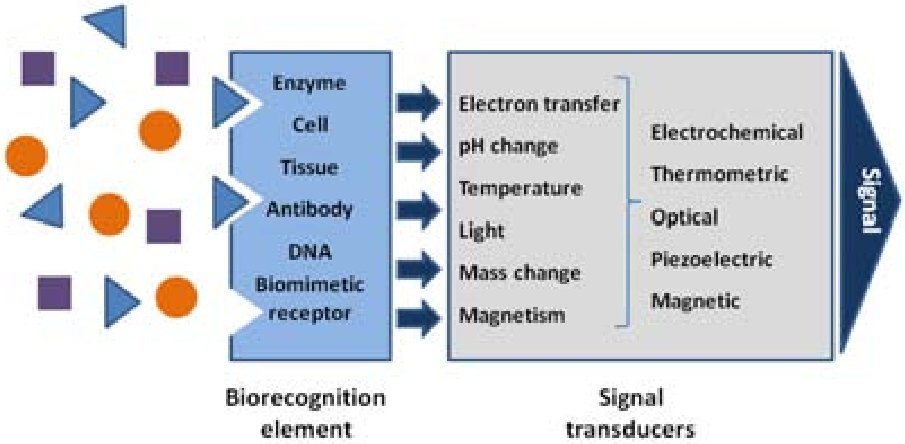
Enzyme
Cell
Tissue
Antibody
DNA
Biomimetic receptor
Electron transfer
pH change
Temperature
Light
Mass change
Magnetism
Electrochemical
Thermometric
Optical
Piezoelectric
Magnetic
Signal
Biorecognition element
Signal transducers

Figure 1.7 Schematic representation of the working principle of a biosensor showing the specific recognition of the analyte, the transducer that detects the physicochemical change and the obtained signal (related to the amount of analyte in the sample).

Biosensors allow the detection of a broad spectrum of analytes in complex sample matrices and have been used in a wide variety of areas such as medicine, food analysis, environment, process industries, security, defense and diagnostics. The emerging field of biosensors seeks to exploit biology in conjugation with other disciplines like analytical chemistry (since they are in fact, chemical sensor), electronics and software technology.[101,107]

The more outstanding features of these devices, which make them very promising analytical tools and good alternatives for the implementation in food control systems (such as HACCP) are listed below:

- *High sensitivity*, achieving in some applications detection limits as low as μg L^{-1} (ppb). The sensitivity of each sensor system may vary depending on the transducer properties and the biological recognizing element.
- *High selectivity*, to be able to distinguish a target analyte from others with similar properties. This aspect is achieved through the use of highly specific recognition elements.
- *Reliability*, since the transduction systems are designed to reduce to the minimum the possible interferences by the sample and the noise problems.
- *Low cost*, due to the fairly inexpensive associated materials and instrumentation.
- *Short analysis time*, allowing a rapid response accordingly with the sensing result.
- *Minimal sample pretreatment* requirements and multi-analysis capability, which provides the saving of time and materials.
- *Easy handling*, not requiring high trained personnel.
- *Portability*, to permit the on-site analysis.
- *Compatibility with automatization and miniaturization* technologies, by applying nanotechnology and microelectronic advances. The first aspect facilitates the integration in the monitoring of industrial processes, while the second aspect allows their application in assays in which the physical size, the sample volume or the point of measurement are limiting factors.
- *Versatility*, which allows the design of devices *à la carte*.

The combination of several of these advantages places biosensors in a preferential position when compared to conventional analytical methods, such as chromatography, spectrometry, etc.[95,107,108]

An ideal biosensing device for the rapid detection of food contaminants or allergens should be thus sensitive, selective, robust, fully automated, inexpensive, and routinely used both in the field and the laboratory. Other desirable properties in some applications would be a high stability, operating life and reduced storage requirements, in order to avoid the need of frequent replacements principally when integrated in an industry production line. These aspects are conditioned by the chemical, physical and mechanical stability of the biological component, but the inconvenient can be minimized or even avoided by the search for highly stable biomaterials, the use of immobilization protocols improving the stability or the application of new technologies based on biomimetic materials. Ideally, the sensing surface should be also renewable in order for several consecutive measurements to be made.

Finally, in many applications, the sensor should be capable of continuously monitoring the analyte on-line. However, disposable, single-use biosensors are satisfactory for some important applications, such as personal blood glucose monitoring by diabetic patients.

1.4.1 Biosensor classification

Biosensors may be classified according to the biological specificity-conferring mechanism, the methodology applied to set the biological interaction (direct or indirect), and the mode of signal transduction.[98]

Based on the nature of the biological recognition process they can be divided into two main categories:

- *Biocatalytic devices*, which incorporate enzymes, whole cells or tissue slices that recognize the target analyte and produce electroactive species. A continuous consumption of substrate is achieved by the immobilized biocatalyst incorporated into the transducer and transient or steady-state responses are monitored by the integrated detector.
- *Affinity biosensors* that rely on the selective and strong binding of the immobilized biological element with the target analyte. In this case equilibrium is reached and there is no net consumption of the analyte by the immobilized biorecognition element. Thus the detection is based in the monitoring by the integrated detector of the equilibrium response and the subsequent analyte-receptor complex formation. Some commonly used biorecognition elements are: antibodies (Ab), membrane receptors, cells, tissues and nucleic acids, being the most applied examples of affinity biosensors the immunosensors (based on the antigen-antibody interaction) and genosensors (based on the recognition of complementary DNA strands). More recently other types of bioreceptors were also used, such as ionic channels, lectines, aptamers, peptidic nucleic acids (PNAs) and molecular imprinted polymers (MIPs).[95,100,108–112]

The biocatalytic biosensors were the most frequently applied to complex matrices since the pioneering work of Clark & Lyons. Biosensors using enzymes as the recognition element often have relatively simple designs and do not require expensive instrumentation, beside the wide commercial availability of the enzymes. Moreover, such sensors are typically easy to use, compact, and inexpensive devices.[113,114] Regarding the bioaffinity sensors, it should be pointed out that the affinity reaction can sometimes be monitored directly, but other times a labeled secondary ligand (which binds to the analyte) or a labeled compound that competes with the analyte for the immobilized receptor is needed. In most of these cases enzymatic labels are used and the detection is based on an indirect biocatalytic reaction in which the steady-state or transient signals are then monitored by the integrated detector.[108]

On the other hand, depending on the transduction technique, biosensors can be classified into the following groups: electrochemical, optical, thermometric, piezoelectric and magnetic.[114,115] Optical transducers are especially attractive as they can allow direct (label-free) and real-time detection, showing in particular the phenomenon of Surface Plasmon Resonance (SPR) good biosensing potential. However, in some applications they lack sensitivity, as for example in the case of food pathogens detection, in which long pre-enrichment steps are needed to reach the required limits of detection.[92] In contrast, electrochemical biosensors offer comparable instrumental sensitivity, being furthermore more robust, easier to use, portable and cheaper, in addition to their capability to operate even in turbid media. As a result, the field of electrochemical biosensors has grown rapidly in the past years, becoming one of the currently most studied areas in analytical chemistry. In principle, any biocatalytic reaction in which a net electron transfer takes place can be analyzed using this type of sensor.[99,110,111,116] Research in this field has focused on novel sensing strategies and was supported by a large number of publications about the enhancement of specificity, sensitivity, and response time.[117]

Given that in the present work electrochemical biosensors were applied for the analysis of the studied targets related with food safety, the next section will be focused on this kind of biosensors.

1.4.2 Electrochemical biosensors

Electrochemical biosensors can be classified in different types according to the electrochemical property measured [98,112,118].

- *Amperometric*, in which the reaction being monitored generates a measurable current resulting from the oxidation or reduction of an electroactive species when a fixed potential is applied.

- *Potentiometric*, based on the measurement of an electric potential or charge accumulation in the electrode interface when there is no significant current flowing in the system.
- *Conductimetric*, in which the reaction of the biological receptor with the analyte generates a measurable change in the conductive properties of the medium between electrodes.
- *Impedimetric*, based on monitoring both resistance and reactance in the biosensor by measuring the electric current at different frequencies when applying a potential in an alternating current circuit.

From these four groups, the first two are the most widely applied. Among the potentiometric sensors the ion selective electrodes (ISEs) have been widely used[119], being within this group the classic pH electrodes, which have been used for over hundred years. In the simplest applications, the exchange reactions occur directly on the electrode surface, by the restoration of redox balance between the target ion, and the electrolyte. Another example of more complex potentiometric sensors are the ion-selective field effect transistors (ISFETs) that can also be used in electrochemical biosensors.[120]

On the other hand, amperometric biosensors have been the most widely developed and represent around the 75 % of the currently commercialized biosensors, with the well-known glucose sensor, which is daily used by millions of people around the world, as the main example, demonstrating the great utility of this technology. The popularity of the amperometric transducers can be attributed to their simplicity, ease of fabrication and use, low cost of the biosensor strips as well as the associated instrumentation and the low limits of detection that can be achieved [121].

The choice of the electrode to be used for an electrochemical biosensor is crucial for several aspects including the sensitivity of the method, the cost of the assay and the possibility to adopt different immobilization procedures. The working electrode should provide a reproducible response, as well as high signal-to-noise ratio. This depends primarily on two factors: the redox behavior of the electroactive species and the background current over the potential region required for the measurement. Other considerations include the potential window, electrical conductivity, mechanical properties, and toxicity. The geometry of the electrodes must also be considered, being the more regularly used: planar disk configuration, thin-layer and thick film technology, including the screen-printed electrodes, which are very promising due to their low-cost fabrication, mass-production compatibility and reduced reagent consumption (allowing the performance of all immunological steps in just a drop). Finally, another important factor is the dependence of the response on the surface state of the electrode, requiring often precise electrode pre-treatment and polishing to obtain reproducible results, which depends on the materials involved.[122–124]

1.4.2.1 Electrochemical immunosensor design

The aforementioned advantageous features turned electrochemical biosensors into one of the most promising alternatives to the optical approaches used in immunoassays, and therefore it is not surprising that during the past decade many research groups made big efforts in adapting optical ELISA approaches to electrochemical platforms for the development of immunosensors. These novel devices couple all the benefits provided by the immunochemical methods (already detailed in Section 1.3) with the advantages of electrochemical detection, solving thus some drawbacks suffered by the ELISAs associated with the type of measurement. Some of these negative aspects include a requirement for generally bulky and power-intensive light sources, detectors, and monochromators, potential false signals arising from complex colored samples, and in addition, the fact of following the Lambert–Beer law makes that a minimum sample volume and path length is required to achieve certain performances.[125]

As a result, electrochemical immunosensors combine the high selectivity conferred by the use of an immunoreagent as biorecognition element (antigen or antibody) with the sensitivity of the electrochemical transducer, which transforms the immunological recognition event in an electrical amplified signal as outlined in Figure 1.8.

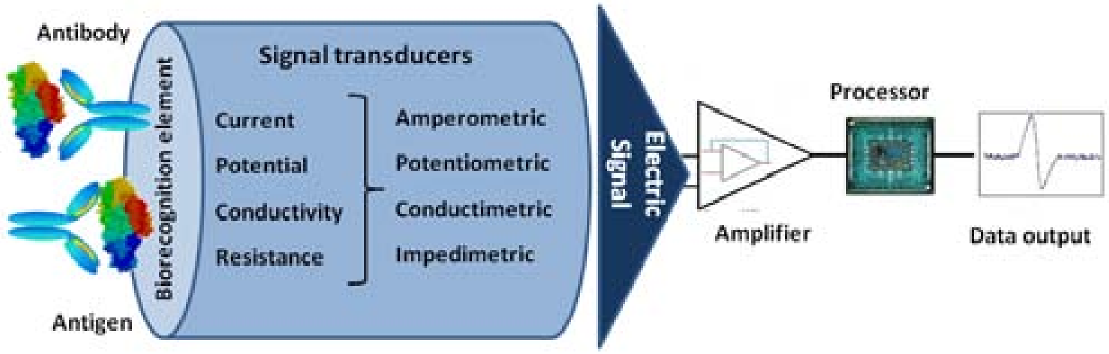
Antibody
Antigen
Biorecognition element
Signal transducers
Current
Potential
Conductivity
Resistance
Amperometric
Potentiometric
Conductimetric
Impedimetric
Electric Signal
Amplifier
Processor
Data output

Figure 1.8 Schematic representation of an electrochemical immunosensor, showing the antibody or antigen as biorecognition element, the four possible transduction types and the processing of the electric signal.

Electrochemical immunosensors are frequently based on the labeling of the immunoreagents with biocatalytic tags, generally enzymatic, just as in the ELISA technique.[126] It should be also pointed out that the possibility of using either antibodies or antigens as biorecognition element, gives a high flexibility and versatility to the immunosensors design[127,128]. One key point in their development is the recognition layer immobilization, for instance the antigen or antibody, depending on the chosen immunoassay format. Some groups have adopted a simple and straightforward adsorption procedure very similar to that adopted for optical ELISA. However, physical immobilization often results in random orientation and weak attachment. A crucial problem is how to maintain the protein conformation maximizing simultaneously the biological recognition capability, by orienting the Fab regions to the sample solution when immobilizing antibodies, or exposing the epitopes for their further antibody recognition in the case of attaching the antigens. Covalent immobilization presents great advantages in the fabrication of electrochemical immunosensors trying to direct the attachment points to side chain-exposed functional groups of the proteins which does not significantly affect their recognition sites. With the aim of achieving a better presentation of the recognition element to the target analyte, the use of ordered layers on the surface of the electrode were introduced, as for example by the formation of self assembled monolayers (SAMs) through thiol-gold chemistry. Alternative methods for the formation of SAMs are based on the use of diazonium salts which can be easily applied to graphite and carbon electrodes. Another approach that has been recently proposed for the immobilization of recognition elements on the electrode surface involves the use of different polymeric matrices such as polysulfone polymer and chitosan. In the case of antibodies orientation some other strategies that can be specifically applied for immobilizing the biomolecules through the Fc region are based on different bioaffinity interactions, with lectin sugar, protein A, G or L.[118,123,129,130]

Finally, the electrode surface to be used as support for the immobilization of the recognition element, the selection of the most appropriate electrochemical technique and the choice of the enzymatic label and substrate (which must lead to an electroactive product) are other important factors to be considered when adapting an optical ELISA to an electrochemical platform.[123]

In the following two sections, the amperometric detection technique as well as the most used transducing materials is explained in more detail, focusing particularly on the conditions applied during this dissertation.

1.4.2.2 Amperometric detection

Among the voltammetric methods applied with analytical purposes, amperometric techniques are the most widely used in the sensors field, for monitoring biorecognition reactions.

Amperometric biosensors are based on the measurement of the electric current resulting from the electrochemical oxidation or reduction of an electroactive species on the electrode surface when a constant potential is being applied[131,132]. The electrochemical cells commonly used in controlled-potential experiments, and as such in amperometric measurements, consist of a three-electrode set-up immersed in the sample solution containing a supporting electrolyte: the working, reference and auxiliary electrodes. While the working electrode is the electrode at which the electrochemical reaction of interest occurs, the reference electrode provides a stable and reproducible potential (independent of the sample composition), against which the potential of the working electrode is compared. The most commonly used reference electrode is Ag/AgCl. An inert conducting material, such as platinum wire or graphite rod, is generally used as the current-carrying auxiliary electrode or counter-electrode, which closes the electric circuit. As a result, the potential is measured in a circuit containing the working and reference electrode in which the current flow is almost zero (due to the high electric resistance of the potentiostat), while the current changes are registered in another circuit including the working and auxiliary electrode. The electrode material, its surface modification or its dimensions affects the detection ability of the electrochemical biosensor and, thus, its performance. Therefore the exact cell design and the material used for its construction are selected according to the experiment at hand and the nature of the sample.[110,124,132,133] Nevertheless, electrodes can be easily miniaturized at a relatively low cost and very small sample volumes (on the order of microliters or even nanoliters) are required, since in fact the sensitivity of electrochemical methods is not affected by the volume used during the measurement.[118,125] Examples of amperometric equipments are shown in Figure 1.9.

The measured current is proportional to the concentration of the electroactive species in the sample, being the intensity directly related to the speed of the electron transfer reaction (reduction or oxidation) occurring at the electrode-solution interface, which can be described by Faraday’s law:

$$I = nF\,(\partial C / \partial t)$$

where I is the current intensity, n the number of transferred electrons per analyte molecule in the redox reaction, F the Faraday constant (96.5 C mol^{-1}) and $\partial C / \partial t$ the reaction rate in mol L^{-1}.

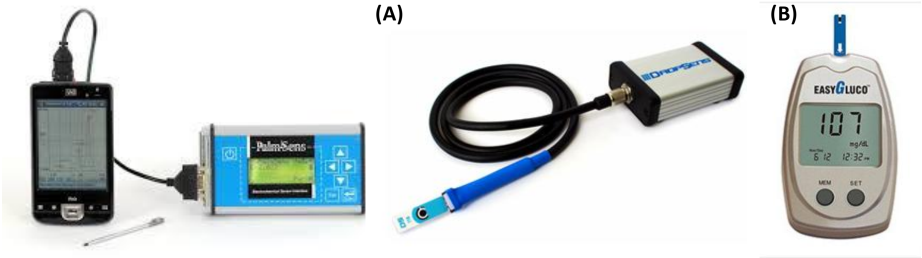

Figure 1.9 Examples of hand-held amperometric devices are shown in (A), while one of the commercially available amperometric glucose sensors is depicted in (B).

The reaction rate is not only affected by the reaction at the electrode itself, but also by the mass transport of the electroactive analyte from the bulk solution to the electrode surface, which depends on different factors such as: concentration, electrode surface, besides the conditions of migration, convection and diffusion. The effect of migration is eliminated by the addition of supporting electrolytes to the electrochemical cell, while convection phenomena are controlled through a constant agitation of the solution. Therefore a steady-state diffusion layer can be considered at the electrode surface, in which mass transport only depends on the diffusion, and the current intensity can thus be expressed as:

$$I = nFADC_s / L$$

where A is the electrode area, D the diffusion coefficient, C_s the electroactive analyte concentration in the solution, and L the thickness of the diffusion layer.[114,132,134]

On the other hand, the selection of the applied potential to carry out the amperometric measurements depends on the redox potential of the electroactive species in the specific conditions of the assay (working electrode used, reference electrode, pH, buffer, etc). In the case of electroactive analytes, the selected potential provides some electrochemical selectivity, by providing the reduction or oxidation of only certain chemical species. However, in the case of immunosensors generally both types of immunoreagents are electrochemically inert and the antigen-antibody complex formation does not provide any electrochemical reaction. Therefore, the use of a label is required that allows the monitoring of the affinity reaction. As previously mentioned, the more commonly used labels producing electroactive species are the enzymes.

While with optical ELISA the enzyme label should catalyze the production of a colored species; in the case of electrochemical immunosensors it is essential that the enzymatic product is electroactive so that it can be easily measured through the amperometric technique. When labeling the antibody or antigen with an enzyme, the substrate is added in excess in order to work in saturation conditions in which the measured current corresponds to the maximal current that can be provided by the enzyme, being thus proportional to its concentration. As a result, the amperometric signal is proportional to the amount of enzymatic conjugate on the electrode surface, related at the same time to the biorecognition event. The signal provided by the enzymatic reaction (after adding the specific substrate) depends on the direct electronic transfer on the electrode surface or through the reaction with a mediator. The product that is formed by the enzyme catalysis should have a low redox potential to minimize interference from other components in the sample, while the substrate should be electro-inactive at the measuring potential to keep the background signal low.[76]

Because of the easiness in which enzymes can be found from commercial sources and their extended application with optical ELISA, horseradish peroxidase (HRP) and alkaline phosphatase (AP) are also the most widely used labels in immunosensors, being the first mentioned the one applied in the present work. HRP is able to react with a huge range of substrates giving a high versatility to the detection schemes. Peroxidases catalyze the reduction of hydrogen peroxide to water in the presence of a mediator, which is a substrate with reversible electrochemical properties that improves the electronic transfer between enzyme and electrode, as shown in Figure 1.10.

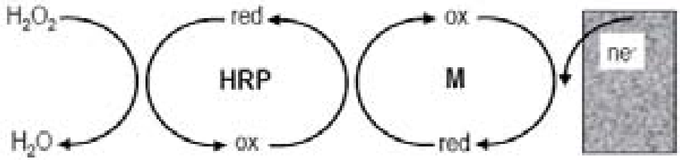

Figure 1.10 Reactions occurring at the surface of the electrochemical transducer when using peroxidase enzyme labeling with hydrogen peroxide as the substrate and with a mediator such as hydroquinone.

As outlined in Figure 1.10, the mediator is regenerated by applying a constant potential to the electrode surface. The mediators are normally compounds of low molecular weight able to transfer electrons from the enzyme active sites to the electrode, fulfilling some conditions: selectivity, stability of both reduced and oxidized form, rapid reaction with the enzyme and fast electron transfer. Furthermore they should also reduce the potential to be applied in order to minimize thus occasional interferences in the reaction.[135,136] In this perspective, good results have been obtained for example with TMB, catechol and hydroquinone (all of them coupled with H_2O_2), being the last one used in the present dissertation.[123,129]

1.4.2.3 Electrochemical transducing materials

There are many kinds of materials that can be used as transducers of the working electrodes, being the most commonly used materials: inert metals such as platinum or gold, and several forms of carbonaceous materials including carbon fiber, carbon paste, glassy carbon, pyrolitic graphite, or graphene. Metals have long been used for electrochemical electrodes due to their excellent electrical and mechanical properties, while carbon-based materials have a high chemical inertness and provide a wide range of anode working potentials with low electrical resistivity. Moreover, they also have a very pure crystal structure that provides low residual currents and a high signal-to-noise ratio. Other alternatives of transducers combine the aforementioned materials with conducting polymers such as polypyrrole and polyaniline, or with nanomaterials, like metallic nanoparticles or carbon nanotubes. More recently, a number of new combined materials have appeared for the preparation of electrodes, called composites.[92,137]

A composite material is formed by the combination of two or more dissimilar materials, in which each material retains its original properties, while giving the composite distinct chemical, mechanical and physical properties that differ from those exhibited by the individual components. Composites are prepared by the dispersion of a solid conducting material (such as platinum, gold or graphite) in a non-conducting polymeric matrix. The properties of the resulting composite depend on the nature of each component, their relative amounts and distribution. Rigid carbon composites can be obtained by mixing carbon powder with a non-conducting polymer giving a paste that can be hardened after curing the material.[138] In this work graphite-epoxy composites were used for the developed detection strategies, which are explained in more detail in Chapter 3. Magneto electrodes based in graphite-epoxy composites for the magnetic immobilization of biomolecules were constructed and evaluated for the integration of magnetic particles and nanoparticles in the bioanalytical procedure. The next section addresses the integration of micro and nanomaterials not only in biosensing devices, but also in bioassays.

1.5 INTEGRATION OF MICRO AND NANOMATERIALS IN BIOSENSORS AND BIOASSAYS

Advances in nanotechnology and nanoscience are having a significant impact on several areas such as the field of diagnostics, environmental monitoring, as well as food safety and security.

Nanodiagnostics involve the use of nanotechnology, where a number of nanoparticle-based assays have been introduced for biomolecular detection, to meet the demands for increased sensitivity and early detection in less time. The promise of increasing sensitivity and speed, and reduced cost and labor makes nanodiagnostics an appealing alternative to current molecular diagnostic techniques. On the other hand, nanobiotechnology is the intersection of nanotechnology and biology. New synthesis, fabrication and characterization methods for nanomaterials, which have dimensions that range from 1 to 100 nm, have evolved to a point that deliberate modulation of their size, shape and composition is possible, thereby allowing control of their properties. The nano versus the bulk size of the material offers larger surface-to-volume ratios and superior electronic and optical properties. Advances in the manipulation of nanomaterials permit the binding of different biomolecules such as proteins, nucleic acids, bacteria, and toxins through surface modification and engineering. One of the major advantages of using nanomaterials is due to their large surface area, allowing a greater number of biomolecules to be immobilized and this consequently increases the number of reaction sites available for interaction with a target species for ultra-sensitive detection. This property, coupled with excellent electronic and optical properties, facilitate the use of nanomaterials in label-free detection and in the development of biosensors with enhanced sensitivities and improved response times.[139–141]

In recent years, remarkable progress in electroanalysis at micro and nanoscales has been achieved, in which the nanoscaled materials can be tailored with tunable dimensions, high specific surface areas and specific chemical properties for high electroactivity to achieve improved sensitivity and specificity, while miniaturized electrodes or devices enable in situ electroanalysis of biological processes with high spatio-temporal resolution.[142]

Carbon nanotubes (CNT), nanofibers, nanowires, as well as nanoparticles, including gold and other metallic nanoparticles, silica nanoparticles, quantum dots, magnetic nanoparticles, liposomes, dendrimers and polymeric nanoparticles, are among the best studied nanosystems for biosensing and imaging, primarily due to the recent progress in their syntheses and structural characterizations. From all these nanomaterials carbon nanotubes, gold nanoparticles, quantum dots and magnetic nanoparticles are the most widely used in nanobiotechnology. A description of this four materials and a brief overview of their useful properties is shown in Table 1.3.[139,143,144]

Table 1.3 Brief description and features of the most widely applied nanomaterials used in nanobiotechnology: carbon nanotubes (CNT), quantum dots (QD), gold nanoparticles (AuNPs) and magnetic particles (MP).[139]

	Description	**Useful properties**
CNT 	Allotrope of carbon consisting of graphene sheets rolled up into cylinders. Multi-walled nanotubes (MWNTs) are essentially a number of concentric single-walled nanotubes (SWNTs).	Exhibit photoluminescence; excellent electrical properties; semi-conductors.
QD 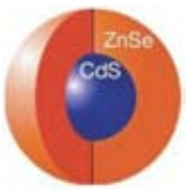	Colloidal semiconducting fluorescent NPs consisting of a semiconductor material core (normally cadmium mixed with selenium or tellurium), which has been coated with an additional semiconductor shell (usually zinc sulphide).	Photostability and tuneable emission spectra and are utilized in assays in a number of modes, including fluorescence emission, fluorescence quenching, or as energy donors.
AuNP 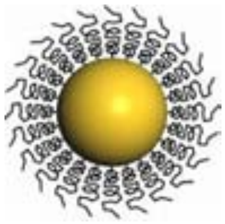	Made of gold, may take the form of spheres, cubes, hexagons, rods or nanoribbons.	Ability to resonantly scatter light; chemically highly stable; change color on aggregation from blue to red; excellent conductivity.
MP 	Made of compounds of magnetic elements such as iron, nickel and cobalt and can be manipulated using magnetic fields.	Used to concentrate particles in assays; excellent conductivity.

Since their discovery, carbon nanotubes (CNTs) have attracted great attention as nanoscale building blocks for micro- and nanodevices. In recent years techniques for the functionalization of CNT with proteins, nucleic acids and antibodies have improved considerably. This, coupled with exceptional electrical, physical, and optical properties, suggests that CNT have great potential for signal amplification and as transducers. However, they present challenges at the fabrication level (for instance, production of pure and uncontaminated nanotubes is costly, continuous growth of defect-free CNTs to macroscopic lengths is difficult to obtain and dispersion of CNTs onto a polymer matrix is very difficult). In addition, another important issue related to the use of CNTs is their toxicity.[139,141]

Colloidal gold nanoparticles (NPs) were the first NPs used in electron microscopy and in immunology. More recent developments involve metal nanoshells and semiconductor quantum dots (QDs). Also, functionalization of NP surfaces is necessary in order to stabilize them in solution or to provide functional groups for further uses. Inorganic NP labels appear to be the most versatile systems for bioanalytical applications (such as, immunoassays and DNA assays). However, other inorganic particles worthy of mention are lanthanide oxides, especially europium oxide (Eu_2O_3), which present long emission lifetime, have large Stokes shifts, narrow emission bands and inherent photostability. Unfortunately, natural or untreated Eu_2O_3 particles can lose their desirable optical properties during activation and conjugation and thus there are only few reports dealing with analytical applications.[144]

NPs can be used for labeling of antibodies or antigens, using direct detection through optical methods based on colorimetric response (AuNPs) or fluorescence emission (QD). Furthermore direct electrical methods can also be applied taking advantage of the excellent electroactivity of AuNPs and heavy metal based QDs (i.e. CdS, ZnS, PbS QDs). However, the most reported way to electrochemically detect AuNPs used in bioassays consists in an indirect electrical detection, involving a preliminary oxidative dissolution in acidic mediums, followed by the detection of the metal ions by a sensitive powerful electroanalytical technique such as anodic stripping voltammetry. Finally, another alternative to detect NPs used as labels consists in using their catalytic properties toward reactions of other species, such as the reduction of other metal ions or other electrochemical reactions.

On the other hand, the presence of nanoparticles on a transducer surface promotes the electron transfer, improving the electrochemical response coming from potentiometric and conductimetric responses. The introduction of NPs into the transducing platform is commonly achieved by their adsorption onto conventional electrode surfaces in various forms including that of a composite.[145]

Magnetic particles consist of an inorganic core of a magnetic element such as iron oxide coated with a stabilizing polymer containing functional groups for further conjugation strategies. They can be easily manipulated using magnetic fields and provide advantageous features such as the concentration of the target molecules in the assays, as well an excellent conductivity. This kind of particles can be used as solid support of immunoassays or as label when coupled to magnetoresistive measurements. While superparamagnetic micron sized beads have been available for some time, magnetic nanoparticles would be advantageous due to their small size and high surface to volume ratio, increased diffusion rates and high capture capacity.[139,146]

Finally, biological nanoparticles, including viruses, ferritins, heat shock proteins and enzyme complexes, can offer well-defined three-dimensional structures that are malleable for genetic and/or chemical modifications with near-atomic precision, which is very attractive for many applications in bioimaging and biosensing. In particular, bacteriophages are viruses that infect and replicate within bacteria.[143] Over time, and with a better understanding of phage‐host kinetics and the realization that there exists a phage specific for nearly any bacterial pathogen, a variety of improved, rapid, sensitive, and easy-to-use phage-mediated detection assays have been developed.[147]

As a result, the integration of nanomaterials in bioanalytical system is a very promising tool. In the next sections two of the aforementioned micro or nanomaterials are described in more detail: the magnetic particles and the bacteriophages, since they were applied in the different strategies developed in this dissertation.

1.5.1 Integration of magnetic particles in bioanalytical procedures

The origins of magnetic particles can be situated around 1976, when the production of spherical polystyrene particles of uniform size was achieved. They have been commercially available for many years being widely used in laboratories to extract desired biological components, such as cells, organelles or DNA from a fluid,[148,149] and are also known to be a powerful and versatile tool in a variety of analytical and biotechnology applications.

Magnetic particles range in size from a few nanometers to a few micrometers and consist of a magnetic material such as iron, nickel, cobalt, neodymium-iron-boron, samarium-cobalt or magnetite, coated with non-conducting polymers, which prevent the formation of aggregates and facilitate the further biological functionalization.[149] Nanometer sized particles (5–50 nm) are usually composed of a single magnetic core with a polymer shell around it, while larger particles (30 nm – 10 µm) can be composed of multiple magnetic cores inside a polymer matrix, giving rise to a special class of magnetic particles called superparamagnetic particles. This kind of particles are composed of thousands of very small magnetic grains, generally between 5 and 15 nm, embedded in a polymer matrix. When magnetic grains are so small, their magnetic moment can randomly flip between different orientations due to the thermal energy, and therefore the grains have no net magnetic moment. However, when a magnetic field is applied a net magnetization is achieved. The magnetization per volume unit is larger than that of paramagnetic materials, hence the name superparamagnetism, but is lower than that of permanent magnetic particles, avoiding thus aggregation problems. Finally, it should be pointed out that many parameters can influence the magnetic properties of superparamagnetic particles, such as the outer diameter, the amount of magnetic material inside the bead, the grain composition of the magnetic material and the shape of the bead.[150] In particular, the magnetic particles used in this dissertation are composed of iron oxide grains, consisting of Fe_3O_4 (ferrimagnetic magnetite) with some Fe_2O_3 (maghemite), embedded in a non-magnetic polystyrene matrix.

A wide range of magnetic particles are commercially available nowadays, allowing a high versatility in their applications. Many companies (e.g. Invitrogen, Pierce, Ademtech, Millipore, etc) provide magnetic particles of different sizes, as well as modified with different kind of chemical groups such as tosyl, amine, carboxyl or epoxy, to facilitate the further biological functionalization, or even already modified with a specific biological molecule attached on their surface like antibodies, oligonucleotides, enzymes, and other active biomolecules of interest such as streptavidin, biotin, protein A or G. A schematic representation is shown in Figure 1.11.

Due to the superparamagnetic behavior, the magnetic particles can be easy manipulated by using permanent magnets or electromagnets. When applying a magnetic field, the particles with the attached biological components, are brought close together allowing the easy removal of the fluid and remaining non-attached content (Figure 1.11, D), and in the absence of the magnet they can be re-dispersed in the new added media of choice. Therefore, their development signified a great advance in bioanalytical separation techniques, by providing a simple and rapid separation, not requiring the use of classical centrifugation or chromatography methods. The analysis of samples performed on magnetic beads can thus be easily achieved without any pre-enrichment, purification or pre-treatment steps, which are normally required for standard methods.

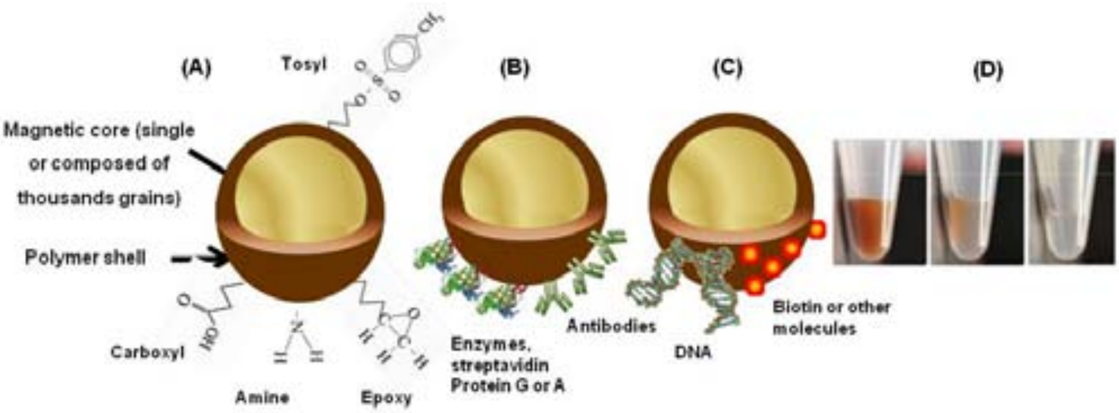
(A)
Tosyl
(B)
(C)
(D)
Magnetic core (single or composed of thousands grains)
Polymer shell
Carboxyl
Amine
Epoxy
Enzymes, streptavidin Protein G or A
Antibodies
DNA
Biotin or other molecules

Figure 1.11 Schematic representation of the magnetic particles (A), as well as of the particles functionalized with antibodies (B) or other proteins (antigens, streptavidin) (C). The magnetic separation of the particles when applying a magnet is also shown in (D).

Moreover, their use as solid support in immunoassays has shown to greatly improve the performance of the biological reactions, due to different factors: i) an increased surface area which improves the efficiency of the reactions, ii) a faster assay kinetics achieved because the particles are in suspension and the analytical target does not have to migrate very far, iii) an easy analyte preconcentration, and iv) a minimized matrix effect thanks to the improved washing and separation steps.[151,152] To optimally use magnetic particles for improving the assay performance, it should be noted that the size is an important factor to be considered. Small particles have a high diffusivity (rotational, translational), which increases the rate of finding reactive sites. However, large particles are generally more magnetic and thus easier to manipulate.[153,154] An additional advantage of the use of magnetic particles is that the immobilization of the recognition element (coating step) can be performed in large quantities in a single step and the coated particles can be stored for several weeks or even months without loss of activity thus shortening the analysis time.

In the last decade extensive research has been done on the use of magnetic particles for a novel generation of biosensors. Particle diameters between 50 nm and 3 µm coupled to different types of biosensors have been reported.[150] Magnetic particles can be used for efficient transport, for faster assay kinetics, for improving binding specificity and as labels for detection.

During the last several years magnetoresistive based detection methods in combination with microfluidics have received significant research interest in biosensing applications. These methods involve the labeling of bioanalyte with magnetic micro- or nanoparticles and the detection of their stray field using integrated magnetoresistive sensors. Magnetic labels in immunoassays require large magnetization values so that the magnetic moment induced in a nanoparticle of small mass is large enough to detect by magnetic field sensors such as giant magneto-resistors () and superconducting quantum interference devices. Using magnetic micro-or nanoparticles as labels is rather advantageous compared to fluorophores because they are stable and thus the measurements can be repeated without a time limitation and without the need of excitation. Another advantage of the magnetic labels is that they can be manipulated on-chip by application of a magnetic field gradient. Additionally, the low production cost and the small size of the microfabricated magnetic sensors promote this method for miniaturization and make it well suited for hand held on-chip biosensing systems. Moreover, the transport of magnetic particles in microfluidic systems or biosensors is investigated in several ways, such as using mechanically moving permanent magnets, sets of electromagnets with specific actuation schemes, or micropatterned and integrated current wires.[146,155,156]

Regarding the use of MPs for the magnetic immobilization of the biorecognition element, beside all the improvements provided to the immunoreaction performance, many advantageous features related to the immobilization and electrochemical detection can also be added in the case of electrochemical immunosensors.

First of all, it should be pointed out that the immobilization of the recognition element directly onto the electrode surface may require several time-consuming steps that are not always suitable for mass-production and could bring some difficulties, which can be avoided through the use of magnetic particles. Some of these drawbacks are: i) the biological component can shield the sensing surface, hindering the electron transfer and reducing the electrochemical signal, ii) the electrode is used in all immunological steps thus leading to possible passivation or poisoning of the electrode surface through the nonspecific adsorption of other species present in the sample, iii) the reusability is limited due to the repeated immobilization of the biomolecules on the electrode surface, and iv) the renewal of the electrode surface can be difficult since it requires also the removal of the biorecognition element bounded to the transducer, affecting thus also the reproducibility of the system. Moreover, since the immunological assay usually requires many washing steps, these can cause defects on the layer of the recognition elements that could compromise the reproducibility of the results. Finally, the confinement of the recognition element onto the surface of an electrode can be an obstacle to the of antibody/antigen reaction rate and can limit the number of biomolecules that can be immobilized on the electrode surface.[123,157]

All these problems can be mainly solved by the use of magnetic particles as solid support, since this approach separates the steps related to the immunoreactions from the magnetic immobilization and electrochemical detection step. As a result the electrode is used only as a sensing surface and no passivation or electrochemical interferents are expected, being the working electrode surface easily accessible by the enzymatic product, which diffuses onto the bare electrode surface.[158]

Previous studies using magnetic particles show how the efficiency of target molecule capture and binding to the surface is increased approximately five-fold in a biosensor when magnetic actuation is used instead of diffusion and sedimentation.[159] Moreover, another work comparing the performance of an electrochemical immunosensor with an electrochemical magneto-immunosensor using carbon-based screen-printed electrodes showed that the separation of magnetic beads for immunoassay and screen-printed electrodes for electrochemical detection, gave the best analytical performances in terms of sensitivity and speed of the analysis.[160]

Finally in our group, very promising results were obtained by the integration of magnetic beads, modified with biomolecules such as antibodies or DNA, in biosensor analytical systems based on magneto graphite epoxy composite electrodes (m-GEC). In this approaches, different strategies for the oriented single-point attachment of proteins (antibodies as well as carrier-hapten conjugates) on functionalized magnetic beads (-COOH, tosyl-activated, Protein A) were developed. The versatility of the magneto immunosensing strategy in different immunological formats (sandwich, direct or indirect competitive assay) and the detection of small molecules (pesticides, antibiotic residues, additives) as well as of pathogenic bacteria in real samples were successfully demonstrated.[130,161–163]

1.5.2 Integration of bacteriophages and virus-like nanoparticles in bioanalytical methods

As addressed in the previous section, inorganic nanostructured materials, including gold, silver and other metallic nanoparticles, carbon nanotubes, silica nanoparticles, quantum dots, magnetic nanoparticles, dendrimers, represent an exciting area due to their unique properties compared to the non-nanostructured counterpart. However, and beside these non-biological nanomaterials, bacteriophages, as other virus-like particles, are attracting much interest due to their outstanding properties. Due to their harmlessness comparing with other nanomaterials, the application of chemically or genetically engineered phages, viral capsids and viral-like particles in biomedicine, biotechnology and nanotechnology are under intensive study.[164] Potential uses include new vaccines, vectors for gene therapy and targeted drug delivery,[165,166] agents for molecular imaging and flow cytometry [167,168] and building blocks for the construction of nanostructured materials and electronic nanodevices.[169–171] Furthermore the highly specific recognition has been employed for the typing of bacteria.[172]

Bacteriophages, are viruses typically of 20–200 nm in size that infect bacteria, being found in abundance in the soil, manure and feces, thermal vents, and water. These viruses are extremely specific, and their long-term survivability and ability to reproduce quickly in suitable hosts make them the major regulators of microbial balance on Earth's ecosystem.

Phages are host-specific obligate intracellular parasites that bind to specific receptors on the bacterial surface in order to inject their genetic material inside the bacteria and use afterwards the bacterial cell machinery for their own multiplication and dissemination of mature virions. As a result, they are self-reproducing, and self-assembling nanostructured particles, with both structure and function encrypted in their genomic DNA. Each phage particle, called a virion, encloses its genome in a protein or lipoprotein coat called capsid, which is composed of multicopies of identical subunits forming icosahedral, T-shape or filamentous nanostructures. Virions bind specifically to host surface receptors and inject genetic material into the bacterial cells, initiating a new cycle of propagation. Depending on their life cycles and means of propagation they can be divided into two categories: lytic or virulent and temperate or reductive phages. The production and release of virions resulting in cell lysis is known as the lytic pathway of phage multiplication. In contrast, temperate phages can incorporate their DNA into the host chromosome by a site-specific integration procedure and become dormant until there is a stimulus to replicate and produce virions (known as the non-lytic pathway or lysogenic propagation).[173–175]

Some phages possess a very broad host range and infect numerous bacteria across strains, species, and/or genera, while others have a very narrow host range, and may infect only a limited number of bacteria within a particular strain. They bind to the bacterial receptors through its tail spike proteins (TSP) by recognizing surface structures such as *pili* and flagella, surface polysaccharides, or certain proteins, lipids, and other receptors protruding from the bacterial cell wall.[43]

Since its discovery in 1952, the bacteriophage P22, which infects *Salmonella enterica*, has been an intensely studied model for virus assembly[176,177]. It is a dsDNA phage of the Podoviridae family, which is characterized by a short non-contractile base plate or tail structure incorporated into a pentameric opening at one of twelve icosahedral capsid shell vertices. A schematic representation is shown in Figure 1.12.

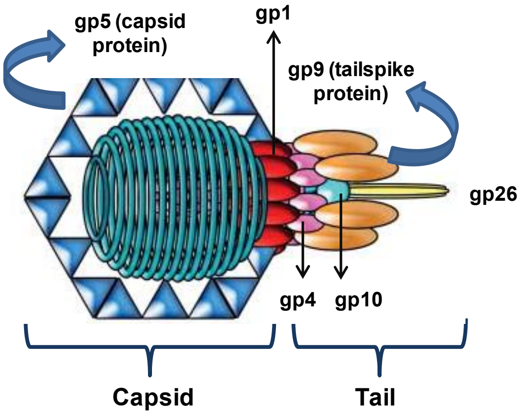

Figure 1.12 Schematic representation of P22 phage structure, which is composed of 415 molecules of coat protein (gp5), 6 tailspike (proteins (gp9) and other structural proteins (gp1, gp4, gp10 and gp26).[176]

P22 TSP is one of the most intensively studied phage receptor binding proteins. It was shown that the P22 virion contains six TSP molecules comprised of three subunits. Thus, each phage particle has 18 individual sites capable of lipopolysaccharide (LPS) binding and cleavage and shows high affinity towards their lipopolysaccharide receptor with binding constants in the 10^6 M^{-1} range[178]. The TSP functions as a viral adhesion protein and binds to the O-antigenic repeating units of *Salmonella* host LPS, its cellular receptor. The number of O-antigenic repeating units of LPS varies greatly within the LPS pool of a cell. The TSP shows a receptor destroying endorhamnosidase activity cleaving the α(1,3)- O-glycosidic bond between rhamnose and galactose of the O-antigenic repeats[179].

Native phages have been used for more than a century as alternative therapy of bacterial infections.[180,181] Instead of broad-spectrum antibiotics, phages ignore every cell but the strain of bacteria they have evolved to inhabit, which makes them safe to mammalian cells and even to non-target bacteria.[182]

The specificity and rapid growth of phages are some of the features which make them also ideal agents for the rapid detection of bacteria. Besides, they are extremely resistant and capable of existing in free form for long periods of time, being not only stable in aqueous solutions but also having high organic solvent resistance (as for example in 99 % acetonitrile, 80 % methanol, 50 % ethanol and 60 % DMF). Moreover, these naturally occurring nanoparticles have other unique properties in comparison with synthetic nanoparticles: for each phage, all the nanoparticles are nearly identical, being mono-disperse in shape and size and stable without the need of further stabilizing agents, a fact difficult to achieve by laboratory synthesis. They are able to be self-synthesized in its specific host, by producing a large amount of viral coat proteins available for further chemical modification. Thus, phages can function as nanoscale scaffolds providing a large surface of proteins that enables the multivalent display of functional groups which can be modified with a variety of signaling agents or on the other hand, the multivalent attachment of functional moieties. Finally, another interesting analytical feature is that only viable cells can be infected by phages.[143,167,183] As a result, phages are promising recognition elements for bacteria detection, presenting distinct advantages over antibodies. On one hand, they have a far longer shelf life as they withstand harsh environments such as pH (in a range from 3 to 11), ionic strength and temperature fluctuations reducing the environmental limitations, and on the other, their production besides being animal-free can be less complicated, faster and less expensive than antibody production. Finally, phages can even be used in the presence of nucleases or proteolytic enzymes, that can be present in the food matrixes, without degradation [172,183–185].

Therefore, a wide range of methods for phage-based bacteria detection have been reported and are extensively compared in many reviews, demonstrating the utility of bacteriophages for both bacteria labeling and capturing [43,147,172,174,186,187]. The use of bacteriophages in bioanalytical procedures for the detection of bacteria will be discussed in detail in § 1.7.3.

1.6 GLIADIN IN GLUTEN-FREE FOODSTUFF. AN OVERVIEW OF THE DETECTION METHODS

Patients with celiac disease should feel confident that food labeled as gluten-free has been assessed for gluten using the best available methodology. In consequence, a range of methods for the detection of gliadin have been reported.

Several analytical methods are used to characterize cereal proteins and their encoding genes: isoelectric focusing (IEF), A-PAGE, SDS-PAGE, reversed-phase high performance liquid chromatography (RP)-HPLC, size-exclusion HPLC (SE-HPLC), high performance resolution capillary electrophoresis (HPCE), matrix-assisted laser desorption ionization time-of-flight mass spectrometry (MALDI-TOF-MS), ELISA, immunoblotting, and PCR. Thus, the detection of gluten is so far principally based on proteomic approaches involving MS, genomic approaches applying PCR, and immunochemical-based tests, as shown in Figure 1.13. The last ones are the most widely applied, with the ELISA as principal technique. In the next sub-sections the available methods for gliadin detection in gluten-free foodstuff are discussed in detail.

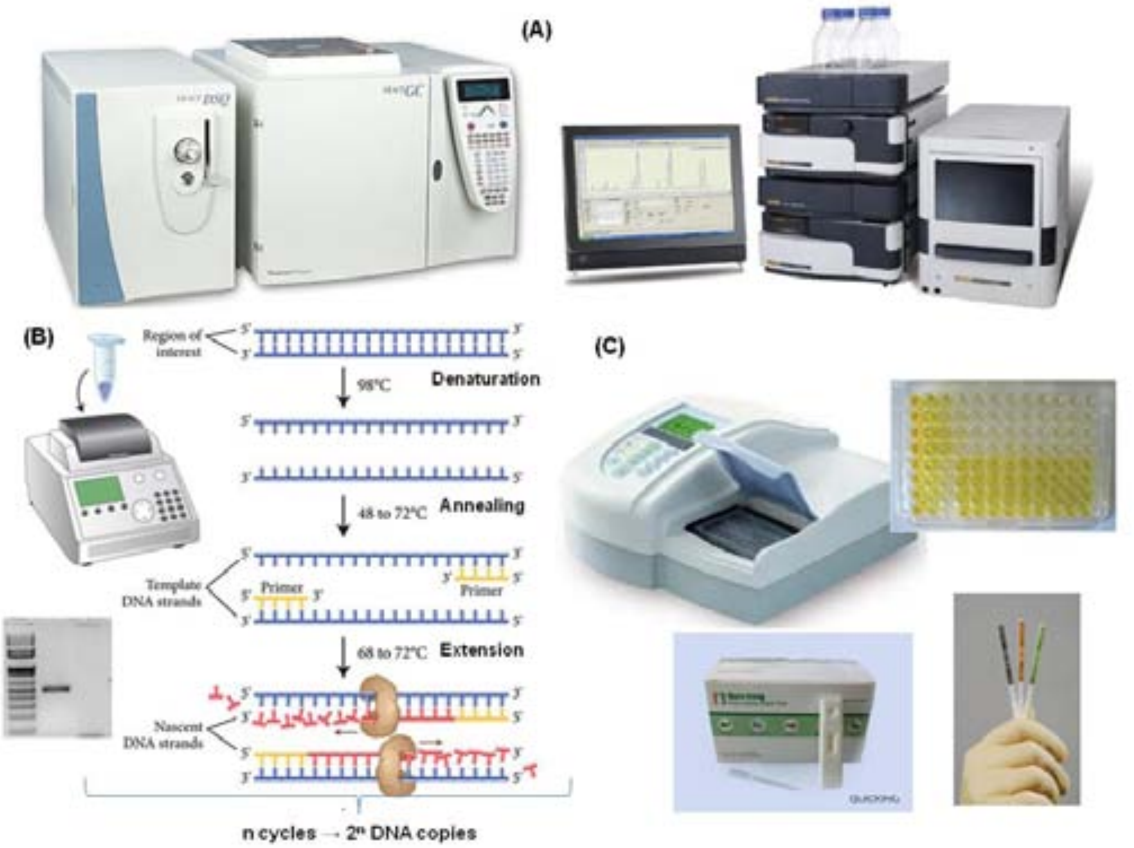

Figure 1.13 Different detection techniques for gluten detection. (A) Proteomic approaches based on classic instrumental methods; (B) genomic approaches based on PCR; and (C) immunochemical strategies based on ELISA with optical detection (up) or rapid kits with visual detection of the immunological reaction in reactive strips or wells (down).

1.6.1. Proteomic and genomic detection methods

Proteomic research is usually based on two components: a high resolution separation of proteins and an identification of individual proteins through a microanalytical process (N-terminal sequencing or MS). The separation of cereal proteins can be performed by electrophoretic techniques such as SDS-PAGE, A-PAGE and two-dimensional electrophoresis, or by chromatographic analysis such as HPLC methods, which are the most widely used. Moreover, SE- and RP-HPLC methods have been used to characterize size distribution, protein polymorphism, and biochemical characteristics based on the differences in molecular size distribution and hydrophobicity of cereal storage proteins. Up-to-date research projects are using chromatography for the separation of proteins on the analytical and preparative scales and applying high-throughput detection methods such as MS for identification. Ultra high-performance LC (UHPLC) can be used either coupled with medium resolution (such as triple quadrupole MS, QQQ) or high resolution (e.g., TOF-MS) detection techniques. Nevertheless, soft ionization techniques are usually used for protein mass spectrometry, i.e., MALDI or electrospray ionization (ESI).[31]

Therefore the first proteomic based procedure for rapidly quantifying gliadins in food was a MALDI/TOF-MS microanalysis, based on the direct observation of the characteristic gliadin mass pattern in food and its subsequent measurement, which allowed the measurement of gliadin concentration in processed and non-processed gluten containing food samples below toxic levels, with a linear response in the 0.4-10 mg per 100 g food range and a similar sensitivity to those of the most efficient conventional ELISA formats previously employed [188,189]. MALDI analysis of proteins, although considered fast and specific, presents a high mass resolution still poor compared with other techniques such as electrospray mass spectrometry. Therefore, to identify the subtle structural differences among gliadins and glutenins, the more resolutive ES-MS in combination with high performance liquid chromatography (HPLC) was later assayed.[190] More recently, a novel combination of direct enzymatic digestion and LC/MS/MS was developed for the quantification of gluten traces in native and processed food samples, which is based on the detection of six gluten marker peptides. The optimized method could detect these gluten marker peptides in the range of 0.01-100 mg L^{-1} with LOD of 0.001-0.03 mg L^{-1} and LOQ of 0.01-0.1 mg L^{-1}. To minimize the matrix effects and improve the selectivity, a 60 min run time and 2.7 µm superficially porous silica C18 column was found to be optimal in the HPLC separation of peptides.[191] Although the good performance achieved with these non-immunological methods, they present the limitation of the expensive equipments, the need of trained personnel for processing the results and the lower sample processing rate when compared to immunochemical methods such as ELISA.

Genomic approaches are based on the amplification of gluten-specific DNA fragments by PCR. In general, the presence of proteins in food indicates the presence of DNA. Therefore a DNA-based method for the detection of celiac-toxic fragments (wheat, barley and rye) in food can be applied.[192] Normally, PCR results are only qualitative. However, by incorporating internal standards, the results provide semi-quantitative results. The first quantitative PCR system to detect simultaneously contamination of wheat, barley and rye in gluten-free food was a quantitative competitive PCR (QC-PCR), which is based on the co-amplification of a competing internal standard of known concentration with the target sequence. The detection limits confirmed the suitability for the analysis of gluten-free foods and the results were evaluated, and compared with ELISA, obtaining a good correlation between the two methods.[193] Finally, by employing real-time PCR (RT-PCR) highly accurate quantitative results can be obtained, but with the drawback of needing expensive laboratory equipment and reagents. Moreover, in some cases, the obtained limits of detection are not low enough for gluten-free control showing LOD values of around 50-100 mg L^{-1}.[194,195] Nevertheless, in a recent developed real-time PCR system detection limits below 1.5 mg kg^{-1} were achieved and a high correlation with the results obtained by the most frequently used commercially available ELISA (based on the R5 monoclonal antibody) was observed. However, in samples submitted to an intensive hydrolysis process, as with syrups and malt extracts, the DNA is practically undetectable due to massive DNA degradation, and therefore impossible to be amplified by Q-PCR.[196] Finally, it should be pointed out that DNA-based methods have the drawback of the expensive equipments required and time-consuming DNA extraction and amplification steps, beside the fact that many food components can act as PCR-inhibitors. Moreover, since the target is a protein, the direct quantification should be more accurate than indirect DNA detection. This becomes evident for example in the case of contamination with gliadin-free wheat starch, which would give a positive result through PCR although gliadin absence.

Table 1.4 summarizes the most prominent proteomic and genomic based techniques for gliadin detection, showing in detail the target, detection technique, tested food sample and the achieved limits of detection.

1.6.2 Immunochemical-based and biosensing detection methods

Some recent reports looked at the use of flow cytometry, a high-throughput technique able to detect as low as 10 ng L^{-1} levels of gliadin,[197] or the application of different immunoassay formats coupled to fluorescence detection. As an example one group reported an innovative fluorescence correlation spectroscopy assay based on a competitive immunoassay, resulting in a detection limit of 0.006 mg kg^{-1}, which would require huge dilution of extracts from gluten-free samples for detection.[198] Another fast and simple method was a fluorescence polarization immunoassay using a ruthenium chelate as a label to develop the method, reporting detection limits of 0.09 mg L^{-1}.[199] Moreover, in 2009 the use of a microfluorimeter device based on a five channel-microfluidic chip for the in situ detection of gliadin in raw and cooked foodstuff was reported. After comparing different fluoroimmunoassay formats, best results were achieved with an indirect competitive assay, reaching detection limits of 4.1 µg L^{-1} (ppb) with high reproducibility.[200]

Table 1.4 Proteomic and genomic-based techniques for gluten detection.

Target	Detection technique	Tested matrix	Limit of detection	Reference
Wheat gliadin	MALDI/TOF-MS	Wheat starch, 11 processed commercial food samples and breads (high gluten food sample)	4 mg kg^{-1}; (good ELISA correlation: 1.1 $^{+}/_{-}$ 0.6)	Camafeita et al. 1997 [188]
Gliadin and glutenins	HPLC/ ES-MS	Non-defatted flour of different wheat varieties	-	Mamone et al. 2000 [190]
Six gluten marker peptides	Direct enzymatic digestion and LC/MS/MS	Native and processed food samples	1 to 30 ng kg^{-1} (0.001-0.03 ppm)	Sealey-Voyksner et al. 2010 [191]
Wheat, barley and rye DNA	Quantitative competitive (QC)-PCR	Four breads, two pastries, one millet product and eight baby food products	10 mg kg^{-1} (good correlation with ELISA: 11 from 15 samples)	Dahinden et al. 2001 [193]
Wheat, barley and rye DNA	rt-PCR	Flours and gluten-free biscuits	100 mg kg^{-1}	Olexová et al. 2006 [195]
Wheat, barley and rye DNA	rt-PCR using Taqman probes	Vegetable food matrixes and meat products	2.5 mg kg^{-1} (in vegetables) and 5 mg/kg (in meat)	Zeltner et al. 2009 [201]
Wheat DNA	rt-PCR	Flours, chocolate, starches, meats, candies, hydrolysates (beers, syrups, malt extracts) and heat-processed food samples (bread, biscuits, baby foods)	below 1.5 mg kg^{-1} (5 ng DNA/kg) (good correlation with R5 ELISA, except in some heat-treated food samples)	Mujico et al. 2011 [196]

Several conventional immunological procedures including immunoblotting and ELISA formats using different monoclonal or polyclonal antibodies against a variety of gliadin components are commonly used in an attempt to quantify gluten in food, being the ELISA-like techniques the most common used for gliadin detection, as already mentioned.

Early assays used principally polyclonal antibodies, but later monoclonal based systems allow more precisely quantization of celiac toxic epitopes. One of the first toxic sequence to be identified was a 19 amino acid peptide of α-gliadin (LGQQQPFPPQQPYPQPQPF), and monoclonal antibodies has been raised against it, for the detection of gliadin and gluten hydrolysates.[202] Other monoclonal antibodies against short heat-stable epitopes (R5 antibodies)[203] or towards the toxic 33-mer from α-gliadin (G12 and A1 antibodies)[204,205] were also reported.

Different approaches for sandwich ELISAs were developed and were the first commercially available methods.[36] One was developed in the early 1990s based on a monoclonal ω-gliadin antibody that recognises the heat- stable ω fraction from wheat, rye and barley prolamins, but not oat avenins.[206] This became the official method of the Association of Analytical Communities (AOAC), but only for gluten levels above 160 mg/kg. It was able to quantify native and heated gluten, but unable to accurately detect and quantify barley prolamins. Moreover, it could over- or underestimate gluten content, and could not accurately quantify hydrolyzed gluten.[36] In addition, the relative amount of ω-gliadin to other gliadin fractions was not consistent between cultivars and species leading to inaccurate results.[207]

The other more recent immunological method is based on a monoclonal antibody R5,[203,208] and was endorsed by Codex Committee on Methods of Analysis and Sampling for gluten determination. In this case, antibodies are directed towards a specific potentially celiac toxic pentapeptide glutamine–glutamine–proline–phenylalanine–proline (QQPFP) and homologous sequences that occur repetitively in gluten of wheat, rye and barley prolamins, but not found in avenins. It was claimed that this antibody does not cross-react with avenin and the method is able to quantify native and heated gluten, being more sensitive than the anti- ω-gliadin ELISA. Gliadins are detected with the R5 ELISA in the range of 2‑5 mg kg^{-1} food, having a LOD of 3 mg kg^{-1} gluten (1.5 ppm gliadin) and a LOQ of 5 mg kg^{-1}.[209] However, some criticism is that it overestimates barley hordein (especially in barley contaminated oats, unless a hordein standard is used for the tests), shows cross-reaction with soya proteins and is also unable to accurately quantify hydrolyzed gluten.[36,207]

It should be noted the gluten proteins are not necessarily intact when present in food. The original version of the R5-ELISA and the anti-ω-gliadin ELISA employ a sandwich format, and this kind of ELISAs require multivalency or at least two epitopes (i.e. two antibody binding sites), which is not always the case when proteins are hydrolyzed leading to the underestimation of small gluten fragments.[36,210] A R5 antibody-based competitive ELISA was specifically developed to overcome this limitation and so hydrolyzed gluten peptides containing single epitopes can be detected.[211] The combination of the competitive R5 ELISA and peptic-tryptic digestion of prolamins was shown to be suitable for the determination of partially hydrolyzed gluten in fermented cereals with LOD 2.3 and LOQ 6.7 mg kg^{-1}.[212] Another recent competitive ELISA test with high sensitivity, reproducibility, and repeatability was reported, showing LOD values of 0.44 mg kg^{-1}.[205] However, none of these methods are still validated.

There are several commercially available test kits currently on the market for gliadin and/or gluten detection: RIDASCREEN Gliadin ELISA kit (R-Biopharm, Darmstadt, Germany), Haven Gluten Assay Kit (Allmark, Chester UK), Gluten Check Assay (Diagnostic Innovations, St. Asaph, UK), Gluten ELISA Kit (Tecna, Trieste, Italy), Gliadin ELISA kit (IM3717, Immunotech, a Beckman Coulter Co., Prague, Czech Republic), BioKits Gluten Assay Kit (Tepnel BioSystems Ltd, Manchester, UK), INGEZIM GLUTEN (Ingenasa, Madrid, Spain), just to cite a few. They mainly consist of a reference material, one or more specifically developed antibody solutions, and other chemicals like buffers and extraction cocktails. However, by comparing the different ELISA-test kits it has been shown that the measured gliadin contents varied depending on the antibody and reference material used for raising the antibody as well as for calibrating the assay, which stresses thus the importance of validating immunochemical methods for gluten detection.[31] Therefore, there is still a requirement for a sensitive and fast assay to screen different foods on the market. Moreover, there is a definitive need for an assay that is easy to use and can be used on site, so that industries generating gluten-free foods can rapidly test incoming raw materials as well as checking for gluten contamination throughout the food production process.[213]

As explained in the previous section, biosensors are promising candidates to cover this demand. The first report of an optical biosensor based on porous silicon (Psi) technology for gliadin detection appeared some years ago, which exploited the use of a recombinant glutamine-binding protein from *Escherichia coli,* that is able to recognize the gliadin in micromolecular concentration.[214,215]

More recently the development of two electrochemical immunosensors was reported by Nassef and colleagues. The first one was based on the measurement of gliadin content using gold electrodes with antibody- modified acidic self- assembled monolayers (SAMs) and a sandwich assay coupled to differential pulse voltammetry for the detection. In this approach a highly sensitive immunosensor with low ppb detection limits (5.5 and 11.6 µg L^{-1} depending on the surface chemistry), very good reproducibility, and an excellent correlation with the ELISA methods was achieved.[213] The second developed immunosensor relied on the spontaneous self-assembly of anti-gliadin Fab fragments on gold surfaces as a means of improving the sensitivity. Once again a sandwich immunoassay format was employed and a limit of detection of 3.29 µg L^{-1} was achieved by using amperometry for gliadin detection.[216]

Table 1.5 summarizes the most prominent immunochemical based techniques for gliadin detection, in which the obtained detection limits were below the 20 mg kg^{-1} (20 ppm) established by the food regulations. The table presents in detail the target, type of assay with the employed antibodies or labeled antigen, detection technique, tested food sample and the achieved limits of detection.

Table 1.5 Immunochemical assays for gluten detection.

Target	Type of assay	Detection technique	Tested matrix	Limit of detection	Reference
Gliadin	Sandwich/ pAb	ELISA		22 µg L^{-1} (ppb) (low reactivity with barley and oats)	McKillop et al. 1985 [217]
Gliadin	Sandwich/ moAb	ELISA	Nominally gluten-free products based on wheat starch	15 µg L^{-1} (low reactivity with barley, rye, oats)	Freedman et al. 1987 [218]
ω-gliadin (and HMW-glutenins)	Sandwich/ moAb (401/21)	ELISA	Meat/gluten blends (cooked), flour/starch blends, flours	100-150 µg L^{-1}	Skerritt and Hill 1990 [206]
Gliadin	Competitive/ pAb	ELISA	Different types of foods and even processed foods including meat products	1 µg L^{-1}	Chirdo et al. 1995 [219]
Gliadin of wheat, barley and rye	Sandwich Competitive biotin-Ab Competitive biotin-gliadin mAb (12A1, and 13B4)	ELISA	Different types of foods and even processed foods including meat products	1 µg L^{-1} 20 µg L^{-1} and 5 µg L^{-1} (No reactivity with oats, rice, soy or maize)	Chirdo et al. 1998 [220]
19mer toxic gliadin peptide	Sandwich/ moAb (PN3)	ELISA	Wheat starches; dried skimmed milk powder, sugar beet bran, flours; cooked & uncooked gluten-free products	Gliadin: 4 µg L^{-1} (0.08 mg kg^{-1}) Rye: 500 µg L^{-1} (10 mg kg^{-1}) ω-gliadin, barley, oats: 1 mg L^{-1} (20 mg/kg) (Also detect oats)	Ellis et al. 1998 [202]
Wheat, barley, rye and oats prolamins	Sandwich/ 3 moAb cocktail	ELISA	Different flours, gluten-free foods and wheat starches	1.5, 0.05, 0.15 and 12 µg L^{-1} (for gliadins, hordeins, secalins and avenins respectively)	Sorell et al. 1998 [221]
Toxic epitopes in wheat, barley and rye gliadin	Sandwich Competitive/ moAb (R5)	ELISA	Unprocessed and heat-processed wheat and barley-based products, hydrolyzed foods, contaminated oat samples	1.5 µg L^{-1} 1.2 µg L^{-1}	Valdés et al. 2003,[203] Ferre et al. 2004 [211]
Gliadin	Competitive/ Gliadins	Homogeneous stopped-flow	Gluten-containing and	4 µg L^{-1}	Sánchez-Martínez et

	labeled with terbium(III) chelate/ pAb	fluorimmunoassay	gluten-free food samples (flours, bread, cocoa, baby food)		al. 2004 [222]
16mer common to α, β, γ and ω-gliadin	Sandwich Competitive/ Gliadin adsorbed to latex or captured by pAb/ second pAb-FITC	Flow Cytometry	Flour, pasta, biscuit and cake samples	10 ng L^{-1} 1 µg L^{-1}	Capparelli et al. 2006 [197]
ω-gliadin and toxic epitopes R5	Sandwich/ moAb (401/21; R5)	ELISA	Barley flour	5 mg L^{-1} (ω-gliadin) 1.5 mg L^{-1} (R5)	Kanerva et al. 2006 [207]
Gliadin	Competitive/ Fluorescein labeled gliadin peptides/ pAb	Fluorescence correlation spectroscopy	Extract of gliadin from a crude preparation and enzyme digestion with pepsin and trypsin	0.006 mg L^{-1}	Varriale et al. 2007 [198]
Gliadin	Competitive/ Gliadin labeled with Ru(II) chelate/ pAb	Long-Wavelength Fluorescence polarization	Maize flour and bread	0.09 mg L^{-1}	Sánchez-Martínez et al. 2007 [199]
Gliadin toxic epitopes (α- and *γ*-gliadin and ω-secalin)	Sandwich/ 2 x moAb, 1x pAb	ELISA	Samples labeled as gluten-free, samples spiked by wheat flour	5 µg L^{-1} (No cross-reactivity with oat, rice, maize, and buckwheat)	Gabrovská et al. 2006 [223], Sánchez et al. 2007 [224]
33mer toxic gliadin peptide (wheat, barley & rye)	Sandwich Competitive/ moAb (G12 and A1)	ELISA	Different kinds of flours	0.6 µg L^{-1} 0.4 µg L^{-1}	Morón et al 2008a and b [204,205]
Gliadin	Sandwich (indirect)/ Capture moAb and secondary pAb	Electrochemical immunosensor (DPV)	Raw materials (bread and cake mix), processed foods (biscuit and pasta) and gluten-containing sample (Tostagrill bread)	5.5 µg L^{-1}	Nassef et al. 2008 [213]
Gliadin	Sandwich (direct)/ Capture Fab fragments and mAb-HRP	Electrochemical immunosensor (impedimetric and amperometric)	Gliadin preparation provided by the Prolamin Working Group (PWG)	0.42 mg L^{-1} (impedance) 3.29 µg L^{-1} (amperometry)	Nassef et al. 2009 [216]
Gliadin	Competitive (indirect)/ biotinylated gliadin to immobilize; moAb	Microfluorimeter device based on a five channel-microfluidic chip	Gluten-free sample (Harisín pasta) and gluten-containing sample ("Tostagrill" toasted bread)	4.1 µg mL^{-1}	Mairal et al. 2009 [200]

In this dissertation, an alternative novel competitive immunochemical method on magnetic particles was developed for the dual detection through a magneto immunoassay with optical detection and a magneto-electrode coupled to amperometric sensing.

1.7 PATHOGENIC BACTERIA. AN OVERVIEW OF THE DETECTION METHODS

Culture-based methods are considered to be the “gold standard” and remain the most reliable and accurate techniques for food-borne pathogen detection. They are known for their cost effectiveness, sensitivity, ability to confirm cell viability and ease of standardization. Although these methods are designed to be able to detect a single target cell in the sample (which size can vary from 10 g to 375 g or more), amplification of the signal is required through the growth of a single cell into a colony.

As a result of the high demand for obtaining rapid information about pathogenic contamination in HACCP programs, in recent years considerably efforts have been directed towards the development of alternative methods that reduce the assay time of microbiological analysis and also save media requirements. These rapid methods are designed to avoid selective culturing and serological/biochemical identification.[225]

1.7.1 Conventional culture-based methods

The general approach for recovering and identifying the bacteria usually includes a morphological evaluation of the microorganism as well as tests for the organism’s ability to grow in different media under a variety of conditions, which involves the following basic steps:[226,227] i) pre-enrichment of the sample in a nutrient non-selective broth such as buffer peptone water (BPW), lactose broth or Luria-Bertani broth; ii) selective enrichment and differential plating on selective agar media; iii) biochemical screening; and iv) serological confirmation.

The purpose of pre-enrichment is to resuscitate injured cells and/ or increase the level of the target pathogen in the sample in order to ensure that any viable microorganism is multiplied and subsequently detected. Pre-enrichment may also be useful for diluting any inhibitory compounds or preservatives found in the sample, as well as rehydrating cells sampled from dried or processed foods. This incubation step takes usually between 18 to 24 h, followed by the selective enrichment in which specialized media are used to selectively increase the concentration of the target pathogen while at the same time suppressing the growth of background microflora through some types of colorants or inhibitors. Overall, cultural enrichment results in exponential amplification of the target organism by as much as a million-fold, becoming thus much easier to be detected. As an example the RV broth (Rappaport-Vassiliadis) is efficient for selective enrichment of *Salmonella*.[228]

The next step in culture-based food-borne pathogen detection is the selective and differential plating, which is facilitated by the use of a combination of selective agents that suppress the growth of competitive microorganisms, and differential agents that allow the organism to be readily distinguished from other present microorganisms. In the particular case of *Salmonella*, some typical selective agar media are: Bismuth Sulfite agar, Xylose Lysine Deoxycholate agar (XLD) and Brilliant Green agar (BGA), as shown in Figure 1.14. If after the selective and differential plating no typical colonies have grown, the analysis is completed and the results are reported as negative. In the case that one or more colonies that fulfill the presumptive positive criteria were isolated, additional biochemical and/or serological testing are needed to confirm that the isolate is indeed the target pathogen. The biochemical tests are usually carried out in tubes and are based on the unique features of the different bacterial species metabolism, such as the presence of specific enzymes and indicators, carbohydrates and cell respiration. In these tests typical macroscopic changes are observed in the tubes after the bacterial growth resulting from their specific metabolism (Figure 1.14).

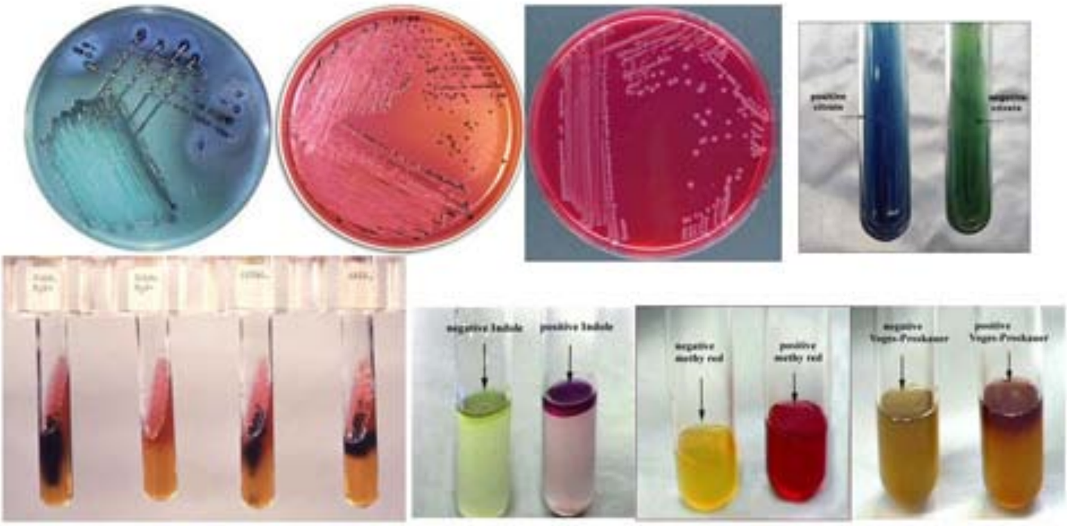

Figure 1.14 Typical *Salmonella* colonies in different selective agar media (from left to right, bismuth sulfite, XLD and BGA) and some biochemical tests for the bacterial identification.

On the other hand, serological tests as agglutination and precipitation are normally performed on plates completing the confirmation. Further tests (e.g., antibiotic resistance, phage typing, immunological recognition, and molecular typing) may provide additional information about the strain, such as the presence of specific virulence factors or the identification of a particular molecular fingerprint.

Performed in the conventional manner, the combined enrichment and plating steps take 24–48 hours each, which means that presumptive detection of a pathogen can take between 2 and 4 days. Moreover, the subsequent confirmation of a positive sample can take up to a week or more. Therefore the major drawback of microbiological methods is the long assay times required, besides their labor-intensiveness. This is an obvious inconvenience in many industrial applications, particularly in the field of foods sector.[2,228]

In spite of their disadvantage, conventional culture methods still represent a field where progress is possible. Automation may be very useful in reducing the time required to prepare culture media, perform serial dilutions, count colonies, etc. There are a wide variety of rapid culture methods that have been designed to replace the standard agar plate, to reduce the workload, facilitate rapid implementation, simplify handling, and/or reduce the need for a complete laboratory infrastructure, which do not necessarily shorten assay times. Some of these modified culture methods are based on the colony counting method using disposable cardboards containing dehydrated media, while others are based on the MPN method. In addition, many companies are trying to shorten the assay times by developing even more selective culturing media. In this perspective, a staggering number of chromogenic and fluorogenic culture media have been developed for the detection and enumeration of specific bacteria in recent years. The addition of these media to culturing protocols facilitates the rapid identification of presumptive colonies of the target microorganism, which has led to its incorporation in some official methods. Moreover, the classical methods are often combined together with other pathogen detection methods like an automated or semi-automated DNA, antibody, or biochemical-based method to yield more robust results.[38,229]

1.7.2 Rapid methods for food pathogen detection

Different instrumental methods have been developed based on a variety of analytical techniques such as chromatography, infrared or fluorescence spectroscopy, bioluminiscence, flow cytometry, electric conductance and impedance. The last two mentioned methods are being used in many laboratories and are based on measuring the conductance changes of the medium, in consequence to the microbial metabolism and growth. The drawback of this kind of technique is the requirement of highly trained personnel and of complex and expensive instrumentation centralized in big laboratories.[92,228] Flow cytometry is another useful high throughput technique that can be used to sort and even identify specific biological cells and particles from liquid samples using fluorescently labeled target-specific ligands (such as antibodies), which gave very promising results achieving low detection limits in milk.[230] However, the complicated optical alignment process and relatively higher cost of flow cytometry equipment, besides the fact that background components of the sample matrix may interfere with fluorescence based detection, are some of the practical hindrances to the routine use of this method.

Due to advances in areas such as genomics and biotechnology, powerful methodologies have been developed to detect both specific pathogens and indicator organisms. Because many microorganisms are not easily cultured or can enter a viable but non-culturable state, the current methods focus on immunological or genetic characteristics to detect the presence of specific pathogenic microorganisms. These methods not only increase the rapidity of analysis, but they are also able to achieve a high degree of sensitivity and specificity without the need for complex cultivation and additional confirmation steps.[141] Most notable amongst these new techniques are the enzyme-linked immunosorbent assay (ELISA), DNA hybridization, and Polymerase Chain Reaction (PCR).

Immunological detection of bacteria has become more sensitive, specific, reproducible and reliable with many commercial immunoassays available for the detection of a wide variety of bacteria and their related biotoxins in food. Advances in antibody production have stimulated this technology, since polyclonal antibodies can be now quickly and cheaply obtained, and do not require the time or expertise associated with the production of monoclonal antibodies. Detection using automated and robotic ELISAs is widely used since they can reduce detection times after enrichment to as low as 1–3 h. Many test kits are available on the market, including immunodiffusion, ELISA and various lateral flow devices that have been validated for detecting different food-borne pathogens.[229,231] Although the promising features of lateral flow systems in terms of their speed and simplicity, they still require high concentrations of target organisms (10^7-10^9 CFU) and have a tendency to produce a relatively higher number of false positive results compared to more traditional microtiter plate ELISA methods.[65] While the immunological-based detection is not much specific and sensitive than nucleic acid-based detection, but it is faster, more robust and has the ability to detect not only contaminating organisms but also their biotoxins that may not be expressed in the organism's genome. In spite of their very less assay time compared to traditional culture techniques and PCR based-methods, antibody-based detection usually requires a minimum of 10^3 to 10^4 CFU for detection and some problems related to low affinity of the antibodies or potential interference from contaminants may arise.[38,141]

Antibodies that recognize bacterial pathogens coupled to micro or nanometer scale magnetic particles have also been used to aid in detection by separating microbial cells from contaminating microflora and interfering components of the food matrix, which is called immunomagnetic separation (IMS). This pre-analytical sample processing is an efficient extraction and concentration method.[232] As pathogens are usually represented in low numbers in food products, the processing of large sample volumes is often required for concentrating and separating bacteria and their further effective detection. As explained in § 1.3, in IMS the antibody functionalized magnetic particles are incubated with the sample to bind target cells and separate them from the sample matrix through application of a magnetic field. The magnetic particle-bound target can then be washed and resuspended into smaller volumes increasing thus their concentration in the testing medium. In comparison to physical separation such as centrifugation and filtration, or chemical separation such as the use of metal hydroxides, resins and lectins, IMS is simpler and generally results in higher capture efficiency due to the greater surface area available for target binding. IMS has been paired with a variety of rapid detection methods for bacterial pathogens, including fluorescence and bioluminescence techniques, enzymatic assays, PCR-based tests and biosensors.[233]

Nucleic acid-based assays consist of two main types, hybridization using probes and amplification by PCR and related techniques. The recent development of microarray technology offers a powerful platform for probe hybridization where millions of probes can be deposited and analyzed simultaneously. The easiest way to detect specific nucleic acid sequences is through direct hybridization of a specific nucleic acid probe, carrying detectable marker molecules, to microbial complementary nucleic acid extracts. The probes may be used to detect genes in the bacterial DNA (Southern blots) or to detect mRNA or rRNA (Northern blots). Fluorescent in situ hybridization (FISH) with oligonucleotide probes directed at rRNA is the most common method among molecular techniques not based on PCR. The probes used by FISH tend to be

15–25 nucleotides in length, and are covalently labeled at their 5' end with fluorescent labels which can be detected using epifluorescence microscopy.

PCR is a method used for the in vitro enzymatic amplification of specific DNA sequences by thermoresistant DNA polymerases. The target DNA, synthetic oligonucleotide primers (20-30 nucleotides in length), a thermostable DNA polymerase and the DNA subunits are combined in a microcentrifuge tube and subjected to temperature changes that facilitate DNA denaturation, annealing of the oligonucleotide primers to the target DNA and extension of the primers across the target sequence. These cycles are repeated many times, thus resulting in increasingly greater quantities of target sequence, being able to generate millions of copies of a single DNA molecule in around 20 to 30 temperature cycles. The PCR amplified products are conventionally separated and detected by electrophoresis on agarose gels.[141,229]

Nucleic acid-based detection coupled with PCR has distinct advantages over culture and other standard methods for the detection of microbial pathogens such as specificity, sensitivity, accuracy and capacity to detect small amounts of target nucleic acid in a sample.[234] Methods linking PCR detection to samples enriched for pathogen proliferation (usually overnight) are available for the majority of foodborne pathogens. For example, the USDA method for detecting *Salmonella* combines enrichment and PCR screening, resulting in reduced numbers of samples for further testing and increased testing sensitivity. Moreover, multiple primers can be simultaneously used to detect different pathogens in one multiplex reaction. Further improvements were provided by the development of real-time PCR which allows instantaneous amplification and detection at the same time, being also meritorious for the capability to quantitatively identify foodborne pathogens in foods when no enrichment is required.

PCR-based methods provide limits of detection on the order of 10^1 to 10^4 CFU mL^{-1}, depending on the DNA extraction efficiency and the nature of the food samples. However, one important limitation of PCR is that it gives also positive signal with death or injured whole cells, and even with free DNA. As such, this approach cannot be applied directly to processed foods because intact DNA will be detected. In addition, PCR is adversely affected by potential inhibitors in the food matrices; therefore it is critical that when designing PCR assays for food testing, internal amplification controls are included.[235] Furthermore, from an industrial point of view routine detection of microbes using PCR can be expensive and complicated, requiring skilled workers to carry out the tests.[38]

Finally, it should be pointed out that to achieve the low limits required by the food regulatory agencies, which in the case of *Salmonella* establish the absence of bacteria in 25 g (or mL) of food sample, some degree of pre-enrichment lasting between 6-8 to 48 h remains essential in both immunochemical as well as nucleic acid-based methods. Although this results in longer total analysis times than the minutes or few hours of the detection strategy itself, the assay time can be shortened to less than one day by indeed replacing the selective culturing and biochemical/ serological testing.

On the other hand, food samples are a complex and heterogeneous matrix consisting of various components including particulate matter, biochemical, and inorganic food components, fats and non-target (harmless) background microflora. Many of these components produce severe interferences in biological reactions, e.g., fat and particulates can interfere with antibody binding, and complex carbohydrates can inhibit nucleic acid amplification.[38]

The development of biosensors is a growing area, in response to the demand for rapid real-time, simple, selective and cost-effective analytical methods. Biosensing devices, due to all their advantageous features detailed in section 1.4, can be considered as ideal tools to be used as an “alarm” to rapidly detect the risk of contamination by pathogens in a rapid and sensitive manner.[236] The specific recognition in such systems is mainly due to the biological probe, such as nucleic acid or antibody, giving rice to genosensors and immunosensors, respectively. Wide varieties of transduction methods have been developed in the past decade for the detection of food-borne pathogens, being optical, mass based and electrochemical the most popular and common.[237] Optical biosensors, and within this group principally the ones based on SPR, are particularly attractive as they can allow direct label-free detection. Although this methodology has been successfully applied for pathogenic detection, it does not reach the required limits of detection to ensure food safety without performing a pre-enrichment step and is limited by the high cost of the associated instrumentation.[92,238] On the other hand, electrochemical detection has several advantages like low cost, ability to work with turbid samples and easy miniaturization. Among the different types of detections, amperometric transduction is the most common electrochemical detection method used for pathogen analysis, having superior sensitivity than potentiometric methods.[38]

Our group has been reporting many methodological improvements in biosensors (immunosensors and genosensors) for the sensitive detection of pathogenic bacteria. In the case of *Salmonella* genosensors, different detection methods were developed in the last 10 years. The first strategies combined the DNA physical adsorption with enzymatic labeling[239] or label free detection using the intrinsic signal of the guanine[240]. Further improvements were achieved by the oriented immobilization of the DNA through the binding of biotinylated oligonucleotides to streptavidin modified magnetic beads.[241] To achieve even higher sensitivities, PCR was performed using two labeled primers giving place to a double-tagged amplicon, in which one of the tags is used for the immobilization while the other can be recognized by enzymatic labels for further amperometric detection. This kind of approach was applied on magnetic beads[242] as well as on GEC electrodes modified with gold nanoparticles by using a thiolated primer.[243] Moreover, a *Salmonella* immunosensing approach was also developed using a sandwich immunoassay format on magnetic beads as solid support, being able to detect 7.5 x 10^3 CFU mL^{-1} of bacteria in milk and as low as 0.1 CFU mL^{-1} after 8 h pre-enrichment.[163]

Finally, in our group (GSB), the detection of *Salmonella* based on P22 phages, inactivated by UV light and, covalently attached on tosyl-activated magnetic particles was recently achieved. In the developed approach the immobilized phage nanoparticles were used for the phagomagnetic separation and pre-concentration of the cells, and the subsequent detection strategy was based on the double-tagging PCR amplification of the bacterial DNA followed by electrochemical magneto-genosensing (PMS/double-tagging PCR/m-GEC genosensing).[244] In the next section the use of bacteriophages for bacteria detection is further discussed.

1.7.3 Bacteriophages for bacteria detection

As previously commented in § 1.5.2, a wide range of methods for phage-based bacteria detection have been reported, using bacteria labeling or capturing.[43,147,172,174,186,187] The detection schemes can be based on the initial binding event with labeled phages or need a productive phage infection, may utilize either phages that have been genetically or physiologically modified in some manner to perform a specific detection task or wild-type phages, as well as modified phage components (like fluorescent labeled endolysin cell wall binding domains or phage tailspike proteins). Moreover in many cases the phage-based approaches have been coupled to immunomagnetic separation to improve the detection limits.

The developed bacteria tagging strategies are classified into different groups, such as:

- *Phage DNA labeling strategy*. Tagging of phage nucleic acid with fluorescent dyes like YOYO-1[245], DAPI[246] or SYBR gold[185]).
- *Phage protein labeling strategy.* Modification of the phage capsid with different tags such as biotin or fluorescent molecules which are displayed upon phage attachment to the target bacteria. In this case the labeling can be performed by expression of specific tags using genetic engineered phages as in the case of biotin binding peptides which are labeled with streptavidin-modified quantum dots[247,248], or by direct conjugation of fluorescent tagging molecules (like Cy3, Alexa 546, Alexa Fluor 488 and 647 C5-aminooxyacetamide) to phage capsid proteins[168,249].
- *Reporter phage strategy.* Use of phages as delivery vehicles to transport measurable markers into the target cells after a productive infection of the host bacterium and the subsequent expression of reporter genes carried in the phage genome. The expressed reporter proteins usually give easy-to-measure signals such as bioluminescence as in the lux reporter genes expression[44,250,251], fluorescence like in the case of green fluorescent protein (GFP)[252,253], or colorimetric signals when based on lacZ encoded β- galactosidase enzyme[254]. Finally, a more unusual application of this strategy involves the ice nucleation gene (*inaW*), which protein product integrates within the bacterial outer cell membrane acting as a catalyst for ice crystal formation[255].
- *Phage amplification strategy.* Reliance on the phage's natural lifecycle after infection and host-based amplification with the subsequent measurement of progeny phages released from the target cells and amplified through the addition of helper cells which are infected to produce a burst of new phages. The progeny phages can be detected through the formation of plaques on a growth plate[256], simple optical density measurement[257] or cell staining methods as means of determining host cell viability[258].
- *Phage-mediated lysis strategy.* Exploitation of phages capability for bacteria lysis and detection of released intracellular specific constituents such as adenosine triphosphate (ATP)[186] or host enzymes (like adenylate kinase and β-galactosidase)[259–261], by applying a routine firefly luciferase based bioluminescent assay or by amperometric measurement of the enzymatic activity through the addition of electroactive substrates, respectively.

Due to the many advantages provided by biosensors, the integration of bacteriophages in biosensor applications are evolving and were recovered and analyzed in diverse reviews.[38,147,172,183,262,263]

Since most studies were based on fluorescence or bioluminescence as detecting principles, immobilization of the phages is not required in these approaches. Electrochemical transducers were principally used for the measurement of enzymatic activity after phage-mediated cell lysis through amperometry or for detection of changes in the microbial growth by impedimetric monitoring[264].

On the other hand, bacteriophages can be immobilized on solid supports for bacteria biosensing, taking advantage of their high specificity to capture their targets. An early version of phage-based biosensor used the passive immobilization onto a polystyrene strip and application as a dipstick device to capture *Salmonella* from foodstuff detecting the bacteria by PCR or epifluorescence microscopy after addition of a fluorescent dye.[265] Later, the use of phages for the creation of pathogenic sensing platforms has been reported by using mainly Surface Plasmon Resonance (SPR) as optical transduction platform[266,267], or mass-sensitive transducers based on quartz crystal microbalance (QCM)[267], surface acoustic wave [268], and magnetoelastic [269–271] sensors. These early reports have mainly relied on physical adsorption for the attachment of the phages on the sensor surface. However, this approaches results in poor phage surface coverage and no orientation, affecting the sensitivity of the platform.

In order to maximize the bacteria capture efficiency, the phage head should ideally be immobilized to the solid phase whereas its tail faces outwards. Chemical attachment of the phages on solid surfaces and transducers would yield better coverage and thus significantly improve the performance of these sensors. Streptavidin-mediated immobilization of biotinylated bacteriophages in which biotin was covalently attached to the capsid proteins[272], directly expressed on the head region[273] or bound to biotin carboxyl carrier peptides expressed on the phage capsid through genetic engineering[274], was reported. Alternatively, phages can be immobilized through electrostatic interaction by taking advantage of the phage head's net charge, which is usually negative, for their physisorption on papers coated with cationic layers[275], silica supports[276] or positively charged cellulose membrane[277]. Thiol-gold chemisorption[278] and hydrogen bonding using different approaches[279] were reported for the immobilization on gold surfaces. Finally, covalent immobilization of bacteriophages through the reaction between phage primary amine functions and amine-reactive groups (NHS ester, carboxyl groups, epoxy, isocyanate, modified SAM, glutaraldehyde, etc) on gold surface[279–281], screen-printed carbon electrode[264], and glass substrates[184,282] for biosensor application were also reported.

Phage receptor binding proteins (RBP) have been also used as novel probes in biosensors.[262] Suitable tags such as cysteine or polyhistidine tags can be added to the RBPs sequence at appropriate positions without altering their binding affinity[283,284], or the overexpression of the RBP as glutathione-S-transferase fusion protein[285] can be performed for the further oriented surface functionalization on biosensor platforms. More recently the RBP of a phage towards Campylobacter jejuni was expressed as a fusion with enhanced green fluorescent protein to label the bacteria for their subsequent detection using an agglutination assay coupled to fluorescent microscopy.[286]

Table 1.6 summarizes the most prominent phage-based detection techniques for *Salmonella* detection in which the obtained detection limits were below 10^3 CFU mL^{-1} and the assay time does not surpass a maximum of 24 h. The table shows in detail the employed phage, the type of assay, detection technique, tested food sample, the assay time and the achieved limits of detection.

Table 1.6 Phage based techniques for *Salmonella* detection.

Phage	Type of assay	Detection technique	Tested matrix	Assay time	Limit of detection	Reference
Felix-01	Phage amplification	HPLC	Milk	24h	<5 CFU mL^{-1}	Hirsh and Martin 1983 [287]
Felix-01	Phage amplification	Plaque counting	Culture media	4h	$6x10^2$ CFU mL^{-1}	Stewart et al. 1998 [256]
SJ2	IMS + Phage amplification	Optical density	Skimmed milk powder, chicken rinses, ground beef	20h	3 CFU in 25 g (mL)	Favrin et al. 2003 [288]
Felix-01 (mutant)	Phage amplification	Plaque counting	Culture media	3-5h	≤10 CFU mL^{-1}	Ulitzur and Ulitzur 2006 [289]
P22	Reporter gene (inaW)	Cell freezing coupled to fluorescent indicator	Milk and eggs	2h	10 CFU mL^{-1}	Wolber and Green 1990[290]
P22	Reporter gene (lux AB)	Bioluminiscence	Culture media/ artificially inoculated egg	6 h/ 16-24	10 CFU mL^{-1}/ 63 CFU mL^{-1}	Chen and Griffiths 1996[250]
P22	Reporter gene (lux AB)	Bioluminiscence	Culture media, poultry and feed samples	16h	$1.6x10^3$ CFU mL^{-1}	Thouand et al. 2008 [44]

SJ2	Phage-based cell lysis and adenylate kinase monitoring	Bioluminiscence (using firefly luciferase assay)	Culture media	2h	10^3 CFU mL^{-1}	Wu et al. 2001 [291]
Lytic phage	Phage-based cell lysis of bacteria absorbed on polypyrrole	Impedance	Culture media	4-5h	10^3 CFU mL^{-1}	Dadarwal et al. 2009 [292]
Filamentous- phage	Phage physically adsorbed on piezoelectric platform	QCM (Quartz Crystal Microbalance)	Buffer	1h	10^2 CFU mL^{-1}	Olsen et al. 2006 [268]
Landscape phage, E2	Phage physically adsorbed on sensor	Magnetoelastic biosensor	Buffer/ water and fat-free milk	30 min-1h	10^3 CFU mL^{-1}/ $5x10^3$ CFU mL^{-1}	Lakshmanan 2007a and b[269,293]; Huang et al. 2009 [294]
E2	Phage physically adsorbed on sensor	Magnetoelastic biosensor	Tomato	30 min	$5x10^2$ CFU mL^{-1}	Li et al. 2010[270]
-E2	Phage physically adsorbed on sensor	Magnetoelastic biosensor	Eggshells	30 min	$1.6x10^2$ CFU mL^{-1}	Chai et al. 2012 [295]
P22 tailspike protein (TSP) with a cysteine tag	TSP immobilized onto gold coated surfaces using thiol-chemistry	SPR (Surface Plasmon Resonance)	Culture media	30 min	10^3 CFU mL^{-1}	Singh et al. 2010 [283]
P22 TSP with cysteine and polyhistidine tags	TSP conjugated to silica encapsulated SERS nanoprobes	Agglutination assay with optical and SEM imaging	Buffer	n.r.	Single cell limit	Tay et al. 2012 [284]
P22, UV inactivated	Phagomagnetic Separation (PMS) coupled to double-tagging PCR	Electrochemical magneto genosensing with amperometric detection	Culture media	4h	3 CFU mL^{-1}	Liébana et al. 2013 [244]

This dissertation addresses a comprehensive study and development of novel and rapid immunological methodologies in different analytical formats by the integration of micro and nanoparticles as well as hybrid bionanoparticles including bacteriophages focused on food safety. The specificity of phages for the biorecognition of pathogenic bacteria was exploited in magnetic particles- based sensing platforms as well as for the development of host-specific nanotags. Both types of strategies were applied in phagoassays and phagosensors for the improved electrochemical or optical detection of the target bacteria.

1.8 REFERENCES

(1) Nawaz, S. In *Encyclopedia of Food Science and Nutrition*; Caballero, B.; Trugo, L.; Finglas, P. M., Eds.; Academic Press: New York, 2003; pp. 4487–4493.

(2) Dwivedi, H. P.; Jaykus, L.-A. *Critical Reviews in Microbiology* **2011**, *37*, 40–63.

(3) Rooney, R.; Wall, P. G. In *Encyclopedia of Food Sciences and Nutrition*; Caballero, B.; Trugo, L.; Finglas, P., Eds.; Academic Press, 2003; pp. 2682–2688.

(4) Food borne diseases http://www.who.int/topics/foodborne_diseases/en/index.html (accessed Jul 29, 2013).

(5) Knura, S.; Gymnich, S.; Rembialkowska, G.; Pettersen, B. In *Safety in Agri-Food Chain*; Luning, P. A.; Devlieghere, F.; Verhé, R., Eds.; Wageningen Academic Publishers: Wageningen (Netherlands), 2006; pp. 19–61.

(6) Roberts, D. In *Encyclopedia of Food Science and Nutrition*; Caballero, B.; Trugo, L.; Finglas, P. M., Eds.; Academic Press: New York, 2003; pp. 2654–2658.

(7) Todd, E. In *Encyclopedia of Food Science and Nutrition*; Caballero, B.; Trugo, L.; Finglas, P. M., Eds.; Academic Press: New York, 2003.

(8) WHO; FAO *UNDERSTANDING THE CODEX ALIMENTARIUS*; CODEX Secretariat; FAO, Eds.; 3rd ed.; Rome, 2006.

(9) Slatter, J. In *Encyclopedia of Food Sciences and Nutrition*; Academic Press: Oxford, 2003; pp. 3023–3028.

(10) Poms, R. E.; Anklam, E. *Frontis* **2005**, *10*, 77–83.

(11) Sampson, H. A. *Journal of Allergy and Clinical Immunology* **1999**, *103*, 717–728.

(12) Wüthrich, B. *Journal of Investigational Allergology and Clinical Immunology* **2000**, *10*, 59–65.

(13) Ortolani, C.; Ispano, M.; Scibilia, J.; Pastorello, E. A. *Allergy* **2001**, *56*, 5–8.

(14) Woods, R. K.; Stoney, R. M.; Raven, J.; Walters, E. H.; Abramson, M.; Thien, F. C. *European Journal of Clinical Nutrition* **2002**, *56*, 31–36.

(15) Taylor, S. *Food Technology* **1992**, *46*, 148–152.

(16) Ciclitira, P. J. *Digestive and Liver Disease* **2002**, *34*, 214–215.

(17) Poms, R. E.; Klein, C. L.; Anklam, E. *Food additives and contaminants* **2004**, *21*, 1–31.

(18) Balkenhohl, T.; Lisdat, F. *The Analyst* **2007**, *132*, 314–22.

(19) Lee, S. K.; Green, P. H. R. *Current Opinion in Rheumatology* **2006**, *18*, 101–107.

(20) Woodward, J. *Medicine* **2007**, *35*, 226–230.

(21) Dewar, D. H.; Ciclitira, P. J. *Gastroenterology* **2005**, *128*, S19–S24.

(22) Wieser, H. *Food microbiology* **2007**, *24*, 115–9.

(23) Da Silva Neves, M. M. P.; González-Garcia, M. B.; Nouws, H. P. A.; Delerue-Matos, C.; Santos-Silva, A.; Costa-García, A. *Analytical and bioanalytical chemistry* **2010**, *397*, 1743–53.

(24) Pividori, M. I.; Lermo, a; Bonanni, a; Alegret, S.; Del Valle, M. *Analytical biochemistry* **2009**, *388*, 229–34.

(25) Kagnoff, M. F. *Gastroenterology* **2005**, *128*, S10–S18.

(26) McGough, N.; Cummings, J. H. *Proc. Nutr. Soc.* **2005**, *64*, 434–450.

(27) Stern, M.; Ciclitira, P. J.; Van Eckert, R.; Feighery, C.; Janssen, F. W.; Méndez, E.; Mothes, T.; Troncone, R.; Wieser, H. *Eur J Gastroenterol Hepatol* **2001**, *13*, 741–747.

(28) Dulay, S.; Lozano-Sánchez, P.; Iwuoha, E.; Katakis, I.; O'Sullivan, C. K. *Biosensors & bioelectronics* **2011**, *26*, 3852–3856.

(29) Shan, L.; Molberg, Ø.; Parrot, I.; Hausch, F.; Filiz, F.; Gray, G. M.; Sollid, L. M.; Khosla, C. *Science (New York, N.Y.)* **2002**, *297*, 2275–9.

(30) Shan, L.; Qiao, S.-W.; Arentz-Hansen, H.; Molberg, Ø.; Gray, G. M.; Sollid, L. M.; Khosla, C. *J. Proteome Res.* **2005**, *4*, 1732–1741.

(31) Haraszi, R.; Chassaigne, H.; Maquet, A.; Ulberth, F. *Journal of AOAC International* **2011**, *94*, 1006–1025.

(32) Collin, P.; Thorell, L.; Kaukien, K.; Mäki, M. *Aliment. Pharmacol. Ther.* **2004**, *19*, 1277–1283.

(33) Khosla, C.; Gray, G. M.; Sollid, L. M. *Gastroenterology* **2005**, *129*, 1362–1363.

(34) Stern, M. *European journal of gastroenterology & hepatology* **2005**, *17*, 523–4.

(35) Catassi, C.; Ratsch, I. M.; Fabiani, E.; Rossini, M.; Bordicchia, F.; Candela, F.; Coppa, G. V.; Giorgi, P. L. *Lancet* **1994**, *343*, 200–203.

(36) Thompson, T.; Méndez, E. *Journal of the American Dietetic Association* **2008**, *108*, 1682–7.

(37) Diaz-Amigo, C.; Popping, B. *Journal of Agricultural and Food Chemistry* **2013**, *61*, 5681–5688.

(38) Velusamy, V.; Arshak, K.; Korostynska, O.; Oliwa, K.; Adley, C. *Biotechnology Advances* **2009**, *28*, 232–54.

(39) Pandey, A.; Joshi, V. K.; Nigam, P.; Soccol, C. R. In *Encyclopedia of Food Microbiology*; Academic Press: Oxford, 2004; pp. 604–610.

(40) Hanes, D. In *International Handbook of Foodborne Pathogens*; Miliotis, M. D.; Bier, J. W., Eds.; Marcel Dekker Inc: New York, 2003.

(41) Slauch, J. M.; Mahan, M. J.; Michettu, P.; Neutra, M. R.; Mekalanos, J. J. *Infection & Immunity* **1995**, *63*, 437–441.

(42) Zhang, S. DEVELOPMENT OF A BIOSENSOR FOR THE RAPID DETECTION OF, Auburn University, 2005.

(43) Smartt, A. E.; Xu, T.; Jegier, P.; Carswell, J. J.; Blount, S. a; Sayler, G. S.; Ripp, S. *Analytical and Bioanalytical Chemistry* **2012**, *402*, 3127–46.

(44) Thouand, G.; Vachon, P.; Liu, S.; Dayre, M.; Griffiths, M. W. *Journal of Food Protection* **2008**, *71*, 380–5.

(45) Valcárcel, M.; Ríos, A. *Trends in Analytical Chemistry* **2000**, *19*, 593–598.

(46) Valcárcel, M.; Lendl, B. *TrAC Trends in Analytical Chemistry* **2004**, *23*, 527–534.

(47) Muñoz-Olivas, R. *TrAC Trends in Analytical Chemistry* **2004**, *23*, 203–216.

(48) Socaciu, C. In *Safety in Agri-Food Chain*; Luning, P.; Devlieghere, F.; Verhé, R., Eds.; Wageningen Academic Publishers: Wageningen (Netherlands), 2006.

(49) Bergwerff, A. A.; Schloesser, J. In *Encyclopedia of Food Science and Nutrition*; Caballero, B.; Trugo, L.; Finglas, P. M., Eds.; Academic Press: New York, 2003; pp. 254–261.

(50) Holbrook, R. In *The microbiological safety and quality of food*; Lund, B.; Baird-Parker, T. C.; Gould, G. W., Eds.; Aspen Publ.: Gaithersburg, Maryland, 2000; pp. 1761–1790.

(51) Alegret, S.; Pividori, I. In *Comprehensive Analytical Chemistry*; Alegret, S.; Mercoçi, A., Eds.; Elsevier B.V., 2007.

(52) Franek, M.; Hruska, K. *Vet. Med. - Czech* **2005**, *50*, 1–10.

(53) Nesterenko, I. S.; Nokel, M. A.; Eremin, S. A. *Journal of Analytical Chemistry* **2009**, *64*, 434–444.

(54) Chu, F. S. *Encyclopedia of Food Sciences and Nutrition.*; Academic Press: Oxford, 2003; pp. 3248–3255.

(55) Spinks, C. A. *Trends in Food Science and Technology* **2000**, *11*, 210–217.

(56) Woof, J.; Burton, D. *Nat Rev Immunol* **2004**, *4*, 89–99.

(57) Abbas, A. K.; Lichtman, A. H. *Cellular and molecular immunology*; 5th ed.; Saunders, 2003.

(58) Sharma, A. In *Encyclopedia of Food Microbiology*; Elsevier: Oxford, 1999; pp. 625–633.

(59) Janeway, C. *Immunobiology*; 5th ed.; Garland Publishing, 2001.

(60) Berg, J. .; Tymoczko, J. L.; Stryer, L. In *Biochemistry*; W H Freeman: New York, 2002; p. Section 4.3.

(61) Kane, M. M.; Banks, J. N. In *Immunoassays: a practical approach*; Goosling, J., Ed.; Oxford University Press: Oxford, 2000.

(62) Switzer, R.; Garrity, L. *Experimental biochemistry*; W.H. Freemen and company: England, 1999.

(63) Bhunia, A. K.; Ball, P. H.; Fuad, A. T.; Kurz, B. W.; Emerson, J. W.; Johnson, M. G. *Infect. Immun.* **1991**, *59*, 3176–3184.

(64) Liddell, E. In *The Immunoassay Handbook*; Wild, D., Ed.; Elsevier Ltd: New York, 2005.

(65) Banada, P. P.; Bhunia, A. K. In *Principles of Bacterial Detection: Biosensors, Recognition Receptors and Microsystems*; Zourob, M.; Elwary, S.; Turner, A., Eds.; Springer: New York, 2008; pp. 567–602.

(66) Hock, B. *Acta Hydrochimica and Hydrobiologica* **2002**, *29*, 375–390.

(67) Kramer, K.; Hock, B. *Analytical and Bioanalytical Chemistry* **2003**, *377*, 417–426.

(68) Emanuel, P. A.; Dang, J.; Gebhardt, J. S.; Aldrich, J.; Garber, E. A. E.; Kulaga, H.; Stopa, P.; Valdes, J. J.; Dion-Schultz, A. *Biosensors & Bioelectronics* **2000**, *14*, 751–759.

(69) Posner, B.; Lee, I.; Itoh, T.; Pyati, J.; Graff, R.; Thorton, G. B.; Lapolla, R.; Benkovic, S. J. *Gene* **1993**, *128*, 111–117.

(70) Hoogenboom, H. R. *Nature Biotechnol.* **2005**, *23*, 1105–1116.

(71) Koivunen, M. E.; Krogsrud, R. L. *Labmedicine* **2006**, *37*, 490–497.

(72) Wilson, K.; Walker, J. In *Principles and Techniques of Biochemistry and Molecular Biology*; Cambridge University Press: Hong Kong, 2005; pp. 292–348.

(73) Schetters, H. *Biomolec Eng.* **1999**, *16*, 73–78.

(74) Antibody Labeling http://www.thermosavant.com/eThermo/CMA/PDFs/Product/productPDF_5058.pdf (accessed Sep 17, 2013).

(75) Hermanson, G. . *Bioconjugate Techniques*; 2nd ed.; Academic Press: Rockford, IL, 2008.

(76) *Immunoassay and Other Bioanalytical Methods*; van Emon, J. M., Ed.; CRC Press: Boca Ratón, FL, 2007.

(77) Wilchek, M.; Bayer, E. A. *Analytical Biochemistry* **1988**, *171*, 1–32.

(78) Wilcheck, M.; Bayer, E. A.; Livnah, O. *Immunology Letters* **2006**, *103*, 27–32.

(79) Orth, R. N.; Clark, T. G.; Craighead, H. G. *Biomedical microdevices* **2003**, *5*, 29–34.

(80) Green, N. M. *Methods Enzymol.* **1990**, *184*, 51–67.

(81) Jones, M. L.; Kurzban, G. P. *Biochemistry* **1995**, *34*, 11750–11756.

(82) ABC Peroxidase Staining Kits Instruction, from Thermo Scientific. http://www.piercenet.com/product/abc-staining-kits (accessed Sep 22, 2013).

(83) Hsu, S. M.; Raine, L.; Fanger, H. *American Journal of Clinical Pathology* **1981**, *75*, 734–738.

(84) Harlow, E.; Lane, D. *Antibodies - a laboratory manual.*; Harbor, C. S., Ed.; Cold Spring Harbor Laboratory Press: New York, 1988; p. 726.

(85) Mahon, C. R.; Tice, D. *Clinical Laboratory Immunology*; Pearson Education, Inc: Upper Saddle River, NJ, 2006; p. 325.

(86) Lequin, R. M. *Clinical Chemistry* **2005**, *51*, 2415–2418.

(87) Jenkins, S. H.; Heineman, W. R.; Halsall, H. B. *Analytical Biochemistry* **1988**, *168*, 292–299.

(88) Kaneki, N.; Xu, Y.; Kumari, A.; Halsall, H. B.; Heineman, W. R.; Kissinger, P. T. *Anal. Chim. Acta* **1994**, 253–258.

(89) Wijayawardhana, C. A.; Halsall, H. B.; Heineman, W. R. *Analytica Chimica Acta* **1999**, *399*, 3–11.

(90) Kenna, J. G.; Major, G. N.; Williams, R. S. *Journal of Immunological Methods* **1985**, *85*, 409–419.

(91) Vogt Jr, R. .; Phillips, D. L.; Henderson, L. O.; Whitfield, W.; Spierto, F. W. *Journal of Immunological Methods* **1987**, *101*, 43–50.

(92) Pividori, M. I.; Alegret, S. In *Biosensors in Food Processing, Safety, and Quality Control*; Mutlu, M., Ed.; CRC Press: Boca Ratón, 2011; pp. 89–117.

(93) Clark, L. C. *Trans Am Soc Art Int Org* **1956**, *2*, 41–48.

(94) Clark, L. C.; Lyons, C. *Ann NY Acad Sci* **1962**, *102*, 29–45.

(95) González, V.; García, E.; Ruiz, O.; Gago, L. *Aplicaciones de biosensores en la industria agroalimentaria. Informe de vigilancia tecnológica de la comunidad de Madrid.*; Elecé Industria Gráfica: Madrid, 2005; p. 113.

(96) Thakur, M. S.; Ragavan, K. V. *Journal of Food Science and Technology* **2012**, *50*, 625–641.

(97) Turner, A. P. F.; Karube, I.; Wilson, G. S. *Biosensors, fundamentals and applications*; Oxford University Press: Oxford, 1987.

(98) Thévenot, D. R.; Toth, K.; Durst, R. A.; Wilson, G. S. *Pure Appl. Chem.* **1999**, *71*, 2333–2348.

(99) Taylor, R. F.; Schultz, J. S. *Handbook of Chemical and Biological Sensors*; Institute of Physics Publishing: Bristol, UK, 1996.

(100) Wang, J. *Nucleic Acids Res.* **2000**, *28*, 3011–3016.

(101) Sharma, S. K.; Sehgal, N.; Kumar, A. *Current Applied Physics* **2003**, *3*, 307–316.

(102) Bučko, M.; Mislovičová, D.; Nahálka, J.; Vikartovská, A.; Šefčovičová, J.; Katrlík, J.; Tkáč, J.; Gemeiner, P.; Lacík, I.; Štefuca, V.; Polakovič, M.; Rosenberg, M.; Rebroš, M.; Šmogrovičová, D.; Švitel, J. *Chemical Papers* **2012**, *66*, 983–998.

(103) Eggins, B. R. *Biosensors, an introduction*; John Wiley & Sons Ltd.: New York, 1996; pp. 31–50.

(104) Gorton, L. *Electroanalysis* **1995**, *7*, 23–45.

(105) Céspedes, F.; Alegret, S. *Trends in analytical chemistry* **2000**, *19*, 276–285.

(106) Nilsson, P. Biosensor technology applied to hybridization analysis and mutation detection, KTH – Royal Institute of technology, Stockholm (Sweden), 1998.

(107) Velasco-García, M.; Mottram, T. *Biosystems Engineering* **2003**, *84*, 1–12.

(108) Mello, L. D.; Kubota, L. T. *Food Chemistry* **2002**, *77*, 237–256.

(109) Grieshaber, D.; MacKenzie, R.; Vörös, J.; Reimhult, E. *Sensors* **2008**, *8*, 1400–1458.

(110) Wang, J. *Analytical Electrochemistry*; 2nd ed.; John Wiley & Sons VCH: Hoboken, New Jersey, 2006.

(111) Eggins, B. R. *Chemical Sensors and Biosensors*; John Wiley & Sons Ltd.: West Sussex, England, 2002.

(112) Alegret, S. In *Biosensores electroquímicos*; Alegret, S.; Yamanaka, H.; Pividori, M. I., Eds.; Cyted, 2007; pp. 7–18.

(113) Karyakin, A. A.; Vuki, M.; Lukachova, L. V.; Karyakina, E. E.; Orlov, A. V.; Karpachova, G. P.; Wang, J. . *Analytical Chemistry* **1999**, *71*, 2534–2540.

(114) Ruiz, J. G. Desarrollo de biosensores enzimáticos miniaturizados para su aplicación en la industria alimentaria, Universidad Autónoma de Barcelona, 2006.

(115) Terry, L. A.; White, S. F.; Tigwell, L. J. *Journal of Agricultural and Food Chemistry* **2005**, *53*, 1309–1316.

(116) Brajter-Toth, A.; Chambers, J. Q. *Electroanalytical Methods for Biological Materials*; Dekker, M., Ed.; New York - Basel, 2002.

(117) Bakker, E.; Qin, Y. *Analytical chemistry* **2006**, *78*, 3965–84.

(118) Ronkainen, N. J.; Halsall, H. B.; Heineman, W. R. *Chemical Society reviews* **2010**, *39*, 1747–63.

(119) Bakker, E.; Diamond, D.; Lewenstam, A.; Pretsch, E. *Analytica Chimica Acta* **1999**, *393*, 11–18.

(120) Yuqing, M.; Jianguo, G.; Jianrong, C. *Biotechnology Advances* **2003**, *21*, 527–534.

(121) Tothill, I. E.; Turner, A. P. F. *Biosensors. Encyclopedia of Food Science and Nutrition*; Elsevier: Oxford, 2003; pp. 489–499.

(122) Wang, J. In *Analytical Electrochemistry*; Wiley-VCH: New York, 2000; pp. 28–40.

(123) Ricci, F.; Adornetto, G.; Palleschi, G. *Electrochimica Acta* **2012**, *84*, 74–83.

(124) Koyun, A.; Ahlatcıoğlu, E.; İpek, Y. K. In *A roadmap of Biomedical Engineers and Milestones*; Kara, S., Ed.; InTech: Rijeka (Croatia), 2012.

(125) Ricci, F.; Volpe, G.; Micheli, L.; Palleschi, G. *Analytica Chimica Acta* **2007**, *605*, 111–129.

(126) Wang, H.; Shen, G.; Yu, R. In *Electrochemical sensors, biosensors and their biomedical applications*; Academic Press: Oxford, 2008; pp. 237–260.

(127) Ghindilis, A. L.; Atanasov, P.; Wikins, M.; Wikins, E. *Biosensors & Bioelectronics* **1998**, *13*, 113–131.

(128) Stefan, R. I.; Van Staden, J. F.; Aboul-Enein, H. Y. *Analitical & Bioanalytical Chemistry* **2000**, *366*, 659–668.

(129) Wan, Y.; Su, Y.; Zhu, X.; Liu, G.; Fan, C. *Biosensors & bioelectronics* **2013**, *47*, 1–11.

(130) Zacco, E.; Adrian, J.; Galve, R.; Marco, M.-P.; Alegret, S.; Pividori, M. I. *Biosensors & Bioelectronics* **2007**, *22*, 2184–91.

(131) O'Conell, P. In *Encyclopedia of Dairy Sciences*; Elsevier: Oxford, 2004; pp. 101–106.

(132) Skoog, D. A.; West, D. A.; Holler, F. J.; Crouch, S. R. *Química analítica*; 8th ed.; Editorial Thomson: Buenos Aires (Argentina), 2006.

(133) Gileadi, E. *Electrode Kinetics for Chemists, Chemical Engineers, and Material Scientists*; VCH Publishers, Inc: New York, 1993.

(134) Lermo, A. Nous dissenys biomoleculars en genosensors i immunosensors per a la seguretat alimentaria, Autonomous University of Barcelona, 2009.

(135) Ferreira, A. A. P.; Riccardi, C. D. .; Yamanaka, H. In *Biosensores electroquímicos*; Alegret, S.; Yamanaka, H.; Pividori, M. I., Eds.; Cyted, 2007; pp. 39–47.

(136) López, G. M. A.; Ortiz de Apodaca, F. O. *Schironia* **2002**, *1*, 51–59.

(137) Zhang, S.; Wright, G.; Yang, Y. *Biosensors & bioelectronics* **2000**, *15*, 273–82.

(138) Céspedes, F.; Martínez-Fábregas, E.; Alegret, S. *Trends in analytical chemistry* **1996**, *15*, 296–304.

(139) Gilmartin, N.; O'Kennedy, R. *Enzyme and microbial technology* **2012**, *50*, 87–95.

(140) Tallury, P.; Malhotra, A.; Byrne, L. M.; Santra, S. *Advanced drug delivery reviews* **2010**, *62*, 424–37.

(141) Theron, J.; Eugene Cloete, T.; De Kwaadsteniet, M. *Critical Reviews in Microbiology* **2010**, *36*, 318–39.

(142) Li, C. M.; Hu, W. *Journal of Electroanalytical Chemistry* **2013**, *688*, 20–31.

(143) Li, K.; Nguyen, H. G.; Lu, X.; Wang, Q. *The Analyst* **2010**, *135*, 21–7.

(144) Cháfer-Pericás, C.; Maquieira, a.; Puchades, R. *TrAC Trends in Analytical Chemistry* **2012**, *31*, 144–156.

(145) De la Escosura-Muñiz, A.; Parolo, C.; Merkoçi, A. *Materials Today* **2010**, *13*, 24–34.

(146) Johnson, C. J.; Zhukovsky, N.; Cass, A. E. G.; Nagy, J. M. *Proteomics* **2008**, *8*, 715–30.

(147) Smartt, A. E.; Ripp, S. *Analytical and Bioanalytical Chemistry* **2011**, *400*, 991–1007.

(148) Pankhurst, Q. a; Connolly, J.; Jones, S. K.; Dobson, J. *Journal of Physics D: Applied Physics* **2003**, *36*, R167–R181.

(149) Tartaj, P.; Morales, M. a D. P.; Veintemillas-Verdaguer, S.; Gonz lez-Carre o, T.; Serna, C. J. *Journal of Physics D: Applied Physics* **2003**, *36*, R182–R197.

(150) Van Ommering, K. Dynamics of Individual Magnetic Particles near a Biosensor Surface, Eindhoven (The Netherlands) Printed by: Ipskamp Drukkers B.V., 2010.

(151) Wang, J.; Erdem, A. In *Nanostructured Materials and Coatings for Biomedical and Sensor Applications*; Gogotsi, I. G.; Uvarova, I. V., Eds.; Springer Netherlands, 2003; pp. 297–303.

(152) Solé, S.; Merkoçi, A.; Alegret, S. *Trends in analytical chemistry* **2001**, *20*, 102–110.

(153) Shoup, D.; Lipari, G.; Szabo, a *Biophysical journal* **1981**, *36*, 697–714.

(154) Baudry, J.; Rouzeau, C.; Goubault, C.; Robic, C.; Cohen-Tannoudji, L.; Koenig, a; Bertrand, E.; Bibette, J. *Proceedings of the National Academy of Sciences of the United States of America* **2006**, *103*, 16076–8.

(155) Gijs, M. A. M. *Microfluidics and Nanofluidics* **2004**, *1*, 22–40.

(156) Giouroudi, I.; Keplinger, F. *International journal of molecular sciences* **2013**, *14*, 18535–56.

(157) Xu, Y.; Wang, E. *Electrochimica Acta* **2012**, *84*, 62–73.

(158) Kourilov, V.; Steinitz, M. *Analytical Biochemistry* **2002**, *311*, 166–170.

(159) Dittmer, W. U.; De Kievit, P.; Prins, M. W. J.; Vissers, J. L. M.; Mersch, M. E. C.; Martens, M. F. W. C. *Journal of immunological methods* **2008**, *338*, 40–6.

(160) Centi, S.; Laschi, S.; Mascini, M. *Talanta* **2007**, *73*, 394–9.

(161) Zacco, E.; Pividori, M. I.; Alegret, S.; Galve, R.; Marco, M.-P. *Analytical Chemistry* **2006**, *78*, 1780–8.

(162) Lermo, a; Fabiano, S.; Hernández, S.; Galve, R.; Marco, M.-P.; Alegret, S.; Pividori, M. I. *Biosensors & Bioelectronics* **2009**, *24*, 2057–63.

(163) Liébana, S.; Lermo, A.; Campoy, S.; Cortés, M. P.; Alegret, S.; Pividori, M. I. *Biosensors & Bioelectronics* **2009**, *25*, 510–3.

(164) Yildiz, I.; Shukla, S.; Steinmetz, N. F. *Current Opinion in Biotechnology* **2011**, *22*, 901–908.

(165) Yacoby, I.; Bar, H.; Benhar, I. *Antimicrobial Agents and Chemotherapy* **2007**, *51*, 2156–2163.

(166) Ashley, C. E.; Carnes, E. C.; Phillips, G. K.; Durfee, P. N.; Buley, M. D.; Lino, C. a; Padilla, D. P.; Phillips, B.; Carter, M. B.; Willman, C. L.; Brinker, C. J.; Caldeira, J. D. C.; Chackerian, B.; Wharton, W.; Peabody, D. S. *ACS nano* **2011**, *5*, 5729–45.

(167) Li, K.; Chen, Y.; Li, S.; Nguyen, H. G.; Niu, Z.; You, S.; Mello, C. M.; Lu, X.; Wang, Q. *Bioconjugate chemistry* **2010**, *21*, 1369–77.

(168) Robertson, K. L.; Soto, C. M.; Archer, M. J.; Odoemene, O.; Liu, J. L. *Bioconjugate chemistry* **2011**, *22*, 595–604.

(169) Lee, L. A.; Niu, Z.; Wang, Q. *Nano Research* **2009**, *2*, 349–364.

(170) Portney, N. G.; Martinez-morales, Ḱ. A. A.; Ozkan, M. *ACS nano* **2008**, *2*, 191–196.

(171) Mateu, M. G. *Protein Engineering, Design & Selection* **2011**, *24*, 53–63.

(172) Zourob, M.; Ripp, S. In *Recognition Receptors in Biosensors*; Zourob, M., Ed.; Springer: New York, 2010; pp. 415–448.

(173) Kutter, E.; Sulakvelidze, A. *Bacteriophages: biology and applications*; CRC Press: Boca Ratón, FL, 2005.

(174) Mandeville, R.; Griffiths, M.; Goodridge, L.; McIntyre, L.; Ilenchuk, T. T. *Analytical Letters* **2003**, *36*, 3241–3259.

(175) Calender, R. *The bacteriophages*; 2nd editio.; Oxford University Press: New York, 2006.

(176) Lander, G. C.; Tang, L.; Casjens, S. R.; Gilcrease, E. B.; Prevelige, P.; Poliakov, A.; Potter, C. S.; Carragher, B.; Johnson, J. E. *Science* **2006**, *312*, 1791–1795.

(177) Kang, S.; Hawkridge, A. M.; Johnson, K. L.; Muddiman, D. C.; Prevelige, P. E. *Journal of Proteome Research* **2006**, *5*, 370–7.

(178) Baxa, U.; Steinbacher, S.; Miller, S.; Weintraub, A.; Huber, R.; Seckler, R. *Biophysical Journal* **1996**, *71*, 2040–2048.

(179) Steinbacher, S.; Miller, S.; Baxa, U.; Budisa, N.; Weintraub, A.; Seckler, R.; Huber, R. *Journal of Molecular Biology* **1997**, *267*, 865–880.

(180) Pirisi, A. *The Lancet* **2000**, *356*, 1418.

(181) Stone, R. *Science* **2002**, *298*, 728–731.

(182) Thiel, K. *Nature Biotechnology* **2004**, *22*, 31–36.

(183) Van Dorst, B.; Mehta, J.; Bekaert, K.; Rouah-Martin, E.; De Coen, W.; Dubruel, P.; Blust, R.; Robbens, J. *Biosensors & Bioelectronics* **2010**, *26*, 1178–94.

(184) Handa, H.; Gurczynski, S.; Jackson, M. P.; Auner, G.; Mao, G. *Surface Science* **2008**, *602*, 1392–1400.

(185) Mosier-Boss, P. A.; Lieberman, S. H.; Andrews, J. M.; Rohwer, F. L.; Wegley, L. E.; Breitbart, M. *Applied Spectroscopy* **2003**, *57*, 1138–1144.

(186) Schmelcher, M.; Loessner, M. J. In *Principles of bacterial detection: biosensors, recognition receptors, and microsystems.*; Zourob, M.; Elwary, S.; Turner, A., Eds.; Springer: New York, 2008; pp. 731–754.

(187) Hagens, S.; Loessner, M. J. *Applied Microbiology and Biotechnology* **2007**, *76*, 513–9.

(188) Camafeita, E.; Alfonso, P.; Mothes, T.; Méndez, E. *Journal of mass spectrometry : JMS* **1997**, *32*, 940–7.

(189) Camafeita, E.; Solís, J.; Alfonso, P.; López, J. a; Sorell, L.; Méndez, E. *Journal of chromatography. A* **1998**, *823*, 299–306.

(190) Mamone, G.; Ferranti, P.; Chianese, L.; Scafuri, L.; Addeo, F. *Rapid communications in mass spectrometry : RCM* **2000**, *14*, 897–904.

(191) Sealey-Voyksner, J. A.; Khosla, C.; Voyksner, R. D.; Jorgenson, J. W. *Journal of Chromatography A* **2010**, *1217*, 4167–4183.

(192) Köppel, E.; Stadler, M.; Luthy, J.; Hubner, P. *Z. Lebensm. Unters. Forsch.* **1998**, *206*, 399–403.

(193) Dahinden, I.; Von Büren, M.; Lüthy, J. *Eur. Food Res. Technol.* **2001**, *212*, 228–233.

(194) Sandberg, M.; Lundberg, L.; Ferm, M.; Malmheden Yman, I. *European Food Research and Technology* **2003**, *217*, 344–349.

(195) Olexová, L.; Dovičovičová, L.; Švec, M.; Siekel, P.; Kuchta, T. *Food Control* **2006**, *17*, 234–237.

(196) Mujico, J. R.; Lombardía, M.; Mena, M. C.; Méndez, E.; Albar, J. P. *Food Chemistry* **2011**, *128*, 795–801.

(197) Capparelli, R.; Ventimiglia, I.; Longobardo, L.; Iannelli, D. *Cytometry A* **2006**, *63A*, 108–113.

(198) Varriale, A.; Rossi, M.; Staiano, M.; Terpetschnig, E.; Barbieri, B.; Rossi, M.; D'Auria, S. *Anal. Chem.* **2007**, *79*, 4687–4689.

(199) Sánchez-Martínez, M. L.; Aguilar-Caballos, M. P.; Gómez-Hens, A. *Analytical chemistry* **2007**, *79*, 7424–30.

(200) Mairal, T.; Frese, I.; Llaudet, E.; Redondo, C. B.; Katakis, I.; Von Germar, F.; Drese, K.; O' Sullivan, C. K. *Lab on a chip* **2009**, *9*, 3535–42.

(201) Zeltner, D.; Glomb, M. a.; Maede, D. *European Food Research and Technology* **2008**, *228*, 321–330.

(202) Ellis, H. J.; Rosen-Bronson, S.; O'Reilly, N.; Ciclitira, P. J. *Gut* **1998**, *43*, 190–5.

(203) Valdés, I.; García, E.; Llorente, M.; Méndez, E. *Eur. J. Gastroenterol. Hepatol.* **2003**, *15*, 465–474.

(204) Morón, B.; Cebolla, Á.; Manyani, H.; Álvarez-Maqueda, M.; Megías, M.; Thomas, M. del C.; Manuel Carlos López, A.; Sousa, C. *Am. J. Clin. Nutr.* **2008**, *87*, 405–414.

(205) Morón, B.; Bethune, M. T.; Comino, I.; Manyani, H.; Ferragud, M.; López, M. C.; Cebolla, A.; Khosla, C.; Sousa, C. *PloS one* **2008**, *3*, e2294.

(206) Skerritt, J. H.; Hill, A. S. *Journal of Agricultural and Food Chemistry* **1990**, *38*, 1771–1778.

(207) Kanerva, P. M.; Sontag-Strohm, T. S.; Ryöppy, P. H.; Alho-Lehto, P.; Salovaara, H. O. *Journal of Cereal Science* **2006**, *44*, 347–352.

(208) Méndez, E.; Vela, C.; Immer, U.; Janssen, F. W. *Eur. J. Gastroenterol. Hepatol.* **2005**, *17*, 1053–1063.

(209) Immer, U.; Vela, C.; Mendez, E.; Jenssen, F. In *Proceedings of the 17th Meeting of the Working Group on Prolamin Analysis and Toxicity (October 3–6, 2002, London, UK)*; Stern, M., Ed.; Verlag Wissenschafliche Scripten: Zwickau, Germany, 2003; pp. 22–23.

(210) Lester, D. R. *Plant methods* **2008**, *4*, 26.

(211) Ferre, S.; García, E.; Méndez, E. In *Proceedings of the 18th Meeting Working Group on Prolamin Analysis and Toxicity*; Stern, M., Ed.; Verlag Wissenschafliche Scripten: Zwickau, Germany, 2004; pp. 65–69.

(212) Gessendorfer, B.; Koehler, P.; Wieser, H. *Analytical and Bioanalytical Chemistry* **2009**, *395*, 1721–1728.

(213) Nassef, H. M.; Redondo, M. C. B.; Paul, J.; Ellis, H. J.; Fragoso, A.; Sullivan, C. K. O.; Ciclitira, P. J. *Analytical Chemistry* **2008**, *80*, 9265–9271.

(214) De Stefano, L.; Rossi, M.; Staiano, M.; Mamone, G.; Parracino, A.; Rotirotti, L.; Rendina, I.; D'Auria, S. *J. Proteome Res.* **2006**, *5*, 1241–1245.

(215) De Stefano, L.; Rendina, I.; Mario Rossi, A.; Rossi, M.; Rotiroti, L.; D'Auria, S. *Journal of Physics: Condensed Matter* **2007**, *19*, 395007 (5pp).

(216) Nassef, H. M.; Civit, L.; Fragoso, A.; O'Sullivan, C. K. *Analytical chemistry* **2009**, *81*, 5299–307.

(217) McKillop, D. F.; Gosling, J. P.; Stevens, F. M.; Fottrell, P. F. *Biochemical Society Transactions* **1985**, *13*, 486–487.

(218) Freedman, A. R.; Galfre, G.; Gal, E.; Ellis, H. J.; Ciclitira, P. J. *Journal of Immunological Methods* **1987**, *98*, 123–127.

(219) Chirdo, F. G.; Añón, M. C.; Fossati, C. A. *Food and Agricultural Immunology* **1995**, *7*, 333–343.

(220) Chirdo, F. G.; Añón, M. C.; Fossati, C. A. *Food and Agricultural Immunology* **1998**, *10*, 143–155.

(221) Sorell, L.; López, J. a; Valdés, I.; Alfonso, P.; Camafeita, E.; Acevedo, B.; Chirdo, F.; Gavilondo, J.; Méndez, E. *FEBS letters* **1998**, *439*, 46–50.

(222) Sánchez-Martínez, M. L.; Aguilar-Caballos, M. P.; Gómez-Hens, a. *Analytica Chimica Acta* **2004**, *523*, 35–41.

(223) Gabrovská, D.; Rysová, J.; Filová, V.; Plicka, J.; Cuhra, P.; Kubík, M.; Baršová, S. *Journal of AOAC International* **2006**, *89*, 154–160.

(224) Sánchez, D.; Tucková, L.; Burkhard, M.; Plicka, J.; Mothes, T.; Hoffmanová, I.; Tlaskalová-Hogenová, H. *Journal of agricultural and food chemistry* **2007**, *55*, 2627–32.

(225) Upmann, M.; Bonaparte, C. In *Encyclopedia of Food Microbiology*; Robinson, R. K.; Batt, C. A.; Patel, P. D., Eds.; Academic Press: London, 2000; pp. 1887–1895.

(226) Tietjen, M.; Fung, D. Y. C. *Crit. Rev. Microbiol.* **1995**, *21*, 53–83.

(227) Amaguaña, R.; Andrews, W. *Encyclopedia of Food Microbiology*; Robinson, R.; Batt, C.; Patel, P., Eds.; Academic Press: New York, NY, 2004; p. 1948.

(228) Humphrey, T.; Stephens, P. In *Encyclopedia of Food Science and Nutrition*; Caballero, B.; Trugo, L.; Finglas, P. M., Eds.; Academic Press: New York, 2003; pp. 5079–5084.

(229) López-Campos, G.; Martínez-Suarez, J. V.; Aguado-Urda, M.; López-Alonso, V. In *Microarray Detection and Characterization of Bacterial Foodborne Pathogens*; Springer: New York, 2012.

(230) McClelland, R. G.; Pinder, A. C. *Applied and Environmental Microbiology* **1994**, *60*, 4255–4262.

(231) Jasson, V.; Jacxsens, L.; Luning, P.; Rajkovic, A.; Uyttendaele, M. *Food Microbiology* **2010**, *27*, 710–730.

(232) Cudjoe, K. S. In *Encyclopedia of Food Microbiology*; Robinson, R. K.; Batt, C. A.; Patel, P., Eds.; Academic Press, 1999; p. 1968.

(233) Setterington, E. B.; Alocilja, E. C. *Biosensors* **2012**, *2*, 15–31.

(234) Wan, J.; King, K.; Craven, H.; Mcauley, C.; Tan, S. E.; Coventry, M. J. *Letters in Applied Microbiology* **2000**, *30*, 267–271.

(235) Ge, B.; Meng, J. *Journal of Laboratory Automation* **2009**, *14*, 235–241.

(236) Leonard, P.; Hearty, P.; Brennan, J.; Dunne, L.; Quinn, J.; Chakraborty, T. O'Kennedy, R. *Enzyme and Microbial Technology* **2003**, *32*, 3–13.

(237) Arora, P.; Sindhu, A.; Dilbaghi, N.; Chaudhury, A. *Biosensors & Bioelectronics* **2011**, *28*, 1–12.

(238) Taylor, A. D.; Ladd, J.; Yu, Q. M.; Chen, S. F.; Homola, J.; Jiang, S. Y. *Biosensors & Bioelectronics* **2006**, *22*, 752–758.

(239) Pividori, M. I.; Merkoçi, A.; Barbé, J.; Alegret, S. *Electroanalysis* **2003**, *15*, 1815–1823.

(240) Erdem, A.; Pividori, M. I.; Del Valle, M.; Alegret, S. *J. Electroanal. Chem.* **2004**, *567*, 29–37.

(241) Erdem, A.; Pividori, M. I.; Lermo, A.; Bonanni, A.; Del Valle, M.; Alegret, S. *Sensors and Actuators B* **2006**, *114*, 591–598.

(242) Lermo, A.; Campoy, S.; Barbé, J.; Hernández, S.; Alegret, S.; Pividori, M. I. *Biosensors and Bioelectronics Bioelectronic* **2007**, *22*, 2010–2017.

(243) Oliveira Marques, P. R. B.; Lermo, A.; Campoy, S.; Yamanaka, H.; Barbé, J.; Alegret, S.; Pividori, M. I. *Analytical Chemistry* **2009**, *81*, 1332–1339.

(244) Liébana, S.; Spricigo, D. A.; Cortés, M. P.; Barbe, J.; Alegret, S.; Pividori, M. I. *Analytical Chemistry* **2013**, *85*, 3079–3086.

(245) Goodridge, L.; Chen, J.; Griffiths, M. *Applied and environmental microbiology* **1999**, *65*, 1397–404.

(246) Kenzaka, T.; Utrarachkij, F.; Suthienkul, O.; Nasu, M. *Health Science* **2006**, *52*, 666–671.

(247) Edgar, R.; McKinstry, M.; Hwang, J.; Oppenheim, A. B.; Fekete, R. A.; Giulian, G.; Merril, C.; Nagashima, K.; Adhya, S. *Proceedings of the National Academy of Sciences of the United States of America* **2006**, *103*, 4841–4845.

(248) Yim, P. B.; Clarke, M. L.; McKinstry, M.; De Paoli Lacerda, S. H.; Pease, L. F.; Dobrovolskaia, M. a; Kang, H.; Read, T. D.; Sozhamannan, S.; Hwang, J. *Biotechnology and Bioengineering* **2009**, *104*, 1059–67.

(249) Carrico, Z. M.; Farkas, M. E.; Zhou, Y.; Hsiao, S. C.; Marks, J. D.; Chokhawala, H.; Clark, D. S.; Francis, M. B. *ACS nano* **2012**, *6*, 6675–6680.

(250) Chen, J.; Griffiths, M. *Journal of Food Protection* **1996**, *59*, 908–914.

(251) Kuhn, J.; Suissa, M.; Chiswell, D.; Azriel, A.; Berman, B.; Shahar, D.; Reznick, S.; Sharf, R.; Wyse, J.; Bar-On, T.; Cohen, I.; Giles, R.; Weiser, I.; Lubinsky-Mink, S.; Ulitzur, S. *International Journal of Food Microbiology* **2002**, *74*, 217–27.

(252) Oda, M.; Morita, M.; Unno, H.; Tanji, Y. *Appl Environ Microbiol* **2004**, *70*, 527–534.

(253) Tanji, Y.; Furukawa, C.; Na, S.; Hijikata, T.; Miyanaga, K.; Unno, H. *J Biotechnol* **2004**, *114*, 11–20.

(254) Goodridge, L.; Griffiths, M. W. *Food Research International* **2002**, *35*, 863–870.

(255) Wolber, P. K. *Adv Microb Physiol* **1993**, *34*, 203–237.

(256) Stewart, G. S. A. B.; Jassim, S. A. A.; Denyer, S. P.; Newby, P.; Linley, K.; Dhir, V. K. *Journal of Applied Microbiology* **1998**, *84*, 777–783.

(257) Favrin, S. J.; Jassim, S. A.; Griffiths, M. W. *Applied and Environmental Microbiology* **2001**, *67*, 217–224.

(258) Jassim, S. a a; Griffiths, M. W. *Letters in applied microbiology* **2007**, *44*, 673–8.

(259) Neufeld, T.; Schwartz-Mittelmann, A.; Biran, D.; Ron, E. Z.; Rishpon, J. *Analytical Chemistry* **2003**, *75*, 580–5.

(260) Squirrell, D. J.; Price, R. L.; Murphy, M. J. *Anal. Chim. Acta* **2002**, *457*, 109–114.

(261) Blasco, R.; Murphy, M. J.; Sanders, M. F.; Squirrell, D. J. *Journal of Applied Microbiology* **1998**, *84*, 661–666.

(262) Singh, A.; Arutyunov, D.; Szymanski, C. M.; Evoy, S. *The Analyst* **2012**, *137*, 3405–21.

(263) Singh, A.; Poshtiban, S.; Evoy, S. *Sensors* **2013**, *13*, 1763–86.

(264) Shabani, A.; Zourob, M.; Allain, B.; Marquette, C. a; Lawrence, M. F.; Mandeville, R. *Analytical Chemistry* **2008**, *80*, 9475–82.

(265) Bennet, A. R.; Davids, F. G.; Valhodimou, S.; Banks, J. G.; Betts, R. P. *Journal of Applied Microbiology* **1997**, *83*, 259– 265.

(266) Balasubramanian, S.; Sorokulova, I.; Vodyanoy, V. I.; Simonian, A. L. *Biosensors & bioelectronics* **2007**, *22*, 948–955.

(267) Nanduri, V.; Sorokulova, I.; Samoylov, A.; Simonian, A.; Petrenko, V.; Vodyanoy, V. *Biosens Bioelectron* **2007**, *22*, 986–992.

(268) Olsen, E. V; Sorokulova, I. B.; Petrenko, V. a; Chen, I.-H.; Barbaree, J. M.; Vodyanoy, V. J. *Biosensors & bioelectronics* **2006**, *21*, 1434–42.

(269) Lakshmanan, R. S.; Guntupalli, R.; Hu, J.; Petrenko, V. A.; Barbaree, J. M.; Chin, B. A. *Sensors and Actuators B* **2007**, *126*, 544–550.

(270) Li, S.; Li, Y.; Chen, H.; Horikawa, S.; Shen, W.; Simonian, A.; Chin, B. a *Biosensors & Bioelectronics* **2010**, *26*, 1313–1319.

(271) Park, M.-K.; Park, J. W.; C. Wikle III, H. *Journal of Biosensors & Bioelectronics* **2012**, *03*, 1–8.

(272) Sun, W.; Brovko, L.; Griffiths, M. *Journal of Industrial Microbiology & Biotechnology* **2001**, *27*, 126–128.

(273) Gervais, L.; Gel, M.; Allain, B.; Tolba, M.; Brovko, L.; Zourob, M.; Mandeville, R.; Griffiths, M.; Evoy, S. *Sensors and Actuators B* **2007**, *125*, 615–621.

(274) Tolba, M.; Minikh, O.; Brovko, L. Y.; Evoy, S.; Griffiths, M. W. *Applied and Environmental Microbiology* **2010**, *76*, 528–35.

(275) Jabrane, T.; Dubé, M.; Mangin, P. J. In *Proceedings of Canadian PAPTAC 95th Annual Meeting 2009*; Montreal (Canada), 2009; pp. 31–314.

(276) Cademartiri, R.; Anany, H.; Gross, I.; Bhayani, R.; Griffiths, M.; Brook, M. a *Biomaterials* **2010**, *31*, 1904–10.

(277) Anany, H.; Chen, W.; Pelton, R.; Griffiths, M. W. *Applied and Environmental Microbiology* **2011**, *77*, 6379–6387.

(278) Torrance, L.; Ziegler, A.; Pittman, H.; Paterson, M.; Toth, R.; Eggleston, I. *Journal of Virology Methods* **2006**, *134*, 164–170.

(279) Singh, a; Glass, N.; Tolba, M.; Brovko, L.; Griffiths, M.; Evoy, S. *Biosensors & bioelectronics* **2009**, *24*, 3645–51.

(280) Arya, S. K.; Singh, A.; Naidoo, R.; Wu, P.; McDermott, M. T.; Evoy, S. *The Analyst* **2011**, *136*, 486–92.

(281) Naidoo, R.; Singh, A.; Arya, S. K.; Beadle, B.; Glass, N.; Jamshid, T.; Szymanski, C. M.; Evoy, S. *Bacteriophage* **2012**, *2*, 15–24.

(282) Handa, H.; Gurczynski, S.; Jackson, M. P.; Mao, G. *Langmuir* **2010**, *26*, 12095–103.

(283) Singh, A.; Arya, S. K.; Glass, N.; Hanifi-Moghaddam, P.; Naidoo, R.; Szymanski, C. M.; Tanha, J.; Evoy, S. *Biosensors & Bioelectronics* **2010**, *26*, 131–8.

(284) Tay, L.-L.; Huang, P.-J.; Tanha, J.; Ryan, S.; Wu, X.; Hulse, J.; Chau, L.-K. *Chemical Communications* **2012**, *48*, 1024–1026.

(285) Singh, A.; Arutyunov, D.; McDermott, M. T.; Szymanski, C. M.; Evoy, S. *Analyst* **2011**, *136*, 4780–4786.

(286) Javed, M. a; Poshtiban, S.; Arutyunov, D.; Evoy, S.; Szymanski, C. M. *PloS one* **2013**, *8*, e69770.

(287) Hirsh, D. C.; Martin, L. D. .

(288) Favrin, S. J.; Jassim, S. a.; Griffiths, M. W. *International Journal of Food Microbiology* **2003**, *85*, 63–71.

(289) Ulitzur, N.; Ulitzur, S. *Applied and environmental microbiology* **2006**, *72*, 7455–9.

(290) Wolber, P. K.; Green, R. L. *Trends in Biotechnology* **1990**, *8*, 276–279.

(291) Wu, Y.; Brovko, L.; Griffiths, M. W. *Letters in Applied Microbiology* **2001**, *33*, 311–315.

(292) Dadarwal, R.; Namvar, A.; Thomas, D. F.; Hall, J. C.; Warriner, K. *Materials Science & Engineering C—Biomimetic and Supramolecular Systems* **2009**, *29*, 761–765.

(293) Lakshmanan, R. S.; Guntupalli, R.; Hu, J.; Kim, D. J.; Petrenko, V. A.; Barbaree, J. M.; Chin, B. A. *Journal of Microbiological Methods* **2007**, *71*, 55–60.

(294) Huang, S.; Yang, H.; Lakshmanan, R. S.; Johnson, M. L.; Wan, J.; Chen, I.-H.; Wikle, H. C.; Petrenko, V. a; Barbaree, J. M.; Chin, B. a *Biosensors & bioelectronics* **2009**, *24*, 1730–6.

(295) Chai, Y.; Li, S.; Horikawa, S.; Park, M.-K.; Vodyanoy, V.; Chin, B. A. *Journal of Food Protection* **2012**, *75*, 631–636.

CHAPTER 2

AIMS OF RESEARCH AND DISSERTATION OUTLINE

This dissertation addresses the development of improved immunoanalytical strategies for the detection of allergens and contaminants affecting food safety, by the integration of micro and nanoparticles on the immunochemical reaction. To achieve this task, two different targets (nano and micro sized) were explored: on one hand, the gliadin in gluten-free foodstuff, and on the other, the pathogenic bacteria *Salmonella enterica* serovar Thyphimurium. The outstanding features of the magnetic particles as platforms for the immunoassay were comprehensible studied in order to minimize the matrix effect and to increase the sensitivity. Moreover, the integration of bionanomaterials as bacteriophages to the immunoassays was also explored.

The general aim was the development and optimization of different immunoassay formats (competitive and sandwich, direct and indirect), performed on micro- or nanostructured magnetic particles, and the evaluation of the matrix effect and analytical performance of the different strategies using spiked samples. For both targets the immunochemical systems were evaluated by dual detection through optical and electrochemical readouts. The capabilities to achieve selective and sensitive detection strategies and to improve the performance of current detection methods were also explored.

Therefore the following specific objectives have been pursued in this work:

- To study novel immobilization strategies for the covalent binding of different bioreceptors on micro and nanosized magnetic platforms in an oriented way.
- To characterize the biomolecule orientation immobilized on the magnetic carriers, as well as to study its coupling efficiency.
- To develop and assess the analytical performance of different immunoassay formats, such as competitive and sandwich, as well as to optimize the incubation conditions and immunoreagents concentration in order to achieve an improved magneto immunoassay system.
- To achieve the labeling of phage nanoparticles for the electrochemical and optical tagging of bacteria and their detection.
- To exploit the use of bottom-up hybrid nanomaterials such as phage-modified gold nanoparticles and phage-modified magnetic nanoparticles as bioanalytical tools for bacteria tagging.

- To study the capabilities of magnetic-phage hybrid nanoparticles to capture and pre-concentrate bacteria from complex food samples.
- To design novel biosensing analytical systems based on phage nanoparticles as a biorecognition element for pathogenic bacteria detection.
- To assess the accuracy of the different immunochemical strategies for the detection of food allergens and contaminants in spiked food samples.

Dissertation outline

The next chapters present the experimental work carried out in this dissertation, as well as the achieved results, discussion and conclusions. **Chapter 3** describes the construction of the magneto-electrodes and their electrochemical characterization, while Chapters 4 to 8 present the developed immunoanalytical strategies using magnetic particles and hybrid bionanoparticles for the optical or electrochemical detection of the model targets, consisting each chapter of a short introduction, a brief description of the specific aim, experimental section, results and discussion, and a conclusion related to each specific work. On one hand, **Chapter 4** shows the integration of magnetic particles in a competitive immunoassay, applied for the detection of gliadin in gluten-free foodstuff. And on the other, **Chapters 5 to 8** describe the design of novel immunoanalytical strategies in non-competitive format for the screen-out of *Salmonella* by the integration of magnetic carriers and bacteriophages. The design of optical immunoassays and electrochemical immunosensors based on bacteriophages can be separated in two main research lines, based on the use of the P22 phage towards *Salmonella* as a model: a) the use of biotinylated bacteriophage as specific and sensitive tagging reagent (Chapters 5 and 6) and, b) the integration of the phagic nanoparticles as biorecognition elements in magnetic micro and nanoparticles (Chapters 7 and 8). Finally, in **Chapter 9** the general conclusions are presented, as well as future perspectives on the application of the developed work.

CHAPTER 3

CONSTRUCTION AND CHARACTERIZATION OF MAGNETO GRAPHITE-EPOXY COMPOSITE ELECTRODES

3.1 INTRODUCTION

One of the main expertise areas in our group is the construction of conducting rigid graphite-epoxy composites (GEC), by using epoxy resin as the polymeric matrix[1,2]. GEC material is highly moldable before curing, permitting the easy construction of amperometric sensors of various shapes and sizes. In addition, once the material is cured, it is very resistant from a mechanical point of view, being stable at moderately high temperatures and even in the presence of organic solvents. Moreover, the surface can be renewed with a simple polishing procedure allowing the indefinitely reuse of the electrodes.

Regarding the electrochemical properties, GEC is made of small conductive graphite particles dispersed in a polymeric matrix. This configuration acts as a microelectrode array, showing higher signal-to-nonspecific adsorption ratio and lower detection limits when compared to other well-known carbon electrodes as glassy carbon. The high sensitivity of this electrochemical transducer, coupled with its compatibility with miniaturization and mass fabrication technologies, makes it very attractive for quick and simple analyses in industrial applications.[3]

On the other hand, their utility as biosensors transducer was widely demonstrated in many applications. Different biomolecules (DNA and proteins) were shown to be tightly immobilized under static conditions to the GEC surface through simple adsorption procedures, obtaining a stable and reproducible biorecognition element for the subsequent electrochemical detection. However, the adsorption in the presence of water and under stirring is negligible, showing thus low nonspecific adsorption. All these features make them good candidates to be integrated in bioinstrumentation.[4]

Other variations of the GEC electrodes were also introduced, showing a high versatility. Firstly, biocomposites were developed by integrating a biological material directly in the composite, acting the GEC in this case not only as transducer but also as a reservoir of the biological material. Biocomposites have the main advantage of a simplification in the methodology, saving time through the elimination of the immobilization step and permitting a very easy renewal of the surface with the integrated biorecognition element through a simple polishing action.[3,5]

On the other hand, the introduction of a small neodymium magnet inside the GEC electrodes (m-GEC) designed in our laboratories allowed the electrochemical genosensing[6] and immunosensing[7]. The performance of immunoassays on magnetic particles as solid support, provide many advantageous features to the immunosensing approach, based on the concept of magnetic bioseparation and minimized matrix effect, [7] as well as the easy magnetic immobilization of the biorecognition element on the transducer surface, as extensively explained in Chapter 1 (§ 1.5.1).

In the present dissertation, m-GEC electrodes were used in all the developed strategies coupled to electrochemical detection and the biorecognition element was attached on the transducer by magnetic immobilization. This chapter describes the construction of the m-GEC working electrodes and their further characterization using cyclic voltammetry.

3.2. AIM OF THE CHAPTER

This chapter is focused on the construction and characterization of the working electrodes and magneto electrodes based on conducting graphite-epoxy composite.

Therefore the specific objectives of this chapter were the following:

- To construct the working electrodes based on magneto graphite-epoxy composites.
- To establish the reduction potential of the benzoquinone on the constructed electrodes (that will be consequently applied for all amperometric measurements).
- To assess the reproducibility of the construction and renewing process of the prepared m-GEC.
- To study the effect of capturing the modified magnetic particles (with gliadin, antibodies or phages as biorecognition element) on the electrode surface.
- To analyze the reusability of the modified m-GEC electrodes.

3.3 EXPERIMENTAL SECTION

3.3.1 Materials

The graphite-epoxy composite was prepared using 50 µm particle size graphite thin powder (product nº 1.04206.2500, Merck, Darmstadt, Germany), an epoxy resin and hardener (product Nº Epo-Tek H77, Epoxy Technology, USA). The body of the electrodes consists of PVC tubes of 6 mm i.d., 8 mm o.d. and 22 mm long provided by a local retail store. For the electrical connection a female connector with a metal end of 2 mm in diameter (product nº 224CN, Onda Radio, Spain) and a copper disk with a diameter of 6 mm (local retail store) were used. The neodymium magnets used for the magneto-electrodes construction were from HALDE GAC (product nº N35D315). Before each use, the surface of the m-GEC electrode was thoroughly smoothed, first with abrasive paper of different thickness (local retail store) and then with alumina paper (polishing strips product nº 301044-001, Orion).

The voltammetric characterizations were carried out using an Autolab PGSTAT Eco-Chemie. A three-electrode setup was used, comprising a platinum auxiliary electrode (Crison 52-67 1, Spain), a double junction Ag/AgCl reference electrode (Orion 900200) with 0.1 mol L^{-1} KCl as the external reference solution, and a magneto graphite- epoxy composite (m-GEC) electrode as the working electrode.

The hydroquinone used as electroactive species for the electrochemical characterization was from Sigma-Aldrich (product nº H9003).

The buffer solutions were prepared with milli-Q water (Millipore Inc., Ω = 18 MΩ cm) and their compositions were: PBST (0.01 mol L^{-1} phosphate buffer, 0.15 mol L^{-1} NaCl, 0.05 % v/v Tween 20, pH 7.5); b-PBST (2 % w/v BSA in PBST as blocking buffer); and PBSE (0.1 mol L^{-1} sodium phosphate, 0.1 mol L^{-1} KCl, pH 7.0) for the electrochemical measurements.

The magnetic microparticles of 1 µm and 2.8 µm diameter with surface tosyl groups (Dynabeads MyOne^{TM} Tosylactivated, product no. 655.01 and Dynabeads M-280 Tosylactivated, product n° 142.03) for the covalent binding of gliadin and bacteriophages (to prepare the gliadin-MP and P22-MP conjugates), respectively, and the microparticles of 2.8 µm diameter coated with the specific high-affinity antibodies for the immunomagnetic separation of *Salmonella* (Dynabeads anti-*Salmonella*, product no. 710.02) were purchased from Invitrogen Dynal AS (Oslo, Norway). They are hydrophobic particles composed of paramagnetic γ-Fe_2O_3 and Fe_3O_4 nanoparticles dispersed in a polystyrene polymer matrix with an average magnetic content of 17 wt %.[8]

The magnetic separation of the particles during the washing steps was carried out using a magnetic separator for Eppendorf tubes Dynal MPC-S (Product no. 120.20D, Dynal Biotech ASA, Norway) and the incubations under shaking and/ or temperature control in Eppendorf tubes were performed using an Eppendorf Thermomixer compact.

3.3.2 Construction of the magneto electrodes based on graphite-epoxy composite (m-GEC)

The process followed for the construction of the m-GEC electrodes is schematically outlined in **¡Error! No se encuentra el origen de la referencia.** 3.1.

Firstly, the body and connection of the electrode had to be prepared (steps *i- iv*). With this aim copper disks used as electrical contact were cleaned to remove all copper oxide present on the surface by dipping it for a few seconds in 1:1 HNO_3 and rinsing immediately well with milli-Q water. The cleaned plates were then soldered to a female electric connector with a metal end of 2 mm diameter (*i*) using a Sn wire (*iii*). Afterwards, the female electric connector was set inside a cylindrical PVC tube (*iv*) using a hammer. A gap with a depth of 3 mm is thus obtained in the end of the body electrode.

In the meanwhile, the graphite- epoxy composite paste was prepared. The epoxy resin (Epo-Tek H77) was initially mixed with its hardener at a 20:3 (w/w) ratio, according to the manufacturer recommendations, and then graphite powder was added to this mix in a 1:4 (w/w) ratio. The mixture was thoroughly hand-mixed to ensure the uniform dispersion of the graphite powder throughout the polymer (approximately for 30 min). The resulting paste was placed in the 3 mm gap of the previous prepared PVC cylindrical sleeve body. A small neodymium magnet (3-mm i.d.) was placed into the center of the electrode after the addition of a thin layer of composite paste in order to avoid the direct contact between the magnet and the electrical connector (*v* and *vi*).

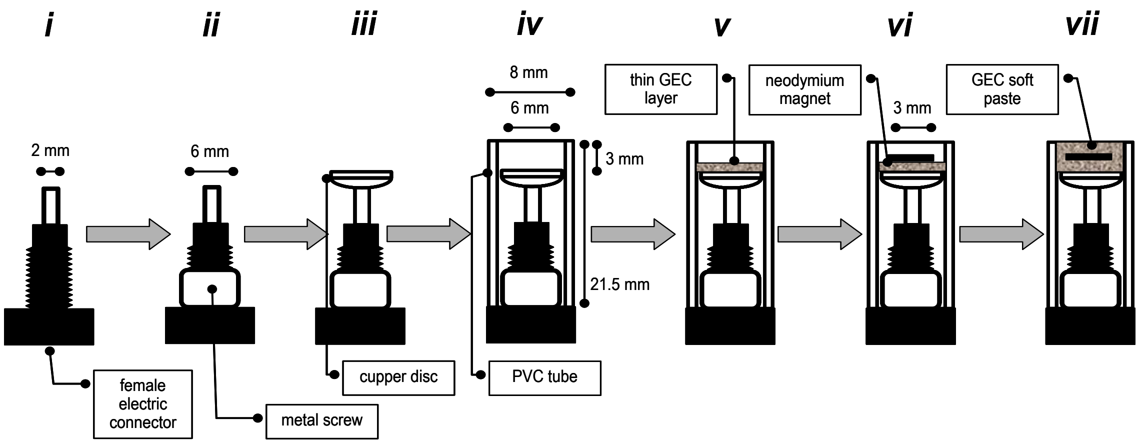
i
ii
iii
iv
v
vi
vii
8 mm
6 mm
thin GEC layer
neodymium magnet
3 mm
GEC soft paste
2 mm
6 mm
3 mm
21.5 mm
female electric connector
metal screw
cupper disc
PVC tube

Figure 3.1 Schematic representation of the steps followed for the construction of m-GEC electrodes.

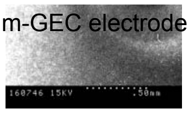
viii
ix
x
modified magnetic beads
m-GEC
150 µl of solution
eppendorf 2 ml
150 µl of solution
xii

Finally, after filling and tightly packing the GEC paste in the electrode body gap (*vii*), the m-GEC electrodes were cured at 90 ºC for 4 days in order to obtain a rigid composite. Before each use, the surface of the m-GEC electrodes were wetted with milli-Q water and then renewed and thoroughly smoothed by a simple polishing procedure, first with abrasive paper of different grit (500, 800 and 1000) and then with alumina paper. When not in use, the electrodes were stored in a dried place at room temperature.

3.3.3 Characterization of the m-GEC electrodes by cyclic voltammetry

Cyclic voltammetry is the most widely used technique for acquiring qualitative information about electrochemical reactions, providing rapidly considerable information on the thermodynamics of redox processes, on the kinetics of heterogeneous electron-transfer reactions, and on coupled chemical reactions or adsorption processes.[9]

The characterization of the previously prepared electrodes is performed through this technique, which consists of scanning linearly the potential applied over a stationary working electrode (in an unstirred solution) between two established potentials, first in one direction and then in the reverse until returning to the starting point. During the potential sweep the potentiostat measures the current and the resulting plot of current *vs.* potential is called voltammogram. This is a complex, time-dependent function of a large number of physical and chemical parameters, offering thus a rapid location of the redox potentials of the electroactive species and being the intensity directly related with their concentration.

The electrochemical properties of the electrodes were affected by the graphite-epoxy composite proportions and homogeneity as well as by the curing and renewing processes, being the electron transfer determined by the active conducting graphite area on the electrode surface. The electrochemical cell used for the voltammetric characterization was composed of a three-electrode setup (previously detailed in § 3.3.1) immersed in 20 mL PBSE buffer and the electrochemical response of the constructed electrodes was evaluated through the redox couple hydroquinone/ benzoquinone in a potential range between -0.6 and +1.0 V at a scan rate of 50 mV s^{-1}. The hydroquinone was added to the cell at a final concentration of 1.8 mmol L^{-1} and the measurements were carried out without stirring. Hydroquinone was chosen as electro-active specie since this was the mediator applied in all subsequent amperometric detection strategies that use horseradish peroxidase as enzymatic label.

Besides giving information about the reproducibility of the construction and renewing process of the prepared m-GEC, the voltammetric characterization provided the reduction potential of the benzoquinone on the constructed electrodes that were consequently applied for all amperometric measurements. The reduction potential was used to regenerate the hydroquinone previously oxidized by the peroxidase enzyme.

In addition to the four principal parameters obtained from the voltammogram, the cathodic and anodic peak currents and potentials (*Ipc, Ipa, Epc and Epa*), as shown in Figure 3.2, A, the position of the peaks on the potential axis is related to the formal potential of the redox process (Eº) and the peak separation (Δ*Ep*) gives information about the number of electrons transferred and the reversibility of the process. The formal potential for a reversible couple is centered between the anodic peak and cathodic peak potentials (*Epa* and *Epc*) and thus the separation between the peak potentials is given by:

$$\Delta Ep = Epa - Epc = (0.059/n)\ \text{V}$$

The redox reaction between benzoquinone and hydroquinone involves the transference of two electrons (*n*=2) as shown in Figure 3.2, B, and thus for a nernstian or reversible diffusion-controlled process a Δ*Ep* of around 30 mV would be expected.

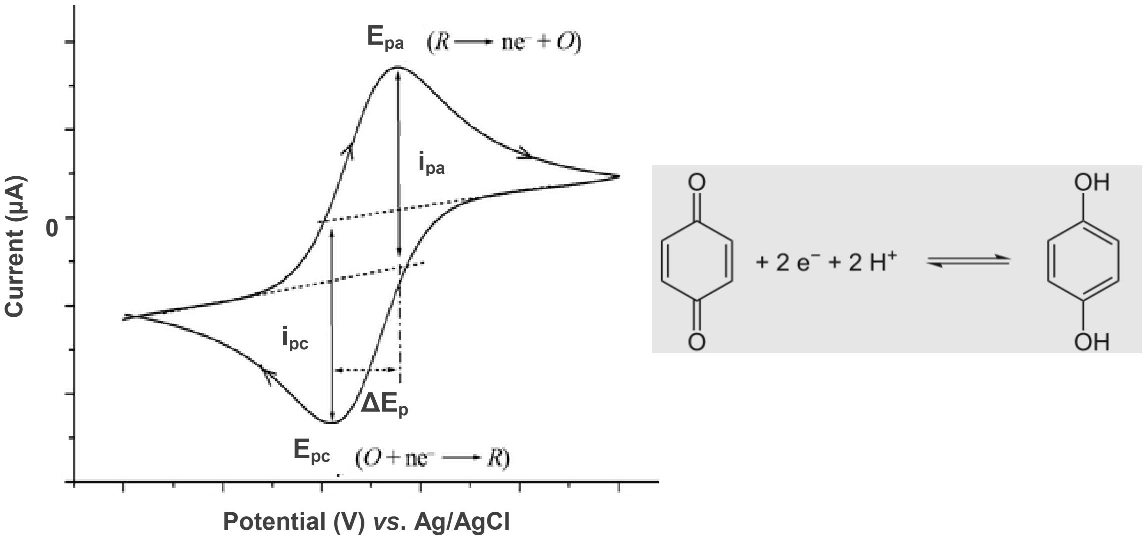
E_{pa} ($R \longrightarrow ne^- + O$)
i_{pa}
Current (μA)
0
i_{pc}
ΔE_p
E_{pc} ($O + ne^- \longrightarrow R$)
Potential (V) *vs*. Ag/AgCl
O
O
+ 2 e⁻ + 2 H⁺
OH
OH

Figure 3.2 (A) Schematic representation of a cyclic voltammogram, showing the anodic and the cathodic peaks (*pa* and *pc*), with the corresponding oxidation and reduction of the electroactive species (being *O* and *R* the oxidized and reduced forms, respectively.) (B) Redox reaction for the exchange between benzoquinone and hydroquinone taking place during the voltammetric measurements.

However, the reversibility of the redox reaction is not only evaluated by the Δ*Ep*, but also by the peak currents. In a reversible electron transfer process the anodic peak current should be the same than the cathodic peak current, being thus their ratio (*Ipa*/*Ipc*) equal to the unity for a simple reversible couple.[9,10]

The effect of the magnetic immobilization, in order to attach the biorecognition element (for instance the gliadin or the antibodies and bacteriophages with the captured bacteria) to the m-GEC transducer by means of the magnetic particles, was also analyzed. The details of the gliadin and phage immobilization procedures, as well as of the bacteria immuno and phagomagnetic separation are given in each corresponding chapter (§§ 4.3.2.2, 8.3.2.1, 5.3.3 and 8.3.3, respectively). The aim of this study was to analyze if the presence of the magnetic particles attached to proteins (in the case of gliadin detection) or bacteria (in the case of phage based detection) on the m-GEC electrode surface, affected the electrochemical behavior of the working electrodes. If some shift in the reduction potential of the benzoquinone was observed in the voltammograms, this should be the applied potential for the amperometric measurements carried out in the further detection strategies.

Finally, the reusability of the m-GEC electrodes was also studied.

3.4 RESULTS AND DISCUSSION

3.4.1 Characterization of the m-GEC electrodes by cyclic voltammetry

Figure 3.3, A illustrates the response of ten m-GEC electrodes of the same batch, i.e., prepared with the same graphite-epoxy paste, while Table 3.1 shows the average potential and current peaks values as well as the Δ*Ep* and *Iap*/*Icp* ratio calculated from the obtained voltammograms. The results demonstrated an outstanding reproducibility of construction as well as of the polishing process, confirming that they could be used equally for the replicates in the amperometric detection. In the case of observing some unusual behavior or peak shift, the affected electrodes were removed and not further used for the detection.

With the bare m-GEC electrodes the reduction peak for the benzoquinone was found to be around -0.100 V, while the oxidation peak of the hydroquinone around +0.180 V (*vs.* Ag/AgCl). Regarding the peak deviation of the electrodes batch, the obtained coefficient of variation (CV) values were 8.9 and 11.7 % for the anodic and cathodic potentials and 12.7 and 12.4 % for the anodic and cathodic currents, respectively.

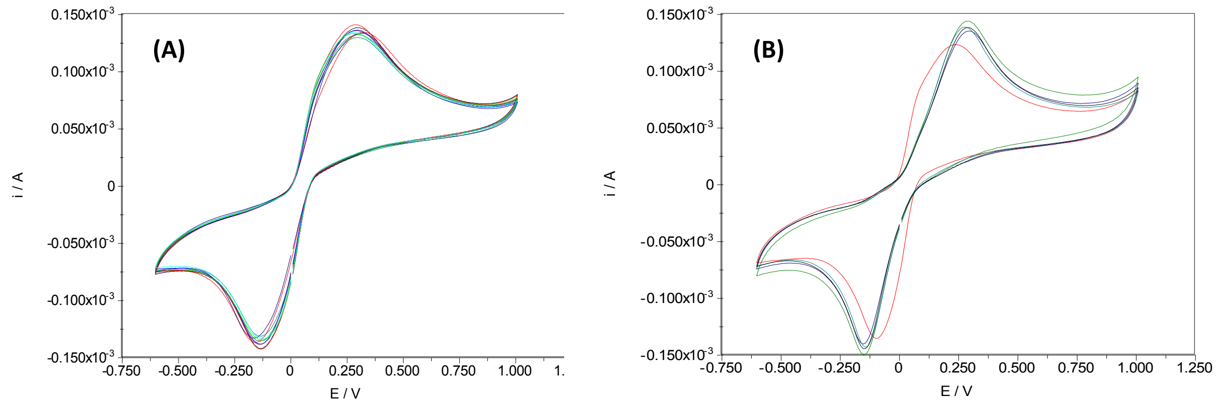

C:\Tamara\Caracterización mGEC abril 2011\HQ 280311 mGEC 1 bis.icw

C:\Tamara\Caracteriz mGEC 05.03.13\Electrodos Michelle\mGEC 6_HQ.icw

Figure 3.3 Electrochemical characterization by cyclic voltammetry of 10 m-GEC electrodes of the same batch (A) and comparison of the bare magneto electrode (in red) with MP modified m-GEC electrodes containing phage and captured bacteria (B). In all cases, 0.1 mol L^{-1} phosphate buffer, 0.1 mol L^{-1} KCl, pH 7.0 and 1.81x10^{-3} mol L^{-1} hydroquinone were used and the potentials were recorded *vs*. Ag/AgCl reference electrode, at a scan rate of 50 mV s^{-1}.

The effect of adding the modified magnetic particles on the electrode surface was also studied. With this aim the modified magnetic particles systems were analyzed, i.e. the gliadin-MP as well as the antibody-modified and phage- modified MP with attached bacteria by capturing the particles on the electrode surface and comparing the obtained cyclic voltammograms with the behavior of the bare magneto-electrodes. In the case of gliadin-MP, the presence of the magnetic particles did not influence the cyclic voltammetry, obtaining approximately the same redox peaks than with the bare electrodes. However, in the case of the phage-modified and antibody-modified magnetic particles with the captured bacteria a shift in the peaks could be observed as can be seen in Figure 3.3, B and Table 3.1. This change in the peak position increased thus the Δ*Ep* value indicating a slight impediment in the electron transfer at the electrode surface. However, the *Ipa*/*Ipc* ratio approached even more to the unity, which is another parameter of reversibility as previously explained.

Table 3.1 Potential and current peak values, ΔEp and Iap/Icp ratios for bare m-GEC electrodes as well as m-GEC modified with *Salmonella*-MP, obtained from the average of ten electrodes voltammograms registered using benzoquinone/ hydroquinone as redox couple.

	***Epa* (V)**	***Epc* (V)**	**Δ*Ep* (V)**	***Ipa* (µA)**	***Ipc* (µA)**	***Ipa*/*Ipc***
bare m-GEC	0.176	-0.096	0.272	137	150	0.91
m-GEC with *Salmonella*-MP	0.263	-0.140	0.403	116	114	0.98

Different magnetic particles concentrations (0.05, 0.1 and 0.2 mg mL^{-1}) were tested showing the same behavior in all cases. Since the average cathodic potential was around -0.140 V, a working potential of -0.150 V was accordingly selected for the subsequent amperometric detection of *Salmonella* in this dissertation. It should be pointed out that the presence of the modified magnetic particles on the electrode surface improved the reproducibility of the m-GEC electrodes, obtaining in this case CV values of 3.3 % in the anodic as well as the cathodic potential, and 7.5 and 6.3 % in the anodic and cathodic currents, respectively, for a batch of 10 electrodes.

Finally, the reusability of the modified m-GEC electrodes was also studied. Figure 3.4 shows the electrochemical characterization performed by cyclic voltammetry of a bare m-GEC electrode compared with a m-GEC electrode with gliadin-MP captured on the surface, after different renewal polishing processes.

As displayed in the figure, the electrochemical behavior of the m-GEC electrode was not modified due to the presence of the magnetic particles before the polishing procedure, thus confirming the reusability of the m-GEC electrode after the renewal process. The Figure shows successive rounds (five) of surface renewal.

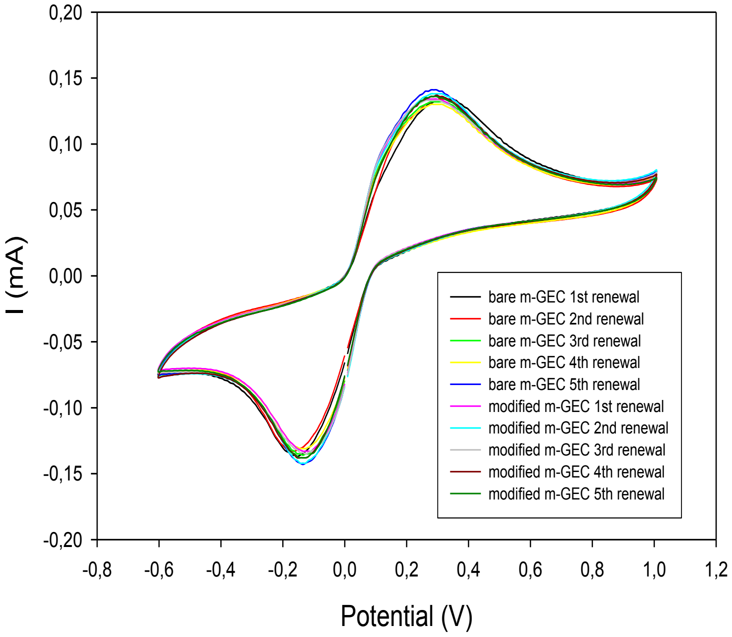

Figure 3.4 The voltammograms comparatively show the electrochemical signal of a bare m-GEC electrode with the m-GEC electrode modified with gliadin-MP 0.1 mg mL^{-1} and antiGliadin-HRP antibody diluted 1/4000, after renewal of the surface by polishing. Five successive rounds of renewal procedure are shown. The conditions were the same as described in Figure 3.3.

3.5 CONCLUSIONS

The constructed m-GEC electrodes were highly reproducible for their subsequent use in the immunochemical strategies based on electrochemical detection developed in this dissertation. Although the peak separation (ΔEp) was bigger than the expected value for a reversible system, the current ratio (Ipa/Ipc) was almost equal to 1, indicating reversibility.

The benzoquinone reduction potential established through the cyclic voltammetry characterization for further amperometric detection was -0.100 V for the gliadin-MP and -0.150 V for the *Salmonella* immuno- and phagomagnetic separation based strategies.

Finally, the reusability of the m-GEC electrodes was also demonstrated.

3.6 REFERENCES

(1) Céspedes, F.; Martínez-Fábregas, E.; Alegret, S. *Trends in analytical chemistry* **1996**, *15*, 296–304.

(2) Alegret, S.; Fabregas, E.; Cespedes, F.; Merkoci, A.; Sole, S.; Albareda, M.; Pividori, M. I. *Química Analítica* **1999**, *18*, 23–29.

(3) Alegret, S. *Analyst* **1996**, *121*, 1751–1758.

(4) Pividori, M. I.; Alegret, S. In *Immobilization of DNA on Chips I, Topics in Current Chemistry, Vol 260*; Wittman, C., Ed.; Springer Verlag: Berlin, 2005; pp. 1–36.

(5) Céspedes, F.; Alegret, S. *Trends in analytical chemistry* **2000**, *19*, 276–285.

(6) Pividori, M. I.; Alegret, S. *Analytical Letters* **2005**, *38*, 2541–2565.

(7) Zacco, E.; Pividori, M. I.; Alegret, S.; Galve, R.; Marco, M.-P. *Analytical Chemistry* **2006**, *78*, 1780–8.

(8) Gijs, M. A. M. *Microfluidics and Nanofluidics* **2004**, *1*, 22–40.

(9) Wang, J. In *Analytical Electrochemistry*; Wiley-VCH: New York, 2000; pp. 28–40.

(10) Bard, A. J.; Faulkner, L. R. *Electrochemical methods: fundamentals and applications*; 2nd editio.; John Wiley and Sons: New York, 2001; p. 833.

CHAPTER 4

INTEGRATION OF MAGNETIC MICRO AND NANOPARTICLES INTO COMPETITIVE IMMUNOASSAYS FOR THE DETECTION OF GLIADIN IN GLUTEN-FREE FOODSTUFF

4.1 INTRODUCTION

The detection of gliadin is of high interest for food safety of celiac patients, as previously mentioned in Chapter 1 (§ 1.1.1). Since the only treatment known until now is a lifelong avoidance of this protein in the diet, gluten has been included in food regulations.[1] Therefore it has been established that foods labeled with the term gluten-free, may not exceed a gluten content of 20 mg L^{-1}.[2] As a result, it is essential to have an easy and reliable method to detect gliadin, not only for the celiac patients, but also for the industries generating gluten-free foodstuffs in order to rapidly test incoming raw materials and check for gluten contamination throughout the food production process.[3,4]

The most commonly used methods for gliadin measurement are based on immunological procedures, including immunoblotting and Enzyme-Linked Immunosorbent Assay (ELISA), using monoclonal or polyclonal antibodies against a variety of gliadin components.[5] As detailed in § 1.6.2, different ELISAs are commercially available. However, the validated methods employ a sandwich format, being thus unable to detect small gluten fragments present in hydrolyzed foodstuff.[2,6]

Since biosensors are promising candidates for the rapid, real-time, simple, selective, and low cost decentralized analysis of foodstuff, two electrochemical immunosensors for gliadin determination based on gold electrodes and using a sandwich format were reported as an antecedent.[4,7]

This chapter is focused on the integration of magnetic particles into competitive immunoassays with electrochemical and optical detection taking as a model target the protein gliadin. To achieve this task, the development of two immunochemical strategies for the sensitive detection of gliadin and small gliadin fragment in natural or pre-treated food were performed: on one hand, a novel magneto immunoassay based on optical detection and on the other, an electrochemical magneto immunosensing approach. In both cases, the immunological reaction was performed on magnetic particles as a solid support in a competitive format. For the first time, the toxic protein fraction of gluten, gliadin, was successfully immobilized in an oriented way by covalent binding on tosylactivated magnetic particles as well as carboxyl-activated nanoparticles. The biorecognition strategy was based on a competitive assay, using commercially available antibodies with horseradish peroxidase (HRP) as enzymatic label. In the case of the electrochemical approach the modified magnetic particles were then captured onto the surface of a magneto electrode based on graphite-epoxy composite (m-GEC) for the further amperometric detection.

Direct, as well as indirect competitive immunoassays were comprehensively studied, achieving the best analytical performance with the direct competitive format. Excellent detection limits (in the order of μg L^{-1}) were achieved, according to the legislation for gluten-free products. Furthermore the matrix effect, as well as the performance of the assays was successfully evaluated using spiked gluten-free foodstuffs, such as skimmed milk and gluten-free beer, obtaining excellent recovery values.

4.2 AIM OF THE CHAPTER

This chapter addresses the covalent immobilization of gliadin on magnetic micro and nanoparticles and the further integration of the modified magnetic carriers in a competitive magneto immunoassay with optical detection as well as a competitive magneto immunosensing approach.

The specific objectives of this chapter were:

- To develop a covalent immobilization strategy for attachment of the antigen gliadin to micro and nanostructured magnetic particles.
- To evaluate the antigen orientation on the magnetic carrier and the coupling efficiency.
- To optimize the competitive magneto immunoassay format to detect the small gliadin fragments valid for both non-treated and hydrolyzed foodstuff, including the incubation conditions and immunoreagents concentration.
- To assess a dual detection system for the competitive magneto immunoassay based on both electrochemical and optical readouts.
- To design a novel competitive magneto immunosensing approach coupled to amperometric detection for the rapid, on-site testing of gliadin.
- To study the extraction procedure for the gliadin analysis in food samples as milk and beer and evaluate the matrix effect.
- To analyze the accuracy of both methods for the detection of gliadin in spiked food samples.

4.3 EXPERIMENTAL SECTION

4.3.1 Materials

4.3.1.1 Chemicals and biochemicals

The magnetic particles (MP) of 1 µm diameter modified with tosyl groups (Dynabeads MyOne^{TM} Tosylactivated, product nº 655.01) were purchased from Invitrogen Dynal AS (Oslo, Norway), while Activ-Adembeads (product discontinued) of 300 nm with already activated surface carboxylic groups were supplied by Ademtech SA (Pessac France). Dynabeads are hydrophobic particles composed of paramagnetic γ-Fe_2O_3 and Fe_3O_4 nanoparticles dispersed in a polystyrene polymer matrix with an average magnetic content of 17 wt %.[8] On the other hand, the magnetic nanoparticles consist of polymer-based magnetic particles with a core-shell structure, in which the core is maghemite γ-Fe_2O_3 (representing 70 wt %), while the shell is a styrene-based copolymer.

Gliadin from wheat was obtained from Sigma-Aldrich (product nº G3375) and stock solutions were prepared with 60 % (v/v) ethanol in carbonate buffer (0.05 M carbonate-bicarbonate, pH 9.6), and stored at room temperature for not longer than a month. Bovine serum albumin (BSA) and the polyclonal antibodies: anti-gliadin (wheat) antibodies (product nº G9144), anti-gliadin (wheat) antibodies- peroxidase conjugate (product nº A1052) (both developed in rabbit), and anti-IgG (rabbit)-peroxidase (product nº A8275) developed in goat, were purchased from Sigma-Aldrich.

Bradford solution (Coomassie Bradford Assay Kit, product nº 23200) and the peroxide and TMB (3,3',5,5'- tetrametylbenzidine) solutions utilized for the optical measurements (TMB Substrate Kit, product nº 34021) were purchased from Pierce.

The hydrogen peroxide 30 % used as a substrate in the electrochemical measurements was purchased from Merck (product nº 1.07209.0250, Germany), while the hydroquinone used as a mediator was from Sigma-Aldrich (product nº H9003).

All buffer solutions were prepared with milli-Q water (Millipore Inc., Ω = 18 MΩ cm) and all reagents were of the highest available grade, supplied from Sigma or Merck.

The composition of the solutions used for the immobilization on tosylactivated particles was: coating buffer (0.1 mol L^{-1} sodium borate, pH 8.5); ammonium sulfate (3 mol L^{-1} prepared in coating buffer), blocking buffer (0.01 mol L^{-1} sodium phosphate, 0.15 mol L^{-1} NaCl, 0.5 % w/v BSA, pH 7.4), washing buffer (0.01 mol L^{-1} sodium phosphate, 0.15 mol L^{-1} NaCl, 0,1 % w/v BSA, pH 7.2); and storage buffer (0.01 mol L^{-1} sodium phosphate, 0.15 mol L^{-1} NaCl, 0.1 % w/v BSA, 0.02 % (w/v) sodium azide, pH 7.4). For the immobilization on magnetic nanoparticles (Active-Adembeads), the activation and storage buffers were provided by the suppliers (Ademtech SA).

The cocktail solution used for the gliadin extraction procedure was constituted by: 5 mM dithiothreitol and 6 % SDS in PBS 1 mM, pH 7.4.

Finally, for the detection assays the following solutions were prepared: carbonate buffer (0.05 M carbonate-bicarbonate buffer, pH 9.6); PBST (0.01 mol L^{-1} phosphate buffer, 0.15 mol L^{-1} NaCl, 0.05 % v/v Tween 20, pH 7.5); b-PBST (2 % w/v BSA in PBST as blocking buffer); and PBSE (0.1 mol L^{-1} sodium phosphate, 0.1 mol L^{-1} KCl, pH 7.0) for the electrochemical measurements.

4.3.1.2 Instrumentation

The gliadin immobilization on the magnetic particles was carried out using a Labinco rotator (Model LD-79) with controlled rotation.

The magnetic separation of the particles was carried out using a magnetic separator for Eppendorf tubes Dynal MPC-S (product nº 120.20D, Dynal Biotech ASA, Norway) or a 96-well plate magnet (product nº 21358, Thermo Fisher Scientific, Waltham, USA). All the incubations and washing steps under shaking and/ or temperature control in Eppendorf tubes were performed using an Eppendorf Thermomixer compact, while the incubations and washing steps with the microtiter plates were performed using a Minishaker MS1 (IKA, Germany).

Polypropylene and polystyrene microtiter plates were purchased from Corning (product nº 153364) and Nunc (product nº 269787, Roskilde, DK), respectively. The first ones were used for the immunoassay performance with the magnetic particles while the second ones were used after the reaction with TMB and stop with H_2SO_4, by transferring the supernatants for the read-out. Optical measurements were performed in all cases on a TECAN Sunrise microplate reader with Magellan v4.0 software, as outlined in Figure 4.1.

In the case of the electrochemical detection, a three-electrode setup was used comprising a platinum auxiliary electrode (Crison 52-67 1), a double junction Ag/AgCl reference electrode (Orion 900200) with 0.1 mol L^{-1} KCl as the external reference solution, and a rigid and renewable magneto graphite-epoxy composite (m-GEC) electrode as the working electrode. Before each use, the surface of the m-GEC electrode was thoroughly smoothed, first with abrasive paper and then with alumina paper (polishing strips 301044-001, Orion). The reproducibility for the construction and the polishing procedure was previously evaluated as described in Chapter 3. Amperometric measurements were performed with a LC-4C amperometric controller (BAS Bioanalytical System Inc, U.S.), while voltammetric characterizations were carried out using an Autolab PGSTAT Eco-Chemie. The assembly for the amperometric detection is shown in Figure 4.2.

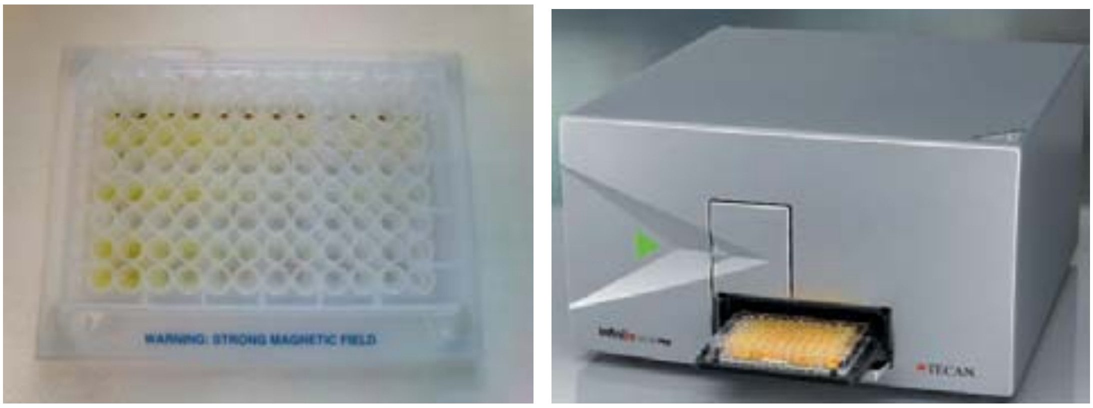

Figure 4.1 Polypropylene microtiter plate placed on the magnet for the capture of the magnetic particles before transferring the supernatants to the polystyrene plates for the final read-out (A) and image of a microplate reader used for the optical detection (B).

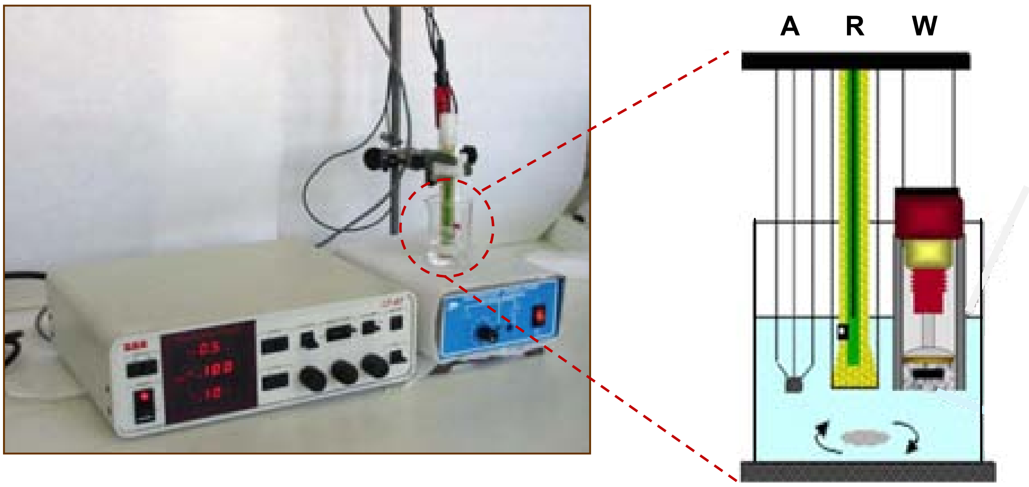

Figure 4.2 Ammeter used for all amperometric measurements with the whole system assembly and zoom in of the three-electrode setup used for the electrochemical measurements, showing the auxiliary (A), reference (R) and working (W) electrodes.

4.3.2 Gliadin binding on magnetic micro and nanoparticles and coupling efficiency

Gliadin was covalently coupled to 1 μm tosylactivated magnetic particles (MP) as well as to 300 nm activated carboxylic magnetic nanoparticles (nMP) through the reaction with the aminated and/ or thiolated aminoacidic moieties of the protein.[9,10] To control the nonspecific adsorption both kinds of magnetic particles were also modified with the inert protein bovine serum albumin, following the same immobilization protocols. Finally, the stability of the gliadin-modified MP was also studied on a monthly basis over a 7-month period.

4.3.2.1 Preparation of the gliadin stock solution

In order to follow the recommended protocol by Dynal, a gliadin stock solution with a concentration of 20 mg mL^{-1} had to be prepared for the immobilization. However, the first challenge was to be able to achieve this concentrated solution. The first attempt was to prepare a 200 mg mL^{-1} stock in milli-Q water but it was impossible to dissolve, not even by shaking and heating. The next try was to prepare directly the 20 mg mL^{-1} solution (0.1 g in 5 mL) in borate buffer (coating buffer) but unsuccessfully after shaking and heating up at 40 ºC overnight.

In parallel, the protein was tried to be dissolved in DMSO achieving the total dissolution by just shaking at room temperature.

Since previous studies about gliadin solubility demonstrated that it was totally soluble in aqueous solutions containing 60 % (v/v) ethanol,[11] the 20 mg mL^{-1} stock was prepared in 60 % ethanol with borate buffer. In this case the protein could be dissolved by shaking and after 20h incubation at 40ºC. This was finally the selected preparation for the stock solution since the suggested coating buffer could be added in this case.

4.3.2.2 Immobilization of gliadin to tosylactivated magnetic microparticles

The binding of the antigenic proteins to the tosylactivated magnetic microparticles (MP) was performed using the coating protocol suggested by the manufacturer. A schematic representation of the reactions is shown in Figure 4.3. A volume of 100 μL of tosyl-modified magnetic particles (100 mg mL^{-1}) was washed twice with 1 mL of coating buffer. Afterwards, the magnetic particles were resuspended in a final volume of 250 µL, comprising 147 µL of coating buffer, 20 µL of the 20 mg mL^{-1} gliadin stock solution (prepared in 60 % ethanol/ 40 % borate buffer 0.1M, pH 8.5) and 83 µL of 3 mol L^{-1} ammonium sulphate. The particles were then incubated during 24 hours (by mixing 2 h at 37 ºC and 800 rpm followed by tilt rotation 22 h at room temperature and 30 rpm). After incubation, the modified-MP were separated with a magnet and the supernatant was removed and placed in another tube to perform the quantification of the remaining protein by Bradford test. The modified particles were then resuspended in the same total volume (250 µL) of blocking buffer and incubated overnight, as previously explained, for inactivating the remaining tosyl groups. The particles were then submitted to three washing steps with the washing buffer and finally resuspended in storage buffer to reach a 25 mg mL^{-1} stock solution, which was stored at 4ºC. Before each assay, gliadin-MPs were washed (X3) with PBST and resuspended to a final volume in order to obtain the desired concentration of magnetic particles.

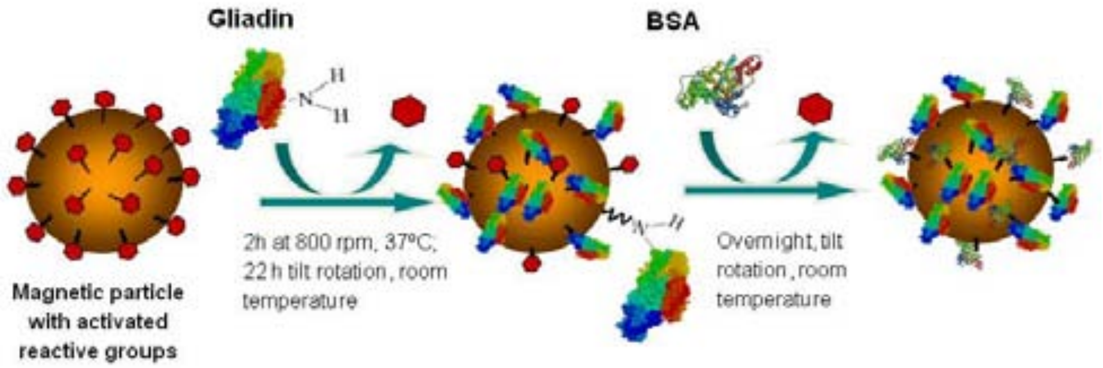
Gliadin
BSA
Magnetic particle with activated reactive groups
2h at 800 rpm, 37ºC; 22 h tilt rotation, room temperature
Overnight, tilt rotation, room temperature

Figure 4.3 Schematic representation of the immobilization of gliadin on the magnetic particles with the subsequent blocking with BSA.

4.3.2.3 Immobilization of gliadin to carboxyl-activated magnetic nanoparticles

In the case of the magnetic nanoparticles (nMP), the immobilization was performed following a very similar protocol in order that the results are comparable. Again 100 µl of the nMP (100 mg mL^{-1}) were washed twice, but in this case in 1 ml of activation buffer provided by the supplier. The magnetic particles were resuspended in 230 µl of activation buffer and 20 µl (20 mg mL^{-1}) of gliadin solution was then added. After homogenization with vortex, the particles were incubated in the same conditions than the microparticles. Subsequent to the immobilization step, the modified-MP were separated with a magnet and the supernatants were kept as well for the further protein detection. The modified nanoparticles were washed once in 250 µl and finally resuspended in 400 μl of storage buffer to reach 25 mg ml^{-1} stock solution, which was stored at 4 ºC until used.

4.3.2.4 Coupling efficiency study

In order to analyze the efficiency of the gliadin coupling to the magnetic particles, the amount of protein present in the supernatants after the immobilization step was determined by Bradford test[12] and was subsequently compared to the concentration before the conjugation.

The Bradford test is a colorimetric method based on the reaction of the proteins with the Coomassie Brilliant Blue G-250 dye. The anionic form of this reagent binds non-covalently principally to the arginine aminoacids in the protein and interacts also to some extent with histidine, lysine, tyrosine, tryptophan and phenylalanine residues. In the absence of proteins the dye has a yellow-brown color, which changes to blue after the reaction with proteins in an acidic medium, generating a concomitant shift in the absorption maximum from 465 nm to around 610 nm.[13] The difference between both forms of the dye is greatest at 595 nm, being this the optimal wavelength to perform the optical read-outs. This method is rapid, sensitive and presents low matrix interference.

The assay was performed according to the manufacturer of the kit (Coomassie Bradford Assay Kit, Pierce) by processing different dilutions of the samples and a standard curve prepared of gliadin dilution series. After the reaction, the plate was shaken for 30 seconds, incubated for 10 minutes at room temperature and finally after a short agitation, the absorbance was measured at 600 nm. The calibration curve was obtained by plotting Abs *vs*. gliadin concentration and the amount of protein in the supernatants was determined by interpolation.

4.3.3 Epitope orientation and nonspecific adsorption study

In order to ensure the correct orientation of the epitope, gliadin-MP and BSA-MP (as negative control to evaluate the non-specific adsorption) were incubated with the specific antibodies to compare the signal-to-non specific adsorption ratio. For the direct immunoassay format antiGliadin-HRP were used, whereas for the indirect format the antiGliadin primary antibody reacts in a second step with the antiIgG-HRP secondary antibody to produce the optical or the electrochemical signal.

4.3.4 Competitive magneto immunoassay for the optical detection of gliadin

A competitive immunoassay was chosen to be developed since this is the most suitable format to be able to detect not only the native protein, but also the hydrolyzed fragments that could result from the heat treatment during food processing. A sandwich format could underestimate the gliadin content in the samples due to the fact that it needs multivalency, which means at least two epitopes for the detection.

Different competitive formats, direct and indirect, were evaluated for the first time using the gliadin modified magnetic microparticles (gliadin-MP). Moreover, some parameters of the magneto immunoassay, like incubation time and reagents concentration, were analyzed in both magnetic carriers, the gliadin modified microparticles (gliadin-MP) and nanoparticles (gliadin-nMP).

The direct and indirect competitive magneto immunoassay with optical detection, were performed in 96-well microtiter plates for the optimization of the main factors affecting the competitive immunological reaction. In the direct assay (Figure 4.4, A), the gliadin in the samples competes with the gliadin immobilized on the magnetic particles for the antiGliadin-HRP antibody, whereas in the indirect assay (Figure 4.4, B), the non-labeled antiGliadin antibody is revealed with a secondary antibody labeled with the HRP enzyme (antiIgG-HRP) as optical reporter.

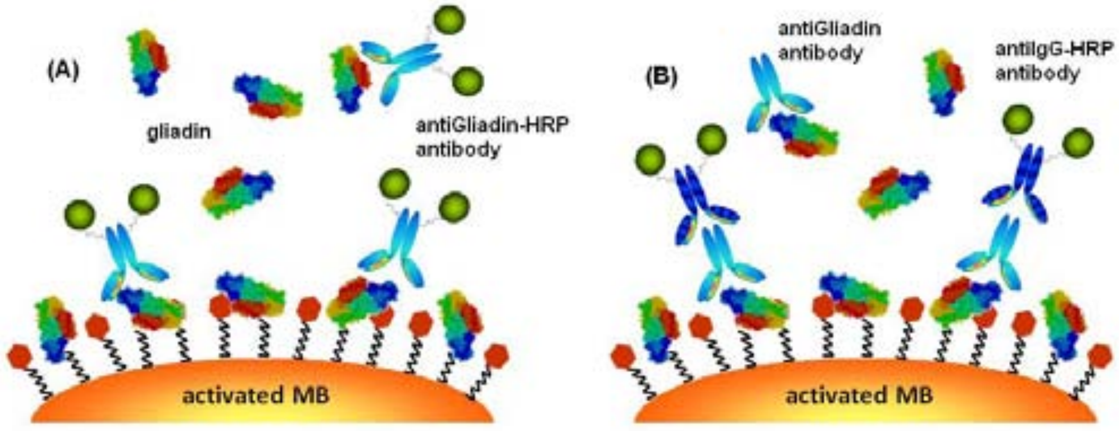

Figure 4.4 Schematic representation for the gliadin determination based on (A) direct and (B) indirect competitive magneto immunoassay.

Two–dimensional (2D) serial dilution experiments were performed using the direct and indirect competitive magneto immunoassay with optical detection in order to select the optimal concentration for both the gliadin modified magnetic particles, as well as the specific gliadin antibodies. With this aim, increasing concentrations of gliadin-MP were tested in one dimension of the microplate and challenged towards different concentration of antiGliadin antibodies in the other direction. In the case of the indirect competitive assay, the antiIgG-HRP antibodies solution was fixed in a 1/2000 dilution, as recommended by the manufacturer, and the concentration of the other two components were varied in the two dimensions of the microplate. The optimal concentrations were chosen to produce a signal ranging from 0.8 to 1.2 absorbance units. Beside the reagent concentration, an important parameter such as the need of a preincubation step[14] was also optimized to improve the immunoassay. Other experimental parameters (like surfactant concentration, ionic strength and pH) were used as optimized in previous works.[15]

The direct competitive magneto immunoassay was performed in microtiter plates with flat-bottomed wells comprising the following steps (referred to the 'amount added per well'): i) Preincubation step with 75 µL of the gliadin standard solutions in PBST with 6 % ethanol (from 2.0×10^{-4} to 50.0 µg mL^{-1}) and 75 µL of the antiGliadin-HRP antibody; ii) Competitive immunological reaction with gliadin-MP (0.040 mg mL^{-1}) and 100 µL of the preincubation mix in shaking conditions at room temperature for 30 min, followed by washing (3X) with 100 µL of PBST.

In the case of an indirect competitive magneto immunoassay, after the step ii), a third step is performed: iii) Immunological reaction with 100 µL of the secondary antiIgG-HRP antibody (diluted 1/2000 in PBST) with shaking for 30 min at room temperature, followed by washing (3X) with 100 µL of PBST.

After each incubation or washing step, the magnetic particles were separated from the supernatant on the bottom corner by using a 96-well magnet plate separator, positioned 2 min under the microtiter plate. Finally, in both cases, the last step was performed as follows: iv) Optical detection with 100 µL of substrate solution, consisting of H_2O_2 and TMB in citrate buffer, incubated for 30 min at room temperature in darkness. The enzymatic reaction was stopped by adding 100 µL of H_2SO_4 (2 mol L^{-1}), which turns the solution to yellow, and the absorbance measurement of the supernatants was performed at 450 nm as schematically outlined in Figure 4.5.

The TMB is a soluble colorimetric substrate for the horseradish peroxidase (HRP) enzyme and is more quickly oxidized than other HRP substrates, resulting in a fast color development and thus a very sensitive immunoassay. In the presence of the enzyme, TMB acts as hydrogen donor for the reduction of the hydrogen peroxide to water, as shown in Figure 4.5, and the resulting diimine causes the colored solution.

The color intensity is proportional to the amount of HRP activity, which in turn is related to the levels of target analyte in the optimized ELISA procedure. One electron oxidation of TMB results in a radical cation that forms a charge transfer complex with the non-oxidized compound. This charge transfer complex absorbs at 652 nm (ε= 39,000), giving the blue color, while the completely oxidized form (diimine), resulting from two sequential one-electron oxidations of TMB, absorbs at 450 nm (ε= 59,000) turning the solution to yellow.[16,17]

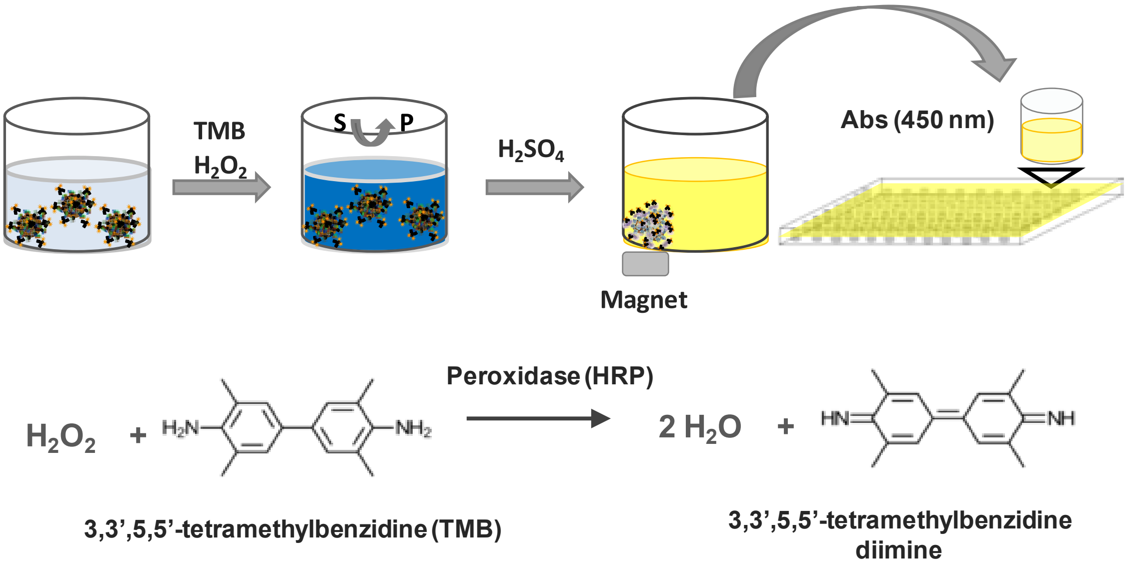
TMB
H2O2
S
P
H2SO4
Abs (450 nm)
Magnet
Peroxidase (HRP)
H2O2
+
H2N
NH2
2 H2O
+
HN
NH
3,3',5,5'-tetramethylbenzidine (TMB)
3,3',5,5'-tetramethylbenzidine diimine

Figure 4.5 Schematic representation for the optical detection in the magneto immunoassay performed on 96-well microtiter plates. Previously the competitive assay was performed on magnetic particles modified with gliadin and using antibodies labeled with HRP. The reaction of the TMB with H_2O_2 in the presence of the HRP is also shown.

The obtained signals were inversely proportional to the amount of gliadin added, since the more analyte was present in the sample, the fewer antibodies were available to react with the gliadin on the magnetic particles. Accordingly, the maximal signal corresponded to that achieved with the samples without gliadin. The obtained results of the standards were fitted to a sigmoidal curve as shown in Figure 4.6, according to the following four-parameter logistic equation:

$$y = \{(A-B)/\ [1+10\ \exp((\log C-\log X) \times D)]\} + B$$

The parameter A is the maximal absorbance, B is the minimum absorbance, C is the concentration producing 50 % of the maximal absorbance (IC50), X is the gliadin concentration and D is the slope at the inflection point of the sigmoid curve.

In a competitive assay the limits of detection (LOD) correspond to the analyte concentration causing a 10 % of inhibition in the attachment of the labeled immunoreagent, being thus obtained as the 90 % of the A value. On the other hand, the working range of the assay is defined between the 20 % (quantification limit) and the 80 % of the maximal signal. Finally, the sensitivity is given by the slope in the linear region of the curve.[18,19]

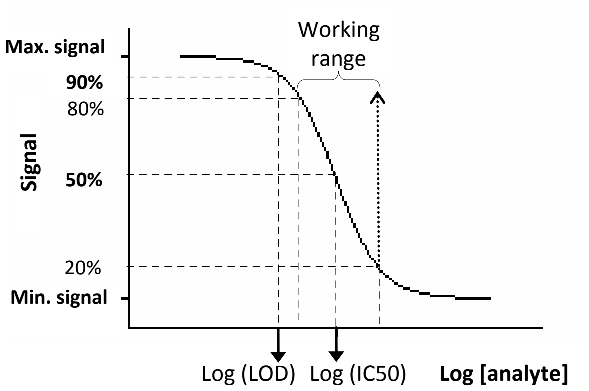

Figure 4.6 Typical sigmoid curve used for the adjustment of the signal obtained with a competitive immunoassay, showing the most important parameters: the limit of detection (LOD), the IC50 value, and the working range comprised between the 80 and the 20 % of the maximal signal.

4.3.5 Study of the matrix effect and gliadin extraction procedure from foodstuff

Two different food samples were analyzed as a model of foodstuff containing gluten as well as gluten-free foodstuff which can be contaminated affecting thus the food safety of the celiac patients: beer and skimmed milk. Beer is one of the naturally gluten containing liquid samples while skimmed milk, although naturally gluten-free, can be easily contaminated during processing of milk derivatives products with cereals.

Two extraction procedures were evaluated: the first one was the most commonly reported ethanolic extraction,[2,6] which consist of a buffer containing 60 % v/v of ethanol, while the second one was a cocktail solution containing, beside the ethanol, 5.0 mM dithiothreitol and 6 % SDS in PBS pH 7.[20,21] For the extraction with ethanol, 0.125 g of the studied sample and 0.125 mL of the gliadin solution at the selected concentration to spike the food matrix were added to 4.750 mL of 60 % ethanol. The mix was placed for 1 h in tilt rotation at 30 rpm and room temperature, following a centrifugation step of 10 min at 3500 rpm. On the other hand, the cocktail extraction was performed by adding to the spiked sample (comprising 0.125 g of the food sample and 0.125 mL of gliadin) 1.25 mL of the cocktail solution and after a vigorous shaking the mix was incubated at 40ºC for 20 min. After some minutes cooling, 3.5 mL of ethanol 85 % were added and the mix was placed for 40 min in tilt rotation at 30 rpm and room temperature, followed by a centrifugation step as previously explained.

During the extraction procedure the samples were diluted (1/40). After the centrifugation the volume is transferred to a new tube and a further 1/10 dilution was performed after the extraction process.

For the evaluation of the matrix effect, the gliadin standard curves obtained in both foodstuffs (skimmed milk and beer) were compared with the standard curve performed in PBST for both kinds of modified magnetic particles, gliadin-MP and gliadin-nMP using the previous optimized magneto immunoassay.

4.3.6 Competitive electrochemical magneto immunosensor for gliadin detection

Optimal concentration of the antiGliadin-HRP antibodies and gliadin-MP was chosen to produce a high amperometric signal related to a low nonspecific adsorption by performing a two-dimensional serial dilution assay. The conditions were selected in order to reach a compromise between obtaining the highest possible signal and at the same time good competition parameters.

The competitive assay was performed in 2 mL Eppendorf tubes, and comprises the following steps (all the referred quantities are the amounts added per tube): i) Preincubation and ii) Competitive immunological reaction. Both steps were performed as explained in § 4.3.4., but using the optimized immunoreagents concentration for the electrochemical measurements. Following the incubation and the washing steps, the magnetic particles were separated from the supernatant by placing the Eppendorf tubes in a magnetic separator until the particles migration towards the tube sides was completed, obtaining a clear solution. The particles were finally resuspended in 140 µL of PBST and captured by dipping the m-GEC electrodes into the tubes, as outlined in Figure 4.7. And finally, the last step is performed as follows: iii) electrochemical detection, in which the amperometric signal was determined by using the gliadin-MP modified m-GEC as a working electrode and dipping the three-electrode setup in 20 mL PBSE buffer. 100 µL of hydroquinone were immediately added at a concentration of 1.81 mmol L^{-1} and under continuous magnetic stirring the m-GEC electrode was polarized at a working potential of −0.100 V (*vs*. Ag/AgCl), which was previously fixed through cyclic voltammetry (as outlined in § 3.4.1). When a stable baseline was reached, 500 µL of H_2O_2 were added into the electrochemical cell to a final concentration of 4.90 mmol L^{-1} (which corresponds to the H_2O_2 concentration capable to saturate the whole enzyme amount employed in the labeling procedure), and the current was measured until the steady state current was reached (normally after 1 min of H_2O_2 addition). The amperometric measurements were related to the amount of HRP conjugated antibodies attached to the gliadin immobilized on the magnetic particles. The signals were proportional to the enzymatic activity since the system works at saturation conditions of the substrate and thus maximal intensity values were obtained. The reactions that occur at the polarized m-GEC electrode surface upon H_2O_2 addition in the presence of hydroquinone are the following (Figure 4.7):

$$\text{HRP (red)} + H_2O_2 \rightarrow \text{HRP (ox)} + H_2O$$

$$\text{HRP (ox)} + \text{HQ (red)} \rightarrow \text{HRP (red)} + \text{HQ (ox)}$$

$$\text{HQ (ox)} + ne^- \rightarrow \text{HQ (red)}$$

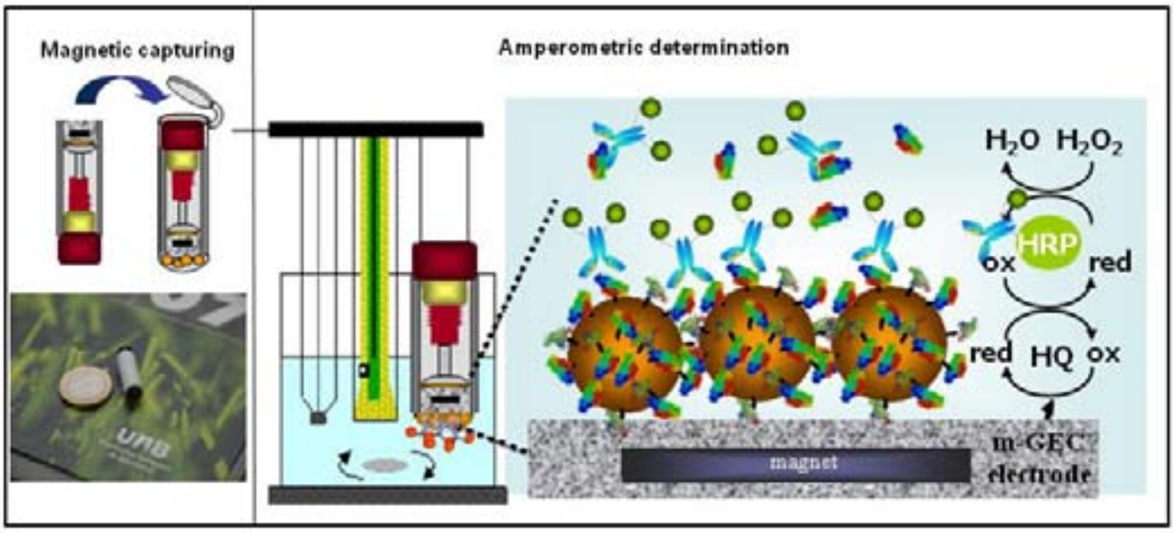

Figure 4.7 Schematic representation of the experimental details for the capture of the magnetic particles by dipping the electrode in the reaction tube and for the amperometric measurement using the magneto immunosensor. The chemical reactions involving the HRP enzyme, H_2O_2 as a substrate and hydroquinone as a mediator occurring during the measurement by polarizing the magneto electrode at -0.100 V (*vs.* Ag/AgCl) are also shown.

The standard curve was fitted to a four-parameter logistic equation as described for the magneto immunoassay procedure. While the modified MP were discarded and not reused after the electrochemical detection, the m-GEC electrodes were renewed by polishing for further uses, as explained in Chapter 3 (§ 3.4.1).

4.3.7 Accuracy study in foodstuff

Gluten-free beer and skimmed milk samples were spiked with increasing gliadin contents from 5 to 200 mg L^{-1}. The gliadin was extracted from the spiked samples using an extraction buffer containing 60 % v/v ethanol. To 0.125 g of the spiked samples, 4.875 mL of the extraction solution were added, and the mixture was shaken for 30 min under rotation. Finally, after a centrifugation step of 10 min at 3500 rpm, the supernatants were diluted 1/10 v/v in PBST buffer, obtaining as a result a 1/400 dilution of the food matrix in 6 % of ethanol. The recovery of gliadin was determined with both the magneto immunoassay procedure as well as with the electrochemical magneto immunosensor.

4.4 RESULTS AND DISCUSSION

4.4.1 Gliadin binding on magnetic micro and nanoparticles and coupling efficiency

The efficiency of coupling to both kinds of magnetic particles was evaluated by Bradford test using a gliadin calibration curve prepared in 50 mM borate buffer with 1 % ethanol in the case of the MP or a dilution 1/5 of activation buffer with 1 % ethanol for the nMP. Firstly, the Bradford test was applied to a wide range of gliadin concentrations (from 0 to 1000 µg mL^{-1}) in order to establish the linear region of the curve (Figure 4.8, A). The linear range was established between 0 and 80 µg mL^{-1} and very similar response was obtained regardless the buffer used, i.e. borate for the gliadin-MP or activation buffer 1/5 for gliadin-nMP, as shown in Figure 4.8, B with a very good linear fit (r^2 = 0.9911 and 0.9916, respectively).

The efficiency of the gliadin binding to the magnetic particles was calculated by subtracting the protein amount in the supernatant to the initial protein concentration taking into account that a concentration of 1600 µg mL^{-1} was added in all cases. The coupling proportion showed to be very reproducible in different days, giving excellent results in both magnetic carriers, with values of 88.5 % for the microparticles and 90.5 % in the case of the nanoparticles.

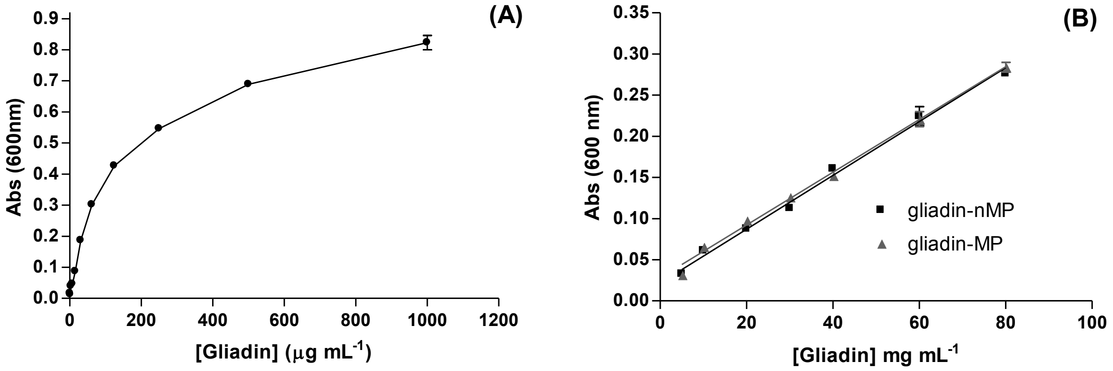

Figure 4.8 (A) Gliadin calibration curve obtained by Bradford test, showing the response at a concentration range from 0 and 1000 µg mL^{-1} of gliadin. (B) Curves obtained in 50 mM borate buffer with 1 % ethanol (for the gliadin –MP) and activation buffer 1/5 with 1 % ethanol (for the gliadin-nMP) by performing the Bradford test in the linear range of gliadin concentration from 0 to 80 µg mL^{-1}. The error bars show the standard deviation for n=4.

Due to the biological nature of the gliadin-modified MP, another important issue that had to be considered was their stability over the time. The stability of the gliadin-modified MP was studied following a monthly basis over a 7 month period, during which time the gliadin-MP were stored as recommended by the manufacturer at 4 ºC. All other experimental conditions were maintained constant. As shown in Figure 4.9, no significant change over this period of time was observed, confirming the stability of the immobilized gliadin on the surface of the MP for at least 7 months.

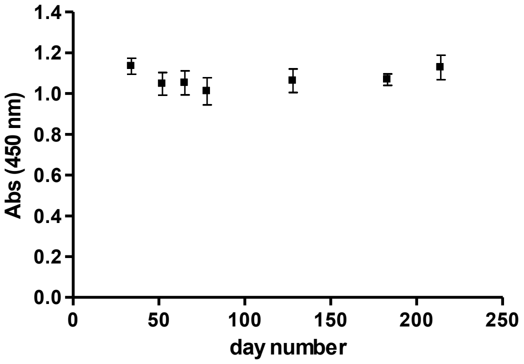

Figure 4.9 Stability study of the gliadin-modified MP performed with a direct magneto immunoassay in PBST buffer. The experimental conditions used in all cases are: gliadin-MP concentration of 0.040 mg mL^{-1}, antiGliadin-HRP antibody dilution of 1/8000. The error bars show the standard deviation for n = 4.

4.4.2 Epitope orientation and nonspecific adsorption study

Although a good coupling efficiency (determined to be of around 90 %) achieved for the gliadin immobilization, this fact does not ensure that the epitopes are appropriately exposed. Due to the randomness of the immobilization procedure, the availability of the epitopes after the conjugation has to be controlled since the binding to the magnetic particles could hinder the subsequent antibody recognition. Beside the efficiency and stability of gliadin coupling it is extremely important to verify the specificity and high affinity reaction between the antibodies and the immobilized gliadin to guarantee the immunoassay performance.

As a result, the correct orientation of the epitopes was evaluated by comparing the signals obtained using the gliadin-MP with the response towards BSA modified magnetic particles (BSA-MP) as a negative control for the determination of the non-specific adsorption of the enzymatic conjugates and antibodies. The results obtained after the reaction of both modified magnetic particles with the specific antiGliadin antibodies for the magneto immunoassay using (A) the direct and (B) indirect format are shown in Figure 4.10. For the direct immunoassay format antiGliadin-HRP antibodies were used, whereas for the indirect format the antiGliadin primary antibody reacts in a second step with the antiIgG-HRP secondary antibody to produce the optical signal.

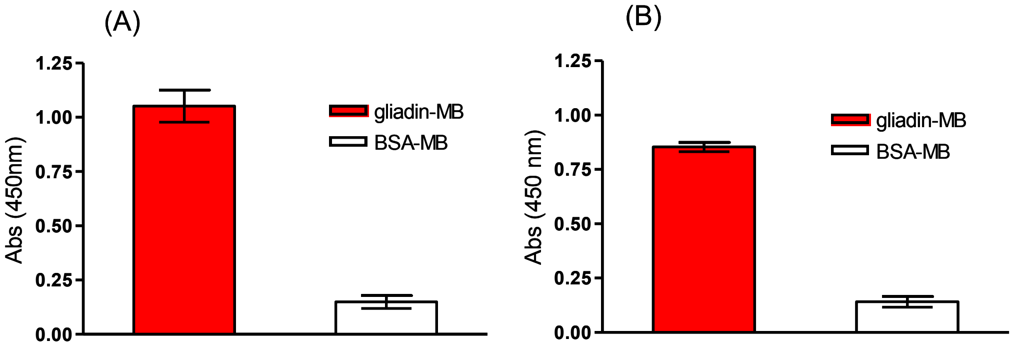

Figure 4.10 Evaluation of the orientation of the immobilized gliadin on the magnetic particles by its reaction with antiGliadin antibodies using the direct (A) and indirect (B) immunoassay format. In both cases, a concentration of 0.04 mg mL^{-1} MPs was used. For the direct immunoassay format the antiGliadin-HRP antibodies were diluted 1/8000, w or the indirect format the antiGliadin primary antibodies were diluted 1/4000, and antiIgG-HRP y antibody 1/2000. Same results are shown for BSA-MP as negative control for the non-specific n evaluation. The error bars show the standard deviation for n=4.

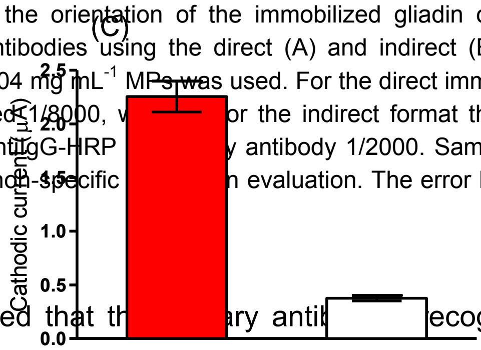

The results confirmed that th ary antib ecognized with high specificity and affinity the toxic gliadin epitopes, since the signal was significantly higher for the gliadin-MP comparing with the BSA-MP, giving signal to-non-specific adsorption ratios of 7.0 and 6.0 for the direct and indirect format, respectively. Moreover, the low optical signals (of around 0.149 and 0.141 a.u. for the direct and the indirect format, respectively) obtained with the BSA-MP indicated an extremely low non-specific adsorption of the antibodies on the surface of the modified-MP.

These results demonstrate that the immobilization to the magnetic particles leaves the epitopes oriented, allowing the subsequent antigen-antibody reaction, which suggests that the reactive groups for the covalent binding are not affecting the epitopes or that there are more than one epitope per protein.

The aminoacidic sequences of the gliadin protein and the within reported epitopes were also studied as shown in Figure 4.11,[22] in order to analyze the positions of the lysine, arginine and cysteine residues which contain the potentially reactive groups that could be affected by the covalent conjugation to the magnetic particles during the immobilization. As can be seen, the epitopes responsible for the protein antigenicity reported in the bibliography [23–25] did not contain any aminoacidic moiety capable to react with the tosyl or carboxylic groups of the magnetic particles. Furthermore the majority of the reactive residues were principally observed in the more distant regions of the protein sequence. In addition, the tertiary protein structure seemed not to affect the immobilization or to hinder the subsequent antigenic recognition of the immobilized protein.

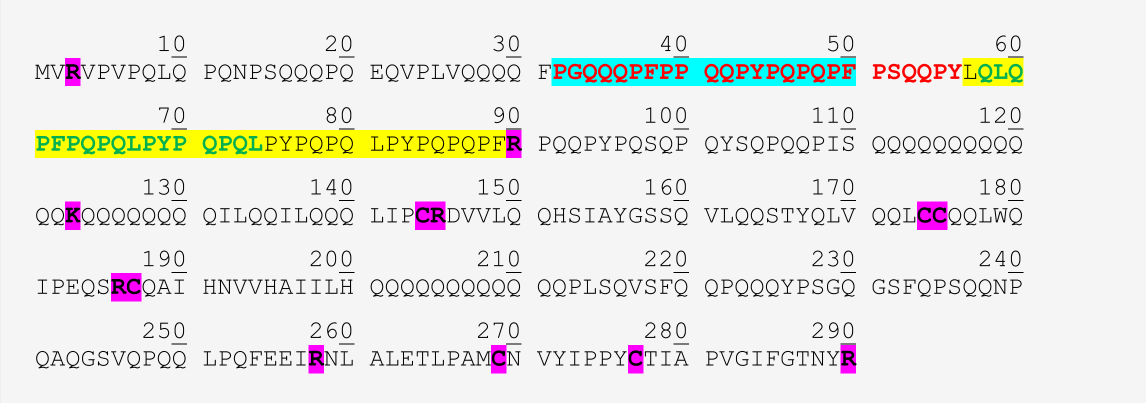

```
        10         20         30         40         50         60
MVRVPVPQLQ PQNPSQQQPQ EQVPLVQQQQ FPGQQQPFPP QQPYPQPQPF PSQQPYLQLQ

        70         80         90        100        110        120
PFPQPQLPYP QPQLPYPQPQ LPYPQPQPFR PQQPYPQSQP QYSQPQQPIS QQQQQQQQQQ

       130        140        150        160        170        180
QQKQQQQQQQ QILQQILQQQ LIPCRDVVLQ QHSIAYGSSQ VLQQSTYQLV QQLCCQQLWQ

       190        200        210        220        230        240
IPEQSRCQAI HNVVHAIILH QQQQQQQQQQ QQPLSQVSFQ QPQQQYPSGQ GSFQPSQQNP

       250        260        270        280        290
QAQGSVQPQQ LPQFEEIRNL ALETLPAMCN VYIPPYCTIA PVGIFGTNYR
```

Figure 4.11 Aminoacidic sequence of α-gliadin (access code in UniProtKB/TrEMPL: Q9M4L6)[22], highlighting different peptides reported to be antigenic for celiac patients: a) 19 aminoacids sequence[26], b) 25 aminoacids sequence that include the previous[23], c) 17 aminoacids sequence[23], and d) 33 aminoacids sequence[24] which includes sequence c and another shorter composed of 14 residues[25]. Lysine, cysteine and arginine residues are also highlighted in violet. As can be observed, the toxic regions are especially rich in glutamine (Q) and proline (P).

4.4.3 Competitive magneto immunoassay for the optical detection of gliadin

Once the efficient and oriented immobilization orientation of the antigen on the magnetic particles was confirmed, other important parameters to be optimized are the immunoassay format (direct or indirect), as well as the immunoreagents concentration (gliadin-MPs and antibodies).

4.4.3.1 Immunoassay optimization using the gliadin-MP

From the two-dimensional serial dilution experiments, the concentration of the immunoreactants was optimized, as shown in Figure 4.12 and 4.13 for the indirect and direct format, respectively. In both cases, the 2D experiments were performed covering a large range of particles and antiGliadin antibodies concentrations to get a global overview of the behavior and make the first adjustments. Then, a finer analysis was done with replicates for each point, in order to determine the better conditions, as shown in the aforementioned Figures.

In the case of the indirect assay (Figure 4.12), the first 2D experiment was carried out by fixing the magnetic particles concentration at 0.15 mg mL^{-1} and varying the antibodies dilutions in the two directions of the microplate: on one hand, the antiGliadin antibodies from 1/3000 to 1/64000, and on the other, the antiIgG-HRP antibodies from 1(1000 to 1/8000). The different dilutions combinations were tested on the gliadin-MP (Figure 4.12, A) as well as on BSA-MP (Figure 4.12, B) as a negative control. Good responses were obtained with the gliadin-MP, achieving in many cases signals above 1 in absorbance related to very low signals obtained with the BSA-MP, with values below 0.2 for all the tested concentration range. This indicated a very low nonspecific adsorption of the antibodies on the magnetic particles.

When analyzing the results the optimal conditions in which the absorbance was around 1 were obtained at a dilution of around 1/6000 of the primary antibodies and between 1/2000 and 1/3000 of the secondary antibodies. As a result the next 2D assay was performed setting in this case the antiIgG-HRP antibodies at 1/2000, by changing the gliadin-MP concentration from 0 to 0.6 mg mL^{-1} and assaying at three different antibodies dilutions (1/2000, 1/4000 and 1/6000), as shown in Figure 4.12, C. Regarding the antibodies dilution it was decided to fix the antiGliadin antibodies at 1/4000 for further studies. However, in the case of the magnetic particles due to the high absorbance signals (around 2) obtained at a concentration above 0.15 mg mL^{-1} a new optimization was performed testing gliadin-MP concentrations between 0 and 0.12 mg mL^{-1} (Figure 4.12, D). The results showed that a concentration of 0.06 mg mL^{-1} could be considered as optimal situation, since the absorbance was around 1 in this case, which is the ideal condition to adjust the maximum of a competitive immunoassay. Moreover, once again the low nonspecific adsorption of the antibodies was demonstrated giving as a result a very good signal to background ratio.

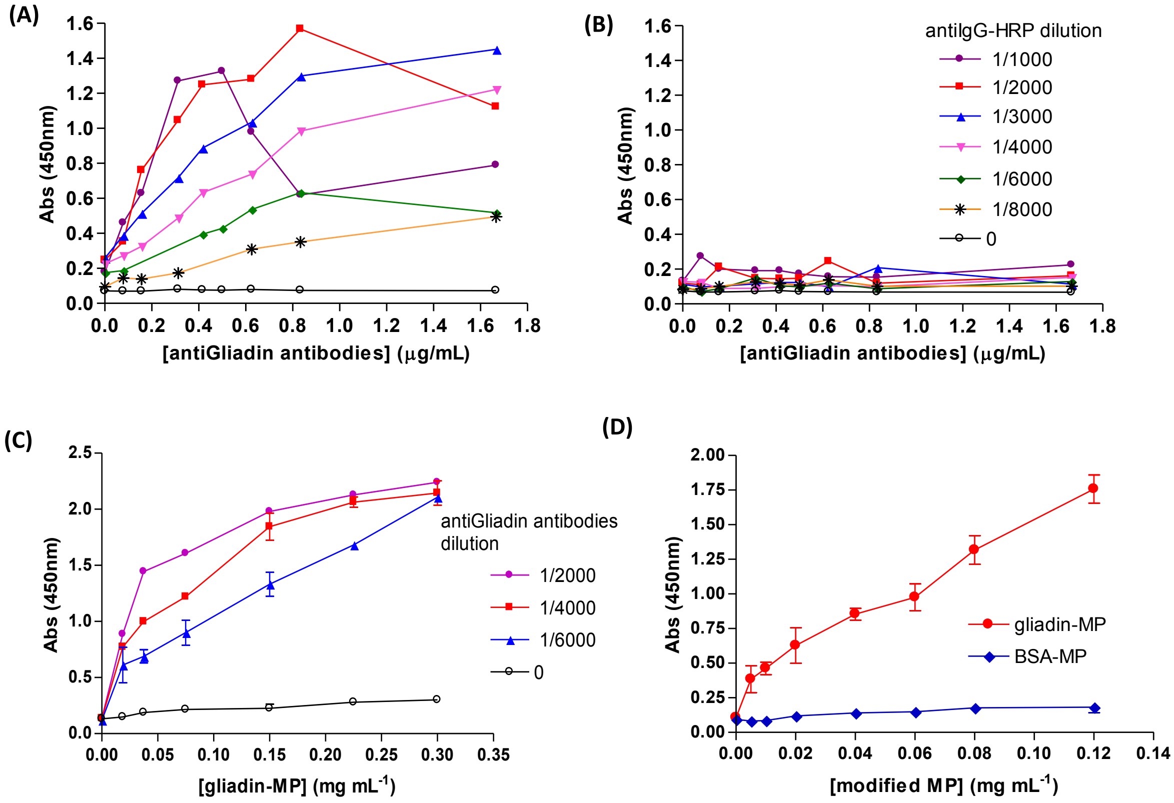

experiments performed with the indirect magneto immunoassay strategy. Top: A wide range of antiGliadin antibodies concentrations and secondary antiIgG-HRP antibodies were tested for the gliadin-MP (A) and BSA-MP (B), as negative control, by fixing the MP amount at 0.15 mg mL^{-1}. In the x-axis different antiGliadin antibodies concentrations are assayed (expressed in µg mL^{-1}), corresponding to the following dilutions: 1/3000, 1/6000, 1/8000, 1/10000, 1/12000, 1/16000, 1/32000 and 1/64000, while the different curves are related to the dilutions of the label showed in the right side. Bottom: Finer optimizations performed by fixing the antiIgG antibody dilution at 1/2000 (C) and finally setting also the antiGliadin antibodies at 1/4000 and comparing the signals of the gliadin-MP with BSA-MP (D). The error bars show the standard deviation for n=3.

Afterwards, the direct immunoassay was also optimized. Again a first 2D experiment was performed covering a wide range of concentrations by varying the gliadin-MP from 0 to 0.15 mg mL^{-1} and the antiGliadin-HRP from 1/2000 to 1/24000 (Figure 4.13, A). Then the antibodies dilutions were focused in a smaller span of dilutions (Figure 4.13, B).

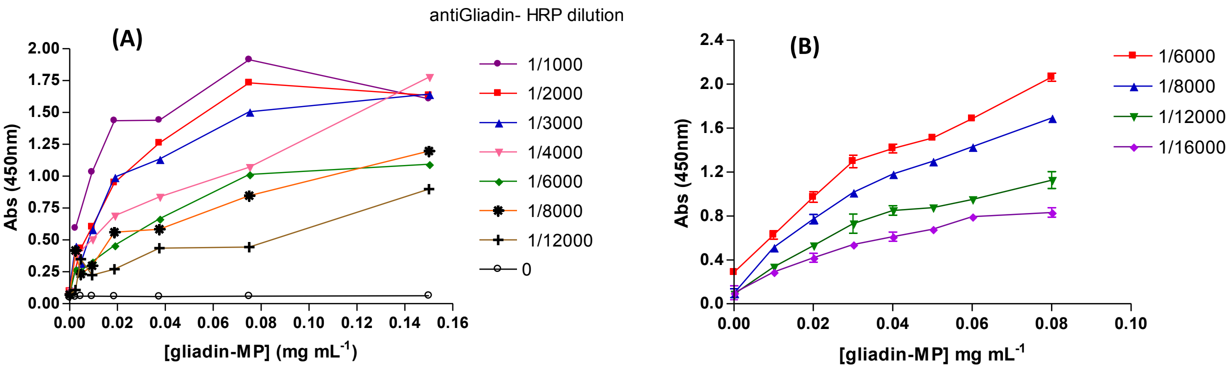

Figure 4.13 Two dimensional serial dilution experiments performed with the direct immunoassay format to optimize the antiGliadin-HRP antibodies dilution and gliadin-MP concentration.

As can be seen in the Figure 4.13, optimal conditions for the direct competitive magneto immunoassay were found to be a gliadin-MP concentration of 0.040 mg mL^{-1} and antiGliadin-HRP diluted 1/8000 and also in this format a very low nonspecific adsorption was shown.

After the optimization of the reagents concentration, the magneto immunoassay was performed by varying the amount of gliadin in PBST buffer, in order to obtain the best competition range, which was found to extend over a gliadin concentration range between 0 and 50 µg mL^{-1}.

A stock solution of 2 mg mL^{-1} of gliadin was prepared, but again the dissolution of the protein was an issue. The first attempt was to dissolve the gliadin directly in PBST and PBST with 20 % DMSO incubating in agitation at 40ºC overnight, but without success. Afterwards the same concentration was prepared directly in DMSO, obtaining positive results, but a 20 % of DMSO was needed when diluting the stock to prepare the calibration curve, with the problem that this amount showed to affect the immunoassay hindering the acquisition of a competitive curve. As a result, different solutions were tested containing 60 % (v/v) of ethanol in water or buffer solution in order to solve the problem: a) water, b) PBST 0.01 M, pH 7.4, c) PBS 0.04 M, pH 7.4, d) carbonate/ bicarbonate 0.05 M, pH 9.6, e) borate 0.02 M, pH 8.5. In all cases the solutions were incubated overnight at 40ºC and shaking. The solution d) was the most efficient being the protein totally dissolved the morning after, while the solution e) showed also good results after a longer incubation time. The solutions a) and c) did not dissolve at all. Therefore, it was decided to store the gliadin stock solution in carbonate buffer containing 60 % (v/v) ethanol.

A last important optimization was to establish if the inclusion of a preincubation step of the gliadin samples with the primary antiGliadin antibodies could improve the immunoassay performance and finally also compare both formats (direct and indirect) in order to determine the better situation. With this aim direct and indirect competitive magneto immunoassay procedures were performed using different preincubation times (0, 45 and 90 min) as shown in Figure 4.14. The signals were obtained using the optimized immunoreagents concentration previously described and assaying gliadin standards of the following concentrations: 0, 0.002, 0.02, 0.1, 0.5, 2.5, 10 and 50 µg mL^{-1}.

As can be seen in the Figure 4.14 and in the competitive parameters detailed in Table 4.1, A and B, improved results in terms of IC50 and LOD values, were achieved with the direct format, which also has the advantage of being simpler and faster to perform since an incubation step and the related washes were removed through the direct labeling. Furthermore, when analyzing the different preincubation times it could be clearly observed that the addition of a preincubation step significantly improved the competition parameters (Absmax/IC50 ratio), related with better LODs for the assay in both formats. Although a slight better LOD was obtained after 90 min preincubation in comparison to 45 min, much better Absmax/IC50 ratio and also a higher slope was obtained with the shorter preincubation, involving in addition a reduction in the assay time.

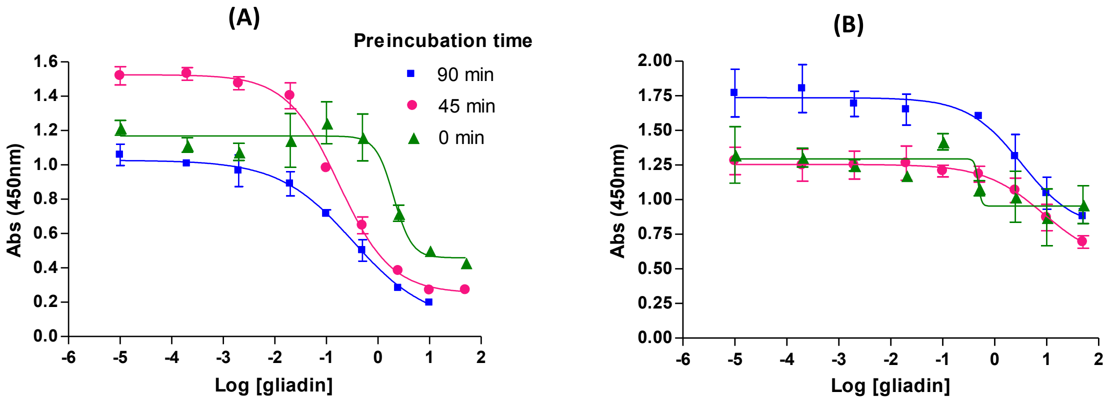

preincubation step between the antiGliadin primary antibodies and the gliadin standards (from 0 to 90 minutes). The experimental conditions were: gliadin-MP 0.04 mg mL^{-1}; antiGliadin-HRP antibody 1/8000 (for the direct competitive immunoassay); antiGliadin primary antibody 1/6000 and antiIgG-HRP secondary antibody1/2000 (for the indirect format). The error bars show the standard deviation for n =3.

When looking at the results of the direct format, the higher signals obtained for the shorter preincubation time could be explained in the fact that as longer the antibodies are preincubated with the gliadin samples, as more favored will be the binding to the free gliadin in solution instead than to the gliadin immobilized on the magnetic particles. Moreover, if no preincubation was performed the recognition of the immobilized gliadin is more favored requiring thus a higher gliadin concentration to be able to notice a signal decrease.

Table 4.1 Competition parameters for the direct (A) and indirect (B) competitive magneto immunoassay after different preincubation times.

(A) Preincubation time (min)	Abs max/IC50	Linear range (µg mL^{-1})	Slope	LOD (µg mL^{-1})
0	0.53	1.107- 14.577	0,95	0.0503
45	7.75	0.020 – 0.844	-0.81	0.0045
90	3.14	0.019 – 1.294	-0.61	0.0034

(B) Preincubation time (min)	Abs max/IC50	Linear range (µg mL^{-1})	Slope	LOD (µg mL^{-1})
0	-	-	-	-
45	0.17	0.997 – 15.58	-1.017	0.188
90	0.24	1.019 – 16.41	-0,938	0.283

As a result, a preincubation time of 45 min was chosen for further studies, giving an IC50 of 129.7 µg L^{-1} and a LOD of 4.5 µg L^{-1}, which is more than 1000 times lower than the 20 ppm required limit, i.e. 20 mg L^{-1}, according to the EC legislation for gluten-free products.

4.4.3.2 Immunoassay optimization using the gliadin-nMP

The 2D experiments with the gliadin-nMP were performed using the previously optimized conditions, i.e. a direct immunoassay with a preincubation step of 45 min. Once again, the gliadin-nMP concentration was varied in one direction of the microplate, while modifying the antiGliadin-HRP antibodies dilution in the other, to find the optimal combination that produce a signal ranging from 0.8 to 1.2 absorbance units. The first broader concentration range optimization (Figure 4.15, A) showed that the optimal results were obtained for a magnetic nanoparticles concentration between 0.04 and 0.08 mg mL^{-1} and using an antibody dilution from 1/6000 and 1/12000. Therefore a finer 2D analysis was performed for magnetic particles concentration below 0.08 mg mL^{-1} and assaying at four different antibodies dilutions: 1/4000, 1/6000, 1/8000 and 1/12000 (Figure 4.15, B). After evaluating the results the optimal conditions were chosen to be a gliadin-nMP concentration of 0.06 mg mL^{-1} and antibodies dilution of 1/6000. When comparing to the tosylactivated microparticles, which optimal concentrations were found to be 0.04 mg mL^{-1} and 1/8000 respectively, it could be observed that slight higher concentration of both reagents were needed in the case of the nanoparticles to achieve similar signals.

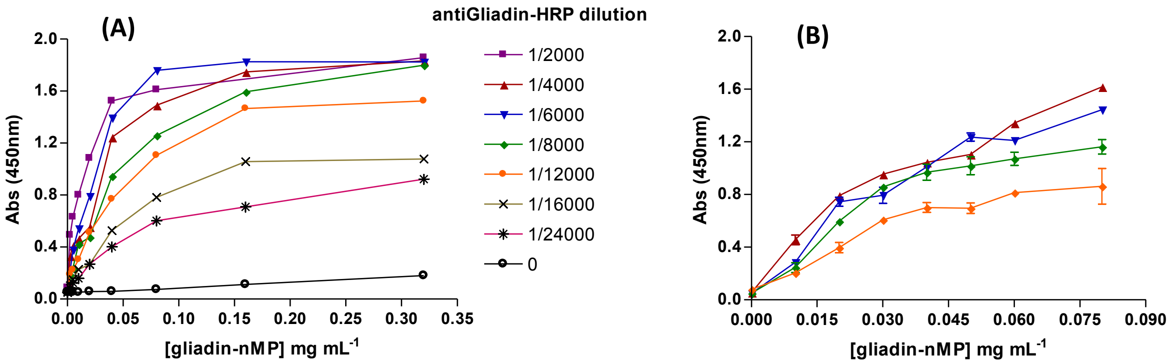

Figure 4.15 Optimization of the antiGliadin-HRP antibodies dilution and gliadin-nMP concentration by two-dimensional serial dilution experiments performed with the direct magneto immunoassay strategy.

Once the immunoreagents were optimized, the competitive curve was performed with the gliadin-nMP in the same gliadin concentration range than previously performed with the microparticles. However, the results showed a high minimal signal (with a value of 0.543) and a low slope (-0.49) of the competitive curve as shown in Figure 4.16. A first attempt to improve the results was done by decreasing the gliadin-nMP concentration to the half, but as can be seen in the graph the minimal signal was still high, obtaining nevertheless a significant signal decrease for the upper region of the sigmoidal curve resulting thus in an even lower slope. In the case of decreasing the antibodies concentration (from a 1/6000 dilution to 1/8000) the minimal signal could be reduced to some extent but the higher signals also decreased not showing therefore any improvement. Finally it was decided to decrease the incubation time of the competition step from 30 min to 15 min, so that the reaction with the antigen immobilized on the magnetic nanoparticles was less favored. The competition curve was greatly improved as shown in Figure 4.16, giving an IC50 of 115.8 µg L^{-1} and a LOD of 7.7 µg L^{-1}. The competitive parameters are shown in Table 4.2. When comparing the results with the response obtained using the microparticles very similar IC50 and LOD values were achieved in both cases. As a result, the nanoparticles did not show a significant improvement as was previously supposed due to the increased reactivity given by their smaller size. The only advantage which could be highlighted was a better sensitivity demonstrated through the higher slope and Abs max/IC50 ratio.

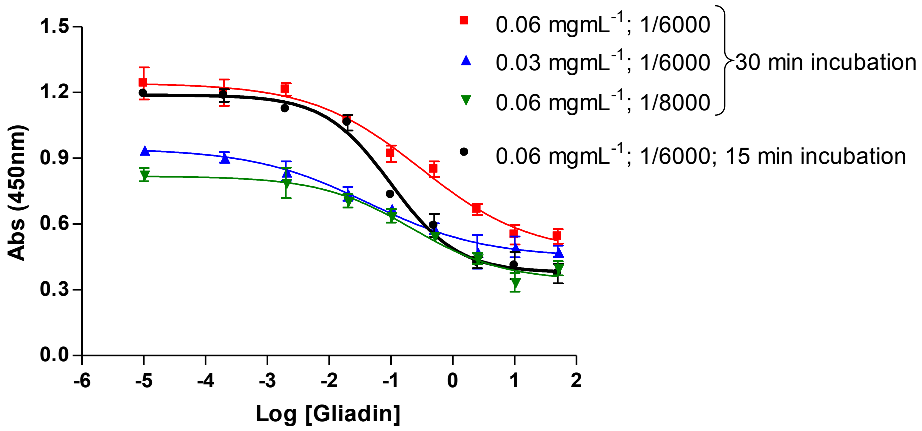

Figure 4.16 Optimization of the direct competitive immunoassay performed with the gliadin-nMP. The results with the optimal immunoreagents concentration (gliadin-nMP 0.06 mg mL^{-1} and antiGliadin-HRP diluted 1/6000) are compared with the curve obtained after reducing the magnetic particles or the antibodies concentration, as well as after changing the incubation time for the competition step from 30 to 15 minutes. The error bars show the standard deviation for n=3.

Table 4.2 Competition parameters for the direct competitive magneto immunoassay performed on the gliadin-nMP.

	Abs max/IC50	Linear range (µg mL^{-1})	Slope	LOD (µg mL^{-1})
Gliadin-nMP	10.22	0.021- 0.811	0.87	0.0077

4.4.4 Study of the matrix effect and gliadin extraction procedure from foodstuff

The matrix effect is related with the combined effect of all components of the sample other than the analyte in the performance of an analytical method,[27] and consists of a bias in the analyte determination performed in different matrixes. The most important type of matrix effect is any that occurs between the matrix used to prepare the calibration curve, and the matrix of the test samples.

Due to the different composition of the chosen food matrixes (skimmed milk, involving high contents of fat, protein and minerals and beer, containing alcohol, non-fermented complex carbohydrates, polyphenols, minerals and proteins), it is expected that these complex food matrixes will produce a bias compared with the standard curve performed in PBST buffer.

In order to overcome matrix effect, general procedures are dilution of the sample or the use of a sample extract in the preparation of the standard curve, although in food samples clean-up may sometimes be necessary.[28]

Two different procedures for the gliadin extraction were evaluated with the direct competitive magneto immunoassay: i) the ethanolic and ii) the cocktail solution extractions. Therefore the first step was to evaluate the effect of the presence of ethanol and of the cocktail solution in the competitive immunoassay as shown in Figure 4.17.

With this aim, different ethanol amounts (3, 6, 9 and 12 %) were added to the calibration curve. The addition of increasing amounts of ethanol did not show a very significant effect on the calibration curve obtaining good competition parameters in all cases as can be seen in Table 4.3, with very good limits of detection as well as IC50 values. However a drop off in the upper signals was evident for the higher ethanol percentages (9 and 12 %) producing thus a decrease in the sensitivity of the curve indicated by the slope decline.

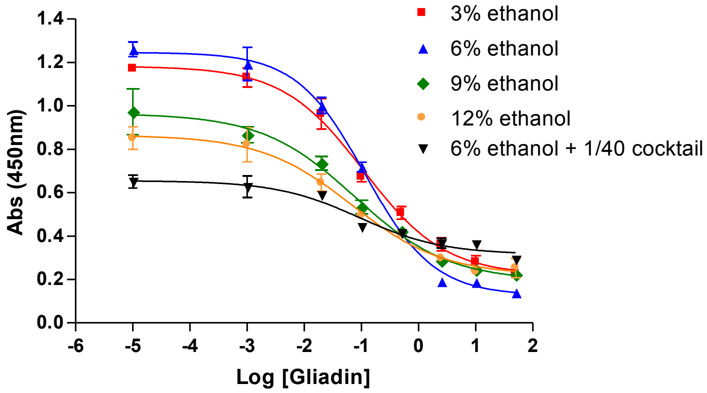

Figure 4.17 Study of the extraction procedure. Effect of adding different ethanol amounts as well as the cocktail solution in the direct competitive magneto immunoassay for the determination of gliadin. In all cases a gliadin-MP concentration of 0.04 mg mL^{-1} and a antiGliadin-HRP dilution of 1/8000 was used.

Regarding the cocktail solution, the influence of the presence of a 1/40 dilution in addition to 6 % ethanol was studied, since this would be the final conditions in the samples after the 1/10 dilution performed subsequent to the extraction protocol. As shown in Figure 4.17, the cocktail solution promoted a signal decrease at low concentration as well as an increase at high gliadin concentration, affecting significantly the competition parameters and even hindering the determination of the LOD value in this competitive curve. This effect was previously reported.[2] As a consequence, this cocktail solution was not further studied, while the classical ethanolic extraction was employed, as also recommended by the manufacturers of commercial kits in competitive (Ridascreen Gliadin competitive 2nd generation, Art. Nº. R7021, r-Biopharm, Germany) and sandwich (Transia Plate Gluten, Art. Nº. GL0301, Diffchamb, UK; Immunotech Gliadin ELISA kit, Ref Nº IM3717, Beckman Coulter, Czach Republic) ELISA formats.

Table 4.3 Comparison of the competition parameters obtained at different ethanol amounts.

Ethanol amount (%)	IC50	Linear range (µg mL^{-1})	Slope	LOD (µg mL^{-1})
3	0.110	0.010- 1.007	-0.61	0.00354
6	0.116	0.015 – 0.708	-0.72	0.00253
9	0.078	0.0050 – 0.673	-0.53	0.00101
12	0.076	0.0091-0.801	-0.54	0.00296

Once the extraction protocol was established, the matrix effect of beer and skimmed-milk spiked with gliadin was evaluated by comparing the results with the standard curve obtained in PBST buffer containing 6 % ethanol.

In the case of the modified nanoparticles, i.e. gliadin-nMP, a high matrix effect was observed in the presence of the milk food matrix, affecting significantly the behavior of the competitive curve as shown in Figure 4.18, A. Thus, further studies were done with the modified magnetic microparticles.

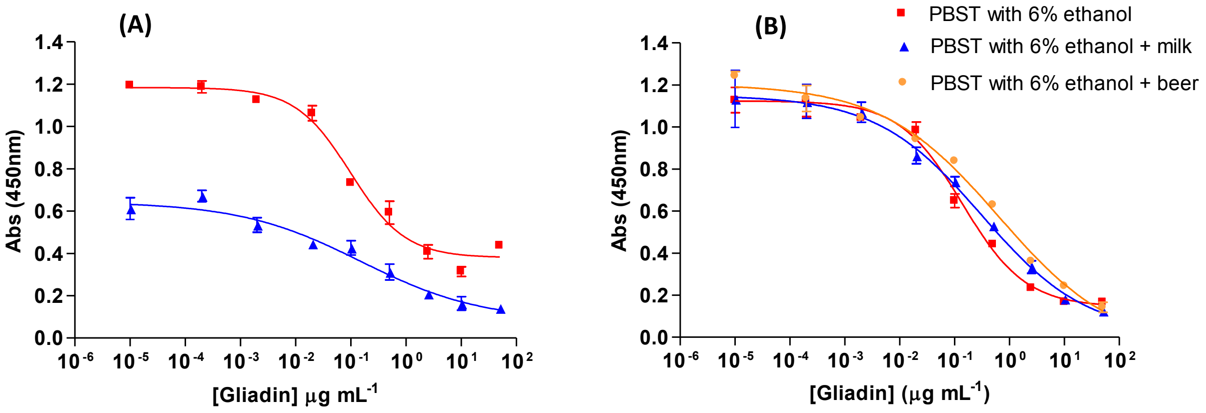

Figure 4.18 Competition curves using the gliadin-nMP (A) and gliadin-MP (B) obtained with the different food matrixes (beer and skimmed milk) compared with the response in PBST buffer after the ethanolic extraction. The experimental conditions in all cases were: gliadin-MP 0.040 mg mL^{-1}; antiGliadin-HRP antibody 1/8000. The error bars show the standard deviation for n= 4.

The curves obtained with the gliadin-MP are presented in Figure 4.18, B, while the detailed results of the competition parameters (such as the linear range, the IC50 and LOD values) are shown in Table 4.4, being the curves and LOD values quite similar for both food matrixes and PBST buffer. Moreover the achieved LOD values were much lower than the required limits of gliadin in gluten-free foodstuff accordingly to the EC food regulations.

However, the matrix effect was not completely avoided with the sample pretreatment through the ethanolic extraction followed by dilution of the sample, as can be seen through the increase of the IC50 value and decrease of the slope in the presence of both food matrixes. In order to overcome this issue, the standard curve for the competitive assay was decided to be performed with the gluten-free references extracts for further studies.

Table 4.4 Comparative results obtained with the magneto immunoassay performed in different matrixes such as PBST, skimmed milk and beer. The results are the average of three calibration curves performed at different days.

	IC50 (ng mL^{-1})	Linear range (ng mL^{-1})	Slope	LOD (ng mL^{-1})
PBST buffer	124.2	19.4-789.2	-0.76	5.71
PBST with milk	249.5	22.4-2381.9	-0.54	5.67
PBST with beer	327.7	12.5-3380.0	-0.46	3.74

4.4.5 Competitive electrochemical magneto immunosensor for gliadin detection

Since the direct immunoassay format and the use of microparticles as solid support gave in general better performance, these conditions were applied for the electrochemical approach. Once again, the first step was to determine the optimal gliadin-MP concentration and antiGliadin-HRP dilution. In both cases, the optimal conditions for the optical system were tested (gliadin-MP 0.04 mg mL^{-1} and antiGliadin-HRP 1/8000) and compared with increasing amounts of both reagents to reach 0.2 mg mL^{-1} magnetic particles and an antibodies dilution of 1/4000, as shown in Figure 4.19, A. As can be seen, significant higher signals were obtained by using a 1/4000 dilution of the labeled antibodies, so this amount was chosen for further studies. Regarding the magnetic particles, an increase in the signal was observed when increasing the concentration. A very good signal to nonspecific adsorption discrimination was obtained in all the condition assayed, even using higher amount of magnetic particles and antibodies concentration as shown in more detail in Figure 4.19, B.

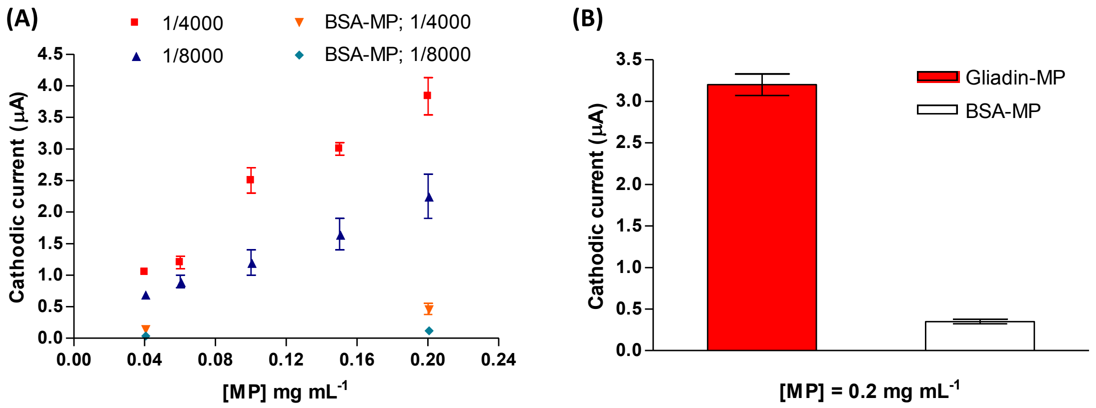

Figure 4.19 (A) Optimization of the immunoreagents amounts by testing five different magnetic particles concentrations (0.04, 0.06, 0.10, 0.15, 0.20 mg mL^{-1}) at two antiGliadin-HRP dilutions (1/4000 and 1/8000) and comparing the signals obtained with gliadin-MP and BSA-MP. (B) Detailed comparison of the signal and non-specific adsorption at 0.2 mg mL^{-1} of magnetic particles and 1/4000 of antibodies. The applied potential was -0.100 V (*vs.* Ag/AgCl).

Although the better magnetic particles concentration seemed to be the highest amount of 0.2 mg mL^{-1}, further studies had to be performed. A compromise situation had to be found in which obtaining high maximal signals but without favoring to much the reaction with the immobilized gliadin. As a result, a shift in the curve, which worsens the competition parameters, should be avoided. Therefore, the whole competitive curve was performed testing the three highest gliadin-MP concentrations (0.1, 0.15 and 0.2 mg mL^{-1}) as shown in Figure 4.20.

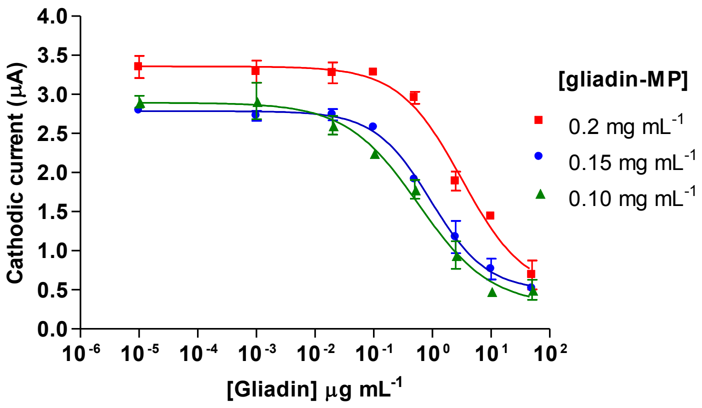

IC50 (ng mL^{-1})	LOD (ng mL^{-1})
2452.2	151.1
910.2	79.1
460.7	20.1

Figure 4.20 Competitive curves obtained at three different gliadin-MP concentrations: 0.1, 0.15 and 0.2 mg mL^{-1} by fixing the antiGliadin-HRP dilution in 1/4000. The table beside shows the IC50 and LOD values obtained for each situation.

As can be seen in the Figures and the related competition parameters, although a slight signal decrease was observed when decreasing the particles concentration, a very significant improvement was obtained at the lower concentration tested. As a result, a gliadin-MP concentration of 0.1 mg mL^{-1} and antiGliadin-HRP antibody dilution of 1/4000 was chosen for further immunoassays with the magneto immunosensor.

Afterwards, the performance of the magneto immunoassay with electrochemical detection in the different food matrixes was evaluated. Figure 4.21 shows a comparison of the competitive curves obtained with the electrochemical magneto immunosensors for skimmed-milk and beer in comparison with the calibration curve in PBST buffer, presenting good and well defined competitive curves for both food samples. In addition, Table 4.5 comparatively shows the parameters extracted from the four-parametric equation for the electrochemical magneto immunosensing approach performed in PBST, in skimmed-milk and beer.

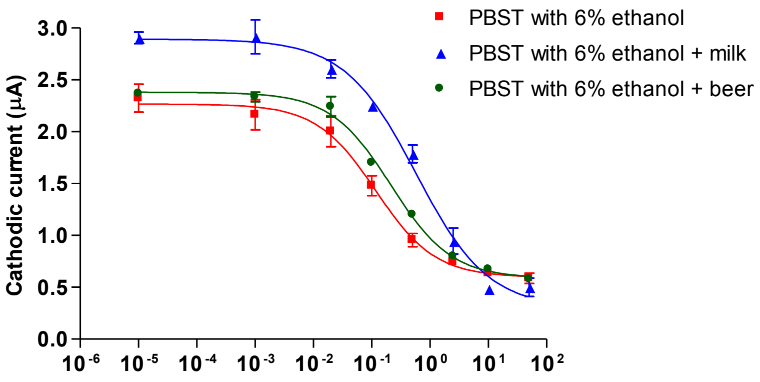

Figure 4.21 Comparative results for the detection of gliadin in PBST buffer, skimmed-milk and beer based on the direct competitive electrochemical magneto inmunosensor. The experimental conditions were: gliadin-MP 0.1 mg mL^{-1} and antiGliadin-HRP antibodies 1/4000. The error bars show the standard deviation for n=3.

Table 4.5 Comparative results of the competition parameters obtained with the electrochemical magneto immunosensor performed in different matrixes such as PBST, skimmed milk and beer.

	IC50 (ng mL^{-1})	Linear range (ng mL^{-1})	Slope	LOD (ng mL^{-1})
PBST buffer	117.4	18.9-589.5	-0.85	5.66
PBST with milk	578.7	66.9-2558.3	-0.72	20.07
PBST with beer	214.5	43.9-1155.6	-0.84	17.54

Excellent results were obtained for the detection of gliadin in skimmed-milk with the electrochemical magneto immunosensor (IC50 578.7 and LOD 20.1 ng mL^{-1}), as well as for the detection in beer (IC50 214.5 and LOD 17.5 ng mL^{-1}). As in the optical detection method, the LODs are once more much lower than the required gliadin limit of 20 mg L^{-1} (20 x 10^{-3} ng mL^{-1}) accordingly to the EC food regulations for gluten-free foodstuff.

When comparing these results with the parameters obtained in the magneto immunoassay (Table 3), similar performance could be observed with both detection strategies. Although slight better LOD values were achieved with the optical detection, much better Absmax/IC50 ratios were obtained in all cases with the electrochemical approach, giving values of 19.3, 6.28 and 11.1 with the immunosensor in comparison to 9.1, 4.6 and 3.5 with the magneto immunoassay in PBST, milk and beer respectively. Besides, fairly better sensitivity was also obtained with the electrochemical detection, showing higher slopes in all the matrixes tested. Moreover, while in the case of the optical system a slope decrease was observed in the presence of both food matrixes, this effect was not present in the case of the immunosensor, suggesting thus a more robust detection method regardless the tested sample.

Finally, when analyzing the coefficient of variation (CV) obtained at a concentration of 100 ng mL^{-1} for both the magneto immunoassay and the electrochemical magneto immunosensing approach, the results were found to be, respectively, 8.5 and 14.2 % in PBST, 7.0 and 11.6 % in skimmed-milk and 8.0 and 14.5 % in beer, for n=4 and n=3.

It should be also pointed out that the obtained LOD values for the magneto immunoassay and the magneto immunosensor are much lower also than the LODs previously reported for the validated R5 sandwich ELISA assays (LOD = 3.2 mg L^{-1})[2], as well as the commercial Ridascreen Gliadin competitive 2nd generation assay (r-Biopharm) (LOD = 1.4 mg L^{-1}). The integration of magnetic particles could play a key role in these improved results. The LODs are also much better than MALDI-TOF procedures as well as other non-immunological methods.[5,29]

Although similar LODs were obtained compared with previously reported electrochemical immunosensors[4,7], the competitive magneto immunosensor showed a wider linear range and the advantage of being able to detect small gluten fragments in pretreated and hydrolyzed foodstuff. A further issue of the renewable magneto immunosensor is that there is no need to perform a modification step after use, as the m-GEC electrodes can be renewed by simple polishing.

4.4.6 Accuracy study in foodstuff

Skimmed milk and gluten-free beer samples spiked with different gliadin concentrations were tested using both, the electrochemical magneto immunosensor as well as the magneto immunoassay procedures. The recovery values are presented in Table 4.6, showing excellent results for the ethanolic extraction followed by both detection methodologies (in skimmed-milk and beer food matrixes), in the concentration range from 5 to 200 mg L^{-1} (ppm). For a gliadin concentration of 20 mg L^{-1} (the required LOD established by the legislation) in beer sample, recovery values of 109.0 % and 121.5 % were obtained respectively with the electrochemical magneto immunosensor and the magneto immunoassay, while in the case of skimmed-milk samples, these values were found to be 112.1 % and 93.5 %.

Table 4.6 Recovery values in spiked skimmed-milk and beer samples based on the magneto immunoassay and the electrochemical magneto immunosensor. In all cases, n =3.

	Spiked skimmed milk sample		**Spiked beer sample**	
Concentration (ppm)	**Found concentration (ppm)**	**Recovery (%)**	**Found concentration (ppm)**	**Recovery (%)**
Magneto immunoassay				
200	194.4	97.2	166.9	83.4
80	76.4	95.5	79.6	99.5
20	18.7	93.5	24.3	121.5
5	6.4	128.0	6.6	132.0
Magneto immunosensor				
200	211.9	106.0	188.9	94.5
80	78.1	97.6	70.6	88.3
20	22.4	112.1	21.8	109.0
5	7.2	144.0	7.0	140.0

In the case of the magneto immunoassay the recovery values obtained by interpolating in the curve performed in PBST- 6 % ethanol without the food matrix were also calculated to control the difference in the gliadin detection. As shown in Table 4.7 the obtained values were significantly affected by the absence of the matrix in the standards, as was already supposed from the competition parameters obtained in Table 4.4 (§ 4.4.4). Once again, it was confirmed that the standard curves for the competitive assay were recommended to be performed with the gluten-free references extracts in the matrix for this system.

Table 4.7 Recovery values obtained after interpolating the spiked samples in the PBST curve containing just 6 % ethanol without the food matrix (milk or beer).

Magneto immunoassay	Spiked skimmed milk sample		Spiked beer sample	
Concentration (ppm)	Found concentration (ppm)	Recovery (%)	Found concentration (ppm)	Recovery (%)
Calibration curve in PBST without matrix				
200	133.2	66.6	60.4	30.2
80	73.6	92.0	39.0	48.8
20	16.7	83.5	20.6	103.0
5	3.9	78.0	8.6	171.5

4.5 CONCLUSIONS

The integration of magnetic micro and nanoparticles in competitive immunoassays for the optical and electrochemical detection of gliadin or gliadin fragments in natural or pre-treated food samples was reported.

For the first time, gliadin was immobilized to tosylactivated magnetic microparticles as well as to carboxyl-activated nanoparticles by covalent binding, achieving excellent immobilization efficiency (near 90 %) in both cases. However, the modified nanoparticles showed higher matrix effect for this application, and thus further studies were done with the magnetic microparticles.

The performance of the electrochemical magneto immunosensor was compared with the magneto immunoassay with optical detection, achieving in both cases similar LOD values. However, better sensitivity was obtained with the magneto immunosensor, which combines the advantages taken from immunochemical assays and magnetic particles separation with the sensitivity and robustness of the electrochemical detection. Beside this, commercially available reagents were used, which makes the implementation of the novel strategy easier. The magneto immunosensor is able to analyze gluten or small gluten fragments in natural or pretreated food and also in gluten-free food samples, as far as the maximal accepted limits are almost 1000 times higher than the achieved limits of detection. Moreover, the food samples could be diluted 400 times, reducing the food matrix effect.

As a result, the usefulness of the magnetic particles integration into both competitive immunochemical techniques was successfully demonstrated and the developed strategies show great promise for celiac patients' food safety.

Due to the outstanding performance of the electrochemical magneto immunosensor, this strategy can be suitable for the rapid and on-site screen-out of gliadin in foodstuff. The high sensitivity of the material used in the m-GEC electrodes, added to its compatibility with miniaturization and mass fabrication technologies, transforms them in very attractive cheap and user- friendly devices for rapid and in-field analysis in food industry applications.

4.6 REFERENCES

(1) Stern, M. *European journal of gastroenterology & hepatology* **2005**, *17*, 523–4.

(2) Thompson, T.; Méndez, E. *Journal of the American Dietetic Association* **2008**, *108*, 1682–7.

(3) Dahinden, I.; Von Büren, M.; Lüthy, J. *Eur. Food Res. Technol.* **2001**, *212*, 228–233.

(4) Nassef, H. M.; Redondo, M. C. B.; Paul, J.; Ellis, H. J.; Fragoso, A.; Sullivan, C. K. O.; Ciclitira, P. J. *Analytical Chemistry* **2008**, *80*, 9265–9271.

(5) Camafeita, E.; Alfonso, P.; Mothes, T.; Méndez, E. *Journal of mass spectrometry : JMS* **1997**, *32*, 940–7.

(6) Kanerva, P. M.; Sontag-Strohm, T. S.; Ryöppy, P. H.; Alho-Lehto, P.; Salovaara, H. O. *Journal of Cereal Science* **2006**, *44*, 347–352.

(7) Nassef, H. M.; Civit, L.; Fragoso, A.; O'Sullivan, C. K. *Analytical chemistry* **2009**, *81*, 5299–307.

(8) Gijs, M. A. M. *Microfluidics and Nanofluidics* **2004**, *1*, 22–40.

(9) Siegel, M.; Khosla, C. *Pharmacology & Therapeutics* **2007**, *115*, 232–245.

(10) Stenberg, P.; Roth, E. B.; Sjöberg, K. *European Journal of Internal Medicine* **2008**, *19*, 83–91.

(11) Van Eckert, R.; Berghofer, E.; Ciclitira, P. J.; Chirdo, F.; Denery-Papini, S.; Ellis, H. J.; Ferranti, P.; Goodwin, P.; Immer, U.; Mamone, G.; Méndez, E.; Mothes, T.; Novalin, S.; Osman, a.; Rumbo, M.; Stern, M.; Thorell, L.; Whim, a.; Wieser, H. *Journal of Cereal Science* **2006**, *43*, 331–341.

(12) Bradford, M. M. *Anal. Biochem.* **1976**, *72*, 248–254.

(13) Mikkelsen, S. R.; Cortón, E. *Bioanalytical Chemistry*; Hoboken, Ed.; John Wiley and Sons: New Jersey, 2004.

(14) Morón, B.; Bethune, M. T.; Comino, I.; Manyani, H.; Ferragud, M.; López, M. C.; Cebolla, A.; Khosla, C.; Sousa, C. *PloS one* **2008**, *3*, e2294.

(15) Lermo, a; Fabiano, S.; Hernández, S.; Galve, R.; Marco, M.-P.; Alegret, S.; Pividori, M. I. *Biosensors & Bioelectronics* **2009**, *24*, 2057–63.

(16) Josephy, P. D.; Eling, T.; Mason, R. P. *The Journal of Biological Chemistry* **1982**, *257*, 3669–3675.

(17) Marquez, L. A.; Dunford, H. B. *Biochemistry* **1997**, *36*, 9349–9355.

(18) Oubiña, A.; Ballesteros, B.; Bou Carrasco, P.; Galve, R.; Gascón, J.; Iglesias, F.; Sanvicens, N.; Marco, M.-P. *Techniques and Instrumentation in Analytical Chemistry* **2000**, *21*, 287–339.

(19) Motulsky, H.; Christopoulos, A. In *A practical guide to curve fitting. GraphPad Prism Software User Manual*; GraphPad Software, Inc: San Diego, 2003.

(20) García, E.; Llorente, M.; Hernando, A.; Kieffer, R.; Wieser, H.; Méndez, E. *European journal of gastroenterology & hepatology* **2005**, *17*, 529–539.

(21) Méndez, E.; Hernando, A. Method for extracting gluten from processed and unprocessed foods by means of heat based on the use of ionic and non-ionic detergents. EP 2 003 448 A1, 2008.

(22) Arentz-Hansen, E. H.; McAdam, S. N.; Molberg, Ø.; Kristiansen, C.; Sollid, L. M. *Gut* **2000**, *46*, 46–51.

(23) Aleanzi, M.; Demonte, A. M.; Esper, C.; Garcilazo, S.; Waggener, M. *Clinical Chemistry* **2001**, *47*, 2023–2028.

(24) Morón, B.; Cebolla, Á.; Manyani, H.; Álvarez-Maqueda, M.; Megías, M.; Thomas, M. del C.; Manuel Carlos López, A.; Sousa, C. *Am. J. Clin. Nutr.* **2008**, *87*, 405–414.

(25) Skovbjerg, H.; Koch, C.; Anthonsen, D.; Sjöström, H. *Biochimica et Biophysica Acta* **2004**, *1690*, 220–230.

(26) Ellis, H. J.; Rosen-Bronson, S.; O'Reilly, N.; Ciclitira, P. J. *Gut* **1998**, *43*, 190–5.

(27) McNaught, A. D.; Wilkinson, A. *IUPAC Compendium of Chemical Terminology*; McNaught, A. D.; Wilkinson, A., Eds.; 2nd editio.; Royal Society of Chemistry: Cambridge, UK, 1997.

(28) Chu, F. S. *Encyclopedia of Food Sciences and Nutrition.*; Academic Press: Oxford, 2003; pp. 3248–3255.

(29) Olexová, L.; Dovičovičová, L.; Švec, M.; Siekel, P.; Kuchta, T. *Food Control* **2006**, *17*, 234–237.

CHAPTER 5

DEVELOPMENT AND CHARACTERIZATION OF BIOTINYLATED BACTERIOPHAGES FOR THE DETECTION OF PATHOGENIC BACTERIA

5.1 INTRODUCTION

Nanostructured materials, including gold, silver and other metallic nanoparticles, carbon nanotubes, silica nanoparticles, quantum dots, magnetic nanoparticles, dendrimers, among others, represent an exciting area due to their unique properties compared to the non-nanostructured counterpart. They can be easily integrated in different procedures and biological reactions for biosensing and bioimaging.[1,2] Beside these non-biological nanomaterials, bacteriophages, as other virus-like particles, are attracting much interest due to their outstanding properties.

As mentioned in Chapter 1 (§ 1.7.3), one of the phage-based bacteria tagging strategies consists of the use of bioconjugation methods to attach signaling molecules at specific, designated positions of virus surfaces. Biotinylation of proteins, nucleic acids, lipids and sugars is without a doubt one of the most important tools of modern cell biology and biotechnology. This is due to the scarcity of naturally biotinylated proteins (< 5 per organism), the chemical flexibility by which biotin can be covalently conjugated to specific moieties of biopolymers and organic ligands, as well as the exceptional high affinity binding between avidin/streptavidin and biotin ($K_A = 10^{15}\ M^{-1}$).[3]

This chapter describes the development and characterization of novel bionanoparticles based on biotinylated bacteriophages. These labeled bionanoparticles were studied for the tagging of the bacteria *Salmonella* Thyphimurium in bioimaging and biosensing approaches with optical and electrochemical detection. The icosahedral-shaped bacteriophage P22 specific to *Salmonella* was studied as a model[4,5]. Its multivalent surface was firstly modified with the small biotin tag and further conjugation with optical and electrochemical reporters for biosensing systems were performed. The biotinylation of two different chemical moieties of the native phages (the amino groups of lysine and the carboxylic acid groups of aspartic or glutamic acid residues on P22 surface) was explored and evaluated, and the recognition capability was studied by classical culture methods. The biotinylated nanotag was characterized through different techniques, such as electrophoresis, confocal microscopy and Transmission Electron Microscopy (TEM) and the degree of labeling (DOL) was determined using a fluorometric assay for biotin detection. The utility of the biotinylated conjugates was demonstrated for the sensitive detection of *Salmonella* in electrochemical and optical biosensing approaches. Finally, the P22 bacteriophages were also explored as scaffold for the bottom-up construction of hybrid bionanomaterials with gold nanoparticles for imaging applications of the bacteria.

5.2 AIM OF THE CHAPTER

This chapter addresses the comprehensive study of the attachment of biotin to potentially reactive chemical moieties of phage capsid proteins for the development of novel bionanoparticles for bacteria tagging, taking as a model the P22 bacteriophage for the detection of the pathogenic bacteria *Salmonella*.

Therefore the specific objectives of this chapter were the following:

- To evaluate different methods for the purification of phage lysates.
- To design a novel method based on electrochemical magneto immunosensing for the purity evaluation of the phage lysates.
- To determine the optimal conditions, such as biotin amount and phage titer, for the phage biotinylation.
- To study the bacteria recognition capability of the biotinylated phages by classical microbiological methods (double agar layered technique), as well as by optical and electrochemical detection using streptavidin conjugated to horseradish peroxidase (Strep-HRP) as enzymatic label.
- To characterize the developed biotinylated P22 phages (biotin-P22) by different techniques such as a fluorometric assay for the evaluation of the labeling degree, electrophoresis and confocal microscopy.
- To exploit bottom-up hybrid nanomaterials such as phage conjugated to gold nanoparticles (AuNPs) for bacteria tagging and further analysis by Transmission Electron Microscopy (TEM).

5.3 EXPERIMENTAL SECTION

5.3.1 Materials

The P22 bacteriophages lysates were concentrated using 25 x 89 mm ultracentrifuge tubes (Ultra-ClearTM Tubes, Beckman, California, USA) in an ultracentrifuge (Optima^{TM} L-80, Beckman, California, USA) with the SW28 Ti rotor (Beckman, California, USA). The filters used in the bacteriophage filtration were Nucleopore Track-Etched Membranes (25 mm Ø, 0.2 µm pore size, product nº 110606, Whatman). The dialysis was performed with cellulose membranes purchased from Sigma (Dialysis Tubing, product nº D-9277, Steinheim, Germany) and the dialysis columns were from Novagen (D-Tube Dialyzer Maxi MWCO12-14 kD, product nº 71510-3). The cesium chloride (CsCl, product nº 10757306001) was supplied by Roche Applied Science (Roche Diagnostic S.L., Spain). For the ultra-filtration technique tested as alternative purification method, the centrifugal devices with filter sizes of 10, 30 and 50K were from Millipore (Amicon Ultra-15 Centrifugal Filter Units, product nº UFC901008, 903008 and 905008, respectively), while the EndoTrap blue columns used for the removal of bacterial endotoxins through affinity chromatography (product nº 311053) were supplied by Hyglos GmbH, Germany.

The NHS-PEG$_4$-Biotin and Amine-PEG$_3$-Biotin were purchased from Thermo Scientific (product nº 21955 and 21347, respectively). The removal of non-reacted biotin after the biotinylation was carried out using desalting columns purchased from Thermo Scientific (Zeba Desalt Spin Columns, product nº 89889). The FluoReporter ® Biotin Quantitation Assay Kit for biotinylated proteins was from Molecular Probes (product nº F30751).

The magnetic particles modified with anti-*Salmonella* antibodies (Dynabeads, product n° 710.02) were supplied by Invitrogen Dynal AS (Oslo, Norway). *N*-(3-Dimethylaminopropyl)-*N'*-ethylcarbodiimide hydrochloride (EDC), *N*-hydroxysulfosuccinimide (sulfo-NHS), Bovine serum albumin (BSA), avidin (product nº A9275) and Strep-HRP (product nº S5512) were obtained from Sigma-Aldrich. The anti-*Salmonella* antibodies conjugated to biotin (biotin-Ab, product nº ab21118), used for the comparison with the biotin-P22 tagging pattern through confocal microscopy, were supplied by Abcam (Cambridge, UK).

The nucleic acid stain Hoechst 33342 and the streptavidin labeled with cyanine 5 (Strep-Cy5) dye used in confocal microscopy were purchased from Life Technologies (product nº H-3570 and SA-1011, respectively), while the streptavidin conjugated to 20 nm colloidal gold nanoparticles (Strep-AuNP, product nº GA-02) were from EY Laboratories, Inc (San Mateo, CA, USA).

The peroxide and TMB (3,3',5,5'- tetrametylbenzidine) solutions utilized for the optical measurements (TMB Substrate Kit, product nº 34021) were purchased from Pierce. On the other hand, the hydrogen peroxide 30 % used as a substrate in the electrochemical measurements was purchased from Merck (product nº 1.07209.0250, Germany), while the hydroquinone used as a mediator was from Sigma-Aldrich (product nº H9003).

All other reagents were of the highest available grade, supplied from Sigma or Merck and all buffer solutions were prepared with milli-Q water (Millipore Inc., Ω = 18 MΩ cm).

For the biotinylation PBS buffer (0.1 mol L^{-1} phosphate, 0.15 mol L^{-1} NaCl, pH 7.2) or MES buffer (0.1 mol L^{-1} MES, 0.15 mol L^{-1} NaCl, pH 5.5) was used, depending on the conjugation strategy. For the evaluation of the biotinylated phages by agarose electrophoresis, 0.5X TAE (40 mM Tris-base pH 7.4, 20 mM sodium acetate, 1 mM EDTA) was prepared, while 2 % uranyl acetate was used in the negative staining performed for TEM analysis.

Finally, the composition of the solutions used in the optical and electrochemical assays were: PBST (0.01 mol L^{-1} phosphate buffer, 0.15 mol L^{-1} NaCl, 0.05 % v/v Tween 20, pH 7.5); b-PBST (2 % w/v BSA in PBST as blocking buffer) and PBSE buffer (0.1 mol L^{-1} sodium phosphate, 0.1 mol L^{-1} KCl, pH 7.0).

The instrumentation and materials used for the incubation and washing steps, the magnetic separations, as well as the optical and electrochemical detection were the same as detailed in Chapter 4 (§ 4.3.1.2). The black flat-bottomed microplates used for the fluorescence assays were from Greiner bio-one (product nº 655900) and the fluorescence measurements were performed with an Infinite M-200 microplate reader from TECAN Iberica Instrumentacion SL.

Regarding the microscopy characterization techniques, Transmission Electron Microscopy (TEM) images were acquired using a JEM-1400 transmission electron microscope equipped with a CCD GATAN 794 MSC 600HP camera, while fluorescence images were acquired using a Leica TCS/SP5 confocal microscope (Leica Microsystems, Exton, PA).

5.3.1.1 Bacterial strain and bacteriophage lysate preparation

The bacteria *Salmonella enterica* serovar Typhimurium LT2 (supplied by J.L. Ingraham, Bacteriology Department, University of California, Davis, USA) were routinely grown in Luria Bertani (LB) broth pH 7.5 or on LB agar plates for 18 h at 37ºC. Bacterial viable counts were determined by plating on LB plates followed by incubation at 37ºC for 24h.

The P22 bacteriophage (ATCC® 19585-B1™), a temperate virus that infects *Salmonella* groups A, B and D was used in the studies as a model. To obtain the lysates exponential cultures of *Salmonella* Typhimurium LT2 (10^8 CFU mL^{-1}) grown in LB medium at 37°C were infected with P22 phage at a multiplicity of infection (MOI) of 1 plaque-forming unit (PFU) per colony-forming unit (CFU) and incubated at 37°C for 5 h. Afterwards, infected cultures were centrifuged at 8000 × g for 10 min and the supernatants were filtered through 0.22 µm Nucleopore membrane to remove any remaining bacteria in the solution. The phage titer was determined by plating adequate dilutions using double agar layered conventional method, as shown in Figure 5.1: 100 µL of each dilution were blended with 100 µL of 10^8 CFU mL^{-1} *Salmonella* Typhimurium LT2 dilution and 2.5 mL of soft agar. The mixture was spilt on LB agar plates and after incubation for 18-24 h at 37 ºC phage plaques were counted. Then, P22 phages were concentrated by ultracentrifugation at 27000 × g for 2 h and finally resuspended in 10 mM $MgSO_4$ to obtain titers of approximately 10^{12} PFU mL^{-1}.

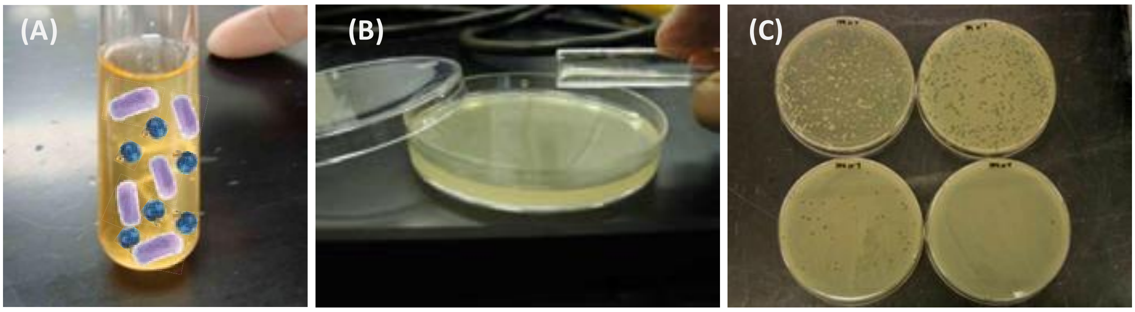

Figure 5.1 Schematic representation of the double agar layered method for titrating active phages. A phage dilution is mixed with 10^8 CFU mL^{-1} *Salmonella* and soft agar (A), pouring the mix on LB agar plates (B) and after 18-24 h incubation at 37ºC the plaques formed at different 10-fold dilution series were counted (C).

5.3.1.2 Bacteriophage purification

Since the phage production is based on their self-synthesizing capability by infecting its specific host, the subsequent purification process to eliminate possible remaining bacterial debris is a really challenging task.

Many methods for phage lysate purification have been reported such as ultra-high speed centrifugation,[6] ultra-filtration through polysulfone membrane followed by chromatography,[7] poly(ethylene glycol) precipitation-gradient centrifugation,[8] chromatofocusing,[9] affinity chromatography,[10] anion exclusion chromatography connected to a fast protein liquid chromatography (FPLC)[11] and size exclusion chromatography[12]. However, the purification by CsCl gradient is still a reference method to ensure high purity of the phages, although it is also quite laborious and time-consuming.

In an attempt to find a simpler, faster and cheaper purification method for preparing the starting phage suspensions different strategies were tested to obtain a pure phage lysate: polyethylene glycol (PEG)/NaCl precipitation (combined or not with a chloroform treatment) followed by ultra-filtration methods using Amicon Ultra devices with different filter sizes (between 10K and 50K), as well as an affinity chromatography column called Endotrap blue, which is commercially available for the efficient removal of bacterial LPS based on a highly cross-linked 4 % sepharose resin. In the last case, the effect of passing repeatedly the phage lysate was also studied. The results were compared to the purity obtained by the CsCl gradient purification method, and its combination with a final dialysis step or with a pass through the aforementioned Endotrap column.

The ultra-filtration and affinity chromatography were carried out following the manufacturer recommendations.

On the other hand, the purification by cesium chloride gradient was performed accordingly to the standard protocol described by Sambrook et al.[13] After a previous step of digestion with DNAase and RNAase, a treatment with NaCl followed by precipitation with PEG and a chloroform extraction, the phage lysate was carefully placed in a CsCl density gradient. Briefly, 15 mL of concentrated bacteriophage suspension was overlaid onto a three-step CsCl gradient containing 7.6 mL of each 1.6 g mL^{-1} CsCl, 1.5 g mL^{-1} CsCl, and 1.45 g mL^{-1} CsCl, respectively, in the ultracentrifuge tubes. Afterwards, P22 bacteriophages were centrifuged for 2 h at 87,000 x g at 4°C in a rotor. Phage-containing bands (translucent white/gray) were extracted through the wall of the centrifuge tube by puncturing with a needle, and the CsCl was subsequently removed by dialysis using a cellulose membrane for 16 hours with three changes of $MgSO_4$ 10 mM at 4ºC. The bacteriophage titer was determined as described in § 5.2.1.1 and finally, the phage stock solutions were maintained in $MgSO_4$ 10 mM solution at 4 °C retaining a constant titer for several months.

5.3.1.3 Purity control of phage lysate by electrochemical magneto immunosensing

The purity control was based on the detection of the *Salmonella* LPS antigens remaining after the purification process and was performed by a sandwich magneto immunoassay for *Salmonella* based on amperometric detection previously developed in our group.[14] As the bacteriophages are used for the specific detection of *Salmonella* and in order to get lower nonspecific adsorption values, the bacteriophage lysate should give no signal due to their host *Salmonella* used to grow them.

The applied protocol for the immunosensing approach was as follows: i) capture of *Salmonella* fragments by adding 140 µL of phage solution to 10 µL of commercial magnetic microparticles modified with specific anti-*Salmonella* antibodies and incubating 10 min at 700 rpm, ii) after removing the supernatant, addition of 140 µL of anti *Salmonella*-HRP antibodies (Ab-HRP) diluted 1/1000 in b-PBST and 30 min incubation at 700 rpm, followed by two 5 min washes with 140 µL of PBST. Finally the last step was iii) the capture of the magnetic particles on the electrode surfaces by dipping the magneto electrode (m-GEC) inside the reaction tube followed by the amperometric detection. The electrochemical measurement was recorded by using the modified m-GEC as a working electrode and immersing the three-electrode setup in 20 mL PBSE buffer, polarizing the m-GEC electrode at a working potential of −0.100V (*vs.* Ag/AgCl), which was fixed through cyclic voltammetry. The amperometric signal was based on the enzymatic activity of the HRP after the addition of hydrogen peroxide (4.90 mmol L^{-1}) as the substrate and hydroquinone (1.81 mmol L^{-1}) as a mediator as explained in Chapter 4 (§ 4.3.6).

Although the developed method is not quantitative, it could give some notion of the bacteria contamination remaining after the purification process. In order to test the applicability of the novel method for the evaluation of LPS contamination, the phage lysates obtained through the different purification methods described in the previous section were tested and the signals were compared with a negative control containing the phage media ($MgSO_4$ 10 mM) and also with the non-purified phages obtained as explained in § 5.3.1.1. If no bacteria interference were present in the samples, the signals should be almost the same than the results of the negative control. Otherwise, some degree of contamination would be suggested.

In parallel to the electrochemical detection, the phage titer was also determined by double agar layered method to control if the phage concentration was affected by the purification procedure.

5.3.1.4 Safety considerations

All the procedures involving the manipulation of potentially infectious materials or cultures were performed following the safe handling and containment of infectious microorganism's guidelines.[15] According to these guidelines, the experiments involving *Salmonella* Typhimurium and *E. coli* were performed in a Biosafety Level 2 Laboratory. Strict compliance with BSL-2 practices was followed and proper containment equipment and facilities were used. Contaminated disposable pipette tips were carefully placed in conveniently located puncture-resistant containers used for sharps disposal. All cultures, stocks, laboratory waste, laboratory glassware and other potentially infectious materials were decontaminated before final disposal by autoclaving. The ultimate disposal was performed according to local regulations.

5.3.2 Bacteriophages biotinylation

The tagging of two different reactive groups, i.e., the amino groups of lysine and the carboxylic acid groups of aspartic or glutamic acid residues on P22 surface, was explored. The reactivity of each group was identified through the conjugation with biotin, which also provided versatility for further modification with optical, fluorescence and electrochemical reporters by using streptavidin conjugates. The linkage between the phage and the biotin tag was performed with water-soluble polyethylene glycol (PEG) spacer arms of different lengths (2.9 and 2.0 nm) to minimize steric hindrance for binding with the optical, fluorescence and electrochemical reporters, providing flexibility to the final three-dimensional structure. Two different biotinylation strategies were evaluated. The first one was based on NHS-PEG$_4$-Biotin, as shown in Figure 5.2, A. The N-hydroxysuccinimide ester (NHS) group reacts specifically with lysine as well as N-terminal amino groups to form stable amide bonds. The hydrophilic PEGylated spacer arm of 2.9 nm imparts water solubility that is transferred to the biotinylated molecule, thus reducing aggregation of the biotin-P22 NPs stored in solution. The second one was based on Amine-PEG$_3$-Biotin, as shown in Figure 5.2, B. The primary amine of the PEGylated biotin reagent was conjugated to carboxyl groups on carboxy termini, aspartate or glutamate residues of the native P22 NPs by using EDC, a water-soluble carbodiimide crosslinker. The EDC was used to activate the carboxyl groups of the P22 phage to bind to the –NH2 group of the amine-biotin, forming an amide bond.

In order to bind the biotin to the amine groups of the phage capsid proteins, the activated NHS-PEG$_4$-Biotin was incubated during 1.5 h at 700 rpm and room temperature with the phage suspension. In the case of the coupling of biotin to the carboxylic groups, EDC and Amine-PEG$_3$-Biotin were added to the phages solution in a biotin:EDC ratio of 10:1 to activate the carboxylic groups on the phage capsid by incubating also 1.5 h at 700 rpm and room temperature.

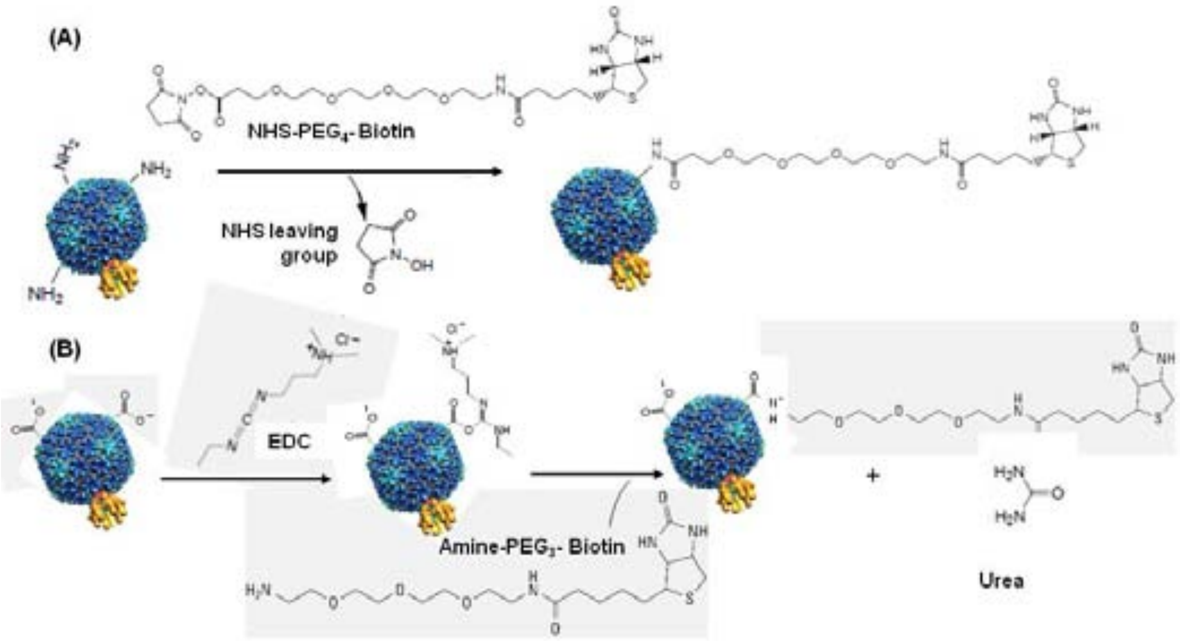

Figure 5.2 Schematic representation of the two paths for the biotinylation: (A) the reaction of NHS-PEG$_4$-Biotin with the primary amines of P22 phages, and (B) the activation of the carboxylic groups of P22 with EDC followed by the reaction with Amine-PEG$_3$-Biotin.

After the biotinylation process, the excess of biotin was removed by passing the sample through an exclusion column (Zeba Desalt Spin Column) through a 2 minutes centrifugation step at 1000 g. A schematic representation of the biotinylation protocol is shown in Figure 5.3. The biotin removal through the column was repeated 3 times to ensure the complete elimination of free biotin from the biotinylated phage suspension for further evaluation of the degree of labeling. However, in the case of using the biotin-P22 for bacteria tagging, the elimination of the free biotin is not as important, since it would anyway be eliminated through the washing steps performed during the immunoassay.

The infectivity of the biotinylated phages was studied by conventional phage titration using the double agar layered method, and by comparing the retained activity after biotinylation with the original titer of the lysate. At the same time, the optical signals at different bacteria concentrations were analyzed to verify which strategy presents best performance. Once the best strategy was established, the phage and biotin amount for the biotinylation process were optimized by evaluating the phage infectivity as well as the optical signals in order to obtain the best results.

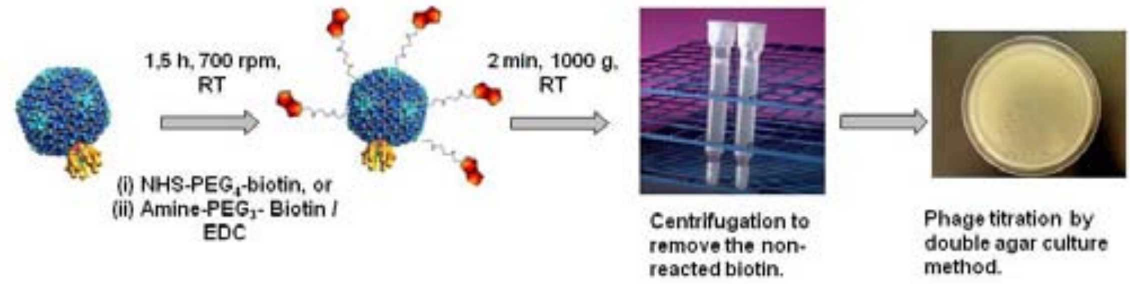
1,5 h, 700 rpm, RT
(i) NHS-PEG$_4$-biotin, or
(ii) Amine-PEG$_3$- Biotin / EDC
2 min, 1000 g, RT
Centrifugation to remove the non-reacted biotin.
Phage titration by double agar culture method.

Figure 5.3 Schematic representation of the biotinylation process.

5.3.3 Immunomagnetic separation and biotin-P22 tagging for the optical and electrochemical detection of *Salmonella*

The utility of the biotin-P22 phage for *Salmonella* tagging and further detection was proved by both optical and electrochemical measurements.

The immunomagnetic separation (IMS) was performed using commercially available magnetic particles modified with the specific antibodies towards *Salmonella*. The exact concentration of the initial inoculum coming from an overnight culture in LB broth was found by serial decimal dilutions plated in LB agar. A negative control of LB broth was also processed. Different concentrations of *Salmonella* in LB (100 µL in the case of optical and 500 µL in the electrochemical detection) were added to anti-*Salmonella* magnetic particles (10 µg for the optical and 50 µg for the electrochemical detection) and an incubation step was performed for 20 min in slight agitation (700 rpm). After that, the magnetic particles with the attached bacteria were separated with a magnet, and washed twice with PBST (5 min, 700 rpm).

The IMS followed by the bacteria tagging with biotin-P22 coupled to optical detection was performed in microtiter plates with flat-bottomed wells comprising the following steps, as shown in Figure 5.4: (i) IMS for attaching the target bacteria to the magnetic particles, as explained above; (ii) bacteria tagging with 100 µL of the biotin-P22 diluted 1/100 (in PBST with $MgSO_4$ 10 mM), incubating 20 min without agitation at 37ºC, followed by washing with 100 µL PBST for 3 minutes; (iii) enzymatic labeling with 100 µL Strep-HRP at a concentration of 1 µg mL^{-1} (in b-PBST), 30 min at 700 rpm and room temperature, followed by washing (2×) with 100 µL of PBST; and (iv) 30 min incubation at 700 rpm, room temperature and in darkness, with 100 µL of substrate solution, containing H_2O_2 and 3,3',5,5'-tetramethylbenzidine (TMB) in citrate buffer, followed by the addition of 100 µL H_2SO_4 to stop the reaction (2 mol L^{-1}) and optical reading at 450 nm (Figure 5.4, B). After each incubation or washing step, the magnetic particles were separated from the supernatant on the bottom corner by using a 96- well magnet plate separator, positioned 1 min under the microtiter plate.

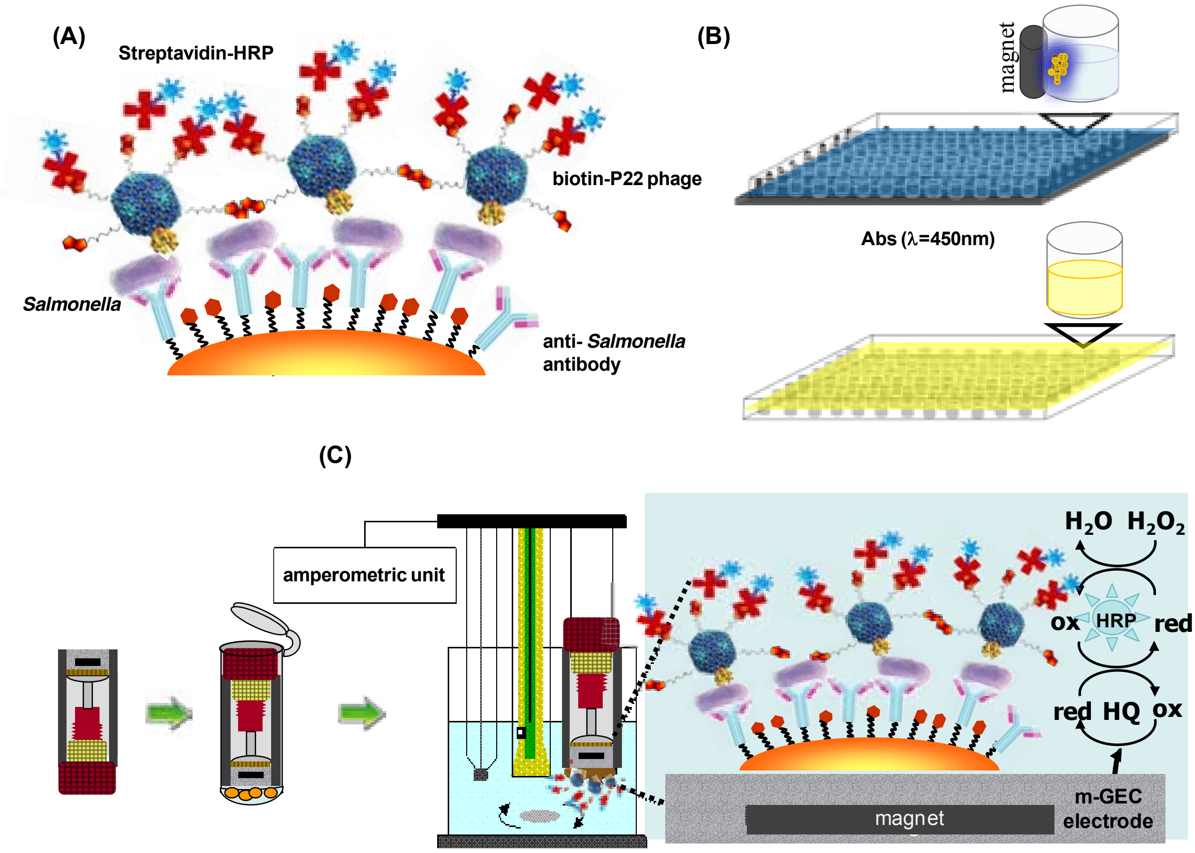

Figure 5.4 Schematic representation of (A) the phagotagging magneto immunoassay showing the immunomagnetic separation of *Salmonella*, the phage tagging and secondary labeling with the conjugate Strep-HRP; (B) on optical detection performed on 96-well microtiter plates and (C) phagotagging electrochemical magneto immunosensor. The magnetic particles capture on the surface of the m-GEC magneto electrode and the chemical reactions occurring during the measurement by polarizing the magneto electrode at -0.150 V (*vs.* Ag/AgCl) are also shown.

On the other hand, the IMS and bacteria tagging with biotin-P22 coupled to electrochemical detection was performed in Eppendorf tubes, similarly than the previous approach, but using 140 µL of the biotin-P22 phage diluted 1/25 and 140 µL of Strep-HRP at a concentration of 40 µg mL^{-1} for the labeling steps, and being the step (iv) the capture of the magnetic particles on the electrode surfaces by dipping the magneto electrode (m-GEC) inside the reaction tube followed by the amperometric detection. The electrochemical measurement was recorded by using the modified m-GEC as a working electrode and immersing the three-electrode setup in 20 mL PBSE buffer, polarizing the m-GEC electrode at a working potential of −0.150 V (*vs.* Ag/AgCl), which was previously fixed through cyclic voltammetry. The amperometric signal was based on the enzymatic activity of the HRP after the addition of hydrogen peroxide (4.90 mmol L^{-1}) as the substrate and hydroquinone (1.81 mmol L^{-1}) as a mediator (Figure 5.4, C). After each incubation or washing step, the magnetic particles were separated from the supernatant on the side wall by placing the Eppendorf tubes in a magnet separator until the particles were migrated to the tube sides and the liquid was clear.

5.3.4 Characterization by gel electrophoresis

The electrophoresis was performed as a way to prove the phage modification and also to control the integrity of the phage nanoparticles. The hypothesis was that for each biotin conjugated to an amine group of the P22, one positive charge of the capsid was removed, which should produce some change in the electrophoretic mobility. Moreover if avidin is added to the biotin-P22 some extra change should occur due to the size increase of the resulting macromolar complex.

In order to run the samples, 10 µL of the non-modified and biotinylated phages at a concentration of 1.75 x 10^{11} PFU mL^{-1}, as well as the biotin-P22 conjugated to avidin (0.2 mg mL^{-1}) were analyzed by conventional gel electrophoresis on a 1.2 % agarose gel containing 0.5X TAE (40 mM Tris-base pH 7.4, 20 mM sodium acetate, 1 mM EDTA). The electrophoresis was run at a constant voltage of 100 V for 45 min. DNA and protein visualization was performed on the same gel using ethidium bromide and Coomassie blue staining, respectively. Both images were obtained using the Gel Doc™ XR+ (Bio Rad) system.

5.3.5 Fluorometric assay for the evaluation of the degree of labeling

The quantification of the number of biotin molecules covalently attached per phage, also called the degree of labeling (DOL), was based on the Biotective™ Green reagent, which consists of avidin labeled with a fluorescent dye and with quencher dye ligands occupying the biotin binding sites.[16] Through fluorescence resonance energy transfer (FRET), the ligand quenches the fluorescence. Biotin molecules attached to the phage displace the quencher dye from Biotective Green reagent, yielding fluorescence proportional to the amount of biotin, as depicted in Figure 5.5.

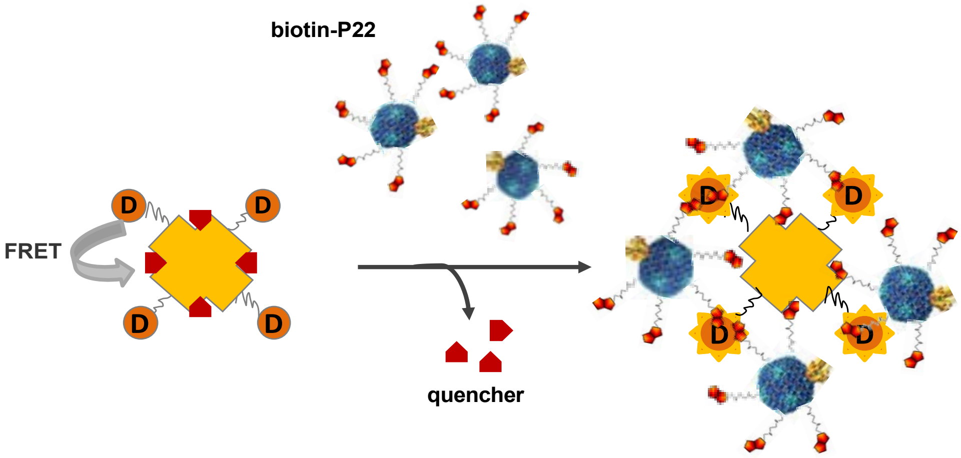

Figure 5.5 Schematic representation of the mechanism of the Biotective Green reagent for the detection of biotin on the modified bacteriophages. The fluorescence of the dye (indicated as D) is quenched by FRET until the quencher dye is displaced according to the amount of biotin.

The experimental procedure was performed following the instructions of the kit manufacturer. In order to expose any biotin moiety sterically restricted and inaccessible to the Biotective Green reagent, protease E was used to disrupt the proteins and establish the total biotin amount. A volume of 50 μL of the biotin-P22 and of a positive control consisting of a biotinylated anti-mouse IgG standard with a known DOL (5 biotin molecules per IgG molecule) were digested overnight at 37ºC in PBS with the protease at a final concentration of 10 U mL^{-1}. To determine the biotin amount in the biotin-P22 a standard curve of biocytin was run within the same assay as the digested and undigested biotin-P22 samples as well as a digested and undigested positive control. The biotin concentration corresponding to the fluorescence intensities of the unknown samples were obtained by interpolation in the resulting sigmoid curve. Once the biotin concentration in each sample was determined, the number of molecules per mL was calculated and divided by the phage or IgG molecules per mL in the same sample in order to obtain the DOL.

5.3.6 Confocal Fluorescence Microscopy

Confocal microscopy was used to characterize the *Salmonella* tagging with the biotin-P22 for bacteria imaging, by using the fluorescent reporter Strep-Cy5. The confirmation of the P22 phage biotinylation and its bacterial recognition ability was also achieved. The general nucleic acid stain Hoechst 33342 was used for labeling the bacteria, by adding 4.5 μL of dye (at 10 mg mL^{-1}) per mL of bacteria at a concentration of 10^6 CFU mL^{-1}. The IMS, as well as the biotin-P22 tagging was performed as previously detailed, but in this case using Strep-Cy5 as fluorescence reporter. To 20 µg of magnetic particles with the captured bacteria and the biotin-P22 phages also attached, 100 µL fluorescent conjugate at a concentration of 2 µg mL^{-1} in b-PBST was added. In order to compare the fluorescence pattern and intensity, the same assay was performed by using biotinylated anti-*Salmonella* antibodies (biotin-Ab), instead of the biotin-P22 phage. Both approaches were imaged using a Leica TCS/SP5 confocal microscope. Finally the 3D Imaris X64 v. 6.2.0 software (Bitplane; Zürich, Switzerland) was applied for processing the images obtained.

5.3.7 Transmission Electron Microscopy (TEM)

A hybrid bionanomaterial was also developed and evaluated for bacteria bioimaging. To achieve this, P22 phages were coupled to AuNP throughout the biotin-streptavidin interaction. Biotin-P22 phages conjugated to Strep-AuNP were prepared adding 5 µL of Strep-AuNP (8 µg mL^{-1}) to 20 µL of biotinylated phages (8 x 10^{10} PFU mL^{-1}) and incubating with slight agitation at room temperature for 30 min. The bacteria tagged with the biotin-P22 and Strep-AuNP complex were prepared performing a previous phagotagging step incubating 100 µL of *Salmonella* (2.3 x 10^{7} CFU mL^{-1}) with 6 µL biotin-P22 (1.5 x 10^{11} PFU mL^{-1}) for 20 min at 37ºC. After a washing step with PBS by centrifugation (5 min at 6000 rpm), 20 µL of the Strep-AuNP label were added and incubated as previously described, performing a washing as the final step. TEM samples were prepared by depositing 10 µL of each sample onto carbon-coated copper grids for 2 min. The grids were then negatively stained for 2 min with 2 % uranyl acetate and viewed with a transmission electron microscope equipped with a CCD GATAN 794 MSC 600 HP camera.

5.4 RESULTS AND DISCUSSION

5.4.1 Bacteriophage purification

Despite the centrifugation steps, the contamination with bacterial lipopolysaccharides (LPS), peptidoglycan fragments, flagella filaments and proteins is very difficult to avoid in a phage lysate,[17] since the phage was grown in a culture of the same host as the target of the assay, in this case, *Salmonella*. As a consequence, the presence of bacteria debris would greatly interfere with the subsequent phage conjugation efficiency, reducing thus the performance of the detection methods. Moreover, since the *Salmonella* detection strategies developed in the present dissertation are based on the combined used of phages and antibodies, the presence of bacterial fragments in the phage suspensions would affect the background values interfering with the results.

Table 5.1 schematizes the most important variations in the purification protocol with the corresponding signal to background ratios obtained after the amperometric measurements of the phage solutions.

Table 5.1 Comparative signal to background ratios after applying the magneto immunoassay with amperometric detection to the phage solutions obtained after different purification protocols.

Phage titer (PFU mL^{-1})	Method	Signal to background
E+11	Non-purified (filtered + ultracentrifugation)	17.1
E+11	PEG/NaCl + chloroform	12.8
E+12	PEG/NaCl + chloroform	14.9
E+11	Ultra-filtration 10K	8.2
E+11	Ultra-filtration 30K	5.8
E+11	Ultra-filtration 50K	5.4
E+10 / E+11	Endotrap,1st pass	5.6
E+10 / E+11	2nd pass	2.95*
E+07 / E+08	3rd pass	1.6
E+12	Endotrap,1st pass	13
E+12	2nd pass	9.6
E+12	CsCl	5.3
E+11	CsCl+dialysis	1.4
E+12	CsCl+dialysis	2.4
E+12	CsCl + Endotrap	3.0

(*) In the case of the Endotrap column two of the five purification replicates showed already in the second pass, a decrease in the phage titer to around 10^8 PFU mL^{-1}.

The results demonstrated a consistent behavior of the developed detection system that became evident after analyzing for example the repeated purification steps through the column, in which a decrease in the signal to background ratio was observed according to each new passing through. Therefore, a correlation between the amount of LPS present in the samples and the obtained signals is observed, demonstrating the capability of the applied sandwich magneto immunoassay with electrochemical detection for the evaluation of the phage lysate purity.

In general, the signals to background ratios suggest that just PEG/NaCl precipitation followed by chloroform extraction was the less efficient purification protocol, while the addition of a further purification method such as ultra-filtration with different filters, or chromatography using the Endotrap colum or CsCl gradient significantly improved the purification level. Regarding the purification with the filters, a slight improvement of the purification seemed to take place while increasing the pore size, obtaining the best results when using the 50K filters.

Finally, comparing all the results the smallest signal to background ratios were achieved using the CsCl gradient purification, and especially if it was followed by dialysis, in which the signal of the purified phage solution almost matched the signal of the blank. A similar value was obtained after three purification steps through the Endotrap column, but with the drawback of presenting an important drop in the phage titer. As a result, the chosen purification protocol was thus the CsCl gradient coupled to a subsequent dialysis step to finally achieve a purified starting reagent, appropriate for the further analytical applications for bacteria detection.

5.4.2 Characterization of phage biotinylation

The bacteriophages bind to specific receptors on the bacterial surface in order to inject the genetic material inside the bacteria. In the case of P22, six homotrimeric tailspike molecules (namely gp9) are involved in the viral adhesion protein which specifically recognizes the O-antigenic repeated units of the LPS on the cell surface of *Salmonella*.[18] The evaluation of the integrity of the phage tailspike protein after biotinylation is, thus, an important issue to be considered, since biotin could hinder the recognition of the bacteria by the biotin-P22 phages. The ideal scenario would be the biotinylation of the capsid monomeric protein (gp5) leaving intact the tailspike protein (gp9) which is involved in the biorecognition. Firstly, the reactive groups of the aminoacidic sequence in both the tailspike protein (gp9) and the main capsid monomeric protein (gp5) were carefully studied, as detailed in Figure 5.6. The number of lysines and glutamic and aspartic acid comparatively in gp5 and gp9 are summarized in Table 5.2.

As stated in the table, the capsid formed by 420 repeated copies of the gp5 monomer, and because of its high surface, has a higher number of addressable moieties compared with the tailspike, composed by the 18 copies of the gp9 monomer (30240 and 1836, respectively). However, among the potentially reactive groups, the tailspike, which represent the biorecognition site of the phage P22, is richer in glutamic and aspartic acid, being the 66 % of the addressable moieties and resulting in much more carboxylic than amine groups in the tailspike protein.

gp5

```
1   MALNEGQIVT LAVDEIIETI SAITPMAQKA KKYTPPAASM QRSSNTIWMP VEQESPTQEG
61  WDLTDKATGL LELNVAVNMG EPDNDFFQLR ADDLRDETAY RRRIQSAARK LANNVELKVA
121 NMAAEMGSLV ITSPDAIGTN TADAWNFVAD AEEIMFSREL NRDMGTSYFF NPQDYKKAGY
181 DLTKRDIFGR IPEEAYRDGT IQRQVAGFDD VLRSPKLPVL TKSTATGITV SGAQSFKPVA
241 WQLDNDGNKV NVDNRFATVT LSATTGMKRG DKISFAGVKF LGQMAKNVLA QDATFSVVRV
301 VDGTHVEITP KPVALDDVSL SPEQRAYANV NTSLADAMAV NILNVKDART NVFWADDAIR
361 IVSQPIPANH ELFAGMKTTS FSIPDVGLNG IFATQGDIST LSGLCRIALW YGVNATRPEA
421 IGVGLPGQTA
```

gp9

```
1   MTDITANVVV SNPRPIFTES RSFKAVANGK IYIGQIDTDP VNPANQIPVY IENEDGSHVQ
61  ITQPLIINAA GKIVYNGQLV KIVTVQGHSM AIYDANGSQV DYIANVLKYD PDQYSIEADK
121 KFKYSVKLSD YPTLQDAASA AVDGLLIDRD YNFYGGETVD FGGKVLTIEC KAKFIGDGNL
181 IFTKLGKGSR IAGVFMESTT TPWVIKPWTD DNQWLTDAAA VVATLKQSKT DGYQPTVSDY
241 VKFPGIETLL PPNAKGQNIT STLEIRECIG VEVHRASGLM AGFLFRGCHF CKMVDANNPS
301 GGKDGIITFE NLSGDWGKGN YVIGGRTSYG SVSSAQFLRN NGGFERDGGV IGFTSYRAGE
361 SGVKTWQGTV GSTTSRNYNL QFRDSVVIYP VWDGFDLGAD TDMNPELDRP GDYPITQYPL
421 HQLPLNHLID NLLVRGALGV GFGMDGKGMY VSNITVEDCA GSGAYLLTHE SVFTNIAIID
481 TNTKDFQANQ IYISGACRVN GLRLIGIRST DGQGLTIDAP NSTVSGITGM VDPSRINVAN
541 LAEEGLGNIR ANSFGYDSAA IKLRIHKLSK TLDSGALYSH INGGAGSGSA YTQLTAISGS
601 TPDAVSLKVN HKDCRGAEIP FVPDIASDDF IKDSSCFLPY WENNSTSLKA LVKKPNGELV
661 RLTLATL
```

Figure 5.6 Protein sequences of the capsid protein gp5 (1-430) and tailspike protein gp9 (1-667) of the P22 phage (UniProtKB/Swiss-Prot, accession number P26747 and P12528, respectively). The potential reactive amino acids are highlighted: lysine (K) in yellow, glutamic (E) in green and aspartic acid (D) in red.

Table 5.2 Number of potential reactive amine moieties on the lysine (Lys) side chains and carboxylic groups on the glutamic (Glu) and aspartic acid (Asp) side chains.

Protein	Copy #/phage	Lys#/copy	Glu#/copy	Asp#/copy	Total Lys#	Total Glu+Asp #
Gp5 (capsid protein)	420	20	20	32	8400	21840
Gp9 (tailspike protein)	18	34	22	46	612	1224

Moreover, previous studies about the interaction of the P22 phage with *Salmonella* have shown that there are more aspartic and glutamic acid residues than lysines involved in the biorecognition event.[19] This preliminary observation suggested that, among the two paths studied for biotinylation, the one involving the carboxylic residues could affect more the biorecognition site. Nevertheless, the two mentioned biotinylation paths were evaluated by comparing the response after the reaction of the modified biotin with the amine groups (NHS-PEG$_4$-Biotin) or the carboxylic groups (Amine-PEG$_3$-Biotin) of the phage proteins.

The study of the infectivity was thus performed after biotinylation and further purification by double agar layered method and enumeration of plaques. The retained lytic activity after biotinylation was thus compared with the original activity of the lysate, as shown in Table 5.3.

Table 5.3 Lytic activity study of the P22 bacteriophages before and after biotinylation in both conjugation paths: the reaction of NHS-PEG$_4$-Biotin with the amine groups of the phage proteins and of Amine-PEG$_3$-Biotin with the carboxylic groups.

	Phage titer (PFU mL^{-1})		**retained lytic activity**
Biotinylating Reagent	**before reaction**	**after reaction**	
NHS-PEG$_4$-Biotin for –NH$_2$ moieties	7.70 x 10^{10}	2.57 x 10^{10}	**33.4 %**
Amine-PEG$_3$-Biotin for –COOH moieties	6.30 x 10^{10}	7.00 x 10^{5}	**0.001 %**

A dramatically drop in the lytic activity was observed when the biotin was attached to the carboxylic groups, confirming that they are involved in the biorecognition site of the bacteria. Furthermore some additional blocking of the phage infectivity could be caused by some degree of polymerization when activating the carboxylic groups by EDC addition, due to the presence of both amine and carboxyl moieties in the phage proteins. On the contrary, the reaction with the amine moieties produced a less significant change.

These results were also confirmed by using the biotin-P22 as tagging reagent for the optical detection of *Salmonella* with a phagotagging magneto immunoassay. The scheme of this procedure for the detection of the bacteria is outlined in Figure 5.4, A and B, and implies the IMS and the *Salmonella* tagging with biotin-P22 as detailed explained in § 5.3.3. The results in Figure 5.7, confirmed that the tagging with the biotin-P22 modified throughout the amine moieties produced higher optical signals, and thus increased sensitivity for the detection of *Salmonella* at a concentration of 10^5 and 10^7 CFU mL^{-1}. Further studies were therefore performed with the biotin-P22 modified throughout the amine moieties.

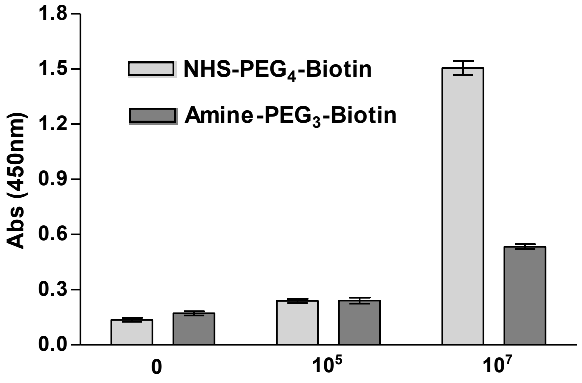

Figure 5.7 Results obtained with the phagotagging magneto immunoassay for the different reaction paths, using the NHS-PEG$_4$-Biotin reacting with the amine groups of the phage proteins or the Amine-PEG$_3$-Biotin reacting with the carboxylic groups, by adding 1 mg of the biotinylating reagent.

Table 5.4 and Figure 5.8, A show the results for the biotinylation using the NHS-PEG$_4$-Biotin at different concentration levels. As can be seen in Table 5.4, the lytic activity was kept almost constant at lower concentrations of biotinylating reagent and decreased when the concentration of NHS-PEG$_4$-Biotin increases. On the other hand, when the biotin amount was maintained constant at 1 mg, doubling the phage titer from 7.7 x 10^{10} to 1.57 x 10^{11} PFU per mL, the retained lytic activity was also doubled accordingly.

Table 5.4 Lytic activity study of P22 bacteriophage before and after the biotinylation by varying the amount of NHS-PEG$_4$-Biotin and the bacteriophage titre.

	Phage titer (PFU mL^{-1})		retained lytic activity (%)
NHS-PEG$_4$-Biotin (mg)	before reaction	after reaction	
0.01	7.70 x 10^{10}	7.49 x 10^{10}	97.3
0.25	5.50 x 10^{10}	5.43 x 10^{10}	98.7
0.50	3.39 x 10^{10}	2.99 x 10^{10}	88.2
1	7.70 x 10^{10}	2.57 x 10^{10}	33.4
1	1.57 x 10^{11}	1.06 x 10^{11}	67.5
4	9.70 x 10^{10}	1.47 x 10^{10}	15.1

The same study was also confirmed by the optical detection of *Salmonella* with the phagotagging magneto immunoassay (Figure 5.8, A). In this approach, not only the integrity of the tailspike protein was evaluated, but also the sensitivity in the detection due to incorporation of the biotin tag.

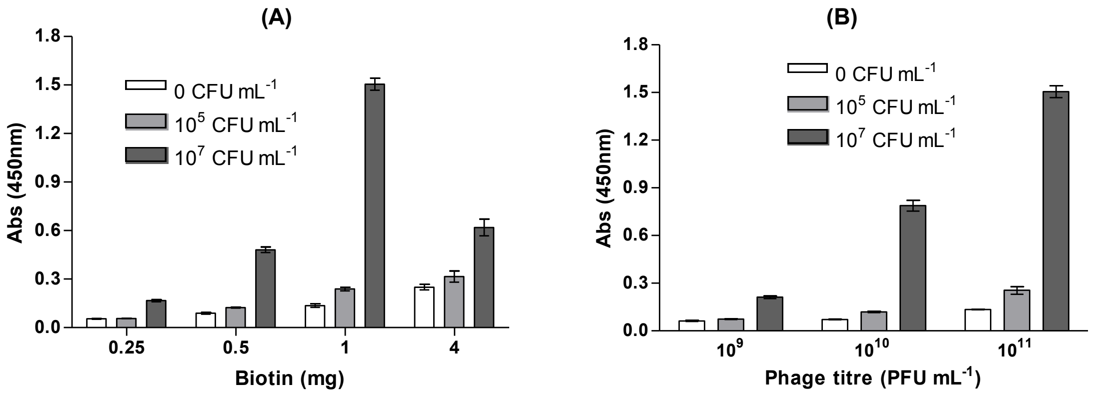

Figure 5.8 Comparison of the signals obtained with the phagotagging magneto immunoassay at 10^5 and 10^7 CFU mL^{-1} of *Salmonella* by increasing the amount of NHS-PEG$_4$-Biotin reacting with the amine groups of the phage (A) and the phage titer (B). The detailed phage titres in (A) are the ones previously reported in Table 5.4 and in (B) the biotin amount was set at 1 mg.

Clearly, although the lytic activity is higher at low concentration (0.25 mg) of biotinylating reagent (NHS-PEG$_4$-Biotin), the optical signal was also very low, indicating a poor degree of biotinylation of the phages. However, by increasing the amount of NHS-PEG$_4$-Biotin, although the lytic activity decreases, an improved sensitivity in the optical detection of the bacteria was observed, up to an optimum value of 1 mg NHS-PEG$_4$-Biotin. A higher amount than 1 mg NHS-PEG$_4$-Biotin implied a higher degree of biotinylation, but with a drop in the biorecognition, suggesting that the tailspike protein was being extensively affected. These results are also confirmed by the drop in the lytic activity observed when using 1 mg to 4 mg during the biotinylation process (Table 5.4).

The phage amount during the biotinylation process was also optimized, obtaining improved results when the concentration was enhanced as shown in Figure 5.8, B.

Therefore, optimal conditions for biotinylation involve the amino groups of the P22 phages and the reaction of 1 mg of NHS-PEG$_4$-Biotin reagent at a phage concentration of 10^{11} PFU mL^{-1}. Finally, the biotinylation with the optimal conditions was repeated five times controlling the phage infectivity of the biotin-P22 by double agar layered method to control the repeatability of the process. Similar retained lytic activity was obtained in all cases as can be seen in Table 5.5, demonstrating that on average around 64 % of the phages are still infective after the biotinylation process.

Table 5.5 Phage infectivity before and after the biotinylation process using the optimal conditions and % of retained lytic activity after the modification.

Phage titer (PFU mL^{-1})		retained lytic activity (%)
before reaction	after reaction	
1.57×10^{11}	1.06×10^{11}	67.5
1.27×10^{11}	8.70×10^{10}	68.5
2.47×10^{11}	1.47×10^{11}	59.5
2.66×10^{11}	1.62×10^{11}	60.9
5.44×10^{11}	3.37×10^{11}	61.9

5.4.3 Characterization of the biotin-P22 phages by gel electrophoresis

To analyze the electrophoretic mobility and structural integrity of the P22 phages after biotinylation through the amine group with the NHS-PEG$_4$-Biotin reagent, the biotin-P22 were analyzed using agarose gel electrophoresis. Figure 5.9, A shows the gel stained with ethidium bromide. The bands observed under UV irradiation indicate that the DNA is inside an intact P22 phage, being the intensity of the non-modified P22 control (lane 2) similar to that of the biotin-P22 (lane 3).

Figure 5.9, B shows the agarose gel stained with Coomassie blue, which interacts with the proteins of the capsid of the P22 phages. The fact that the bands in lanes 2 and 3 fit in both cases (A and B) indicates that the biotin moeities were coupled to intact P22 phages. When comparing the electrophoretic mobility of the unlabeled P22 control (lanes 1) and the biotin-P22 (lanes 2), it can be observed that the biotin-P22 phages have a higher negative net charge compared with the control, and thus ran farther into the agarose gel. This effect was previously reported for proteins [20] and for the bacteriophage T4 modified with the fluorescent dyes Cy3 and Alexa Fluor 546 [21] and it was mostly ascribed to the addition of negative charges associated with the binding of the dyes, since both have a net negative charge. However, the change of mobility due to the biotinylation of the phage P22 with the NHS-PEG$_4$-Biotin was only related with the elimination of one positive charge upon reaction with each amine group on the P22 surface, increasing thus the net negative charge and the electrophoretic mobility. Lane 4 also confirmed biotinylation, since upon the addition of avidin to the biotin-P22 phages, non electrophoretic mobility was observed, due to the formation of big complexes related to the multivalency of avidin and biotin-P22.

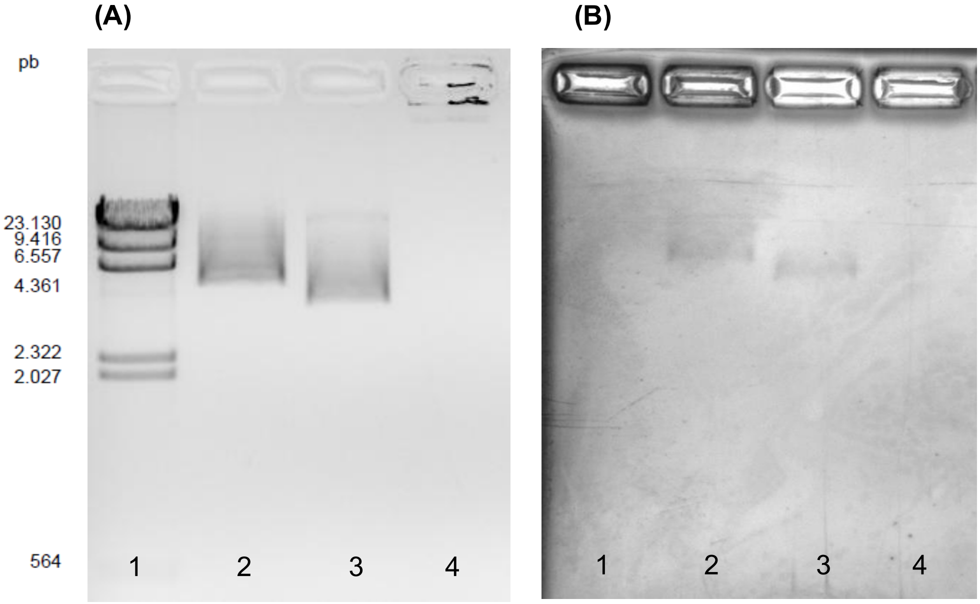

Figure 5.9 Characterization of the biotin-P22 by agarose gel visualized under (A) UV irradiation after ethidium bromide staining, (B) visible light after Coomassie blue staining. Lane 1: DNA marker. Lane 2: non-modified P22 phage negative control. Lane 3: biotin-P22. Lane 4: biotin-P22 reacted with avidin.

5.4.4 Fluorometric assay for the evaluation of the degree of labeling

A calibration curve of biocytin ranging from 0 to 40 pmol was prepared and the fluorescence was plotted *vs*. concentration. The fluorescence signals for each standard (0, 2.5, 5, 10, 20, 30 and 40 pmol in a volume of 50 µL added per well) were obtained using the typical fluorescein wavelengths, with excitation/ emission maxima of 485/ 530 nm. The optimal z-position was previously determined by comparing the signals of the highest biocytin concentration with the one of the blank in order to find the maximal signal to background ratio, which was set at 18539 µm as detailed in Figure 5.10, A. The graph was adjusted to a sigmoidal response curve with an excellent fit (r^2= 0.9996) as shown in Figure 5.10, B and the biotin amount in the samples was obtained by interpolation.

The DOL was evaluated on the biotin-P22 modified through the amine groups with 1 mg of NHS-PEG$_4$-Biotin reagent at a phage concentration of 2.5 x 10^{11} PFU mL^{-1} after purification by an exclusion column. Since the column efficiency guaranteed by the manufacturers is 95 %, in order to ensure the elimination of the excess of biotin, the purification process was repeated three times. The phage titer was controlled in the successive steps and after the initial decrease to 1.7 x 10^{11} PFU mL^{-1} due to the biotinylation process, the titer was kept almost constant during the purification process.

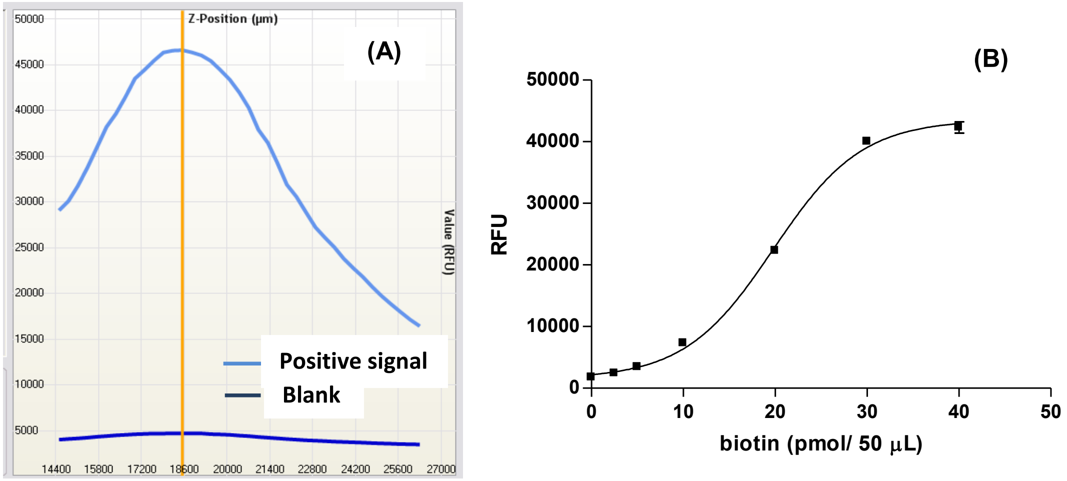

Figure 5.10 (A) Z position optimization for the fluorescence measurements. (B) Standard curve showing the relative fluorescence signals for the biocytin standards in the presence of Biotective Green reagent. After 5 minutes incubation at room temperature in the dark, fluorescence was measured in a microplate reader using excitation at 485 nm and emission at 530 nm.

The steric hindrance of a biotin attached to the P22 phage could effectively decrease the affinity of the biotin for the Biotective Green reagent. Alternatively, multiple biotins could be attached very close to one another on the phage during the chemical modification of the lysines on the phage by the biotin succinimidyl ester labeling. Thereby, biotins close to each other would inevitably result in at least one cryptic or masked biotin. The fluorometric assay using the Biotective Green reagent directly applied to the biotinylated sample is thus useful for the evaluation of the effective biotin amount, not the total, being the effective biotin those able to bind (strept)avidin molecules. The effective biotin concentration is the total biotin concentration minus the cryptic and sterically hindered biotins. In order to determine the total amount of biotinylation, the biotin-P22 was submitted to digestion by using Pronase E.[22] A biotinylated IgG antibody standard solution with a known DOL, was also processed as positive control, calculating the biotin amount in both digested and undigested samples. The antibody was reported to be modified with five biotins per IgG and quantifying with the assay a DOL of 4.8 was obtained in the digested sample and 3.27 for the undigested one, which is in agreement with the results obtained in previous reports.[16] The calculated amounts of unknown biotin in the fluorometric assay of the digested and undigested biotin-P22 phage samples were 2286 and 2189, respectively. When this results are compared to the 9012 potentially reactive lysine moieties present in the sequence of the main phage external proteins gp5 and gp9 it can be concluded that almost 25 % of the lysine residues were modified with the biotinylated reagent.

In contrast to previous reports in the literature [22,23] which showed underestimation of biotin DOL in macromolecules due to steric hindrance of the access to avidin-binding sites, unexpectedly the DOL obtained for the digested as well as for the undigested biotin-P22 was found to be almost the same value. This result suggest that the total amount of biotin attached to the phage can also be considered the effective biotin amount, and thus, able to bind (strept)avidin. It was previously reported that the avidin component can only resolve biotins that are further apart than the four biotin binding sites on avidin, a few nanometers.[24] As this result indicated that the number of cryptic biotins is very low, the hydrophilic, water soluble and highly flexible PEG_4 spacer arm of 2.9 nm used in the biotinylation could clearly play a role to avoid steric hindrance, giving further flexibility, and facilitating the access to the (strept)avidin binding sites.

When analyzing previous works using bioconjugation methods to attach signaling molecules at specific designated positions of virus surfaces, in general lower labeling performances were reported. As an example, the attachment of 40 Cy5 dyes to an icosahedral plant virus of 30 nm in size was demonstrated.[25] Similarly, a spherical plant virus with an average diameter of 28 nm, was loaded with up to 40 fluoresceins, which is equal to a local concentration of 4.6 mM of dyes surrounding the virus.[26] Regarding biotin labeling, also lower DOLs were achieved, reporting the attachment of 400 biotin molecules per phage [27] and of 1350 after the reaction with the M13 phage, a larger cylindrical shaped phage with a length of 880 nm and a diameter of 6 nm [28].

Finally more recently, the conjugation of Cy3 and Alexa 546 to T4 bacteriophages[21] and of Alexa Fluor 488 and 647 C5-aminooxyacetamide dyes to filamentous fd phages were reported.[29] It should be highlighted that only in these two cases using fluorescent dyes higher DOL values were achieved, yielding the incorporation of 1.9×10^4 dyes per T4 phage and 3000 molecules per fd phages. However, the dimension of these phages is significantly larger (100 x 90 nm and 7 nm wide per 890 nm length for T4 and fd phages, respectively) than the P22 (60 nm) used in this work.

5.4.5 Characterization of biotin-P22 phagotagging by fluorescence confocal microscopy

The confirmation of the P22 biotinylation and its bacterial recognition ability was also achieved through confocal microscopy. This technique allows also the study of the labeling pattern of the biotin-P22 for bacteria tagging. The images showed in Figure 5.11 depicted the immunoseparation of the bacteria through the magnetic particles and the labeling with the fluorescent reporter Strep-Cy5 that binds to the biotin-P22. The autofluorescence of the coating polymer of the magnetic particles was exploited for their visualization.

Figure 5.11 shows the differential pattern of the phagotagging (A) in comparison with labeling using a biotinylated antibody (B). As can be seen in the images, biotinylated phages showed brighter dots in the tagging sites, indicating a higher local concentration of dyes due to extensive biotinylation of the surface of P22 phage, while antibodies on the contrary, displayed a less bright signal uniformly distributed on the whole bacterial cell.

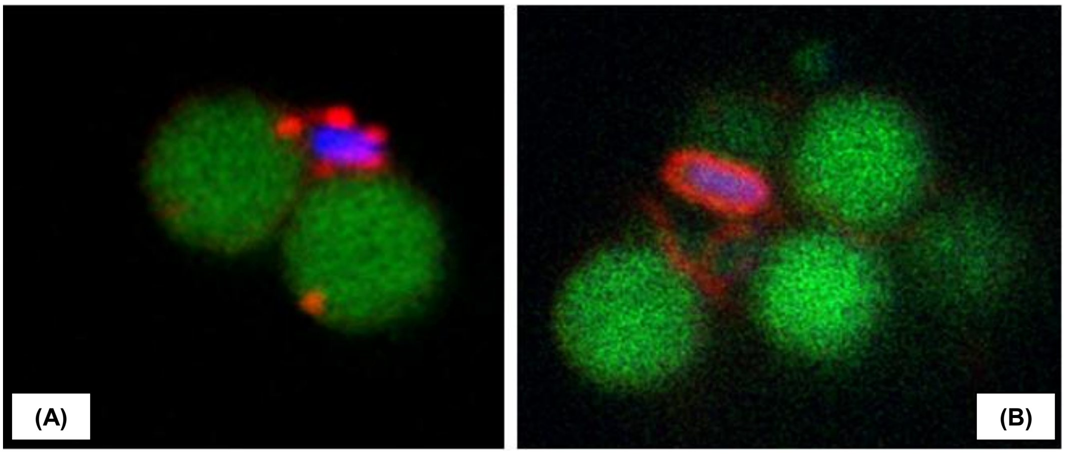

Figure 5.11 Confocal microscopy images of the *Salmonella* phagotagging with biotin-P22 (A) in comparison to biotinylated antibodies (B), attached to *Salmonella* cells which were previously captured to antibody modified magnetic particles used as a support. It can be seen in green the magnetic particles (autofluorescent), in blue the DNA of the bacteria stained with Hoechst 33342 and in red the biotinylated compounds labeled with Strep-Cy5 which gives rise to a red fluorescent signal.

5.4.6 Phagotagging magneto immunoassay for the optical and electrochemical detection of *Salmonella*

The phagotagging magneto immunoassay was performed to analyze the response of the system at different bacteria concentrations (0, 10^2, 10^4 and 10^6 CFU mL^{-1} The sensitivity of both the optical and electrochemical detection strategies was also compared The electroctrochemical and optical reporter used for the detection in both cases was the same Strep-HRP conjugate. As shown in Figure 5.12, in both cases, the signal increases with the bacteria concentration, being the electrochemical detection more sensitive than the optical detection as can be also seen through the signal to nonspecific adsorption ratios detailed in Table 5.6.

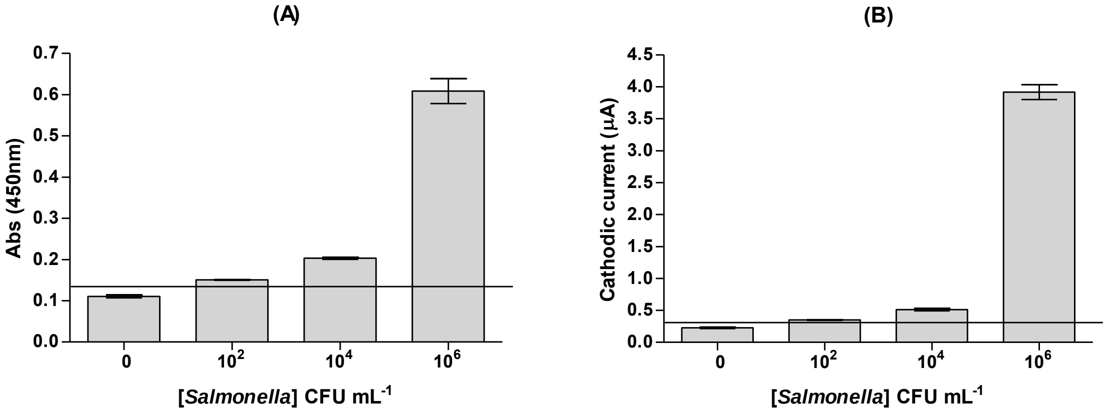

Salmonella at a concentration level of 0, 10^2, 10^4 and 10^6 CFU mL^{-1}, using the biotin-P22 phage. The experimental conditions were as follows: (A) 100 µL *Salmonella* and 100 µL biotin-P22 at a concentration of 2.5 x 10^9 PFU mL^{-1} were added to 10 µg antibody-modified MP, using then 100 µL of Strep-HRP at 0.5 µg mL^{-1} as enzymatic label; and (B) 500 µL *Salmonella* and 100 µL biotin-P22 1 x 10^{10} PFU mL^{-1} were added to 50 µg antibody-modified MP, labeling finally with 100 µL of Strep-HRP 60 µg mL^{-1}. In both cases n=3, except for the negative control in which n=6.

Table 5.6 Comparison of the signal to background ratios at different bacteria concentrations using the phagotagging magneto immunoassay with optical and electrochemical detection.

[*Salmonella*] CFU mL^{-1}	Signal to background ratio	
	Optical	Electrochemical
10^2	1.36	1.54
10^4	1.84	2.25
10^6	5.50	17.18

Further studies in order to demonstrate the utility of the biotin-P22 phages for the detection of *Salmonella* will be shown in the next chapter of this dissertation.

5.4.7 P22 bacteriophages as scaffold for the conjugation of gold nanoparticles

The biotin-P22 phages were reacted with Strep-AuNPs, to achieve the hybrid bionanomaterial biotin-P22/ AuNPs (shown in Figure 5.13, A) used for the bacteria tagging. The Figure 5.13, B shows the TEM image of a *Salmonella* cell decorated with AuNPs throughout the strong biotin-streptavidin interaction with the attached biotin-P22 particles, whereas Figure 5.13, C shows a zoom of a section of *Salmonella* membrane with many Au-NPs labeled biotin-P22 attached. The results demonstrate the utility of the hybrid bionanomaterial for bacteria tagging and bioimaging. Moreover, once again the biotinylation of the P22 phages could be confirmed.

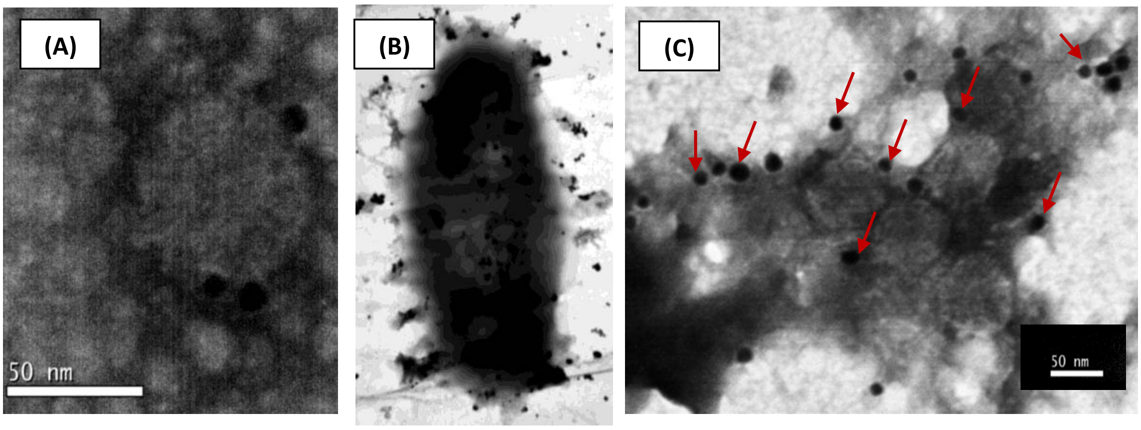

Figure 5.13 Characterization by TEM of the biotin-P22 labeled with Strep-AuNP, for the tagging of *Salmonella*, at a concentration of 2 x 10^7 CFU mL^{-1}. The biotin-P22 labeled with Strep-AuNPs is shown in (A), while the bacterial AuNP tagging pattern is shown in (B) with a scale bar of 0.2 μm. In (C), a zoom with a scale bar of 50 nm is exposed, showing the biotin-P22/ AuNPs complexes, signaled with arrows, binding to the bacteria.

5.5 CONCLUSIONS

The sandwich magneto immunoassay with electrochemical detection was an effective, fast and low cost technique for the purity control of the phage lysates before their use in bacteria tagging and detection. However, further studies should be done in order to validate the method and also to relate the obtained signals with the amount of LPS remaining in the phage solutions after the purification, by comparing the results with current available endotoxin detection methods such as the chromogenic Limulus Amebocyte Lysate (LAL) assay.[30] Nevertheless, the better purification of the phage lysates was achieved using CsCl gradient according to Sambrook et al., followed by a dialysis step since the signals were almost the same than the blank. Therefore this was the chosen technique for preparing a pure starting phage solution to use in all the further strategies developed in this dissertation.

The results from the biotinylation study show that biotin-P22 phages are novel, versatile and robust virus-like particles for the sensitive tagging of bacteria, using fluorescent, optical and electrochemical reporters, with different applications ranging from bioimaging to biosensing. The phages showed a unique surface to display targeting and signaling moieties, enhancing the sensitivity of bacteria detection.

The tagging of two different reactive groups, i.e., the amino groups of lysines and the carboxylic acid groups of aspartic or glutamic acid residues on P22 surface were explored, showing the first one, undoubtedly, advantages in terms of bacterial biorecognition. Around 2200 biotin molecules per phage unit were attached on the capsid, with a PEGylated spacer arm of 2.9 nm, showing a tiny amount (4.2 %) of cryptic biotin. Most of the attached biotin moieties were thus able to bind (strept)avidin molecules. This fact can be also related with the outstanding sensitivity showed for the bacteria detection after the coupling with optical, fluorescent or electrochemical reporters based on (strept)avidin conjugates. The phagotagging magneto immunoassay, as well as the phagotagging electrochemical magneto immunosensor, showed outstanding analytical performance for the sensitive detection of *Salmonella* Thypimurium. The potential of this material for detecting the bacteria deserved further study in real food samples.

Finally, the P22 bacteriophages also demonstrated good performances and versatility as scaffold for the conjugation of other nanomaterials, such as gold nanoparticles, for the specific bacteria tagging and imaging.

The main advantage of using a phage for bacteria tagging instead of a labeled antibody relies mainly on the use of the bacteriophage for biorecognition. Contrary to antibody generation, phages are animal-free, cost-efficiently produced by bacteria infection. Another feature which makes them suitable as a biorecognition element is their outstanding stability and specificity. The specificity is mainly conferred by the P22 bacteriophage specific to serotypes A, B, and D1, being thus an extremely useful tool to trace the source of outbreaks by phage typing.

5.6 REFERENCES

(1) Tallury, P.; Malhotra, A.; Byrne, L. M.; Santra, S. *Advanced drug delivery reviews* **2010**, *62*, 424–37.

(2) Gilmartin, N.; O'Kennedy, R. *Enzyme and microbial technology* **2012**, *50*, 87–95.

(3) Smelyanski, L.; Gershoni, J. M. *Virology journal* **2011**, *8*, 495.

(4) Lander, G. C.; Tang, L.; Casjens, S. R.; Gilcrease, E. B.; Prevelige, P.; Poliakov, A.; Potter, C. S.; Carragher, B.; Johnson, J. E. *Science* **2006**, *312*, 1791–1795.

(5) Kang, S.; Hawkridge, A. M.; Johnson, K. L.; Muddiman, D. C.; Prevelige, P. E. *Journal of Proteome Research* **2006**, *5*, 370–7.

(6) Singh, a; Glass, N.; Tolba, M.; Brovko, L.; Griffiths, M.; Evoy, S. *Biosensors & bioelectronics* **2009**, *24*, 3645–51.

(7) Boratynski, J.; Syper, D.; Weber-Dabrowska, B.; Lusiak-Szelachowska, M.; Pozniak, G.; Gorski, A. *Cellular & Molecular Biology Letters* **2004**, *9*, 253–259.

(8) Humphrey, S. B.; Stanton, T. B.; Jensen, N. S.; Zuerner, R. L. *Journal of Bacteriology* **1997**, *179*, 323–329.

(9) Brorson, K.; Shen, H.; Lute, S.; Perez, J. S.; Frey, D. D. *Journal of Chromatography A* **2008**, *1207*, 110–121.

(10) Merabishvili, M.; Pirnay, J.-P.; Verbeken, G.; Chanishvili, N.; Tediashvili, M.; Lashkhi, N.; Glonti, T.; Krylov, V.; Mast, J.; Van Parys, L.; Lavigne, R.; Volckaert, G.; Mattheus, W.; Verween, G.; De Corte, P.; Rose, T.; Jennes, S.; Zizi, M.; De Vos, D.; Vaneechoutte, M. *PloS one* **2009**, *4*, e4944.

(11) Monjezi, R.; Tey, B. T.; Sieo, C. C.; Tan, W. S. *Journal of chromatography. B, Analytical technologies in the biomedical and life sciences* **2010**, *878*, 1855–9.

(12) Naidoo, R.; Singh, A.; Arya, S. K.; Beadle, B.; Glass, N.; Jamshid, T.; Szymanski, C. M.; Evoy, S. *Bacteriophage* **2012**, *2*, 15–24.

(13) Sambrook, S.; Russell, D. W. *Molecular Cloning: A laboratory manual*; 2nd ed.; Cold Spring Harbor Laboratory Press: New York, NY, 1989; pp. 273–276.

(14) Liébana, S.; Lermo, A.; Campoy, S.; Cortés, M. P.; Alegret, S.; Pividori, M. I. *Biosensors & Bioelectronics* **2009**, *25*, 510–3.

(15) U.S. Department of Health and Human Services, C. for D. C. and P. and N. I. of H. *Biosafety in Microbiological and Biomedical Laboratories*; Chosewood, L. C.; Wilson, D. E., Eds.; U. S. Government Printing Office: Washington DC, 2007; pp. 44–49.

(16) Batchelor, R.; Sarkez, A.; Gregory Cox, W.; Johnson, I. *BioTechniques* **2007**, *43*, 503–507.

(17) Singh, A.; Arutyunov, D.; Szymanski, C. M.; Evoy, S. *The Analyst* **2012**, *137*, 3405–21.

(18) Handa, H.; Gurczynski, S.; Jackson, M. P.; Mao, G. *Langmuir* **2010**, *26*, 12095–103.

(19) Steinbacher, S.; Miller, S.; Baxa, U.; Budisa, N.; Weintraub, A.; Seckler, R.; Huber, R. *Journal of Molecular Biology* **1997**, *267*, 865–880.

(20) Huang, S.; Wang, H.; Carroll, C. A.; Hayes, S. J.; Weintraub, S. T.; Serwer, P. *Electrophoresis* **2004**, *25*, 779–784.

(21) Robertson, K. L.; Soto, C. M.; Archer, M. J.; Odoemene, O.; Liu, J. L. *Bioconjugate chemistry* **2011**, *22*, 595–604.

(22) Rao, S. V.; Anderson, K. W.; Bachas, L. G. *Bioconjugate chemistry* **1997**, *8*, 94–98.

(23) Lu, J.; Zenobi, R. *Analytical Biochemistry* **1999**, *269*, 312–316.

(24) Pugliese, L.; Coda, A.; Malcovati, M.; Bolognesi, M. *Journal of Molecular Biology* **1993**, *231*, 698–710.

(25) Soto, C. M.; Blum, A. S.; Vora, G. J.; Lebedev, N.; Meador, C. E.; Won, A. P.; Chatterji, A.; Johnson, J. E.; Ratna, B. R. *J. Am. Chem. Soc.* **2006**, *128*, 5184–5189.

(26) Barnhill, H. N.; Reuther, R.; Ferguson, P. L.; Dreher, T.; Wang, Q. *Bioconjugate Chemistry* **2007**, *18*, 852–859.

(27) Li, K.; Chen, Y.; Li, S.; Nguyen, H. G.; Niu, Z.; You, S.; Mello, C. M.; Lu, X.; Wang, Q. *Bioconjugate chemistry* **2010**, *21*, 1369–77.

(28) Hess, G. T.; Cragnolini, J. J.; Popp, M. W.; Allen, M. A.; Dougan, S. K.; Spooner, E.; Ploegh, H. L.; Belcher, A. M.; Guimaraes, C. P. *Bioconjugate Chemistry* **2012**, *23*, 1478–1487.

(29) Carrico, Z. M.; Farkas, M. E.; Zhou, Y.; Hsiao, S. C.; Marks, J. D.; Chokhawala, H.; Clark, D. S.; Francis, M. B. *ACS nano* **2012**, *6*, 6675–6680.

(30) Vanhaecke, E.; Pijck, J.; Vuye, A. *Journal of Clinical Pharmacy and Therapeutics* **1987**, *12*, 223–235.

CHAPTER 6

BIOTINYLATED BACTERIOPHAGE AS NANOTAG FOR THE SENSITIVE DETECTION OF PATHOGENIC BACTERIA

6.1 INTRODUCTION

As it was previously discussed in the Introduction (§ 1.7), the detection of pathogenic bacteria plays a vital role in biological threat surveillance, food safety and medical diagnosis.

Conventional culture methods remain the most reliable and accurate techniques for pathogen detection. However, their major drawbacks are their labor-intensiveness and time-consuming as it takes 2–3 days for initial results, and up to 7–10 days for confirmation. This is a clear inconvenience in many industrial applications, particularly in the food sector.[1] As a result, alternative assay methods are continuously being developed, tested, and optimized for improved detection.

The inclusion of nanotechnology can also help to meet the demands of increased sensitivity and rapidity allowing the imaging, tracking, as well as real-time detection of a few microorganisms based on different nanomaterials as for example quantum dots, magnetic and metallic nanoparticles. However, limits of detection below 10^3 CFU mL^{-1} are only achieved when integrating the nanomaterials to methodologies such as microscopy, flow cytometry or PCR, which are all expensive, laborious and time-consuming.[2]

As previously discussed in Chapter 5, biological nanoparticles are also a promising tool for bacteria analysis, and in particular bacteriophages provide a natural source for the specific detection of food-borne pathogens. A wide range of methods have been reported and are extensively compared in many reviews, demonstrating the utility of bacteriophages for both bacteria capturing and labeling,[3–5] as detailed in § 1.7.3 of the Introduction. The inherent ability of phages to bind their bacterial target has been exploited in the integration of these bionanoparticles to bioanalytical procedures for the biorecognition of bacteria in different ways, for instance to capture the bacteria onto surfaces and transducers, using phages previously attached on solid supports.

On the other hand, different methods based on the use of phages for bacteria tagging have been reported. The direct conjugation of fluorescent molecules at specific positions of virion surfaces, decorating addressable amino acids, such as glutamic/aspartic acids, lysines and cysteines was reported. Some examples were described in Chapter 5 (§ 5.3.4). The use of biotinylated phages as labels for bacteria detection has been also reported using T7 and λ bacteriophages genetically modified to display small peptides containing biotin acceptor domains on their capsid proteins (derived from portions of biotin acceptor- type proteins, e.g., biotin carboxyl carrier protein or BCCP). These peptides were biotinylated *in vivo* by specific enzymes of the host bacterium (*E.coli*) and labeled after the bacteria biorecognition with streptavidin-modified quantum dots.[6,7] Recently, the biotinylation of M13 phage using engineered capsid proteins and sortase-based reactions were also evaluated.[8]

In the present chapter, the biotinylated P22 phages (biotin-P22) studied in Chapter 5, were explored as a labeling reagent towards *Salmonella* Thyphimurium. Two different approaches based on phage tagging were studied, i) magneto immunoassay with optical detection and ii) electrochemical magneto immunosensor, for the sensitive detection of *Salmonella*. In both approaches, after the immunomagnetic separation (IMS) of the target bacteria by anti-*Salmonella* antibody modified magnetic particles (Ab-MP), the tagging strategy was based on the use of the biotin-P22 coupled to streptavidin conjugated to horseradish peroxidase (Strep-HRP) acting as both electrochemical and optical reporter. First of all, the bacteria tagging capability of the biotin-P22 conjugates was characterized by Scanning Electron Microscopy (SEM) and further fluorescence microscopy studies were performed. Afterwards, the optimal conditions for the IMS and phagotagging procedures, as well as the reagents concentration were established. Once the phagotagging magneto immunoassay was optimized, both approaches based on phage tagging, i.e. the magneto immunoassay with optical detection and the electrochemical magneto immunosensor were compared in terms of the analytical performance. Moreover, both approaches were evaluated for the detection of the bacteria in both LB broth and milk as a complex matrix. Finally, specificity studies were also performed.

6.2. AIM OF THE CHAPTER

This chapter addresses the integration of biotinylated phages for the bacteria tagging in optical magneto immunoassays and electrochemical magneto immunosensing devices, taking as a model the P22 bacteriophage for the detection of the pathogenic bacteria *Salmonella*.

The specific objectives of this chapter were the following:

- To evaluate the bacteria phagotagging using the biotinylated P22 phages (biotin-P22) by microscopic techniques, such as Scanning Electron Microscopy (SEM) and fluorescence confocal microscopy.
- To optimize the conditions for the immunomagnetic separation step as well as for the bacteria tagging with the biotin-P22.

- To establish the optimal reagents concentration for the phagotagging magneto immunoassay, i.e. the biotin-P22 tag and Strep-HRP label.
- To assess different protocols for the electrochemical magneto immunosensor based on phage tagging in order to simplify the analytical procedure.
- To evaluate the use of the biotin-P22 as nanotag in optical magneto-immunoassay and electrochemical magneto immunosensor based on phage tagging for the sensitive detection of *Salmonella* in milk.
- To compare both approaches based on phage tagging in terms of the analytical performance (LOD, sensitivity and matrix effect).
- To study the specificity of the system by evaluating the presence of cross-reaction towards *E. coli* using both optical and electrochemical detection.

6.3 EXPERIMENTAL SECTION

6.3.1 Materials

The bacteria *Salmonella enterica* serovar Typhimurium LT2 and *Escherichia coli* K12 strains were routinely grown in Luria Bertani (LB) broth or on LB agar plates for 18 h at 37ºC. Bacterial viable counts were determined by plating on LB plates followed by incubation at 37ºC for 24 h. The preparation of the P22 phage lysates (ATCC® 19585-B1™), their titration and purification using CsCl are described in Chapter 5 (§§ 5.3.1.1 and 5.3.1.2, respectively). The lysates were concentrated using 25 x 89 mm ultracentrifuge tubes (Ultra-ClearTM Tubes, Beckman, California, USA) in an ultracentrifuge (Optima™ L-80, Beckman, California, USA) with the SW28 Ti rotor (Beckman, California, USA). The filters used in the bacteriophage filtration as well as a support for SEM samples preparation were Nucleopore Track-Etched Membranes (25 mm Ø, 0.2 µm pore size, product nº 110606, Whatman). The cesium chloride (CsCl, product nº 10757306001) used for the phage purification was supplied by Roche Applied Science (Roche Diagnostic S.L., Spain). The dialysis was performed with cellulose membranes purchased from Sigma (Dialysis Tubing, product nº D-9277, Steinheim, Germany) and the dialysis columns were from Novagen (D-Tube Dialyzer Maxi MWCO12-14 kD, product nº 71510-3).

The NHS-PEG$_4$-Biotin (product nº 21955) and the desalting columns (Zeba Desalt Spin Columns, product nº 89889) used for the removal of non-reacted biotin after the biotinylation process were purchased from Thermo Scientific.

The magnetic particles modified with anti-*Salmonella* antibodies (Dynabeads, product n° 710.02) were supplied by Invitrogen Dynal AS (Oslo, Norway). The anti-*Salmonella* antibodies conjugated to HRP (product nº ab20771) used for the optimization of the IMS step and the biotinylated anti-*Salmonella* antibodies (biotin-Ab, product nº ab21118) used for the tagging comparison in confocal microscopy were from Abcam (Cambridge, UK). Bovine serum albumin (BSA) and Strep-HRP (product nº S5512) were obtained from Sigma-Aldrich.

All buffer solutions were prepared with milli-Q water (Millipore Inc., Ω = 18 MΩ cm) and all reagents were of the highest available grade, supplied from Sigma or Merck. For the biotinylation, PBS buffer (0.1 mol L^{-1} phosphate, 0.15 mol L^{-1} NaCl, pH 7.2) was prepared. The SEM characterization was done with a fixation buffer consisting of 2.5 % v/v glutaraldehyde (EM grade, from Merck) in 0.1 mol L^{-1} sodium phosphate (PB), pH 7.4, and a post-fixation buffer containing 1 % w/v OsO_4 (TAAB Lab) in 0.1 mol L^{-1} PB, pH 7.4.

The reagents used for confocal microscopy, as well as the reagents used for the optical and electrochemical measurements and the composition of the solutions used in the optical and electrochemical assays were the same as previously described in Chapter 5.

The instrumentation and materials used for the incubation and washing steps, the magnetic separations, as well as the optical and electrochemical detection were the same as detailed in Chapter 4 (§ 4.3.1.2).

Scanning electron microscopy (SEM) images were taken with the microscope MERLIN FE from Carl Zeiss Microscopy GmbH and the K850 Critical Point Drier Emitech (Ashford, UK) was used for the preparation of the samples. On the other hand, fluorescence images were acquired using a Leica TCS/SP5 confocal microscope (Leica Microsystems, Exton, PA).

6.3.2 Evaluation of the immunomagnetic separation and phagotagging of the bacteria by microscopy techniques

For the microscopic evaluation by SEM, the IMS, as well as the tagging of the bacteria with the biotin-P22 were performed, using 50 µg of the antibody modified magnetic particles (Ab-MP), 500 µL of *Salmonella* 10^6 CFU mL^{-1} and 100 µL of biotin-P22 at a concentration of 1.4 x 10^{10} PFU mL^{-1}, which were incubated 20 min without shaking at 37ºC, followed by two washing steps with PBST. Finally, 100 µL of the modified magnetic particles were added to 5 mL of milli-Q water, and filtered through a Nucleopore membrane (25 mm Ø, 0.2 µm pore size). The filters were then fixed in 2.5 % (v/v) glutaraldehyde in PB overnight at 4ºC. After four 10 min washes in PB, samples were post-fixed in 1 % (w/v) osmium tetraoxide in PB for 2 h at 4ºC, washed four times for 10 min in water, dehydrated in a graded ethanol series (30, 50, 70, 90, 95 and 100 %) and dried by critical point with CO_2. Samples were then mounted on metallic stubs with adhesive carbon films and observed with the scanning electron microscope (MERLIN FE) operating at 15 kV.[9]

Fluorescence microscopy was also applied in order to visualize the developed detection system and evaluate the attachment ability of biotin-P22 to the bacterial cells. The nucleic acid stain Hoechst 33342 was used to label the bacterial cells, by adding 4.5 µL of a 10 mg mL^{-1} stock solution per mL of *Salmonella* at a concentration of 10^6 CFU mL^{-1} and streptavidin conjugated to the fluorescent dye cyanine 5 (Strep-Cy5) was used to visualize the attached biotin-P22. Biotinylated anti-*Salmonella* antibodies (biotin-Ab) were used to compare the nonspecific adsorption of the tagging reagent and fluorescent reporter on the magnetic particles. The same procedure already described in Chapter 5 (§ 5.3.6) was performed for the samples preparation. The samples were then imaged using a Leica TCS/SP5 confocal microscope (Leica Microsystems, Exton, PA). Finally the 3D Imaris X64 v. 6.2.0 software (Bitplane; Zürich, Switzerland) was applied for processing the obtained images.

6.3.3 Optimization of the phagotagging magneto immunoassay

The concentration of the commercial Ab-MP as well as the incubation time for the IMS step was optimized by a direct sandwich magneto immunoassay with optical detection using HRP labeled anti-*Salmonella* antibodies (Ab-HRP) as enzymatic reporter. Briefly, the applied protocol for the immunoassay was as follows: i) IMS of *Salmonella* by adding 100 µL of bacteria suspension solution to 10 µg of Ab-MPs and incubating at 700 rpm; ii) after removing the supernatant and performing a washing step of 5 min at 700 rpm, addition of 100 µL of Ab-HRP diluted 1/1000 in b-PBST; iii) 30 min incubation at 700 rpm, followed by two 5 min washes with 100 µL of PBST; and iv) addition of 100 µL of substrate solution containing H_2O_2 and 3,3',5,5'-tetramethylbenzidine (TMB) incubating 30 min at 700 rpm in darkness, followed by the addition of 100 µL H_2SO_4 to stop the reaction, and finally performing the optical read-out at 450 nm.

Optimization experiments were also performed in order to determine the most suitable biotin-P22 dilution as well as the best Strep-HRP concentration. With this purpose, the signals to nonspecific adsorption ratios were evaluated to find the best conditions for achieving high positive signals as well as low background values. Besides the reagents concentration, the conditions of temperature and shaking during bacteria tagging procedure as well as the incubation time were some other important parameters optimized in order to improve the sensitivity of the assay. The phagotagging magneto immunoassay with optical detection was used for these optimizations following the protocol described in § 5.3.3. Regarding the electrochemical magneto immunosensor based on phage tagging, the concentration of the labeling reagents, i.e. the biotin-P22 and the Strep-HRP, were also optimized following the protocol described in § 5.3.3. The applied phagotagging immunoassay, which can be coupled with optical as well as electrochemical detection, is schematized in Figure 6.1.

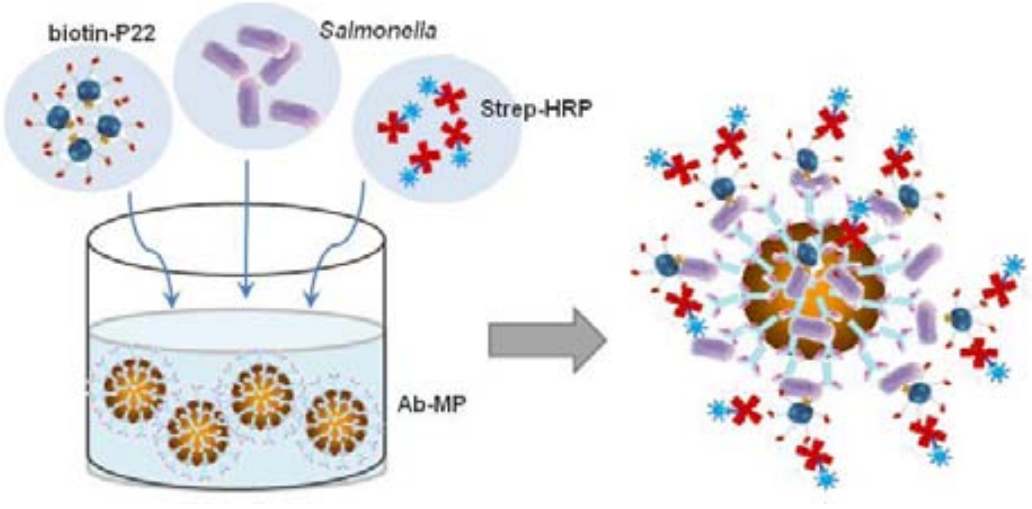

Figure 6.1 Schematic representation of the phagotagging magneto immunoassay showing the IMS of *Salmonella*, the phage tagging with biotin-P22 and secondary labeling with Strep-HRP.

6.3.4 Evaluation of different strategies for the electrochemical magneto immunosensor based on phage tagging

In an attempt to shorten and simplify the analytical procedure of the electrochemical magneto immunosensor based on phage tagging, five different protocols were evaluated by varying the order and number of incubation and washing steps, as detailed outlined in Table 6.1.

6.3.5 Magneto immunoassay with optical detection *vs*. electrochemical magneto immunosensor based on phage tagging for the detection of *Salmonella* in milk

For the evaluation of the matrix effect, the response of the phagotagging magneto immunoassay approach for artificially inoculated *Salmonella* samples (ranging from 10^1 to 10^8 CFU mL^{-1}) in LB broth and in milk diluted 1/10 in LB were compared. The standard curves were fitted to a four-parameter logistic equation according to $y = \{(A-B)/[1 + 10 \exp((\log C - \log X)\times D)]\} + B$, where A is the maximal absorbance, B is the minimum absorbance, C is the concentration producing 50 % of the maximal absorbance, X is the bacteria concentration and D is the slope at the inflection point of the sigmoid curve. The cut-off values and limits of detection with both optical and electrochemical detection were analyzed.

6.3.6 Specificity study

The specificity of these methods was also evaluated by comparing the response to *Salmonella* with the signal obtained in the presence of an equivalent amount of another gram negative bacterium as *E.coli* and finally a mix of both pathogens artificially inoculated in milk samples. A negative control was also processed. If the detection is not affected by any cross reaction, the signal for *E.coli* should be the same as the blank, and on the other hand, the presence of these bacteria in the mix should not interfere in the response towards *Salmonella*.

Table 6.1 Different procedures for the optimization of the electrochemical magneto immunosensor based on phage tagging.

(A) Stepwise	**(B) *Salmonella* + biotin-P22 preincubation**	**(C) IMS + phage tagging in one step**	**(D) Biotin-P22 + Strep-HRP preincubation**	**(E) All reagents in one step**
1- IMS of *Salmonella* (20 min, shaking)	1- *Salmonella* tagging with biotin-P22 (20 min, still, 37ºC)	1- Incubation of Ab-MP, *Salmonella* and biotin-P22 (20 min, shaking)	1- Enzymatic labeling of the biotin-P22 with Strep-HRP and in parallel IMS	1- Mixing of Ab-MP, *Salmonella*, biotin-P22 and Strep-HRP (20 min, shaking)
2- Washing step (1X, 5 min)	2- Addition of 10µL Ab-MP for the IMS (20 min, shaking)	2- Incubation (20 min, still, 37ºC)	2- Washing step (1X, 5 min)	2- Incubation (20 min, still, 37ºC)
3- Tagging with biotin-P22 (20 min, still, 37ºC)	3- Washing step (1X, 5 min)	3- Washing step (1X, 5 min)	3- Addition of biotin-P22+ Strep-HRP complex and incubation (20 min, shaking)	3- Incubation (20 min, shaking)
4- Washing step (1X, 3 min)	4- Enzymatic labeling with Strep-HRP (30 min, shaking)	4- Enzymatic labeling with Strep-HRP (30 min, shaking)	4- Incubation (20 min, still, 37ºC)	4- Washing step (2X, 3 min)
5- Enzymatic labeling with Strep-HRP (30 min, shaking)	5- Washing step (2X, 3 min)	5- Washing step (2X, 3 min)	5- Washing step (2X, 3 min)	
6- Washing step (2X, 3 min)				

6.4 RESULTS AND DISCUSSION

6.4.1 Evaluation of the immunomagnetic separation and phagotagging of the bacteria by microscopy techniques

The IMS of the bacteria and phagotagging with the biotin-P22 was analyzed by SEM and confocal microscopy. These techniques allow the confirmation of the biorecognition capability of the developed nanotag and the labeling with a fluorescent streptavidin conjugate.

6.4.1.1 SEM analysis

The biotin-P22 conjugate was visualized and its bacteria biorecognition capability was verified by SEM microscopy. Figure 6.2 shows the microscopic characterization by SEM of the *Salmonella* phagotagging with the biotin-P22 phages. The IMS of *Salmonella* with the Ab-MPs of 2.8 μm diameter used as support is shown in Figure 6.2, A, while a zoom showing the biotin-P22 phages (~60−70 nm in diameter) attached to the bacterial surface can be seen in Figure 6.2, B and C. The spherical structures of the P22 phages uniformly distributed on the *Salmonella* surface are compared to a negative control containing the attached bacteria without the biotin-P22 label (Figure 6.2, D). A confirmation of the biotin-P22 recognition capacity towards *Salmonella* was thus achieved.

6.4.1.2 Confocal microscopy

Confocal microscopy was used as a technique for the confirmation of the bacteriophage biotinylation and its bacterial recognition ability. The images in Figure 6.3 show a blank without the bacteria (A), the IMS of the bacteria through the magnetic particles without the phage tagging (B) and the labeling with the Strep-Cy5 conjugate that binds to the attached biotinylated phages (C). As can be seen in Figure 6.3, A and B, any nonspecific adsorption of the fluorescent label was observed when no bacteria were present in the sample and no fluorescent labeling was observed if the biotin-P22 was not previously added for the biorecognition.

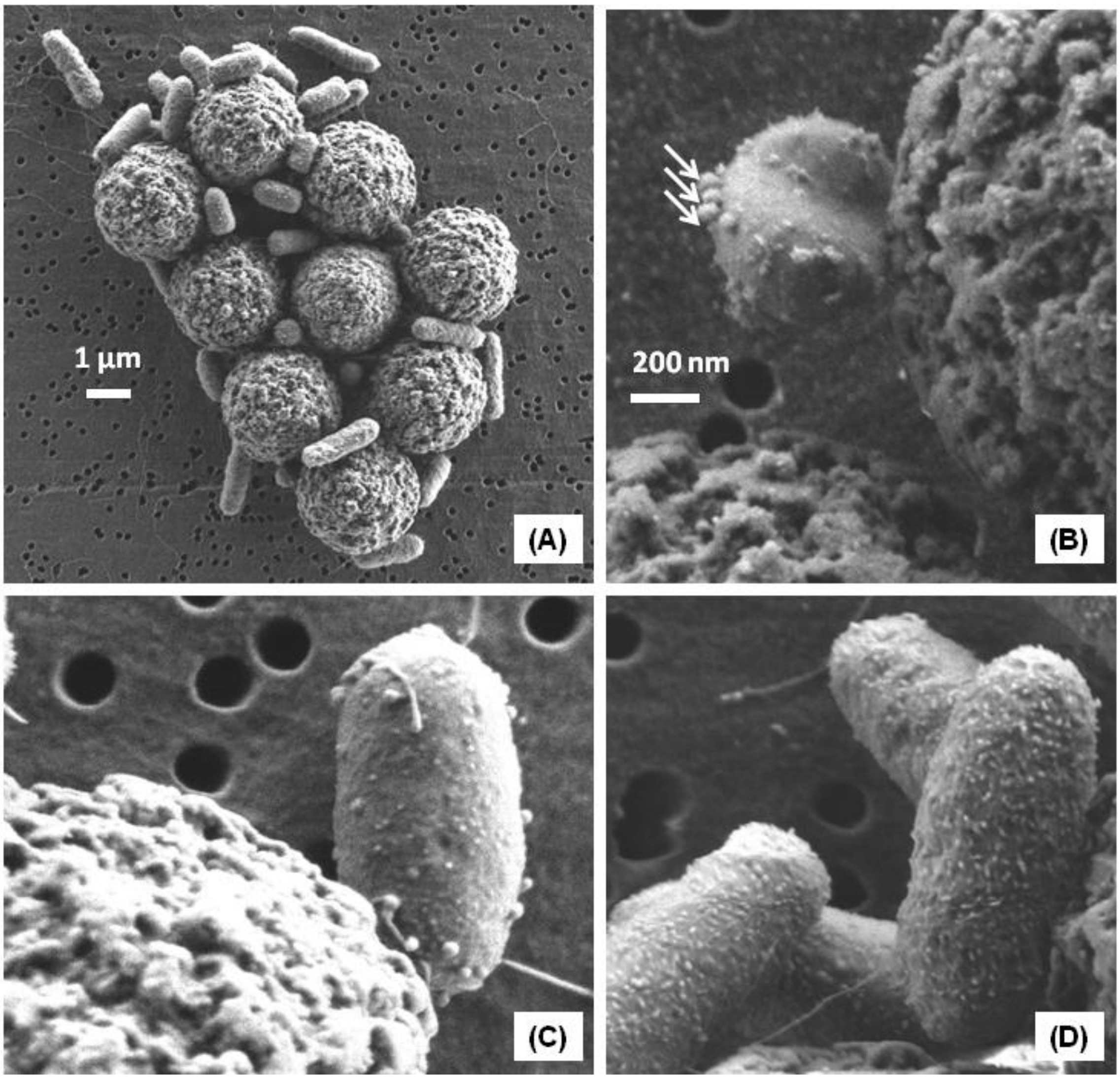

Figure 6.2 Characterization of biotin-P22 phagotagging by SEM, after the addition of 1.6 x 10^6 CFU of *Salmonella* and 10^{10} PFU of biotin-P22 to 50 µg anti-*Salmonella* MP of 2.8 µm (A). A negative control with 0 PFU biotin-P22 is also shown (B). In all cases, identical acceleration voltage (15 kV) was used.

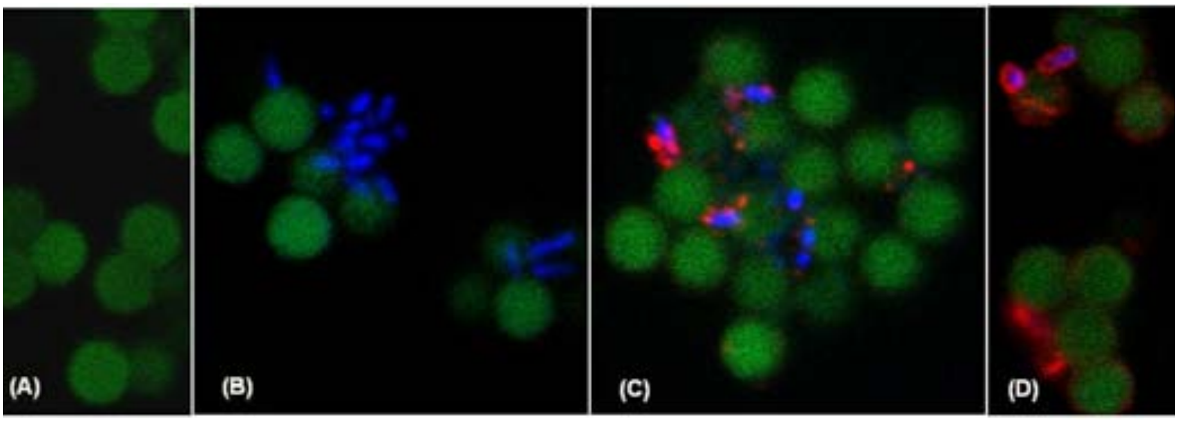

Figure 6.3 Confocal microscopy images of the negative control (A), the captured bacteria on the Ab-MPs (B), and the biotin-P22 attached to *Salmonella* labeled with Strep-Cy5 (C). It can be seen in green the magnetic particles (autofluorescent), in blue the bacteria stained with Hoechst 33342 and in red the biotin-P22 labeled with Strep-Cy5.

Finally, it should be also highlighted that phages showed a different labeling pattern than biotinylated antibodies as described in the previous chapter (§ 5.4.5). Moreover, a lower nonspecific adsorption seemed to take place in the case of phagotagging, since antibodies showed a slight red signal around some magnetic particles as shown in Figure 6.3, D, not observed in the case of biotin-P22 (Figure 6.3, C).

6.4.2 Optimization of the phagotagging magneto immunoassay

6.4.2.1 Study of the conditions for the immunomagnetic separation

In order to establish the optimal conditions for the IMS, a direct sandwich immunoassay was performed using Ab-HRP at a dilution of 1/1000.

As shown in Figure 6.4, three different incubation times were tested (10, 20 and 30 minutes) and the signal obtained for the higher *Salmonella* concentration (10^7 CFU mL^{-1}) was almost the same in all cases, indicating a possible saturation of the detection system at this concentration. However, for a lower bacteria concentration (10^5 CFU mL^{-1}), higher signals were obtained after 20 and 30 minutes in comparison to 10 minutes incubation, showing better signal to nonspecific adsorption ratios.

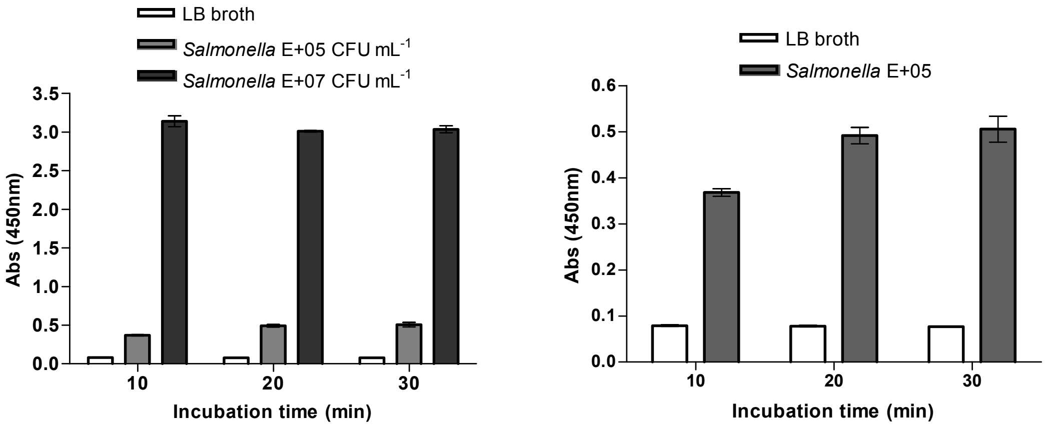

Figure 6.4 Optimization of IMS time, by performing a direct sandwich immunoassay using 0.1 mg mL^{-1} of Ab-MP for the bacteria capturing and Ab-HRP diluted 1/1000 as enzymatic label. The absorbance obtained in LB broth (negative control) was compared with the signals obtained at 10^5 and 10^7 CFU mL^{-1} of *Salmonella* (A). A zoom of the difference between the signal at 10^5 CFU mL^{-1} and the blank is also shown (B).

The concentration of the Ab-MP was also optimized comparing the signals obtained at 0, 10^3, 10^4 and 10^6 CFU mL^{-1} of *Salmonella*, using increasing concentrations of magnetic particles: 0.03, 0.06, 0.10, 0.25, 0.5 mg mL^{-1}, as shown in Figure 6.5.

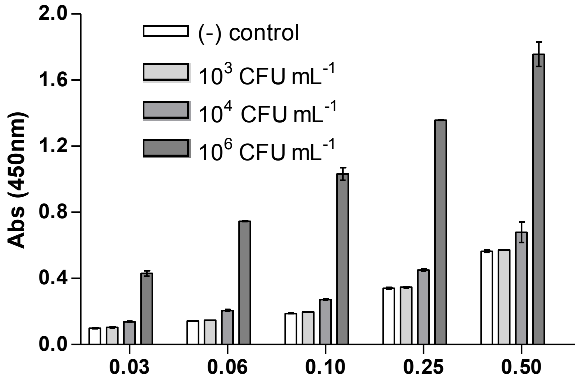

Figure 6.5 Comparison of the results obtained for increasing amounts of Ab-MP when performing a direct sandwich immunoassay using Ab-HRP (1/1000) as enzymatic label.

A signal increase was observed when increasing the Ab-MP concentration, but also the negative controls changed accordingly. When analyzing the corresponding signal to background ratios, better results were obtained at a magnetic particle concentration of 0.1 mg mL^{-1}, as detailed in Table 6.2.

Table 6.2 Comparison of the signal to background ratios obtained for each *Salmonella* concentration at different Ab-MP concentrations using the direct sandwich immunoassay with optical detection.

Signal to background ratio	**[Ab-MP] mg mL^{-1}**				
[*Salmonella*] CFU mL^{-1}	**0.03**	**0.06**	**0.1**	**0.25**	**0.5**
10^3	1.05	1.03	1.05	1.02	1.01
10^4	1.39	1.44	1.45	1.32	1.21
10^6	4.34	5.23	5.50	3.99	3.11

6.4.2.2 Optimization of the concentration for the biotin-P22 and Strep-HRP

Other optimizations which were performed to improve the detection were the adjustment of the concentration of the primary tagging reagent, the biotin-P22, and the enzymatic label, Strep-HRP for both the optical magneto immunoassay and electrochemical magneto immunosensor.

In the case of the optical detection system, four biotin-P22 dilutions and different Strep-HRP concentrations were assayed and the signals to background ratios were evaluated to establish the optimal conditions, as shown in Figure 6.6. Regarding the biotin-P22 tagging, the experiments were done using a phage lysate with an initial titer of around 2.5 x 10^{11} PFU mL^{-1}, which was modified with 1 mg biotin obtaining a final concentration of approximately 1.5 x 10^{11} PFU mL^{-1} after the biotinylation process. The tagging reagent was diluted from 1/10 to 1/200 and the better results were obtained using a 1/100 dilution, as shown in Figure 6.6, B, which corresponded thus to a concentration in the order of 1.5 x 10^{9} PFU mL^{-1} of biotin-P22. On the other hand, when analyzing the response while increasing the enzymatic label, the positive signal reached a plateau after a concentration of 0.5 µg mL^{-1}. However, a slight increase in the blanks was still observed (Figure 6.6, C). Thus, this was the chosen concentration for the detection, since it showed the highest signal to nonspecific adsorption ratio of the studied concentration range (Figure 6.6, D).

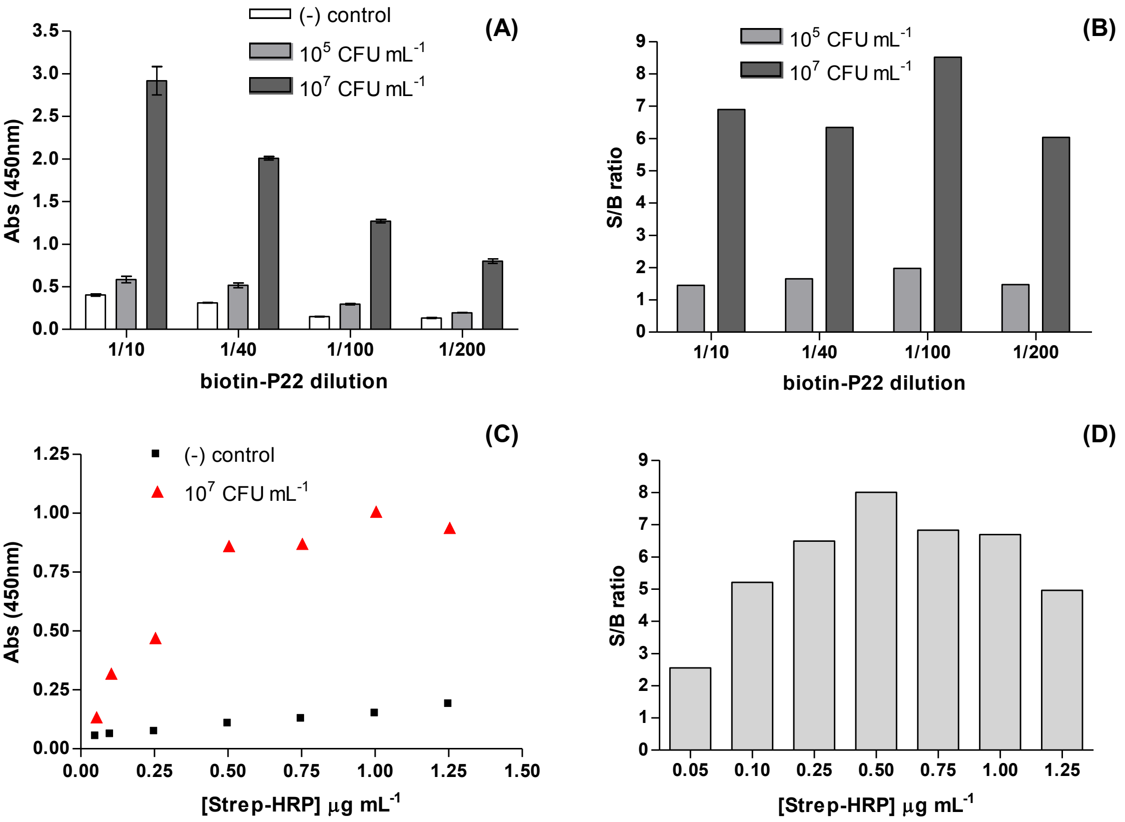

Figure 6.6 Optimization of biotin-P22 dilution (A) and Strep-HRP concentration (C), and signal to background ratios obtained respectively (B and D) by optical detection. For the biotin-P22 optimization the secondary label Strep-HRP was fixed at 1 µg mL^{-1}, while in the case of the Strep-HRP optimization a biotin-P22 dilution of 1/100 was used.

For the electrochemical detection, the amount of Strep-HRP added for the final labeling step was fixed in 6 µg mL^{-1} following optimizations performed in previous works, whereas the concentration of the primary tag biotin-P22 was optimized by analyzing the response at 10^{7} CFU mL^{-1} in comparison to the negative controls using four different phage dilutions (1/10, 1/25, 1/50 and 1/100), as shown in Figure 6.7. A signal increase was observed when increasing the biotin-P22 concentration until the dilution of 1/25, where the maximum response was achieved, while at a 1/10 dilution a lower positive signal and higher background value was obtained. As a result the highest signal to background ratio was obtained at 1/25 and this was the selected dilution, corresponding to a concentration of around 6 x 10^{9} PFU mL^{-1}.

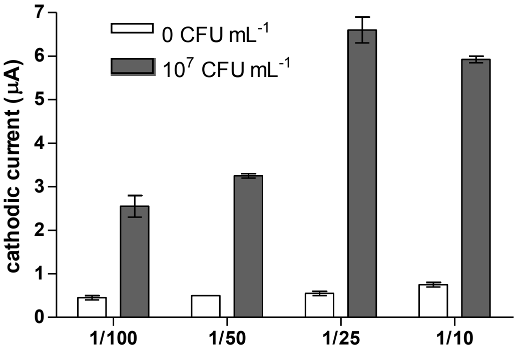

Figure 6.7 Optimization of the biotin-P22 dilution used for the bacteria labeling in the electrochemical approach, using 6 µg Strep-HRP as secondary label.

6.4.2.3 Study of the phagotagging procedure

The phages bind to specific receptors on the bacterial surface in order to inject the genetic material inside the bacteria. In the case of P22, six homotrimeric tailspike molecules (namely gp9) are involved in the viral adhesion protein which specifically recognizes the O-antigenic repeated units of the cell surface lipopolysaccharides of *Salmonella*.[10] Incubation time as well as shaking and temperature conditions during the phage tagging are important factors to be evaluated since they could affect the bacteria biorecognition by the P22 phage. These factors were studied using the phagotagging magneto immunoassay with optical detection and the results obtained when changing some of these parameters are outlined in Figure 6.8.

Analyzing the Figure 6.8, A significant improvement can be seen when incubating without agitation, since higher positive signals and lower nonspecific adsorption were obtained. This result could be explained due to the fact that probably a certain contact time is required in order to achieve the bacteria recognition by the phages and during shaking the phage has more difficulties to bind strongly enough to the *Salmonella* receptors.[11–13] Regarding the incubation time, no significant signal increase were obtained with longer incubation times, while a slight increase of the negative controls were observed. The signal to nonspecific adsorption ratio decreases from around 7.5 for 20 min incubation to 5.5 for longer incubation times. Therefore, the better results were obtained after 20 min incubation without agitation.

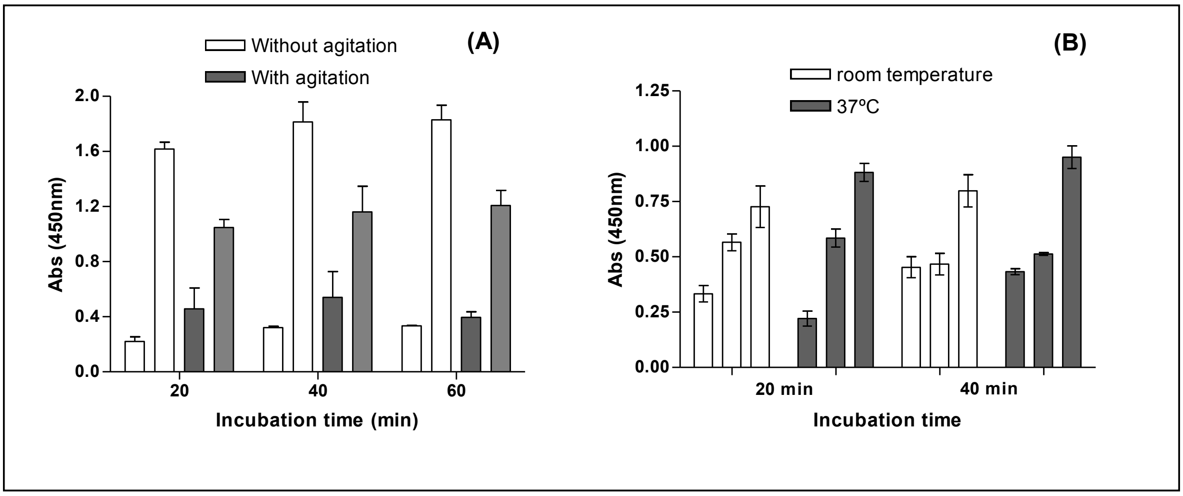

Figure 6.8 Optimization of the incubation conditions for the bacteria recognition by the biotinylated phages. Effect of the agitation (A) and temperature (B) at different incubation times showing the signal of the blank compared with the signals in the presence of *Salmonella*. In (A) only one *Salmonella* concentration was assayed (10^7 CFU mL^{-1}) while in (B) the signals were obtained at two bacteria concentrations (10^5 and 10^6 CFU mL^{-1}).

On the other hand, in order to evaluate the effect of temperature on the recognition step the signals obtained at room temperature after 20 and 40 minutes incubation were compared with the ones obtained at 37ºC, as shown in Figure 6.8, B. As can be seen in the Figure, better signal to background ratios were obtained when performing the incubation at 37ºC compared to the results at room temperature, since higher positive signals and lower blank values were obtained. Furthermore, the reproducibility of the signals was also improved when the temperature was settled at 37ºC. Regarding the incubation time, no advantage in increasing the time from 20 to 40 minutes was observed, since the positive signals were almost the same, but an increase in the blank values were shown. This result was consistent with those obtained in the previous optimization.

6.4.3 Evaluation of different strategies for the electrochemical magneto immunosensor based on phage tagging

Five different strategies were assayed by varying the incubation and washing steps as previously explained in Table 6.1 and schematized in Figure 6.9. The optimal protocol was evaluated by following the different procedures and comparing the responses at two different bacteria concentrations (10^5 and 10^7 CFU mL^{-1}) using the phagotagging immunosensing approach with electrochemical detection.

The results were compared in Figure 6.10. As shown in the Figure, very slight differences between the positive and background signals were observed in the strategies D and E. In both cases, the biotin-P22 was expected to react with the Strep-HRP conjugate before than the bacteria, due to the huge affinity constant of the biotin-streptavidin. These results suggest that the previous attachment of the enzymatic conjugate to the biotin-P22 could hinder the biorecognition required for the bacteria tagging. Although in the remaining three cases the bacteria were clearly detected, improved results were obtained with the strategy C, by performing IMS and phagotagging in one step, showing very low background values and the highest positive signals. A comparison of the signal to background ratios for the different strategies is shown in Table 6.3, demonstrating that strategy C provided by far the better results.

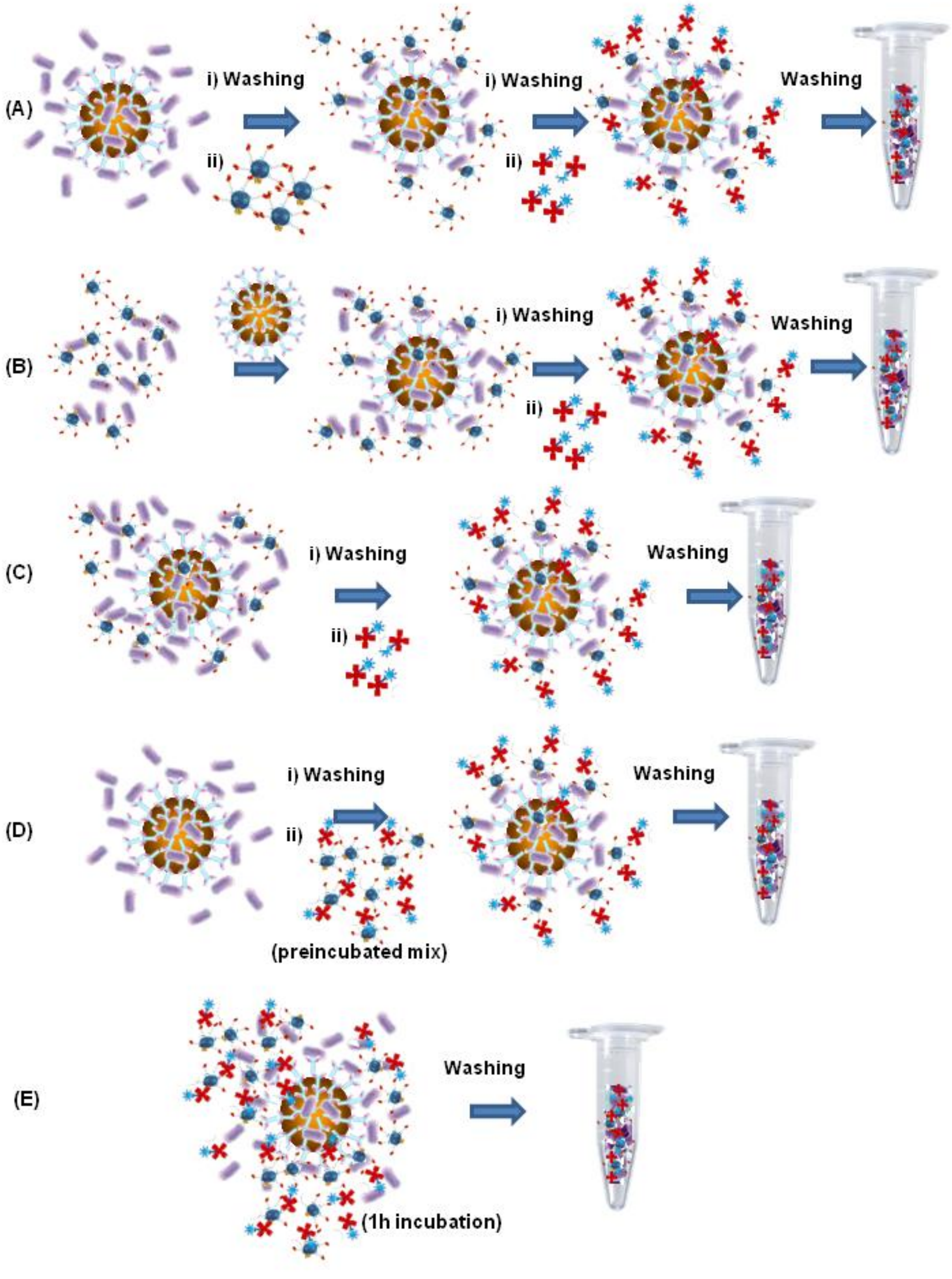
(A)
i) Washing
ii)
i) Washing
ii)
Washing
(B)
i) Washing
ii)
Washing
(C)
i) Washing
ii)
Washing
(D)
i) Washing
ii)
(preincubated mix)
Washing
(E)
Washing
(1h incubation)

Figure 6.9 Schematic representation of the different procedures applied for the optimization of the phagotagging magneto immunoassay protocol. The five strategies were performed as described in Table 6.1: (A) stepwise protocol; (B) preincubation of *Salmonella* with biotin-P22; (C) IMS and phage tagging in one step; (D) preincubation of biotin-P22 with Strep-HRP; and (E) addition of all reagents in one step.

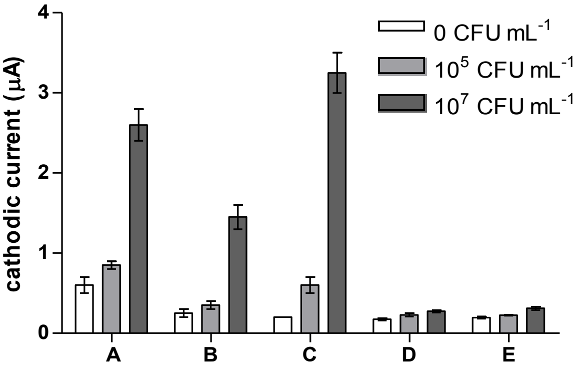

Figure 6.10 Evaluation of the optimal strategy for the phagotagging immunosensing approach. The procedures A to E correspond to the five protocols described in Table 6.1 and schematic represented in Figure 6.9.

Table 6.3 Signal to nonspecific adsorption ratios for the five different strategies tested.

Signal to background ratio	**Strategy**				
[*Salmonella*] CFU mL^{-1}	**A**	**B**	**C**	**D**	**E**
10^5	1.93	1.40	4	1.31	1.15
10^7	5.64	5.8	17.83	1.57	1.59

6.4.4 Magneto immunoassay with optical detection *vs*. electrochemical magneto immunosensor based on phage tagging for the detection of *Salmonella* in milk

Once the reagents concentration, incubation conditions and optimal protocol were established, the response to *Salmonella* concentration as well as the matrix effect in the presence of milk was evaluated for both approaches, i.e. the magneto immunoassay with optical detection and the electrochemical magneto immunosensor based on phage tagging. With this aim, calibration curves were prepared with *Salmonella* artificially inoculated and serially diluted from 10^1 to 10^8 CFU mL^{-1} in LB broth and in milk diluted 1/10 in LB. As cells are injured when exposed to adverse conditions during food processing, a pre-enrichment step is usually included in classical culture methods to achieve the proliferation of stressed *Salmonella* cells, since otherwise bacteria that have not fully repaired may be underestimated.[14] The pre-enrichment step is normally performed with a nonselective broth medium, such as LB broth, leading to a 1/10 dilution of the food matrix. The results obtained for both matrixes using both methods are shown in Figure 6.11. As can be seen in the Figure, a signal variation was observed in the presence of milk, indicating a slight matrix effect throughout the whole calibration curve, which has to be considered for the detection and was more evident at higher bacteria concentrations.

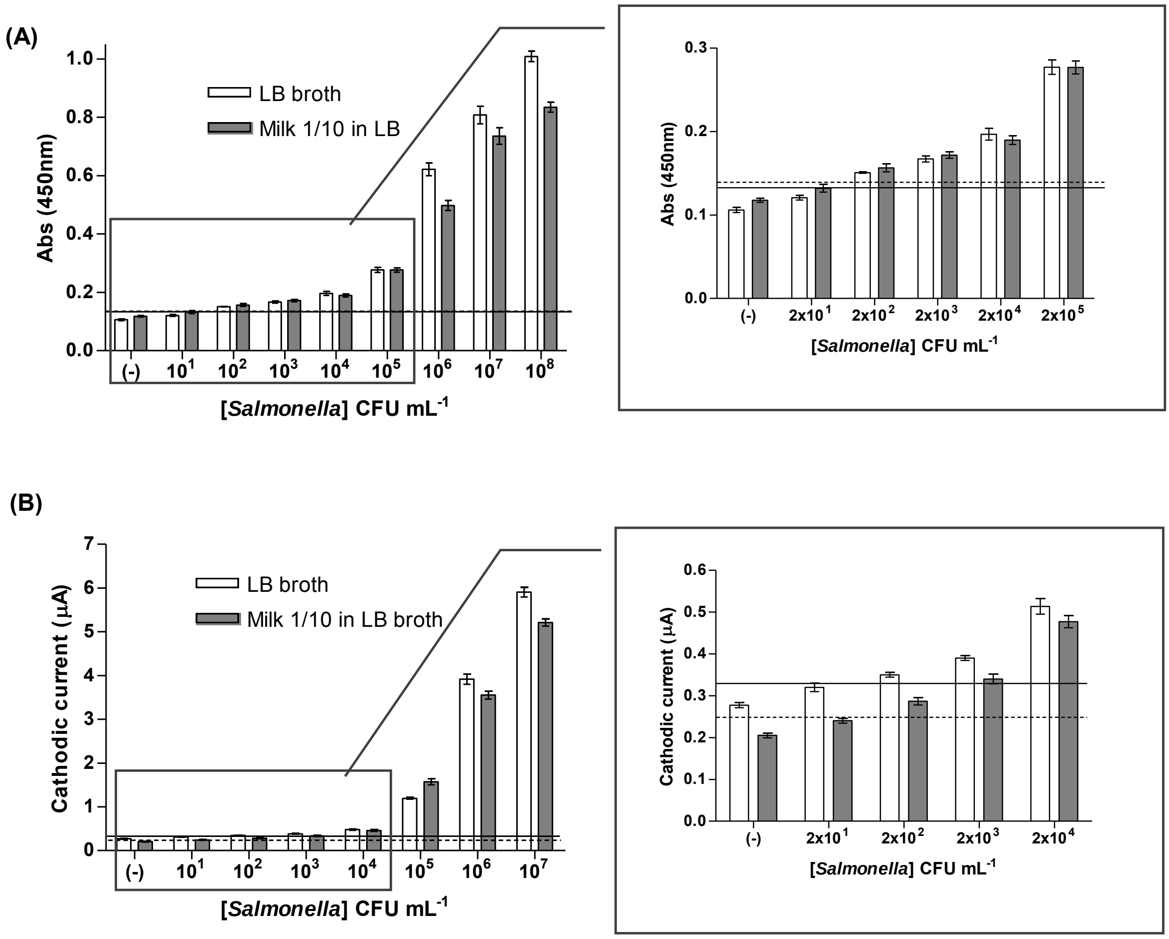

Figure 6.11 Results obtained in LB broth (white bars) and milk diluted 1/10 (grey bars), showing the signals (optical and electrochemical) by increasing the concentration of *Salmonella* from 2 ×10^1 to 2 × 10^8 CFU mL^{-1} (left). The insets in the right panel show a zoom in the lower bacteria concentration range. The reagents concentration were: 0.1 mg mL^{-1} Ab-MP, biotin-P22 diluted 1/100 and Strep-HRP 0.5 µg mL^{-1} for the optical magneto immunoassay (A), and 0.5 mg mL^{-1} Ab-MP, biotin-P22 diluted 1/25 and 6 µg mL^{-1} Strep-HRP for the electrochemical magneto immunosensor based on phage tagging (B). The cut-off values in LB broth and milk are represented in both cases through a solid and dotted line, respectively and in all cases, n=3, except for the 0 CFU mL^{-1} negative control (n=10). The electrochemical measurements were performed in phosphate buffer 0.1 M, KCl 0.1 M, pH 7.0, with hydroquinone 1.81 mM as a mediator and H_2O_2 4.90 mM as a substrate, applying a potential of -0.150 V (*vs*. Ag/AgCl).

The results obtained at 10^8 CFU mL^{-1} based on the electrochemical detection were discarded from the curve, since a significant signal drop was observed at this point when compared to the intensity at 10^7 CFU mL^{-1} (from 5.9 to 3.8 µA in LB), which was not concordant with the expected behavior. This fact could be explained by a blocking of the current transduction at the electrode surface caused through the extremely high bacteria number immobilized on the magnetic particles. Moreover, the addition of high bacteria amounts favor the formation of aggregates due to the multivalence of the magnetic particles and the bacteria as well as the possibility of additional bridges resulting from the tetrameric streptavidin label.

The cut-off and LOD values were evaluated by processing 10 negative samples (0 CFU mL^{-1}) obtaining for the optical detection a mean value of 0.106 and 0.118 absorbance units (a.u.) with a standard deviation of 0.0088 and 0.0073 for the assay performed in LB broth and in milk diluted 1/10 in LB, respectively. The cut-off values were then extracted with a one-tailed *t* test at a 99 % confidence level, calculated as the mean of the blank in addition to the corresponding *t* value multiplied by the standard deviation of the blank. The obtained results were 0.132 (solid line) and 0.139 a.u (dotted line) in LB and in milk respectively, showing that the system is able to give a positive signal for the second point of the curve in both matrixes (Figure 6.11, A), which corresponds to a concentration in the order of 10^2 CFU mL^{-1} of *Salmonella*. The LOD values were calculated by interpolation of the cut-off signals in the sigmoidal dose response curve obtained after plotting the absorbance *vs*. the logarithm of *Salmonella* concentration (Figure 6.12, A), obtaining LODs of 180 CFU mL^{-1} in LB broth and 104 CFU mL^{-1} in milk. The detailed results of the curves parameters are shown in Table 6.4, A demonstrating a good fit in both matrixes (0.9946 in LB and 0.9882 in milk).

In the case of the electrochemical magneto immunosensor based on phage tagging, the mean values for the blanks after processing 10 negative samples were 0.277 and 0.205 µA with standard deviations of 0.018 and 0.016 for the assay performed in LB broth and in milk diluted 1/10 in LB, respectively. The signals corresponding to the LOD values were then extracted obtaining a cut-off value of 0.328 (solid line) and 0.249 µA (dotted line) in LB and in milk, respectively (Figure 6.11, B). The amperometric signals were also plotted *vs*. the logarithm of *Salmonella* concentration and adjusted to a sigmoidal dose response curve (Figure 6.12, B and Table 6.4, B), obtaining a good fit in both matrixes (0.9992 in LB and 0.9981 in milk). The LOD values were then calculated by interpolating the cut-off signals, obtaining 494 CFU mL^{-1} in LB broth and 331 CFU mL^{-1} in milk. However when analyzing the graphs the second point of the curve was already above the aforementioned cut-offs in both matrixes (as shown in Figure 6.11), which corresponds to a *Salmonella* concentration of 200 CFU mL^{-1}.

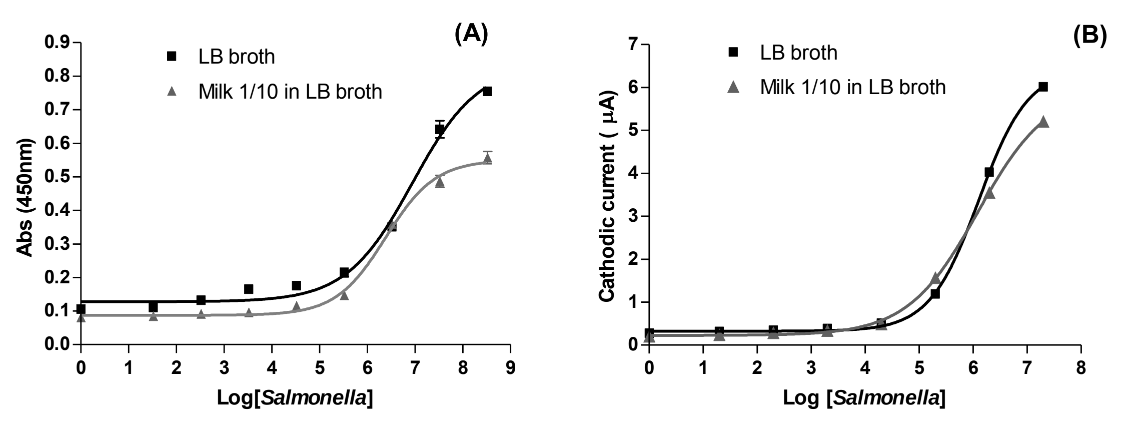

Figure 6.12 Sigmoidal dose response curves obtained in both matrixes after plotting the signal *vs.* the logarithm of *Salmonella* concentration for the optical (A) and electrochemical (B)detection.

Table 6.4 Parameters of the sigmoidal dose response curves obtained after plotting the optical (A) or electrochemical (B) signals *vs*. logarithm of the *Salmonella* concentration when applying the phagotagging magneto immunoassay approach in LB broth and milk.

(A) Optical detection	CV (%) for (-) control	CV (%) at 10^8 CFU mL^{-1}	R^2	Slope	Cut-off	LOD (CFU mL^{-1})
LB broth	8.3	3.1	0,9946	0,57	0,1324	180
Milk 1/10 in LB broth	6.2	3.6	0,9882	0,65	0,1394	104

(B) Electrochemical detection	CV (%) for (-) control	CV (%) at 10^8 CFU mL^{-1}	R^2	Slope	Cut-off	LOD (CFU mL^{-1})
LB broth	6.5	3.2	0,9992	0,95	0,328	494
Milk 1/10 in LB broth	7.8	2.7	0,9981	0,67	0,249	331

(*) The second point of the calibration curve, corresponding to 200 CFU mL^{-1}, was already above the cut-off value in both matrixes and was thus taken as the limit of detection.

Similar detection limits were achieved with both detection strategies, with values in the order of 10^2 CFU mL^{-1}. However, the electrochemical system showed better sensitivity demonstrable through its higher slope in both curves and also through the higher signal to background ratios that were obtained throughout almost the whole calibration curve as can be seen in detail in Table 6.5. Moreover, better fit to the sigmoidal dose response curves and also lower matrix effect were obtained in the case of the electrochemical magneto immunosensor based on phage tagging in contrast to the optical magneto immunoassay. Besides, a lower assay time is required in this case since the last 30 min incubation for the color formation through the reaction with the substrate is not necessary. In addition, the use of electrochemical magneto immunosensors is more promising to cover the demand of rapid and on-site testing required for the implementation in HACCP for food safety.

Table 6.5 Signal to background ratios obtained in both matrixes (LB broth and milk diluted 1/10 in LB) throughout the calibration curve performed with the optical magneto immunoassay and electrochemical magneto immunosensor based on phage tagging.

Signal to background ratio	**Optical**		**Electrochemical**	
[*Salmonella*] CFU mL^{-1}	**LB**	**Milk**	**LB**	**Milk**
2 x 10^1	1,14	1,12	1,13	1,17
2 x 10^2	1,42	1,32	1,26	1,40
2 x 10^3	1,58	1,45	1,41	1,66
2 x 10^4	1,86	1,61	1,85	2,33
2 x 10^5	2,61	2,34	4,31	7,67
2 x 10^6	5,86	4,22	14,14	17,33
2 x 10^7	7,62	6,23	21,05	25,41

Many ELISA-based methods for *Salmonella* detection have been reported due to their advantage of easy automation and high sample throughput capability given by the 96-well microplate format. However, most of them have the disadvantage of their high limits of detection, above 10^5 CFU mL^{-1}.[15] These values are 1000 times higher than the results obtained through the phagotagging magneto immunoassay with optical detection developed in this work. Only in recent approaches based on IMS coupled with the integration of nanomaterials-based labels such as quantum dots[16] or gold nanoparticles[17], or in the case of magneto immunoassays coupled with electrochemical detection using for example ion-sensitive field-effect transistors[18] and intermittent pulse amperometry[19,20], improved sensitivities were reported, with values down to 1-10^2 CFU mL^{-1}.

Moreover, when analyzing the results reported in other strategies based on phage tagging for bacteria detection, lower limits of detection (between 1 and 100 CFU mL^{-1}) were only achieved in a few works. Some examples were the expression of reporter genes (e.g. lux genes ore ice nucleation genes),[21,22] the labeling of the phage DNA with YOYO-1 dye[23] or the use of streptavidin modified quantum dots to label engineered phages previously modified to display biotin binding peptides on their capsid, as explained in § 6.1[6,7].

However, in all the aforementioned cases, more expensive reagents and instrumentation, longer assay times, or in the examples of phagotagging strategies also more complex phage engineering methodologies were needed.

On the other hand, compared with other biosensing methodologies for detecting pathogenic bacteria [24], excellent detection limits were achieved with the developed procedure. As an example, in comparison with a previous work of our group using the same modified magnetic particles for the IMS but antibody labeling [25] instead of phage tagging, the limit of detection was reduced in one order (from 10^3 to 10^2 CFU mL^{-1}). Furthermore, the phage tagging gave better coefficient of variation (CV) values for the negative controls in both LB broth (6.5 *vs*. 9.3 %) as well as in milk (7.8 *vs*. 30 %), indicating a higher reproducibility. The lower limits of detection obtained with the biotin-P22 tagging could be ascribed to the signal amplification achieved through the high biotinylated phage capsid containing around 2000 biotin molecules per phage in contrast to the antibodies labeled with just 2-3 HRP molecules per IgG.

Finally, it is important to point out that although lower limits of detection were achieved using electrochemical methods based on magnetic separation coupled to nucleic acid-based polymerase chain reaction (PCR)[26,27], the present method is more rapid and simple and avoids the tedious and expensive DNA extraction and amplification steps, being thus more suitable for the rapid and on-site testing required for food safety.

6.4.5 Specificity study

Figure 6.13 shows the results for 10^7 CFU mL^{-1} of *Escherichia coli*, 10^7 CFU mL^{-1} of *Salmonella* and finally, a mix containing 10^7 CFU mL^{-1} of each bacteria, artificially inoculated in milk diluted 1/10 in LB broth and compared to a negative control. The results obtained by the phagotagging magneto immunoassay with optical detection are shown in Figure 6.13, A, while the signals obtained with the electrochemical magneto immunosensor based on phage tagging are presented in Figure 6.13, B. As could be expected for a specific assay, in both methods the signals obtained for the *E.coli* samples were almost identical to the negative controls, while the response to the mix of both bacteria were quite similar to the signals obtained with a pure culture of *Salmonella*. These results confirmed the high specificity of both approaches, which can be ascribed to the double biorecognition, coming from: (i) the IMS step with the specific antibodies towards *Salmonella* which are coating the magnetic particles, and (ii) the phage tagging with the specific interaction between the membrane receptor of the bacteria and the tailspike of the P22 phage.

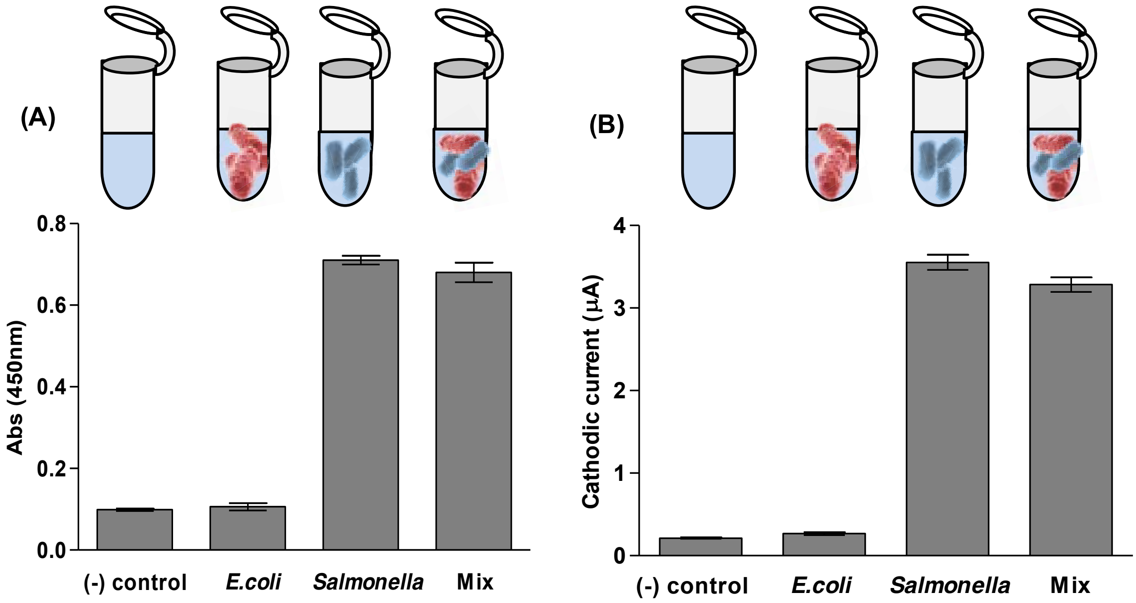

Figure 6.13 Comparative study of the specificity for (A) the phagotagging magneto immunoassay with optical detection and (B) the electrochemical magneto immunosensor based on phage tagging. The bars show the (A) optical and (B) electrochemical signals for milk diluted 1/10 in LB artificially inoculated, respectively, with: 0 $CFUmL^{-1}$ (negative control); 1.8×10^7 $CFUmL^{-1}$ of *E. coli*; 2.3×10^7 $CFUmL^{-1}$ of *Salmonella*; and a mix solution containing both pathogens. The error bars show the standard deviation for n=3. The conditions for the electrochemical measurements are the same as in Figure 6.10.

6.5 CONCLUSIONS

The developed strategy based on the IMS coupled to phage tagging showed outstanding analytical performance for the detection of *Salmonella* Thyphimurium. The labeling with biotinylated bacteriophages was demonstrated through microscopy techniques, as SEM and confocal microscopy. The results demonstrated that biotin-P22 are novel sensitive, versatile and selective bacterial tags that coupled to fluorescent and optical or electrochemical reporters allow the sensitive imaging and detection of the bacteria *Salmonella*. The main advantages of using the phage for bacteria tagging instead of an antibody rely on the outstanding stability and specificity, as well as animal-free, cost-efficiently production of the P22 bacteriophages. Moreover, the huge phage surface available for the modification with a high number of biotin tags allows the amplification of the signal when compared with antibodies directly labeled with only 2-3 HRP molecules, as previously discussed (§ 6.4.4). Also in the case of using biotinylated antibodies instead of biotin-P22 coupled to streptavidin-HRP, lower signal amplification would be achieved since biotinylation of antibodies results normally in a molar substitution between 2 to 5 biotin moieties per antibody, or in some commercially available biotinylated IgG (Abcam, UK), biotin/antibody ratios between 10-20 were reported. Nevertheless, both values are significantly below the 2000 biotin moieties attached per phage in the biotin-P22 tags developed in this dissertation.

Regarding the analytical performance, low matrix effect and excellent limits of detection were achieved in both LB broth and diluted milk using the phagotagging magneto immunoassay coupled to optical detection as well as with the electrochemical magneto immunosensor. Both strategies were able to detect bacteria concentrations in the order of 10^2 CFU mL^{-1}, reducing considerably the time of the assay from 3-5 days needed in the microbiological techniques, to around 3 h with the optical magneto immunoassay and, even further (below 2.5 h) when using the electrochemical magneto immunosensor based on phage tagging.

Better results were obtained with the immunosensing approach as discussed in § 6.4.3, obtaining a rapid and sensitive detection method suitable for *Salmonella* screening-out in HACCP programs. However, it should be pointed out that as long as the methodologies were not fully validated, positive samples should be considered presumptive infected, requiring the further confirmation by approved culture based methods.

Finally, it should be also highlighted that a very specific approach was achieved, capable of clearly distinguishing between different gram negative pathogenic bacteria such as *Salmonella* and *Escherichia coli*. This high specificity is mainly conferred by the antibody-modified magnetic particles employed for the IMS step and the biotinylated P22 phages used for the further labeling step. P22 is specific to serotypes A, B, and D1, being thus an extremely useful tool to trace the source of an outbreak.

The main novelty of the developed approach is the phagotagging procedure for the sensitive detection of bacteria. To the best of our knowledge, this was the first time that phages are used for bacteria tagging in biosensors instead of using them as a biorecognition element immobilized on a solid support for bacteria capturing. As a conclusion, the high sensitivity is given by the signal amplification through the large biotinylated surface provided by the bacteriophages in connection with the m-GEC electrochemical sensing, which result in a rapid, robust and sensitive procedure.

6.6 REFERENCES

(1) Velusamy, V.; Arshak, K.; Korostynska, O.; Oliwa, K.; Adley, C. *Biotechnology Advances* **2009**, *28*, 232–54.

(2) Tallury, P.; Malhotra, A.; Byrne, L. M.; Santra, S. *Advanced drug delivery reviews* **2010**, *62*, 424–37.

(3) Hagens, S.; Loessner, M. J. *Applied Microbiology and Biotechnology* **2007**, *76*, 513–9.

(4) Li, K.; Nguyen, H. G.; Lu, X.; Wang, Q. *The Analyst* **2010**, *135*, 21–7.

(5) Smartt, A. E.; Xu, T.; Jegier, P.; Carswell, J. J.; Blount, S. a; Sayler, G. S.; Ripp, S. *Analytical and Bioanalytical Chemistry* **2012**, *402*, 3127–46.

(6) Edgar, R.; McKinstry, M.; Hwang, J.; Oppenheim, A. B.; Fekete, R. A.; Giulian, G.; Merril, C.; Nagashima, K.; Adhya, S. *Proceedings of the National Academy of Sciences of the United States of America* **2006**, *103*, 4841–4845.

(7) Yim, P. B.; Clarke, M. L.; McKinstry, M.; De Paoli Lacerda, S. H.; Pease, L. F.; Dobrovolskaia, M. a; Kang, H.; Read, T. D.; Sozhamannan, S.; Hwang, J. *Biotechnology and Bioengineering* **2009**, *104*, 1059–67.

(8) Hess, G. T.; Cragnolini, J. J.; Popp, M. W.; Allen, M. A.; Dougan, S. K.; Spooner, E.; Ploegh, H. L.; Belcher, A. M.; Guimaraes, C. P. *Bioconjugate Chemistry* **2012**, *23*, 1478–1487.

(9) Brambilla, C.; Sánchez-Chardi, A.; Pérez-Trujillo, M.; Julián, E.; Luquin, M. *Microbiology* **2012**, *158*, 1615–21.

(10) Handa, H.; Gurczynski, S.; Jackson, M. P.; Mao, G. *Langmuir* **2010**, *26*, 12095–103.

(11) Andres, D.; Baxa, U.; Hanke, C.; Seckler, R.; Barbirz, S. *Biochemical Society transactions* **2010**, *38*, 1386–9.

(12) Baxa, U.; Steinbacher, S.; Miller, S.; Weintraub, A.; Huber, R.; Seckler, R. *Biophysical Journal* **1996**, *71*, 2040–2048.

(13) Siqueira, R. S. De; Dodd, C. E. R.; Rees, C. E. D. *Brazilian Journal of Microbiology* **2003**, *34*, 118–120.

(14) Amaguaña, R.; Andrews, W. *Encyclopedia of Food Microbiology*; Robinson, R.; Batt, C.; Patel, P., Eds.; Academic Press: New York, NY, 2004; p. 1948.

(15) Odumeru, J. A.; León-velarde, C. G. In *Salmonella- A Dangerous Foodborne Pathogen*; Mahmoud, B. S. ., Ed.; InTech: Rijeka (Croatia), 2012; pp. 373–392.

(16) Wang, H.; Li, Y.; Wang, A.; Slavik, M. *Journal of Food Protection* **2011**, *74*, 2039–2047.

(17) Cho, I.; Irudayaraj, J. *International Journal of Food Microbiology* **2013**, *164*, 70–75.

(18) Starodub, N. F.; Ogorodnijchuk, J. O. *Electroanalysis* **2012**, *24*, 600–606.

(19) Croci, L.; Delibato, E.; Volpe, G.; Medici, D. De; Palleschi, G. *Applied and Environmental Microbiology* **2004**, *70*, 1393–1396.

(20) Delibato, E.; Volpe, G.; Romanazzo, D.; De Medici, D.; Toti, L.; Moscone, D.; Palleschi, G. *Journal of agricultural and food chemistry* **2009**, *57*, 7200–4.

(21) Wolber, P. K.; Green, R. L. *Trends in Biotechnology* **1990**, *8*, 276–279.

(22) Chen, J.; Griffiths, M. *Journal of Food Protection* **1996**, *59*, 908–914.

(23) Goodridge, L.; Chen, J.; Griffiths, M. *Applied and environmental microbiology* **1999**, *65*, 1397–404.

(24) Van Dorst, B.; Mehta, J.; Bekaert, K.; Rouah-Martin, E.; De Coen, W.; Dubruel, P.; Blust, R.; Robbens, J. *Biosensors & Bioelectronics* **2010**, *26*, 1178–94.

(25) Liébana, S.; Lermo, A.; Campoy, S.; Cortés, M. P.; Alegret, S.; Pividori, M. I. *Biosensors & Bioelectronics* **2009**, *25*, 510–3.

(26) Liébana, S.; Lermo, A.; Campoy, S.; Barbé, J.; Alegret, S.; Pividori, M. I. *Analytical Chemistry* **2009**, *81*, 5812–20.

(27) Liébana, S.; Spricigo, D. A.; Cortés, M. P.; Barbe, J.; Alegret, S.; Pividori, M. I. *Analytical Chemistry* **2013**, *85*, 3079–3086.

CHAPTER 7

BIOTINYLATED BACTERIOPHAGES ON STREPTAVIDIN MAGNETIC PARTICLES FOR PHAGOMAGNETIC SEPARATION AND DETECTION OF PATHOGENIC BACTERIA

7.1 INTRODUCTION

From the past decades until today, enzymes, antibodies, nucleic acids and biomimetic materials are used as biomolecular recognition elements for the detection of pathogenic bacteria and they have both merits and demerits when compared to one another.[1] The use of phagomagnetic separation (PMS) instead of immunomagnetic separation (IMS) ensures a better stability of the biorecognition element due to the higher resistance towards harsh conditions of phages in contrast to antibodies. As a result, from all the advantageous features already mentioned, their outstanding selectivity, high sensitivity and exceptional stability are three ideal attributes for any biorecognition probe that makes them more suitable for *in situ* monitoring of contaminants in food and environmental samples. [2,3]

As a precedent, the direct chemical biotinylation of phage coat proteins was reported for the development of a phage-based biosorbent through the immobilization of SJ2 phages on streptavidin-modified surfaces for *Salmonella enteritidis* detection.[4] In that case the bacteria capturing efficiency was evaluated by *in vivo* bioluminescence.

In this chapter, the use of biotinylated phages (biotin-P22) for the capture and phagomagnetic separation of *Salmonella* is described. The immobilization of the biotin-P22 on streptavidin-modified magnetic particles (Strep-MP) was performed for the phagomagnetic separation of the target bacteria. Finally the detection was carried out using peroxidase labeled anti-*Salmonella* antibodies (Ab-HRP) as optical reporter. Microscopy techniques were applied for the confirmation of the phage capture on the magnetic particles and of the further bacteria biorecognition, and in addition conventional culturing methods were performed to complete these studies. After performing all necessary optimizations to establish the most suitable conditions for this strategy, the response of the system to the bacteria concentration as well as the matrix effect and specificity were evaluated through a phagomagnetic immunoassay with optical detection. The performance was finally compared to the results obtained with the preceding optical magneto immunoassay and electrochemical magneto immunosensor based on phage tagging using the biotin-P22.

7.2. AIM OF THE CHAPTER

This chapter addresses the integration of biotinylated bacteriophages on streptavidin magnetic particles for phagomagnetic separation of bacteria and further optical detection with a magneto immunoassay, taking the biotin-P22 phage as a model for *Salmonella* detection.

The specific objectives can be summarized as follows:

- To analyze the biotin-P22 phage capturing on streptavidin magnetic particles by microbiology techniques (double agar layered method) and confocal microscopy.
- To study the utility of the biotin-P22 phage immobilized on magnetic particles as biorecognition element for the phagomagnetic separation of *Salmonella* by classical culture methods and Scanning Electron Microscopy (SEM).
- To design and evaluate a novel method for the detection of *Salmonella* based on a phagomagnetic immunoassay with optical detection.
- To assess the analytical performance of the developed strategy in terms of LOD values, matrix effect and specificity, comparing with the optical magneto immunoassay and electrochemical magneto immunosensor based on phage tagging of the pathogenic bacteria.

7.3 EXPERIMENTAL SECTION

7.3.1 Materials

The bacteria *Salmonella enterica* serovar Typhimurium LT2 and *Escherichia coli* K12 strains were routinely grown in Luria Bertani (LB) broth or on LB agar plates for 18 h at 37ºC. The preparation of the phage lysates, as well as their titration and purification using CsCl are described in Chapter 5 (§§ 5.3.1.1 and 5.3.1.2, respectively), while the materials used for the phage lysate preparation are the same detailed in Chapter 6.

The magnetic particles of 2.8 µm in diameter with streptavidin covalently bound for capturing biotinylated ligands (Dynabeads, product n° 112.05) were supplied by

Invitrogen Dynal AS (Oslo, Norway). Anti-*Salmonella* antibodies conjugated to HRP (product nº ab20771) were purchased from Abcam (Cambridge, UK).

The materials used for the bacteriophage biotinylation and the SEM characterization are described in Chapter 6, while those used for the confocal microscopy analysis and the optical and electrochemical assays were the same as previously described in Chapter 5.

Finally, the instrumentation used for the incubation and washing steps, the magnetic separations, as well as the optical and electrochemical detection were the same as detailed in Chapter 4 (§ 4.3.1.2).

7.3.2 Evaluation of the optimal conditions for the phagomagnetic immunoassay based on biotin-P22

The biotin-P22 phagomagnetic immunoassay with optical detection comprised the following steps, as schematized in Figure 7.1: (i) Biotin-P22 capture on the Strep-MP; (ii) phagomagnetic separation (PMS) through 20 min incubation at room temperature with agitation followed by 20 min at 37 °C without agitation; (iii) enzymatic labeling with 100 μL of anti-*Salmonella* antibodies labeled with horseradish peroxidase (Ab-HRP) incubating 30 min at room temperature and 700 rpm, followed by two washing steps with 100 μL of PBST. And finally, the last step, (iv) addition of 100 μL of substrate solution containing H_2O_2 and 3,3',5,5'-tetramethylbenzidine (TMB) incubating 30 min at 700 rpm in darkness, followed by the addition of 100 μL H_2SO_4 to stop the enzymatic reaction, and finally performing the optical read-out of the supernatants at 450 nm.

The first step, i.e. the attachment of the biotin-P22 on the streptavidin-modified magnetic particles (Strep-MP), was performed by adding 100 μL of the modified phages to the magnetic particles. The mix was incubated 30 min at 700 rpm and room temperature, in order to allow the biotin-streptavidin recognition taking place. Afterwards, two washing steps with PBST were performed in order to eliminate the excess of phages.

Regarding the incubation conditions for the bacteria biorecognition by the biotin-P22/MP, a further optimization was performed in order to improve the assay since in this system the phages are immobilized on the magnetic particles, in contrast to their presence in solution in the case of the phagotagging based methods (Chapter 5 and 6).

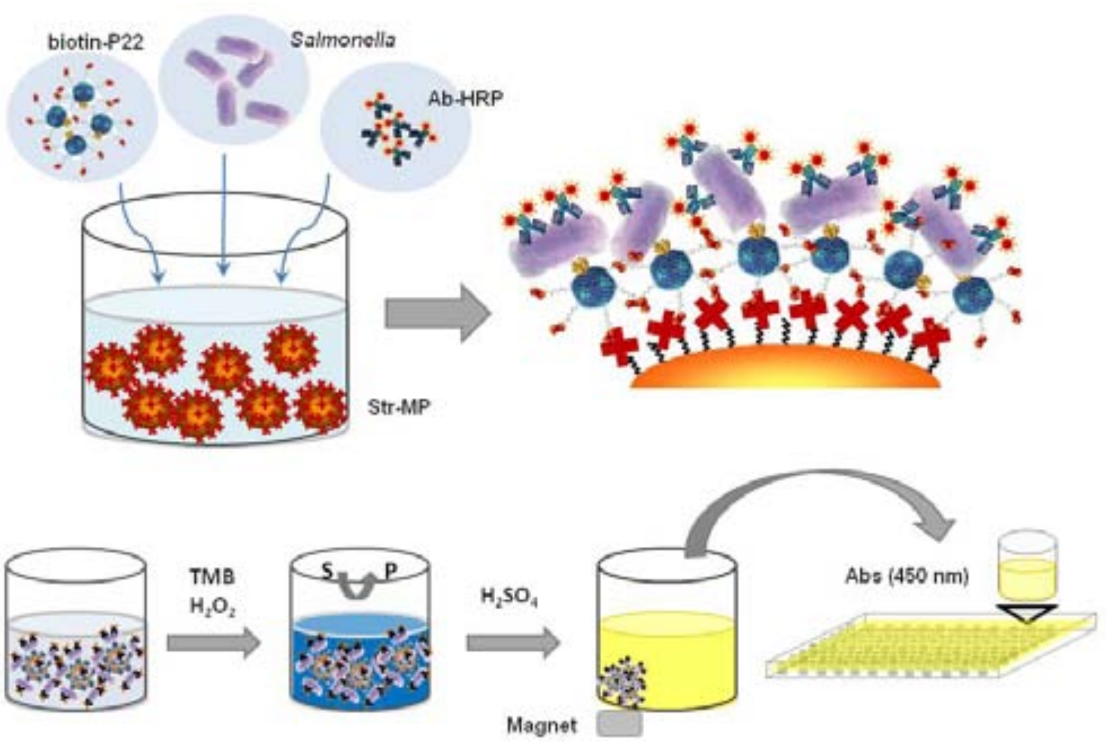

Figure 7.1 Schematic representation of the biotin-P22 phagomagnetic immunoassay with optical detection showing the attachment of the biotin-P22 on the Strep-MP, the bacteria capture and final enzymatic labeling using Ab-HRP. The steps for the optical detection are also shown in the lower panel.

In order to determine the biotin-P22 dilution and Strep-MP concentration, optimization experiments were performed applying the aforementioned optical detection system to different reagents concentration combinations. Another parameter which was adjusted was the enzymatic label concentration, testing also different antibodies dilutions. In all cases the results were evaluated analyzing the signal to nonspecific adsorption ratios to find the optimal conditions for achieving high positive signals related to low background values.

7.3.3 Study of the capturing of biotin-P22 on the Strep-MP

The efficiency of the coupling was evaluated by double agar layered method. In this approach, tenfold serial dilutions of the supernatant and first wash after the reaction with the Strep-MP were plated onto lawns of the bacterial strain and the phage titer was compared to the initial amount added. For the evaluation of the phage orientation and infectivity, several tenfold dilutions of the biotin-P22 modified streptavidin magnetic particles (biotin-P22/MP) were also plated by double agar layered method.

In order to verify the presence of the immobilized biotin-P22 phages on the Strep-MP, confocal fluorescence microscopy was used. With this aim, the biotin-P22 were captured on the magnetic particles as previously described and after washing, 100 µL of streptavidin conjugated to cyanine 5 dye (Strep-Cy5) at a concentration of 2 µg mL^{-1} was added to label the immobilized phages. A sample without the immobilized biotin-P22 was also processed as negative control.

7.3.4 Evaluation of the biotin-P22 phagomagnetic separation of *Salmonella* by SEM and conventional culture method

The capturing performance of the biotin-P22/MP conjugates was evaluated by SEM microscopy. A 1/25 dilution of a biotin-P22 stock solution with an initial titer of around 2.0 x 10^{11} PFU mL^{-1}, was immobilized on 50 µg of Strep-MP and then 500 µL of a *Salmonella* Typhimurium LT2 sample at a concentration of 10^{7} CFU mL^{-1} in LB broth was added to the biotin-P22/MP and incubated 20 min at room temperature with agitation followed by 20 min at 37 °C without agitation. After the PMS of the bacteria, the magnetic particles with the attached bacteria were separated with a magnet, and a washing step in PBST was performed. Finally, the modified magnetic particles were resuspended in 100 µL PBS and after adding it to 5 mL of milli-Q water the SEM samples were prepared as previously explained in Chapter 6 (§ 6.3.2).

In order to study the efficiency of the PMS step, different bacterial dilutions were prepared in LB broth and the capture of *Salmonella* in these samples was performed. A volume of 500 µL of different concentrations of bacteria were added to 10 µg of biotin-P22/MP and incubated under the same conditions. Once again, the magnetic particles with the attached bacteria were separated with a magnet, the supernatant was transferred to a new tube for further plating, and then two washes were performed with PBST for 5 min at room temperature followed by the resuspension in 100 µL PBST. The supernatants were plated in LB agar and grown for 18−24 h at 37°C to compare the bacteria counting with the initial amount added to the particles.

7.3.5 Biotin-P22 phagomagnetic immunoassay for the optical detection of *Salmonella* in milk

In an attempt to shorten as well as simplify the analytical procedure, seven different protocols were evaluated by varying the order and number of incubation and washing steps, as detailed outlined in Table 7.1.

Once the optimal conditions were established, the matrix effect was evaluated by comparing the response of the immunoassay for artificially inoculated *Salmonella* samples (ranging from 10^1 to 10^8 CFU mL^{-1}) in LB broth and in milk diluted 1/10 in LB. Finally, the cut-off and LOD values were also evaluated.

In order to fulfill the legislation about the presence of *Salmonella* in food samples, the detection system should be able to detect 1 CFU in 25 mL of milk, which is only possible if a pre-enrichment step is included. After spiking 25 mL of milk sample with 1-3 CFU of *Salmonella*, an overnight pre-enrichment step (16 h) was performed in LB broth (nonselective broth) at 37 ºC to evaluate the capability of the system to detect the target bacteria. Simultaneously, a positive control with 10X of bacteria (around 10 CFU in 25 mL milk) and a negative control were also processed.

7.3.6 Specificity study

The specificity of the phagomagnetic immunoassay was also evaluated by comparing the response to *Salmonella* with the signal obtained in the presence of an equivalent amount of another gram negative bacterium as *E.coli* artificially inoculated in milk samples at two different bacteria concentrations (10^6 and 10^7 CFU mL^{-1}) . A negative control was also processed. If the detection is not affected by any cross reaction, the signal for *E.coli* should be the same as the blank.

Table 7.1 Different procedures performed with the biotin-P22/MP as a magnetic carrier for the optimization of the phagomagnetic immunoassay.

(A) Stepwise	**(B) *Salmonella* + biotin-P22 preincubation**	**(C) Phage capture + PMS in one step**	**(D) Strep-MP addition as final step**	**(E) *Salmonella* + Ab-HRP preincubation**	**(F) *Salmonella* + Ac-HRP addition in one step**	**(G) All reagents in one step**
1- Biotin-P22 capture on Strep-MP (30 min, shaking)	1- *Salmonella* tagging with biotin-P22 (20 min, still, 37ºC)	1- Incubation of Ab-MP, biotin-P22 and *Salmonella* (30 min, shaking)	1- *Salmonella* tagging with biotin-P22 (20 min, still, 37ºC)	1- Biotin-P22 capture to Strep-MP, and *Salmonella* labeling with Ab-HRP (30 min, shaking)	1- Biotin-P22 capture to Strep-MP (30 min, shaking)	1- Short preincubation of 10 µL Strep-MP with biotin-P22 (10 min, shaking)
2- Washing step (1X, 5 min)	2- Addition of 10µL Strep-MP for the capture of biotin-P22 (30 min, shaking)	2- Incubation (20 min, still, 37ºC)	2- Enzymatic labeling with Ab-HRP (30 min, shaking)	2- Washing step (1X, 5 min)	2- Washing step (1X, 5 min)	2- Incubation with *Salmonella* + Ac-HRP (30 min, shaking, 20 min still at 37ºC)
3- PMS of *Salmonella* (20 min shaking at RT and 20 min still at 37ºC)	3- Washing step (2X, 5 min)	3- Washing step (2X, 5 min)	3- Addition of 10µL Strep-MP for the attachment to the biotin-P22 (30 min, shaking)	3- Incubation with *Salmonella* + Ab-HRP mix (30 min, shaking and 20 min still at 37ºC)	3- *Salmonella* + Ab-HRP addition and incubation (30 min shaking, 20 min still at 37ºC)	3- Washing step (3X, 3 min)
4- Washing step (1X, 5 min)	4- Enzymatic labeling with Ab-HRP (30 min, shaking)	4- Enzymatic labeling with Ab-HRP (30 min, shaking)	4- Washing step (3X, 3 min)	4- Washing step (2X, 3 min)	4- Washing step (2X, 3 min)	
5- Enzymatic labeling with Ab-HRP (30 min, shaking)	5- Washing step (2X, 3 min)	5- Washing step (2X, 3 min)				
6- Washing step (2X, 3min)						

7.4 RESULTS AND DISCUSSION

7.4.1 Evaluation of the optimal conditions for the phagomagnetic immunoassay based on biotin-P22

First of all, the biotin-P22 phagomagnetic immunoassay was performed following the same conditions than the previously developed phagotagging magneto immunoassay detailed described in Chapter 6, to compare the performance of the new strategy. In this case, the protocol was similar to that described in § 6.3.2, but the PMS step was performed for 20 min at 37ºC and without shaking, following the same conditions used in the phagotagging strategy.

The results obtained when using a 1/100 dilution of the biotin-P22 (corresponding to a phage titer of around 2 x 10^9 PFU mL^{-1}), 0.1 mg mL^{-1} of Strep-MP and a 1/2000 dilution of the Ab-HRP are presented in Figure 7.2, A. As can be seen, lower signals were obtained with this approach which used the biotin-P22 for PMS than the phagotagging strategy combined with the immunomagnetic separation (IMS) (Chapter 6).

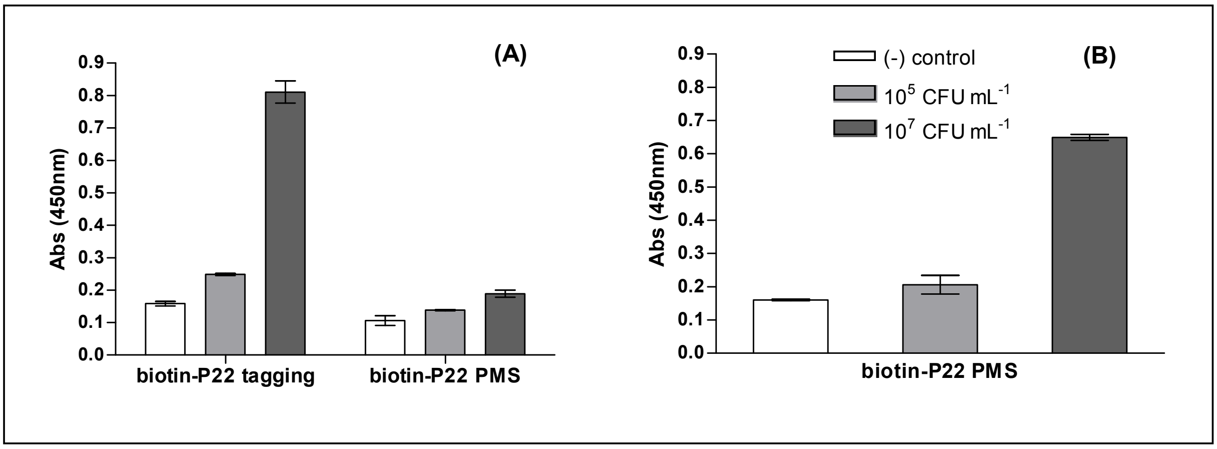

Figure 7.2 (A) Comparison of the results obtained using the biotin-P22 for bacteria tagging or for the PMS when performing the bacteria recognition step through 20 min incubation at 37ºC without shaking; and (B) results obtained after changing the bacteria recognition step to 20 min incubation under shaking followed by 20 min at 37ºC without agitation.

Analyzing the bacteria biorecognition conditions, the phages are in this case immobilized on a solid support and not free in solution, which could decrease considerably the flexibility of the biotin-P22 phages making the binding more difficult. The fact of performing the incubation step without agitation could make the particles settle on the bottom of the wells, hindering thus the bacteria biorecognition. As a result, it was decided to modify the assay by favoring the biorecognition during the PMS step, including a previous 20 min incubation step with shaking before the 20 min without agitation at 37ºC. As shown in Figure 7.2, B a significant improvement was achieved with this modification obtaining similar results than with the phagotagging strategy.

The next step was to optimize the biotin-P22 dilution and Strep-MP concentration for the preparation of the biotin-P22/MP conjugate. Three magnetic particles concentrations (0.1, 0.2 and 0.5 mg mL^{-1}) and three phage dilutions (1/100, 1/50 and 1/25, corresponding to 2 x 10^{9}, 4 x 10^{9} and 8 x 10^{9} PFU mL^{-1}) were assayed at a concentration of 10^{7} CFU mL^{-1} of *Salmonella* and compared to a negative control to determine the optimal combination of reagents concentration, as shown in Figure 7.3. Similar results were obtained in all tested concentrations, without any clear tendency when increasing neither the particles nor the phage concentration. Analyzing the signal to background ratios, the obtained values were also almost the same, although a very slight improvement can be seen at a biotin-P22 dilution of 1/100, which corresponds to a concentration of around 2 x 10^{9} PFU mL^{-1}.

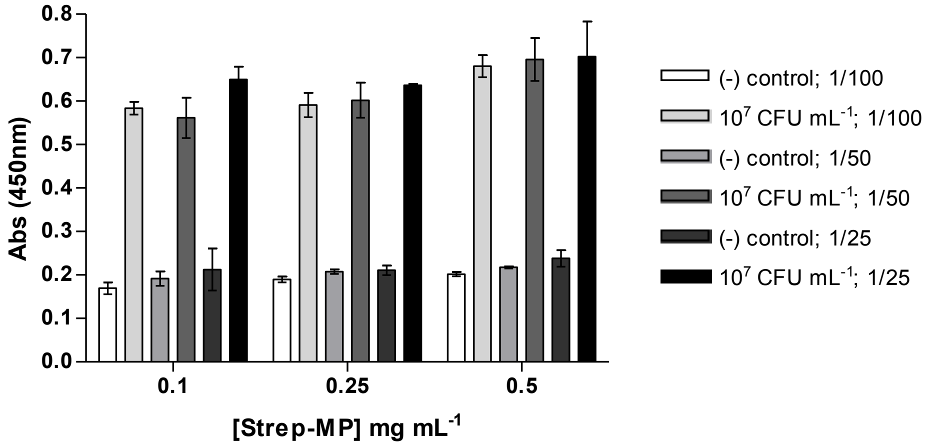

[Strep-MP] mg mL^{-1}	**0.1**			**0.25**			**0.5**		
CFU mL^{-1}	**1/100**	**1/50**	**1/25**	**1/100**	**1/50**	**1/25**	**1/100**	**1/50**	**1/25**
S/B ratio	3.44	2.93	3.06	3.12	2.90	3.02	3.37	3.20	2.95

Figure 7.3 Results obtained for the negative control and 10^{7} CFU mL^{-1} of *Salmonella* with different Strep-MP concentrations (0.1, 0.25 and 0.5 mg mL^{-1}) and biotin-P22 dilutions (1/100, 1/50 and 1/25) when the Ab-HRP dilution was set in 1/1000. The table below shows the signal to background (S/B) ratio for each combination of reagent concentrations. In all cases n=3.

According to the previous results, it was decided to set the Strep-MP concentration in 0.1 mg mL^{-1}, and test even lower biotin-P22 concentrations (1/200, 1/400 and 1/800, corresponding respectively to 1 x 10^9, 5 x 10^8 and 2.5 x 10^8 PFU mL^{-1}) using four different Ab-HRP dilutions (1/4000, 1/2000, 1/1000 and 1/500), and detecting the response at two bacteria concentrations (10^5 and 10^7 CFU mL^{-1}), as shown in Figure 7.4. The results demonstrated a raise in the signal when increasing the antibody concentration. However, an increase in the negative signals was also observed.

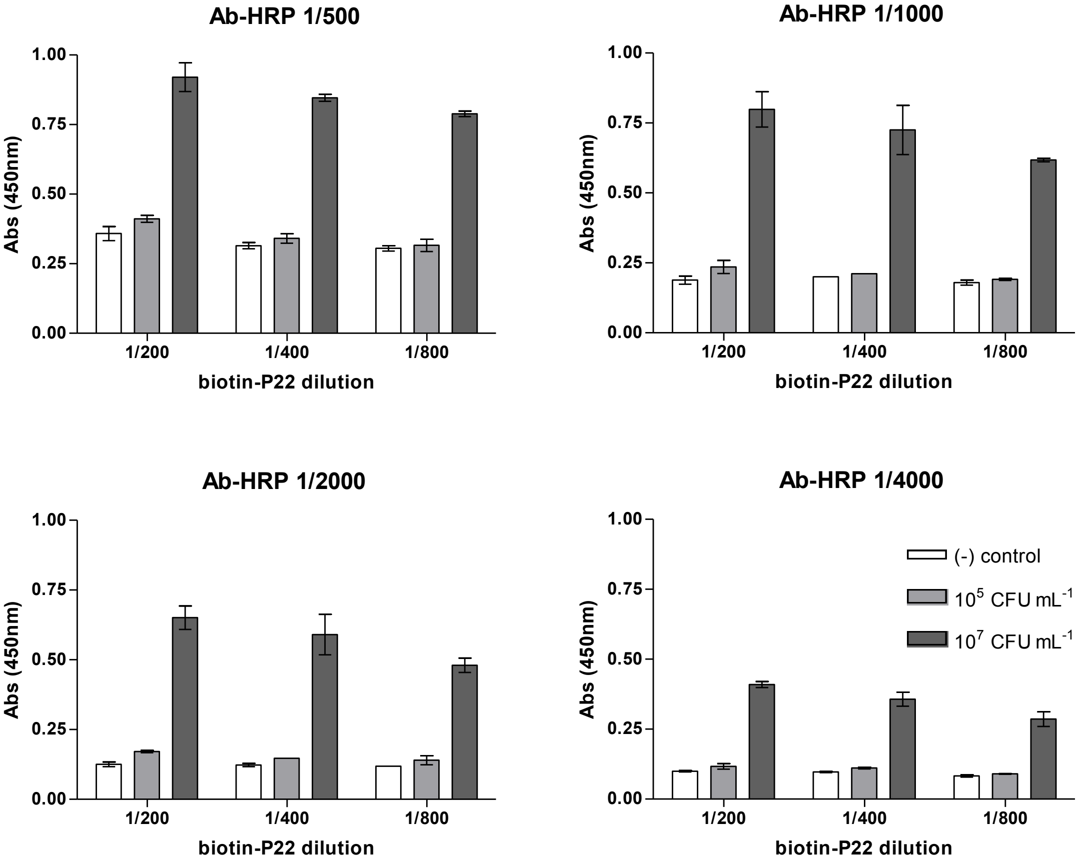

Figure 7.4 Optical signals obtained at different Ab-HRP and biotin-P22 concentrations when performing the biotin-P22 PMS based magneto immunoassay. The Strep-MP concentration was set in 0.1 mg mL^{-1} and the results of the negative control are compared with the signals obtained at 10^5 and 10^7 CFU mL^{-1} of *Salmonella*. In all cases *n*=3.

Analyzing the obtained signal to background ratios obtained at each Ab-HRP dilution shown in Table 7.2, it can be concluded that in general higher ratios were obtained when a biotin-P22 dilution of 1/200 was used in comparison with the lower phage concentrations tested (dilution 1/400 and 1/800). In contrast, in the case of the Ab-HRP, the results improved while decreasing the concentration until the dilution of 1/2000, and then at 1/4000 the response was reduced again. This results suggested that a compromise situation is needed, in which the concentration should not be as elevated to give a high nonspecific adsorption, but neither too low to cause an excessive reduction of the positive signals. Therefore, the optimal conditions were obtained at a 1/2000 dilution of the enzymatic label obtaining the highest signal to background ratios in that case, with values of 5.19 and 1.36 for 10^7 and 10^5 CFU mL^{-1} of *Salmonella*, respectively.

Table 7.2 Signal to background ratios obtained for the different reagent concentration combinations shown in Figure 7.4.

Signal to background ratio	**Ab-HRP**											
	1/500			**1/1000**			**1/2000**			**1/4000**		
biotin-P22	**1/200**	**1/400**	**1/800**	**1/200**	**1/400**	**1/800**	**1/200**	**1/400**	**1/800**	**1/200**	**1/400**	**1/800**
Salmonella **10^5 CFU mL^{-1}**	1.15	1.08	1.04	1.25	1.06	1.06	1.36	1.20	1.18	1.18	1.14	1.08
Salmonella **10^7 CFU mL^{-1}**	2.57	2.69	2.59	4.24	3.63	3.44	5.19	4.80	4.04	4.12	3.68	3.45

7.4.2 Study of the capturing of biotin-P22 on the Strep-MP

The immobilization efficiency of the biotin-P22 on the magnetic carrier was studied by reacting two different phage amounts with the Strep-MP and by evaluating the phage concentration before and after the phage attachment through the biotin-streptavidin reaction. In order to calculate the coupling efficiencies, the amount of phages in both the supernatant and the first wash, were compared with the initial amount before the immobilization. Following the previous described assay optimizations, 100 µL of Strep-MP at a concentration of 0.1 mg mL^{-1}, which corresponds to an amount of 7 x 10^5 magnetic particles, were reacted with 100 µL of the biotin-P22 diluted 1/200 and 1/1000 (1 x 10^9 and 2 x 10^8 PFU mL^{-1}, respectively), being the first one the optimal dilution above determined. The coupling efficiencies of the biotin-P22 on the magnetic particles were found to be 34.9 and 61.0 % for the 1/200 and 1/1000 dilution of the modified phages, respectively, as detailed shown in Table 7.3. Although a lower coupling percentage was obtained at the more concentrated biotin-P22 solution (1/200 dilution), the number of phages per magnetic particle was almost three times higher in this case when compared to the lower concentration (1/1000 dilution), obtaining an immobilization efficiency of nearly 21 in contrast to just 7.5 phages per magnetic particle. This fact demonstrated that a more efficient biotin-P22/MP conjugate was obtained at the 1/200 dilution, which is also in agreement with the results obtained by optical detection showed in detail in Table 7.2, suggesting also an improved bacteria capture capability at this concentration.

Table 7.3 Phage amounts before and after the immobilization and calculated phage amounts attached to the Strep-MP, coupling efficiencies and phages per magnetic particle at two biotin-P22 dilutions (1/200 and 1/1000).

	Phage stock dilution	
	1/200	**1/1000**
Phage amount (PFU)		
Initial	4.18 x 10^7	8.45 x 10^6
Supernatant	2.70 x 10^7	3.20 x 10^6
First wash	2.30 x 10^5	5.50 x 10^4
Attached to Strep-MP	1.46 x 10^7	5.19 x 10^6
Capture efficiency (%)	34.9	61.5
Phage/particle ratio	20.8	7.4

As mentioned in previous chapters, phages bind to specific receptors on the bacterial surface in order to inject the genetic material inside the bacteria. In the case of P22, six homotrimeric tailspike molecules (gp9) are part of the viral adhesion protein which specifically recognizes the O-antigenic repeating units of the cell surface lipopolysaccharide of *Salmonella*.[5] In order to evaluate the phage infectivity after the attachment to the magnetic carrier through the biotin-streptavidin reaction, the biotin-P22/MP conjugate was cultured by the double agar layered method. Using plaque enumeration it is not possible to establish the number of bacteriophages per magnetic particle since each modified magnetic particle is able to produce a unique plaque, regardless of how many phages are correctly oriented on its surface. Nevertheless, by plating the modified magnetic carriers it is possible to evaluate their global lytic activity. The phage amount obtained by plating the modified magnetic particles was 6.3 x 10^4 PFU and 2.0 x 10^4 PFU for a biotin-P22 dilution of 1/200 and 1/1000, respectively. When relating this results to the amount of particles added for the phages capture which was around 7 x 10^5, the biotin-P22/MP conjugate showed a very poor lytic activity in just 9 % and 3 % of the magnetic particles for 1/200 and 1/1000 dilution of the phages, respectively. These results could be explained by a blocking of the binding ability of the biotinylated phages through the immobilization on the solid support, or also by some degree of particle agglomeration during culturing which could affect the counting.

Finally, confocal microscopy was used to study the capture of the biotin-P22 phages on the Strep-MP surface. The images in Figure 7.5 show the fluorescence background in a sample containing the magnetic particles without the biotin-P22 (A) and the Strep-

MP after capturing the biotin-P22 through the streptavidin-biotin interaction (B). For the visualization of the samples, the fluorescence reporter Strep-Cy5 was added after the phage capture and subsequent washing steps. Given the high biotinylation efficiencies achieved when preparing the biotinylated conjugates (previously described in Chapter 5), many biotin molecules were attached per phage particle being thus suitable to be recognized by the fluorescent labeled streptavidin.

As can be seen in Figure 7.5, A the nonspecific adsorption of the fluorescent label was negligible in the absence of the biotin-P22 in the sample, while Figure 7.5, B shows a red labeling in the case of the biotin-P22/MP conjugate. This result confirmed the immobilization of the biotin-P22 on the Strep-MP and the subsequent recognition by the Strep-Cy5 due to the presence of multiple biotin molecules attached per P22 phage. The Figure shows also the pattern of phage immobilization on the magnetic carriers. Each red dot can be ascribed to a phage unit immobilized on the magnetic carrier, showing a quite scarce covering, consistent with the phage counting of 20 phages/ MP.

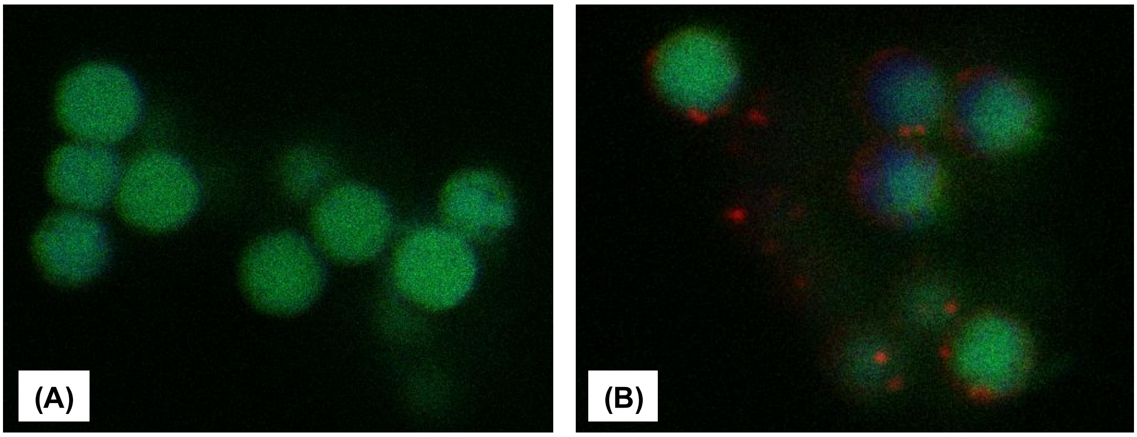

Figure 7.5 Confocal microscopy images of the negative control, corresponding to the Strep-MP without biotin-P22 (A), and immobilized biotin-P22 on the Strep-MP labeled with streptavidin-Cy5 (B). In green the magnetic particles (autofluorescent), in blue the bacteria stained with Hoechst 33342 and in red the biotin-P22 labeled with Strep-Cy5.

7.4.3 Evaluation of the biotin-P22 phagomagnetic separation of Salmonella by SEM and conventional culture method

The PMS of the bacteria by the biotin-P22/MP conjugate was visualized by SEM microscopy. Figure 7.6, A shows a negative control without the modified phages immobilized on the Strep-MP, while Figure 7.6, B is a zoom in the Strep-MP control. No bacteria nonspecific captured on the Strep-MP were observed in the absence of the immobilized phages. On the other hand, when the biotin-P22 were attached to the magnetic carrier, the PMS was able to take place and, as a result, bacteria cells were observed captured by the biotin-P22/MP conjugate, as shown in Figure 7.6, C and D. Moreover, analyzing in more detail the Figure 7.6, D, some nanoparticles were observed on the binding site to the bacterium at the limit of resolution of the technique, which can be ascribed to the biotin-P22 immobilized on the Strep-MP and recognizing the bacteria receptors. These particles are not present in the Strep-MP surface of the negative control shown in 7.6, B.

A confirmation of the biotin-P22 recognition capability towards *Salmonella* was thus achieved. However, the binding efficiency seemed to be lower than the previous developed method presented in Chapter 6, since in general lower amounts of *Salmonella* were observed in the prepared samples, and also smaller particle-bacteria conglomerates, suggesting lower capture ability.

The capability for *Salmonella* capturing of the biotin-P22/MP conjugate was also analyzed by conventional culturing method. For this evaluation, the PMS of a bacteria sample was performed and the initial bacteria amount added to the particles was compared with the counting in the supernatant after the capture. A bacterial solution with a concentration of 2.1 x 10^5 CFU mL^{-1} was prepared in LB broth and the PMS of *Salmonella* Typhimurium LT2 in this sample was performed as described in § 7.3.4, plating afterwards 50 µL of the corresponding supernatant in LB for 18-24 h at 37°C. Bacterial colonies were enumerated in the initial suspension and the supernatant by plate counting, and the number of captured cells was estimated by subtraction for the efficiency calculation obtaining a result of 22.6 %, which is fairly below the capture efficiency obtained by immunomagnetic separation.[6] One possible explanation could be once again the formation of the aggregates produced by several bacterium cells but growing at a unique colony point in the agar plate or, for instance, the infection by some lytic active phages which could be causing under growing of the attached bacteria. Furthermore, if some excess of biotin was present in the used biotin-P22 stock solutions, it could interfere in the immobilization efficiency of the phages on the Strep-MP and also in the subsequent bacteria capturing when performing the PMS step.

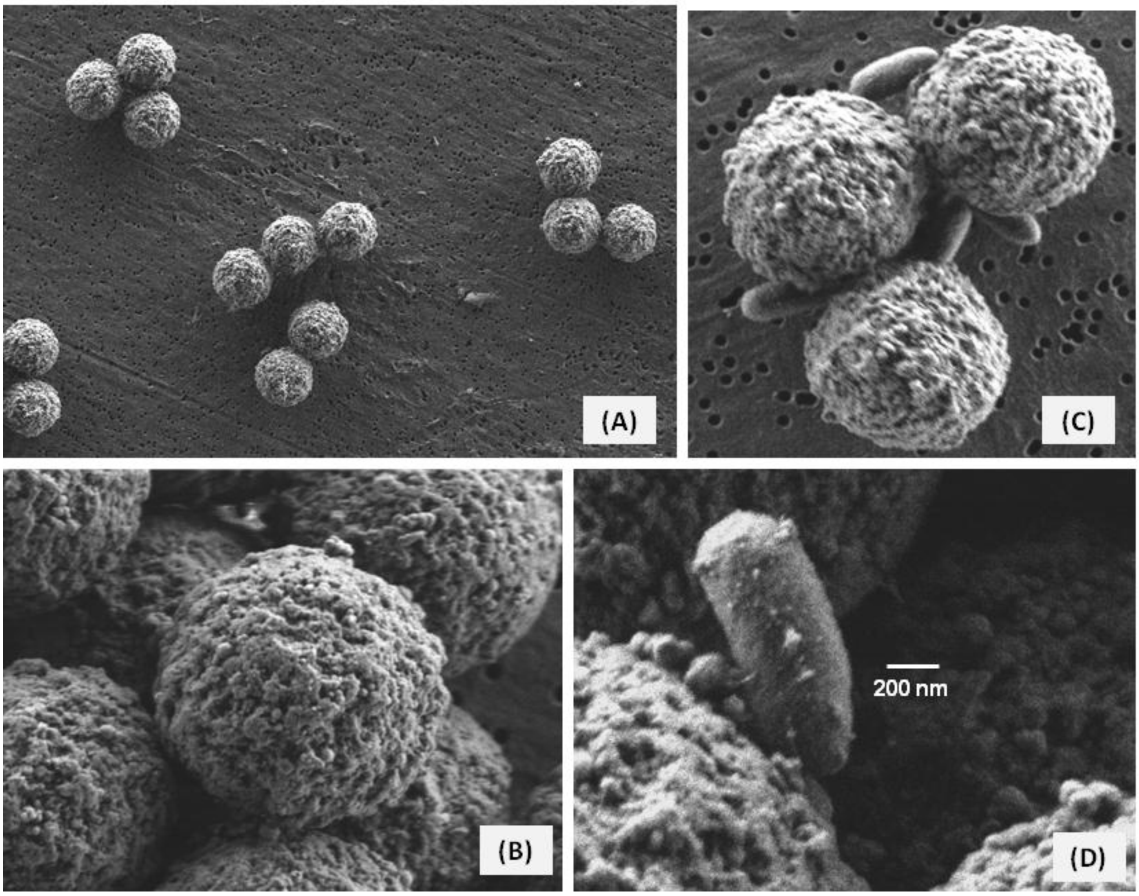

Figure 7.6 Evaluation by SEM of the PMS through the biotin-P22/MP conjugate using a *Salmonella* concentration of 2.3 x 10^7 CFU mL^{-1} (C and D). The biotin-P22-MP was prepared by reacting 8 x 10^8 PFU of biotin-P22 with 7 x 10^5 (10 µg) of Strep-MP (2.8 µm). Negative controls without the biotin-P22 are also shown (A and B). In all cases, identical acceleration voltage (15 kV) was used.

7.4.4 Biotin-P22 phagomagnetic immunoassay for the optical detection of *Salmonella* in milk

The optimal protocol was evaluated by following different procedures and comparing the responses at two different bacteria concentrations (10^5 and 10^7 CFU mL^{-1}) using the biotin-P22 PMS based magneto immunoassay. Seven different strategies were assayed by varying the number and order of the incubation and washing steps as previously explained in Table 7.1 (§ 7.3.5) and schematized in Figure 7.7 below.

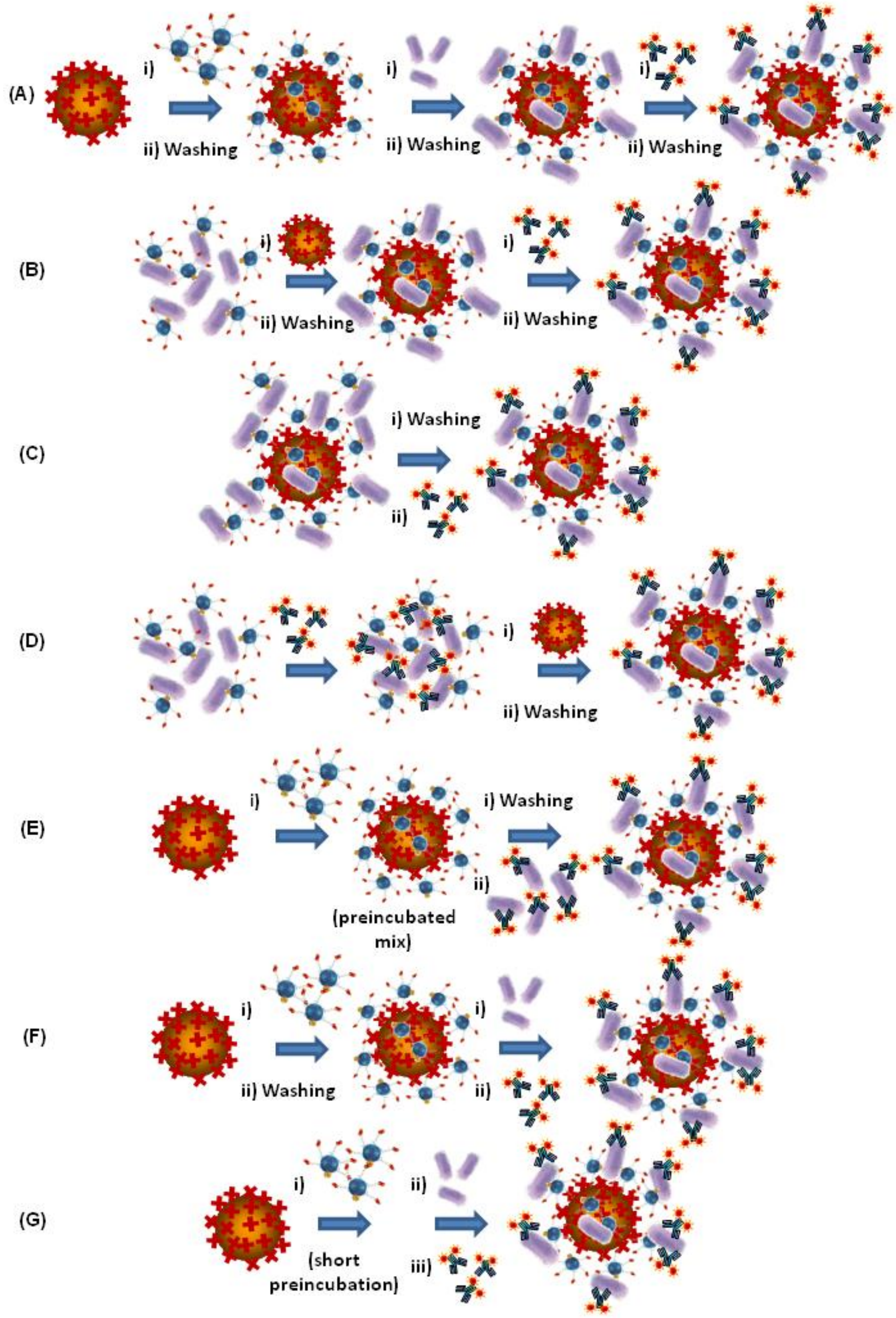
(A)
i)
ii) Washing
i)
ii) Washing
i)
ii) Washing
(B)
i)
ii) Washing
i)
ii) Washing
(C)
i) Washing
ii)
(D)
i)
ii) Washing
(E)
i)
i) Washing
ii)
(preincubated mix)
(F)
i)
ii) Washing
i)
ii)
(G)
i)
(short preincubation)
ii)
iii)

Figure 7.7 Schematic representation of the different procedures applied for the optimization of the biotin-P22 PMS based magneto immunoassay protocol. The seven strategies are detailed in Table 7.1: (A) stepwise protocol; (B) preincubation of *Salmonella* with biotin-P22; (C) phage capture and PMS in one step; (D) Strep-MP addition as final step; (E) preincubation of *Salmonella* with Ab-HRP; (F) simultaneous addition of bacteria and Ab-HRP; and (G) addition of all reagents in one step.

The results are compared in Figure 7.8. Very low signals were obtained with the strategies D and G, which correspond to the addition of the magnetic particles as the final step and de simultaneous addition of all reagents, respectively. This behavior suggest that the joining together of incubation steps without any washings in between is unfavorable for the assay performance, possibly because one of the advantageous features of the magnetic particles, specifically the improved washing steps, is missed using these strategies.

On the other hand, when analyzing the other four strategies by comparing the signal to background ratios (Table 7.4), very low differences between the signal at a bacteria concentration of 10^5 CFU mL^{-1} and the negative control were observed in the cases of preincubating some of the reagents, as much the bacteria with the phage (strategy B) as the bacteria with the antibodies (strategy E). In addition, similar results were obtained in the case of joining the phage capture with the PMS step (Strategy C), although a better response was acquired at the higher bacteria concentration. Finally, strategies A and F were those showing the better performances, being in fact the strategy F just a shortening of the step by step protocol in strategy A, in which the bacteria and Ab-HRP addition was performed simultaneously. Nevertheless, the highest signal to background ratios at both assayed bacteria concentrations were obtained with the strategy A by performing the protocol step by step, with each incubation step carried out separately and with washings in between.

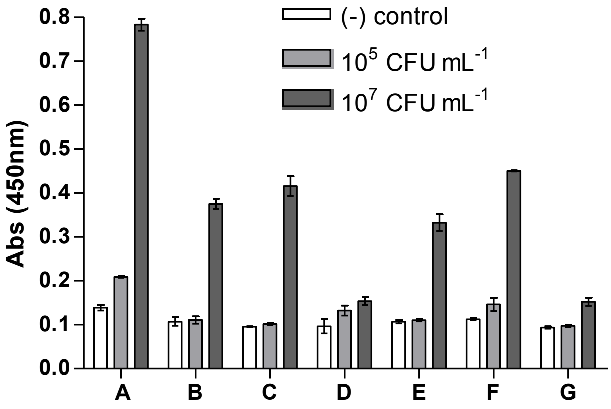

Figure 7.8 Optimization of the protocol for the biotin-P22 PMS based magneto immunoassay. The strategies A-G correspond to the seven protocols described in Table 7.1 and depicted in Figure 7.7. The experimental conditions were the previously optimized: a Strep-MP concentration of 0.1 mg mL^{-1}, a biotin-P22 solution at a 1/200 dilution and an Ab-HRP dilution 1/2000. In all cases, n=3.

Table 7.4 Signal to nonspecific adsorption ratios for the seven different strategies tested.

Signal to background ratio	**Strategy**						
[*Salmonella*] CFU mL^{-1}	**A**	**B**	**C**	**D**	**E**	**F**	**G**
10^5	1.51	1.03	1.06	1.37	1.03	1.30	1.03
10^7	5.56	3.50	4.34	1.59	3.11	4.00	1.63

Afterwards, the response towards the bacteria concentration and the matrix effect were evaluated by preparing two calibration curves with *Salmonella* artificially inoculated and serially diluted in a concentration range from 3.3 x 10^1 to 3.3 x 10^8 CFU mL^{-1} in LB broth and in milk diluted 1/10 in LB. The results obtained for both matrixes are shown in Figure 7.9.

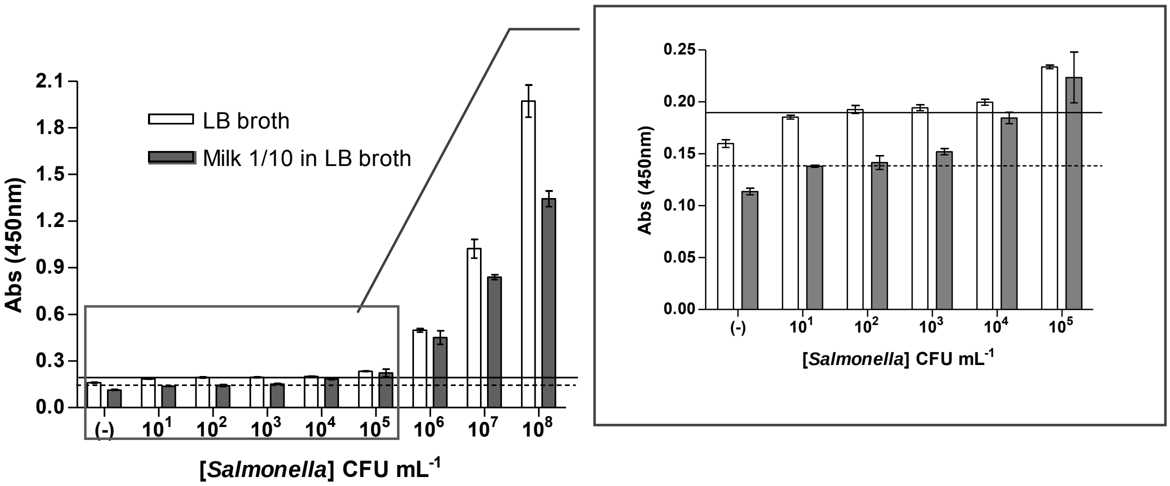

Figure 7.9 Calibration curves obtained in LB broth (white bars) and milk diluted 1/10 (grey bars), showing the signals by increasing the concentration of *Salmonella* from 3.3 ×10^1 to 3.3 × 10^8 CFU mL^{-1}. The inset in the right panel shows a zoom in the lower bacteria concentration range. The reagent concentrations were as follows: 0.1 mg mL^{-1} Strep-MP, biotin-P22 diluted 1/200 (1 x 10^9 PFU mL^{-1}) and Ab-HRP diluted 1/1000. The cut-off values in LB broth and milk are represented in both cases through a solid and dotted line, respectively and in all cases, n=3, except for the 0 CFU mL^{-1} negative control (n=10).

As can be seen in the figure, a signal drop was observed in the presence of milk, indicating some degree of matrix effect throughout the whole calibration curve which was more significant at high bacteria concentration, similar to the behavior observed in the methods based on bacteria tagging explained in Chapter 6. However, the effect seemed to be more pronounced when using the biotin-P22 phagomagnetic immunoassay. This could be explained by the fact that in the current approach the matrix is present during the phage recognition step, which is principally occurring when incubating without agitation and hence the interference of the sample components would be higher than in the case of shaking conditions. In addition, the presence of the biotin-P22 immobilized on the solid support also reduces the flexibility of the modified phages in comparison to the previously developed approaches based on phage tagging. Thus, the availability of the tailspike proteins for the bacteria recognition will be more affected by the presence of interfering matrix components.

For the cut-off and LOD values analysis, 10 negative samples (0 CFU mL^{-1}) were recorded, obtaining a mean value of 0.157 and 0.112 absorbance units (a.u.) with a standard deviation of 0.0105 and 0.0084 for the assay performed in LB broth and in milk diluted 1/10 in LB, respectively. The signals corresponding to the LOD, or cut-off values, were then extracted with a one-tailed *t* test at a 99 % confidence level as already explained in Chapter 6 (§ 6.4.4) obtaining a result of 0.189 (solid line) and 0.138 a.u (dotted line) in LB and in milk, respectively. Thus, the third point of the curve was above the cut-off value in both matrixes (as shown in Figure 7.9), which corresponds to a concentration in the order of 10^{3} CFU mL^{-1} *Salmonella*. The LOD values were finally calculated by interpolation of the cut-off signals in the sigmoidal dose response curve (Figure 7.10 and Table 7.5), obtaining a result of 8.51 x 10^{3} CFU mL^{-1} in LB broth and 2.40 x 10^{3} CFU mL^{-1} in milk. These values are one order bigger than the ones obtained with the phagotagging magneto immunoassay, indicating thus a poorer performance of the biotin-P22 phagotagging immunoassay. More precisely, the achieved limits of detection were 47 times and 23 times higher in LB and milk, respectively.

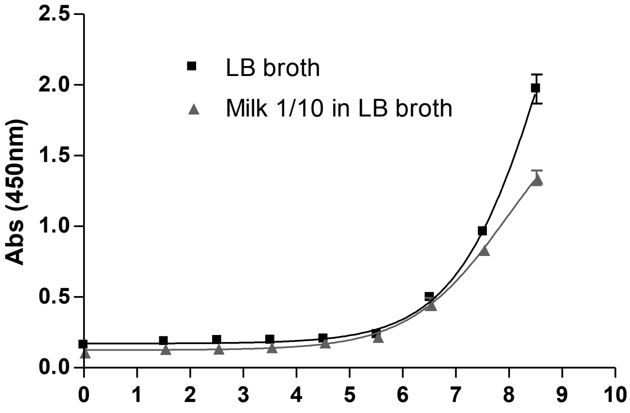

Figure 7.10 Sigmoidal dose response curves obtained in both matrixes after plotting the signal *vs*. the logarithm of *Salmonella* concentration.

The detailed results of the curves parameters are shown in Table 7.5, demonstrating an acceptable fitting in both matrixes (r^2 = 0.9949 in LB and 0.9921 in milk). However, when comparing the obtained results with the previous phagotagging method, the poorer analytical performance became also evident, since lower sensitivity was demonstrated through the inferior slopes and also worse reproducibility of the measurements were indicated by the higher coefficients of variation (% CV).

Table 7.5 Parameters of the sigmoidal dose-response curves obtained with the biotin-P22 biosorbent based magneto-immunoassay in LB broth and milk.

	CV (%) for (-) control	CV (%) at 10^8 CFU mL^{-1}	R^2	Slope	Cut-off	LOD (CFU mL^{-1})
LB broth	6.7	10.3	0,9949	0,4877	0,1888	8510
Milk 1/10 in LB broth	7.5	10.4	0,9921	0,4734	0,1377	2397

Moreover, when comparing the signal to background ratio obtained at the different *Salmonella* concentrations with the same results achieved using the phagotagging strategy lower ratios were acquired throughout almost the whole calibration curves as shown in Table 7.6. These results confirmed once again the lower sensitivity of the biotin-P22 phagomagnetic immunoassay.

Table 7.6 Comparison of the signal to background ratios obtained in both matrixes (LB broth and milk diluted 1/10 in LB) throughout the calibration curves using the biotin-P22 PMS based approach and phagotagging magneto immunoassay.

Signal to background ratio	**Biotin-P22 PMS**		**Biotin-P22 tagging**	
[*Salmonella*] CFU mL^{-1}	**LB**	**Milk**	**LB**	**Milk**
3.3 x 10^1	1,16	1,21	1,14	1,12
3.3 x 10^2	1,21	1,24	1,42	1,32
3.3 x 10^3	1,22	1,34	1,58	1,45
3.3 x 10^4	1,25	1,62	1,86	1,61
3.3 x 10^5	1,46	1,82	2,61	2,34
3.3 x 10^6	3,11	3,59	5,86	4,22
3.3 x 10^7	6,40	7,38	7,62	6,23
3.3 x 10^8	12,33	11,81	9,52	7,07

An exception seemed to occur at the higher bacteria concentrations, since at 10^7 CFU mL^{-1} the signals turned very similar for both strategies and at 10^8 CFU mL^{-1} the tendency was even inverted. This behavior could be explained by a higher aggregation at very high bacteria concentration in the case of the strategies based on phage tagging (Chapter 6), due to the multivalency of the different reagents: magnetic particles, bacteria, as well as the Strep-HRP label. In the case of the biotin-P22 PMS the label is Ab-HRP which is not able to react simultaneously with more than one bacteria, leading thus to less agglomeration.

Despite the worse analytical performance of the biotin-P22 phagomagnetic immunoassay in comparison to the phagotagging strategy, it was decided to evaluate the capability of the system to detect the target bacteria at a concentration of around 1 CFU in 25 mL of milk in order to follow the established food regulations. With this aim, a preenrichment step was performed overnight (16 h) in LB as a nonselective broth at 37 ºC. In this procedure the samples were diluted 1/10 in the LB broth. Afterwards, the spiked milk sample, a 10X positive control and a negative control were assayed using the biotin-P22 phagomagnetic immunoassay, obtaining the results shown in Figure 7.11. After the exact concentration of the overnight culture used to contaminate the milk samples was determined by classical culture method, the bacteria concentration in the positive control was found to be 12 CFU in 25 mL, while the spiked sample contained around 1.2 CFU in 25 mL milk.

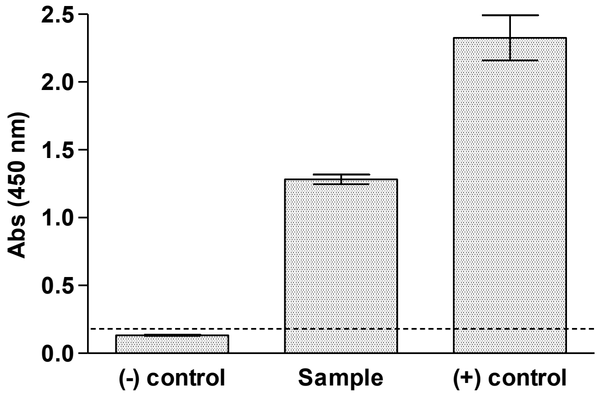

Figure 7.11 Results obtained after 16 h preenrichment when the spiked milk sample, the negative control and positive control were assayed using the biotin-P22 phagomagnetic immunoassay. The experimental conditions were the same explained in Figure 7.9 and in all cases n = 3, with exception of the negative control for which n = 6. The dotted line represents the cut-off value.

The bacteria amounts in the sample, the positive and the negative controls after the 16 h preenrichment were also determined by microbiological culturing, obtaining concentrations of 1.4 x 10^8 CFU mL^{-1}, 5.2 x 10^8 CFU mL^{-1} and 0 CFU mL^{-1}, respectively. These amounts of bacteria were thus consistent with the very high optical signals obtained for the sample as well as the positive control using the phagomagnetic immunoassay, as shown in the Figure. Moreover, the signal of the negative control was below the cut-off value as expected.

As a result, it should be highlighted that although the lower detection limits obtained with this strategy, the challenging bacteria limit of 1 CFU in 25 mL of milk sample could be achieved after performing an overnight preenrichment.

7.4.5 Specificity study

The specificity of the system was evaluated by performing the biotin-P22 phagomagnetic immunoassay in samples artificially inoculated with 10^6 and 10^7 CFU mL^{-1} of both *Escherichia coli* and *Salmonella*, as well as a negative control (Figure 7.11).

Although the signal obtained at 10^6 CFU mL^{-1} of the non-target gram negative bacteria was almost the same than the background adsorption, the result at 10^7 CFU mL^{-1} was above the cut-off value, indicating that at this high concentration of *E.coli* a false positive could take place. The slight raise in the signal observed when increasing the *E.coli* concentration suggested the presence of some degree of cross reaction and thus, a poorer specificity of this strategy when compared to the phagotagging method.

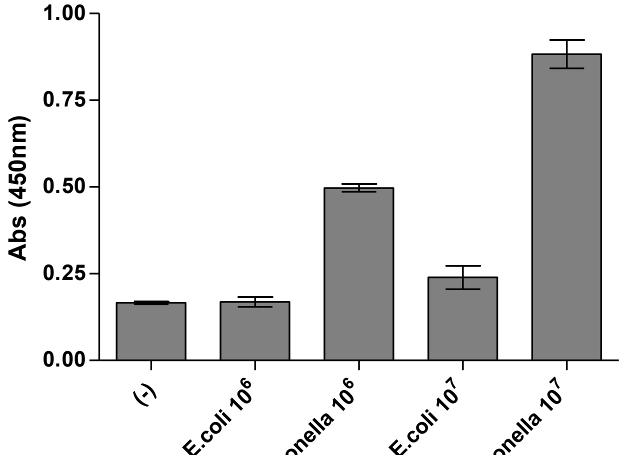

Figure 7.11 Specificity study of the biotin-P22 biosorbent based magneto immunoassay. The bars show the optical signals for the samples artificially inoculated, respectively, with: 0 $CFUmL^{-1}$ (negative control), 2.2 × 10^6 CFU mL^{-1} *E. coli*, 2.8 × 10^6 CFU mL^{-1} *Salmonella*, 2.5 × 10^7 CFU mL^{-1} *E. coli* and 2.6 × 10^7 CFU mL^{-1} of *Salmonella.* The error bars show the standard deviation for n=3.

This behavior could be ascribed to some nonspecific adsorption of the non-target bacteria and/or the enzymatic label to the streptavidin-modified magnetic particles used as solid support. Another possible explanation could be the presence to some extent of biotin in the *E.coli* bacteria, given by the biotin carboxyl carrier protein (BCCP) subunit present in the acetyl-CoA carboxylase enzyme responsible for the fatty acids synthesis in these bacteria.[7] Thus, the biotin covalently bound as a cofactor to the BCCP, could also be recognized by still available streptavidin molecules present on the solid support surface giving place to some degree of nonspecific bacteria capturing. If this would be the case, a slight cross-reactivity of the anti-*Salmonella* polyclonal antibody used as optical reporter should simultaneously occur.

7.5 CONCLUSIONS

The presented strategy based on the phagomagnetic immunoassay using biotin-P22 immobilized on Strep-MP coupled to immunological labeling allowed the detection of *Salmonella*. The capturing of the phages on the magnetic particles to form the biotin-P22/MP conjugates and the subsequent *Salmonella* biorecognition capability was demonstrated using microscopy tools, in particular confocal fluorescence microscopy and SEM, respectively. Moreover, the obtained results were also confirmed by classical culture methods.

Good limits of detection were achieved in both studied matrixes using the biotin-P22 phagomagnetic immunoassay, being able to detect 8.51 x 10^3 CFU mL^{-1} of *Salmonella* in LB broth and 2.40 x 10^3 CFU mL^{-1} in milk. These results were of the same order than previous reported assays based on immunomagnetic separation[6], achieving in the phagomagnetic strategy even 3 times lower detection limits in the case of the milk matrix, although the lower bacteria capturing efficiencies. Moreover, the use of phages as a biorecognition element has the advantage of the outstanding stability, which makes the use of phages more appropriate for the application in food samples analysis, which matrixes at times provide unfriendly media for the less stable antibodies.

However, as already discussed along the previous sections, the analytical performance of the biotin-P22 based phagomagnetic immunoassay was to a great extent underneath the results obtained by the preceding strategy based on phage tagging, in terms of sensitivity, reproducibility, as well as specificity.

Regarding the specificity of the system, a slight cross-reaction was observed at a concentration of 10^7 CFU mL^{-1} of *E.coli*, which did not occur in the phagotagging strategy. Nevertheless, food regulations in dairy products for these gram-negative bacteria establish a maximum of two of five samples contaminated with 10^4 to 10^5 CFU mL^{-1} in the more older regulations (Real Decreto 1679/1994, BOE 24-09-94), while more up-to-date regulations establish a maximum between 10^2 and 10^3 CFU mL^{-1} (REGLAMENTO (CE) 2073/2005 DE LA COMISIÓN de 15 de noviembre de 2005). Thus, a concentration of 10^7 of *E.coli* would be really excessive and, in fact, this cross-reactivity would not be a problem in the majority of food control studies. As a result, it would only affect in the case of processing other kind of samples containing a very high accompanying microflora.

Due to the worse results obtained in comparison to the phagotagging approach, instead of performing further studies for the development of a biosensor with the biotin-P22/MP conjugates, another strategy for phagomagnetic separation based on covalently immobilized phages was evaluated, as explained in the next chapter.

7.6 REFERENCES

(1) Velusamy, V.; Arshak, K.; Korostynska, O.; Oliwa, K.; Adley, C. *Biotechnology Advances* **2009**, *28*, 232–54.

(2) Van Dorst, B.; Mehta, J.; Bekaert, K.; Rouah-Martin, E.; De Coen, W.; Dubruel, P.; Blust, R.; Robbens, J. *Biosensors & Bioelectronics* **2010**, *26*, 1178–94.

(3) Mao, C.; Liu, A.; Cao, B. *Angew Chem Int Ed Engl.* **2009**, *48*, 6790–6810.

(4) Sun, W.; Brovko, L.; Griffiths, M. *Journal of Industrial Microbiology & Biotechnology* **2001**, *27*, 126–128.

(5) Steinbacher, S.; Miller, S.; Baxa, U.; Budisa, N.; Weintraub, A.; Seckler, R.; Huber, R. *Journal of Molecular Biology* **1997**, *267*, 865–880.

(6) Liébana, S.; Lermo, A.; Campoy, S.; Cortés, M. P.; Alegret, S.; Pividori, M. I. *Biosensors & Bioelectronics* **2009**, *25*, 510–3.

(7) Choi-Rhee, E.; Cronan, J. E. *The Journal of biological chemistry* **2003**, *278*, 30806–30812.

CHAPTER 8

BACTERIOPHAGE COVALENT IMMOBILIZATION ON MAGNETIC MICRO AND NANOPARTICLES FOR PHAGOMAGNETIC SEPARATION AND DETECTION OF PATHOGENIC BACTERIA

8.1 INTRODUCTION

The inherent ability of phages to bind their bacterial target has been exploited to capture the bacteria onto different kind of surfaces and transducers, using phages previously attached on solid supports. Different immobilization strategies have been reported on native phages, for instance, physical adsorption,[1–3] ionic interaction,[4] and chemical attachment between reactive groups in the native phage capsid proteins and chemical groups on the solid support.[5–8] The interaction between high affinity molecules and peptides expressed in the capsid through phage display techniques were also described.[9,10] This variety of methods can be applied not only to the use of wild-type phages, but also to engineered phages genetically manipulated to display specific peptides or to carry selected reporting genes, and purified phage's receptor binding proteins- the tailspike proteins, which determine the phage host specificity. Moreover, this recognition elements can be coupled with different transduction platforms such as optical (e.g. SPR), micromechanical (e.g. QCM) and electrochemical biosensors (e.g. amperometric), as extensively analyzed in previous reviews.[11–13]

This chapter addresses the use of P22 phages for the biorecognition and pre-concentration of pathogenic bacteria when they are conjugated with magnetic micro and nanocarriers. Phages were covalently immobilized throughout the amine moieties present in their capsid proteins to tosylactivated magnetic microparticles (P22-MP) or carboxylic nanoparticles (P22-nMP). The phage-modified magnetic carriers were then used for the pre-concentration of *Salmonella* followed by the rapid detection of the whole bacterial cells by a specific labeled antibody, as optical or electrochemical reporter.

The coupling of phages with magnetic particles provides many advantageous features for food safety applications, and as already mentioned the exceptional stability of phages in a wide range of conditions makes them promising alternative candidates for *in situ* testing of food samples. The phagomagnetic separation (PMS) was recently reported in our group but using inactivated phages and coupled with the double-tagging polymerase chain reaction (PCR) amplification of the DNA of the captured bacteria followed by electrochemical magneto-genosensing.[14] Here, the aim was to simplify the analytical procedure and to avoid the complex and more interference susceptible PCR which has high technical requirements.

The next sections describe the preparation of the hybrid phage modified magnetic particle conjugates for bacteria capturing in a PMS step, and their optimization and characterization by Scanning Electron Microscopy (SEM) technique. The analytical performance of the micro and nanoparticles for the PMS was also studied and compared in terms of LODs, specificity and sensitivity. Moreover, the development of the PMS coupled with an electrochemical immunosensing approach was also evaluated, besides the phagomagnetic separation capability of the developed hybrid P22-MP material. Finally, pre-enrichment studies were carried out in order to determine the time that is required for the detection of 1 CFU of *Salmonella* in 25 mL of milk, in order to fulfill the legislation.

8.2. AIM OF THE CHAPTER

This chapter addresses the covalent immobilization of bacteriophages on magnetic micro and nanoparticles for phagomagnetic separation of bacteria and further detection with an optical magneto immunoassay as well as with an electrochemical magneto immunosensing approach, taking the P22 phage as a model for *Salmonella* detection.

The specific objectives of this chapter were:

- To develop phage-based solid supports by the covalent immobilization of the P22 bacteriophage on micro- and nanostructured magnetic particles.
- To evaluate the coupling efficiency and establish the optimal phage/particle ratio.
- To analyze the phage orientation for the bacteria biorecognition by microbiological techniques (double agar layer technique) and SEM analysis.
- To apply the developed phage-modified hybrid magnetic particles in phagomagnetic immunoassays with optical detection.
- To compare the analytical performance of micro and nanostructured magnetic carriers.
- To analyze the phagomagnetic separation of *Salmonella* by conventional culture methods and confocal microscopy.
- To assess the phagomagnetic immunoassay coupled with electrochemical detection for the screen-out of bacteria in milk samples.
- To study the sample pre-enrichment requirements for the detection of *Salmonella* in contaminated milk accordingly to the current food regulations.

8.3 EXPERIMENTAL SECTION

8.3.1 Materials

The bacteria *Salmonella enterica* serovar Typhimurium LT2 and *Escherichia coli* K12 strains were routinely grown in Luria Bertani (LB) broth or on LB agar plates for 18 h at 37ºC. The preparation of the phage lysates, as well as their titration and purification using CsCl are described in Chapter 5 (§§ 5.3.1.1 and 5.3.1.2, respectively), while the materials used for the phage lysate preparation are the same detailed in Chapter 6.

Tosylactivated magnetic particles (MP) (Dynabeads M-280, product n° 142.03) were purchased from Life Technologies, Invitrogen Dynal AS (Oslo, Norway) and Carboxyl-Adembeads (nMP) (product nº 0213) were obtained from Ademtech SA (Pessac France).

Anti-*Salmonella* antibodies conjugated to HRP (product nº ab20771) and unlabeled mouse monoclonal anti-*Salmonella* antibodies (product nº ab8274) were purchased from Abcam (Cambridge, UK). Bovine serum albumin (BSA), *N*-(3-Dimethylaminopropyl)-*N'*-ethylcarbodiimide hydrochloride (EDC), *N*-hydroxysulfosuccinimide (sulfo-NHS) and Tween 20 were supplied by Sigma-Aldrich.

Regarding the reagents used for the visualization of the system by confocal microscopy, the Hoechst 33342 and the anti-mouse IgG antibodies labeled with cyanine 5 dye (anti IgG-Cy5) were purchased from Life Technologies (product nº H-3570 and M-35011, respectively).

All buffer solutions were prepared with milli-Q water (Millipore Inc., Ω = 18 MΩ cm) and all reagents were of the highest available grade, supplied from Sigma or Merck.

The composition of the solutions used for the immobilization on tosylactivated particles was: coating buffer (0.1 mol L^{-1} sodium borate, pH 8.5); ammonium sulfate (3 mol L^{-1} prepared in coating buffer), blocking buffer (0.01 mol L^{-1} sodium phosphate, 0.15 mol L^{-1} NaCl, 0.5 % w/v BSA, pH 7.4), washing buffer (0.01 mol L^{-1} sodium phosphate, 0.15 mol L^{-1} NaCl, 0.1 % w/v BSA, pH 7.2); and storage buffer (0.01 mol L^{-1} sodium phosphate, 0.15 mol L^{-1} NaCl, 0.1 % w/v BSA, 0.02 % (w/v) sodium azide, pH 7.4).

For the immobilization on magnetic nanoparticles the following solutions were used: MES activation buffer (0.1 M MES buffered saline, 0.9 % (w/v) sodium chloride, pH

5.5), PBS coating buffer (0.1 M PBS, 0.15 M NaCl, pH 7.2) and the commercial storage buffer shipped with the particles adding 10 mM $MgSO_4$.

The solutions used for the SEM samples preparation were: fixation buffer (2.5 % v/v glutaraldehyde in 0.1 mol L^{-1} sodium phosphate, pH 7.4) and post-fixation buffer (1 % w/v OsO_4, 0.1 mol L^{-1} sodium phosphate, pH 7.4).

The reagents and buffer solutions used for the magneto immunoassays as well as the optical and electrochemical measurements were the same as previously described in Chapter 5.

Finally, the instrumentation used for the incubation and washing steps, the magnetic separations, as well as the optical and electrochemical detection are detailed in Chapter 4 (§ 4.3.1.1), while the bacterial strains and phage lysate preparation and purification are explained in Chapter 5 (§ 5.2.1).

8.3.2 Covalent immobilization of bacteriophages on magnetic micro and nanocarriers

P22 phages were covalently coupled to 2.8 µm tosylactivated magnetic particles (P22-MP) as well as to 300 nm carboxylic magnetic nanoparticles (P22-nMP) through the amine moieties of their capsid proteins (gp5). In both cases 150 µL of a purified phage stock solution with a concentration in the order of 10^{11} plaque-forming units (PFU) mL^{-1} was added to 1 mg magnetic particles or nanoparticles and the results were compared. In the case of the tosylactivated MP no pre-activation step was needed, while when using the nMP a previous step was required in which EDC and sulfo-NHS were added in order to activate the carboxylic groups of the magnetic particles. A schematic representation of both immobilization procedures is shown in Figure 8.1. Before each assay, the required amount of P22-MP or P22-nMP were washed twice with PBST and resuspended in the appropriate volume in order to obtain the desired concentration of magnetic particles.

8.3.2.1 Immobilization on tosylactivated magnetic particles

In this case, a volume of 35 µL of tosyl-modified MP (30 mg mL^{-1}, 2 x 10^9 magnetic particles mL^{-1}) was washed twice with 1 mL of borate buffer. Afterwards, 150 µL of the purified P22 phage solution followed by 100 µL of $(NH_4)_2SO_4$ were added and mixed properly. The bacteriophage titer was previously determined by serial dilutions plating onto Luria Bertani (LB) plates using the double agar layered method. The MPs were incubated a total of 17 h at 37ºC under shaking. During this time, the amine moieties of the phage reacted with the tosylactivated groups on the MPs surface as shown in Figure 8.1, A. After incubation, the supernatant was removed and placed in another tube to perform the counting of the active phages by double agar layered conventional method. The P22-MPs were then blocked with 1 mL PBS blocking buffer through 2 h incubation at 37ºC with agitation for inactivating the remaining tosyl groups. Afterwards, the P22-MPs were submitted to five washing steps for 5 minutes at room temperature in PBS washing buffer, and finally resuspended in storage buffer to reach a 1.0 mg mL^{-1} stock solution, which was stored at 4ºC.

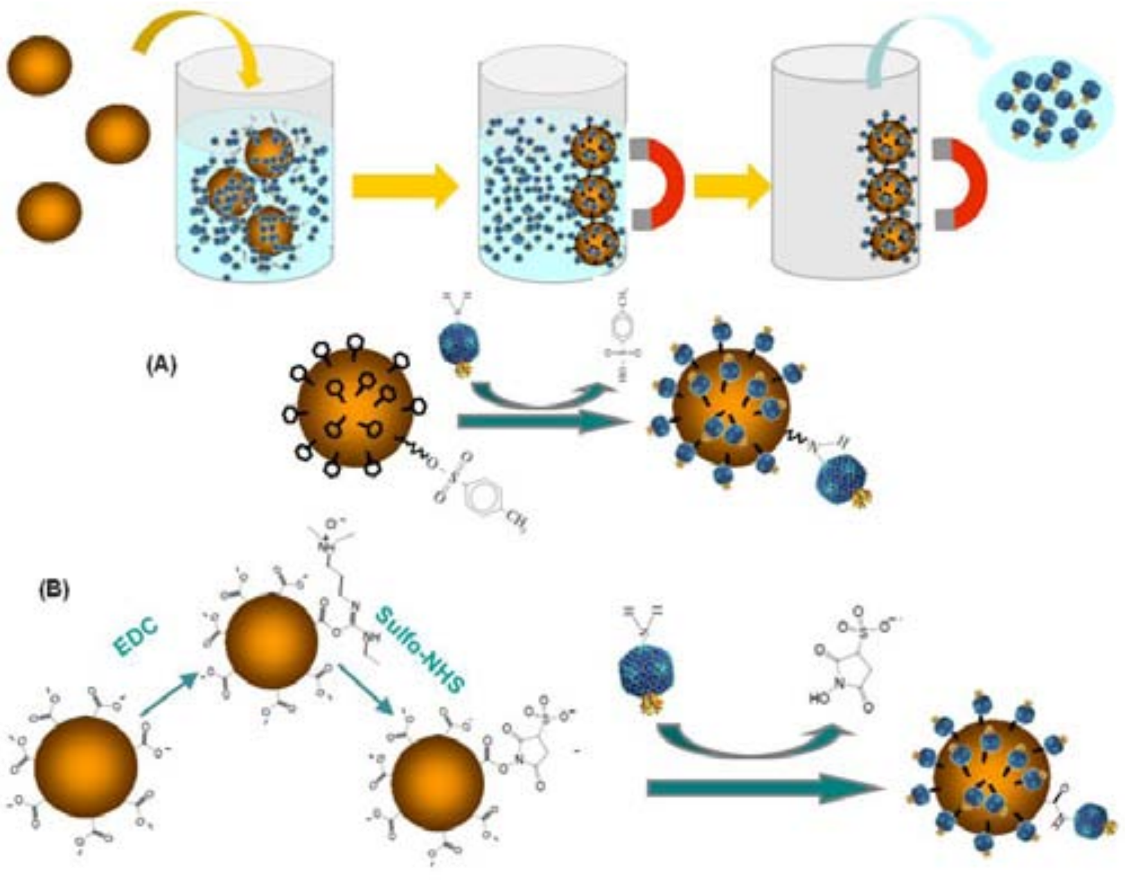

Figure 8.1 Schematic representation of the strategy for immobilizing P22 NPs the magnetic particles. The mix was incubated (17 h at 37 ºC under shaking) and the supernatant was removed to perform the phage counting by double agar layered method. In (A) the reaction of the amine moieties of the phage with the tosyl groups of the MPs is shown, while (B) schematizes the reactions performed to immobilize the P22 on the nMPs. The carboxylic groups were first activated with EDC and sulfo-NHS (8 h at room temperature under shaking) and then excess EDC and sulfo-NHS were eliminated followed by the addition of purified P22 bacteriophages in order to react through the amine groups of their capsid proteins.

8.3.2.2 Immobilization on carboxyl-modified magnetic nanoparticles

For the immobilization on the nMP, 35 µL of the nanoparticles (30 mg mL^{-1}, 3.8 x 10^{10} particles mL^{-1}) were washed twice in MES activation buffer and then the carboxylic groups were activated with 80 µL EDC (4 mg mL^{-1}) and 80 µL sulfo-NHS (9 mg mL^{-1}) incubating for 8 h at room temperature under shaking. During this time EDC reacts with the carboxylate nMPs forming an unstable reactive o-acylisourea ester, which immediately reacts with sulfo-NHS giving a semi- stable amine- reactive NHS ester, suitable for the further immobilization reaction. After two washes to eliminate the excess of EDC and sulfo-NHS, 150 µL of the purified P22 phage solution and 100 µL of activation buffer were added. The mix was incubated 17 h at 37 ºC under shaking in order that the amine groups of the phage proteins react with the NHS ester to form the stable amide bonds of the P22-nMPs. All the aforementioned reactions are schematized in Figure 8.1, B. Finally, the supernatant was transferred to another tube to perform the counting of the active phages and the following blocking and washing steps were performed in the same way than with the tosylactivated magnetic particles.

8.3.2.3 Coupling efficiency and phage/particle ratio studies

After the immobilization, the efficiency of the coupling strategies was evaluated by the double agar layered method. In this approach, tenfold serial dilutions of the supernatants and first wash after the covalent attachment were plated onto lawns of the bacterial strain, and compared with the concentration before immobilization.

The phage/particle ratio was also optimized in the case of the P22-MP analyzing the effect of increasing the magnetic particles amount to 5 mg or the phage concentration up to 10^{12} PFU mL^{-1}.

8.3.3 Evaluation of phage infectivity and biorecognition towards *Salmonella* of the immobilized P22 phages

The availability and integrity of the tailspike proteins (TSP) after the immobilization on the magnetic carriers is an important issue to be considered to ensure the biorecognition towards the bacteria. For the evaluation of the phage orientation and infectivity, several tenfold dilutions of the phage-modified magnetic particles were cultured by double agar layered method. Afterwards, the capture abilities of the modified magnetic carriers were evaluated by Scanning Electron Microscopy (SEM). A bacterial solution in the order of 10^6 CFU mL^{-1} in LB broth was added to P22-MP or P22-nMP and the PMS of *Salmonella* Typhimurium LT2 in these samples were performed. The samples (500 µL) were mixed with 10 µg of P22-MP or P22-nMP and incubated 20 min at room temperature with agitation followed by 20 min at 37 °C without agitation. After that, the magnetic particles with the attached bacteria were separated with a magnet, and then two washes were performed with PBST for 5 min at room temperature. Finally, the modified magnetic particles were resuspended in 100 µL PBS and after adding it to 5 mL of milli-Q water the SEM samples were prepared as previously explained in Chapter 6 (§ 6.3.2).

8.3.4 Comparison of the performance of both magnetic nano and microcarriers

The performance of both kinds of magnetic particles was compared using a magneto immunoassay with optical detection and studying the matrix effect, limits of detection, as well as the specificity of the systems, as detailed in the next sections.

8.3.4.1 Phagomagnetic immunoassay with optical detection for **Salmonella** *in milk*

The phagomagnetic immunoassay was designed in order to be performed in 96-well microtiter plates and comprised the following steps schematically outlined in Figure 8.2 (all the referred quantities are 'the amounts added per well'): (i) PMS of 100 µL *Salmonella* for attaching the target bacteria on the magnetic carriers as previously described; (ii) labeling with 100 µL of anti-*Salmonella* antibodies conjugated to peroxidase (Ab-HRP) incubating 30 min at room temperature and 700 rpm; and finally, the last step, (iii) optical detection with 100 µL of substrate solution, consisting of a mix of H_2O_2 and 3,3',5,5'-tetramethylbenzidine (TMB), incubated for 30 min at room temperature in darkness. The enzymatic reaction was stopped by adding 100 µL of H_2SO_4 (2 mol L^{-1}) and the absorbance measurement of the supernatants was performed at 450 nm.

For the evaluation of the results, the exact concentration of the initial inoculum coming from an overnight culture in LB broth was found by dilution and plating in LB agar. A negative control of LB broth was always also processed.

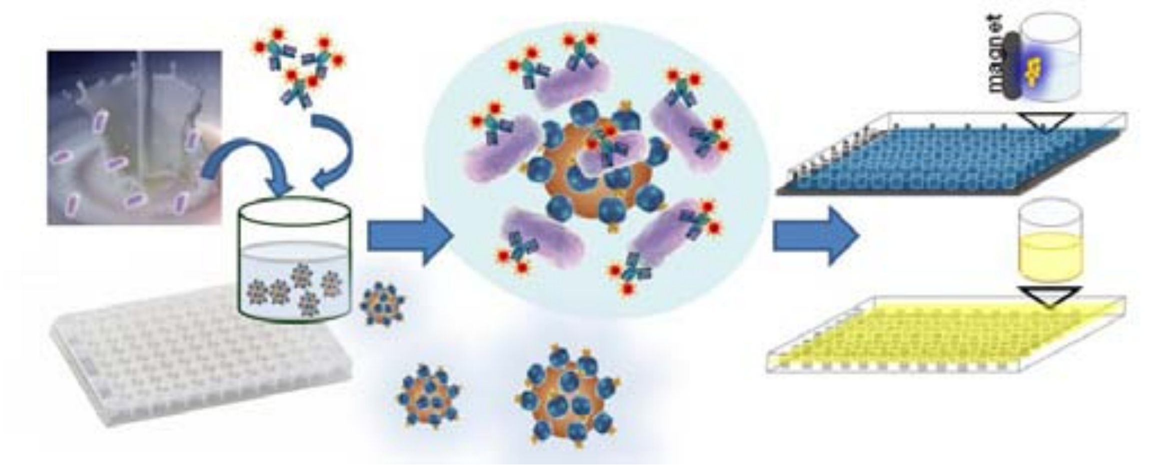

Figure 8.2 Schematic representation of the phagomactic immunoassay with optical detection, comprising the phagomagnetic separation (PMS) of the bacteria and the labeling using anti-*Salmonella* antibody conjugated to horseradish peroxidase (Ab-HRP), followed by the TMB reaction stopped with H_2SO_4 and read at 450 nm.

Different parameters (such as Ab-HRP and magnetic carrier concentrations) were optimized in order to find the optimal conditions for achieving high positive signals related to low background values. Moreover, in an attempt to shorten as well as to simplify the analytical procedure, four different protocols were also evaluated, by varying the number of washing steps, as shown in detail in Table 8.1.

Table 8.1 Different procedures performed with the P22-MP as a magnetic carrier for the optimization of the phagomagnetic immunoassay.

(A) Stepwise	(B) No washing between incubation steps	(C) Antibody addition without supernatant discard	(D) All reagents in one step
1- PMS of *Salmonella* (20 min shaking and 20 min still at 37ºC)	1- PMS of *Salmonella* (20 min shaking and 20 min still at 37ºC)	1- PMS of *Salmonella* (20 min shaking and 20 min still at 37ºC)	1- PMS of *Salmonella* (20 min shaking and 20 min still at 37ºC) and labeling with Ab-HRP at once
2- Washing step (2X, 3 min)	2- Supernatant discard and enzymatic labeling with Ab-HRP (30 min, shaking)	2- Addition of Ab-HRP and enzymatic labeling (30 min, shaking)	2- 30 min incubation at 700 rpm
3- Enzymatic labeling with Ab-HRP (30 min, shaking)	3- Washing step (3X, 3 min)	3- Washing step (3X, 3 min)	3- Washing step (3X, 3 min)
4- Washing step (3X, 3 min)			

Other experimental parameters such as temperature and agitation during the PMS (combining 20 min agitation followed by 20 min without agitation at 37ºC), surfactant concentration, ionic strength, and pH were used as optimized in previous works.

The evaluation of the matrix effect on artificially inoculated *Salmonella* samples (from 10^1 to 10^8 CFU mL^{-1}) in LB broth and in milk diluted 1/10 in LB were compared for both kinds of P22 bacteriophage modified magnetic carriers (P22-MP and P22-nMP), as well as the cut-off values and limits of detection.

8.3.4.2 Specificity study

A preliminary specificity study of the system was performed by comparing the response to *Salmonella* with the signal obtained in the presence of an equivalent amount of another gram negative bacterium as *E.coli* artificially inoculated in the samples, and compared to a negative control.

8.3.5 Evaluation of the phagomagnetic separation (PMS) of *Salmonella* by conventional culture methods and confocal microscopy

In the case of the tosylactivated particles the efficiency of the PMS step was studied, by preparing different bacterial dilutions and capturing the *Salmonella* Typhimurium LT2 in these samples. 500 µL of different concentrations of bacteria were added to 10 µg of P22-MP and incubated 20 min at room temperature with agitation followed by 20 min at 37 °C without agitation. After that, the magnetic particles with the attached bacteria were separated with a magnet, the supernatant was transferred to a new tube for further plating, and then two washes were performed with PBST for 5 min at room temperature followed by the resuspension in 100 µL PBST. Finally, the supernatants were plated in LB agar and grown for 18−24 h at 37°C to compare the bacteria counting with the initial amount added to the particles.

Moreover, to evaluate the bacteria capturing ability and pattern of the immobilized phages, fluorescence microscopy was used. For the samples preparation, the PMS step was performed as previously explained. The nucleic acid stain Hoechst 33342 was used to label the bacterial cells, by adding 4.5 µL of a 10 mg mL^{-1} stock solution per mL of *Salmonella* at a concentration of 10^6 CFU mL^{-1}. The detection was performed by adding 0.4 µg of anti-*Salmonella* antibodies and 1.6 µg of anti IgG-Cy5 as secondary label. The final detection sandwich was imaged using a Leica TCS/SP5 confocal microscope (Leica Microsystems, Exton, PA). Finally the 3D Imaris X64 v. 6.2.0 software (Bitplane; Zürich, Switzerland) was applied for processing the obtained images.

8.3.6 Phagomagnetic electrochemical immunosensor for the detection of *Salmonella* in milk

The phagomagnetic immunosensing approach was performed in 2 ml Eppendorf tubes comprising the following main steps (all the referred quantities are 'the amounts added per tube'): (i) PMS of 500 µL *Salmonella* with the P22-MP as previously described; (ii) labeling with 100 µL of anti-*Salmonella* antibodies conjugated to HRP (Ab-HRP) incubating 30 min at room temperature and 700 rpm; and finally after two washes with PBST (3 min under shaking) and resuspending the modified particles in 140 µL, (iii) the modified magnetic particles were captured by dipping the magneto electrode (m-GEC) inside the reaction tube and the electrochemical detection was performed as previously explained in Chapter 4 (§ 4.3.6).

The P22-MP and Ab-HRP concentration were optimized to improve the amperometric responses, while matrix effect as well as specificity studies were already performed with the phagomagnetic immunoassay with optical detection. As a result, to study the response of the phagosensor to the *Salmonella* concentration, a calibration curve comprising tenfold dilution series of *Salmonella* ranging from 10^8 to 10^1 CFU mL^{-1} was performed in milk diluted 1/10 in LB broth.

8.3.7 Pre-enrichment studies for the detection of *Salmonella* in contaminated milk

Current regulations stipulate that no *Salmonella* should be detectable in 25 g of food, sampled in five portions of 5 g each in different points (Real Decreto 1679/1994, BOE 24-09-94). Standard methods require four steps, namely pre-enrichment, selective enrichment, reisolation step, and finally, identification. The time required for completion of these tests is ranged from 66 to 72 h, which is extended to 4 days when the ISO 6579 2002 standard method is used. [15]

In order to fulfill the legislation, the detection system should be able to detect 1 CFU in 25 mL of milk (that is, 0.04 CFU mL^{-1}), which is only possible if a pre-enrichment step is included. This is performed with a nonselective broth medium such as LB broth, leading to a 1/10 dilution of the food matrix. With the aim of evaluating the pre-enrichment time required to reach the aforementioned LOD, the milk samples were preenriched in LB broth at 37 ºC, and assayed at 4, 6, 8 and 16 h.

8.4 RESULTS AND DISCUSSION

8.4.1 Covalent immobilization of bacteriophages on magnetic micro and nanocarriers

As previously mentioned, the integrity of the phage tailspike protein (TSP) gp9 is an important factor to be considered since the conjugation to the magnetic carriers could hinder the bacterial recognition. The chemical reaction for the covalent immobilization is not controlled in terms of the orientation since amine groups exist, for instance, both on the head and TSP domains of P22. However, the shape could also play a role, since the large and smooth capsid head seems to be favored over the pointy tail spikes of the gp9 proteins in immobilization procedures.[6]

The immobilization efficiency of the P22 phage on the magnetic particles was studied and compared by immobilizing phage amounts in the order of 10^{10} PFU to 1 mg magnetic carriers and evaluating the phage concentration before and after the immobilization step. In order to calculate the coupling efficiencies, the amount of phages in both, the supernatant and the first wash, were compared with the initial amount, before immobilization. The coupling efficiency of the P22 phage on the magnetic carriers was found to be 92.4 and 83.6 %, for MP and nMP, respectively, as detailed shown in Table 8.2.

Table 8.2 Comparative results of the phage amount before and after the immobilization with the calculated coupling efficiencies for both types of magnetic particles.

	Magnetic particles (MP)	**Magnetic nanoparticles (nMP)**
Phage amount (PFU)		
Initial	1.44×10^{10}	1.99×10^{10}
Supernatant	9.90×10^{8}	3.25×10^{9}
First washing step	1.10×10^{8}	9.00×10^{6}
Coupling efficiency (%)	92.4	83.6

When comparing the response of both magnetic micro and nanoparticles at a *Salmonella* concentration of 10^5 and 10^7 CFU mL^{-1} (as shown in Figure 8.3, A), although a higher signal was obtained with the P22-nMP for 10^7 CFU mL^{-1}, a better signal to non specific adsorption ratio was obtained with the P22-MP for the lower bacterial concentration (at 10^5 CFU mL^{-1}), suggesting improved features of the magnetic microparticles in terms of non-specific adsorption and LODs.

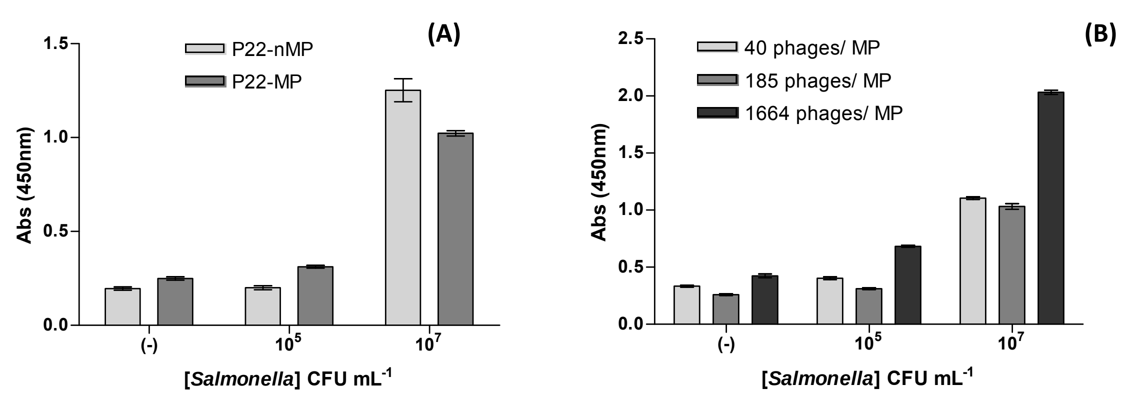

Figure 8.3 Comparative responses for both magnetic carriers (P22-MP and P22-nMP) at bacteria concentrations of 0, 10^5 and 10^7 CFU mL^{-1} (A) and evaluation of different magnetic particles concentrations and phage amounts (B).

Further studies about covalent immobilization were performed on P22-MP, by immobilizing 1.44 x 10^{10} PFUs on increasing amounts of MP, in detail 7 x 10^7 (1 mg) and 3.5 x 10^8 (5 mg). Coupling efficiencies of 92.4 and 98.9 % and phage/MP ratios of 185 and 40 were respectively obtained. The increase in the amount of phages per MP when decreasing the particle concentration was in agreement with the expected results indicating that the particles were not saturated yet. On the other hand, when the amount of phage was increased by immobilizing 2.01 x 10^{11} and 6.42 x 10^{11} PFU on 7 x 10^7 MPs, a decrease in the coupling efficiency was observed. Nevertheless, the number of phages per MP increased considerably obtaining a plateau in the immobilization efficiency at a phage/MP ratio of 1650 (by the immobilization of up to 2.0 x 10^{11} phages on 7 x 10^7 MPs), in agreement with previous studies.[14] The detailed comparative results are presented in Table 8.3.

Furthermore, the signals obtained by increasing the phage/MP ratios from 40 to 1664 and assaying at a *Salmonella* concentration of 0, 10^5 and 10^7 CFU mL^{-1} showed better analytical performance –in terms of higher signals to nonspecific adsorption ratio– for fully-covered magnetic particles (around 1650 phage per MP), as shown in

Figure 8.3, B and in Table 8.4. All these results suggest that a better response was obtained by immobilizing higher phage titer (up to 10^{11} PFU) on lower MP amount (7 x 10^7 MPs), achieving in this condition full coverage of the phages on the magnetic particles, and thus increased PMS efficiency.

Table 8.3 Coupling efficiency and final number of phages per magnetic particle for different phages and magnetic particles amounts.

Initial phage amount (PFU)	Magnetic particles amount/number	Coupling efficiency (%)	Phage/ MP ratio
1.44×10^{10}	5 mg / 3.5×10^8	98.9	40
1.44×10^{10}	1 mg / 7×10^7	92.4	185
2.01×10^{11}	1 mg / 7×10^7	58.0	1664
6.42×10^{11}	1 mg / 7×10^7	18.0	1648

Table 8.4 Signal to nonspecific adsorption ratios for the different phage to particle amounts tested.

	Signal to background ratio		
[*Salmonella*] CFU mL^{-1}	MP: 5 mg/ 3.5×10^8 phage: 1.44×10^{10} PFU ratio: 40 phages/MP	MP: 1 mg/ 7×10^7 phage: 1.44×10^{10} PFU ratio: 185 phages/MP	MP: 1 mg/ 7×10^7 phage: 2.01×10^{11} PFU ratio: 1664 phages/MP
10^5	1.20	1.20	1.61
10^7	3.31	3.98	4.80

8.4.2 Evaluation of phage infectivity and biorecognition towards *Salmonella* of the immobilized P22 phages

In order to evaluate the phage infectivity after the covalent attachment to the magnetic carriers, both the P22-MPs and the P22-nMPs were cultured by the double agar layered method and enumeration of plaques. By this method it is not possible to establish the number of bacteriophages per magnetic particle since each modified magnetic particle is able to produce a unique plaque, regardless of how many bacteriophages are correctly oriented on its surface. Nevertheless, by plating the modified magnetic carriers it is possible to evaluate their global lytic activity. The P22-MPs showed lytic activity of 100 % approximately at a phage/MP ratio of 1650 (full-coverage), but it dropped appreciably to 43 % for a phage/MP ratio of 40.

On the other hand, the P22-nMPs showed lytic activity in as low as 0.001 % of the nanoparticles. This result is not concordant with the immobilization efficiency above 80 %, and could we explained by the high particle agglomeration during culturing which was also observed in the SEM images.

The captured bacteria on the magnetic carriers after the PMS can be seen in the SEM images shown in Figure 8.4. While the P22-MP were able to attach more than one bacteria (Figure 8.4, C and D), the pattern observed with the magnetic nanoparticles was the opposite, showing single bacteria tagged with more than one P22-nMP (Figure 8.4, A and B).

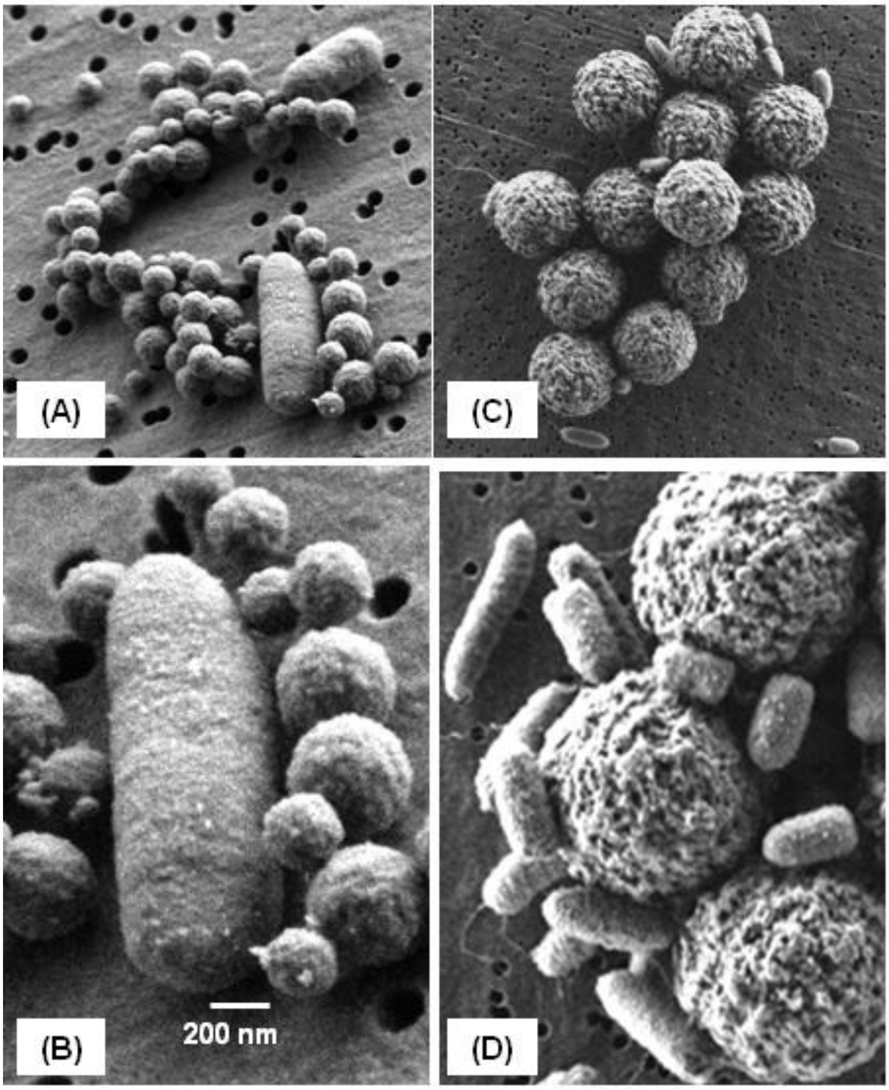

Figure 8.4 Evaluation of the PMS by SEM at a *Salmonella* concentration of 3.2 x 10^6 CFU mL^{-1} using carboxyl-activated magnetic nanoparticles (A and B) and tosylactivated magnetic particles (C and D). In all cases, identical acceleration voltage (15 kV) was used.

Due to multivalency in both magnetic carrier and bacteria, aggregates were clearly observed in both types of particles. However, in the case of the magnetic nanoparticles, the degree of aggregation was higher, and mostly due to self-aggregation, in accordance with the poor lytic activity obtained by culturing. These results suggest that the biorecognition in the nanostructured carrier may be hindered due to agglomeration. The Figure 8.4, B also shows the P22 phages immobilized on the surface of the nMP.

8.4.3 Comparison of the performance of both magnetic nano and microcarriers

8.4.3.1 Phagomagnetic immunoassay with optical detection for Salmonella in milk

First of all, the concentration of anti-*Salmonella* antibody (Ab-HRP) as optical reporter for the phagomagnetic immunoassay was optimized by testing three different dilutions (1/1000, 1/2000 and 1/3000) using the P22-MP as solid support for the immunoassay, and evaluating the signal to non-specific adsorption ratios at two different bacteria concentrations (10^5 and 10^7 CFU mL^{-1}) as detailed in Figure 8.5. The highest signal to background (S/B) ratios were obtained with the 1/1000 dilution, using thus this label concentration for further assays.

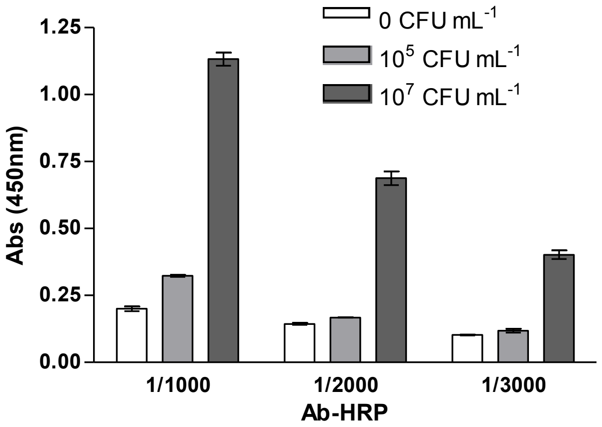

Ab-HRP dilution	1/1000		1/2000		1/3000	
CFU mL^{-1}	10^5	10^7	10^5	10^7	10^5	10^7
S/B ratio	1.62	5.66	1.17	4.79	1.15	3.92

Figure 8.5 Signals obtained at 0, 10^5 and 10^7 CFU mL^{-1} of *Salmonella* using three different Ab-HRP dilutions (1/1000, 1/2000 and 1/3000). The table below shows the corresponding signal to background (S/B) ratios. In all cases, n=3.

On the other hand, the concentration of the P22-MP and P22-nMP were also optimized by analyzing the signal to background ratios at two bacteria concentrations (10^5 and 10^7 CFU mL^{-1}) using different particle concentrations (0.05, 0.1 and 0.2 mg mL^{-1}), as shown in detail in Figure 8.6. The highest signal to background values was obtained in both cases when using a magnetic particle concentration of 0.05 mg mL^{-1}.

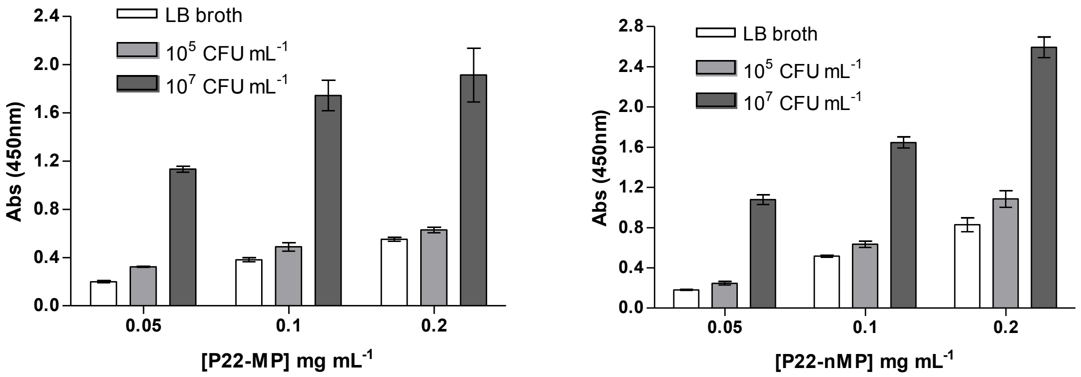

[P22-MP] (mg mL^{-1})	0.05		0.1		0.2	
CFU mL^{-1}	10^5	10^7	10^5	10^7	10^5	10^7
S/B ratio	1.62	5.66	1.28	4.56	1.14	3.47

[P22-nMP] (mg mL^{-1})	0.05		0.1		0.2	
CFU mL^{-1}	10^5	10^7	10^5	10^7	10^5	10^7
S/B ratio	1.36	5.95	1.20	3.06	1.21	2.79

Figure 8.6 Signals obtained at 0, 10^5 and 10^7 CFU mL^{-1} of *Salmonella* using different magnetic particles concentrations for P22-MP (A) and P22-nMP (B), respectively, at a Ab-HRP dilution of 1/1000. The tables below show the corresponding signal to background ratios. In all cases, n=3.

Finally, to establish the optimal strategy for the phagomagnetic immunoassay with optical detection, four different procedures were compared by varying the incubation and washing steps as previously explained in Table 8.1 (§ 8.3.3.1) and depicted in Figure 8.7. To perform this comparative study, this approach was assayed at 0, 10^5 and 10^7 CFU mL^{-1} of *Salmonella* using P22-MP as a magnetic carrier, as shown in Figure 8.8.

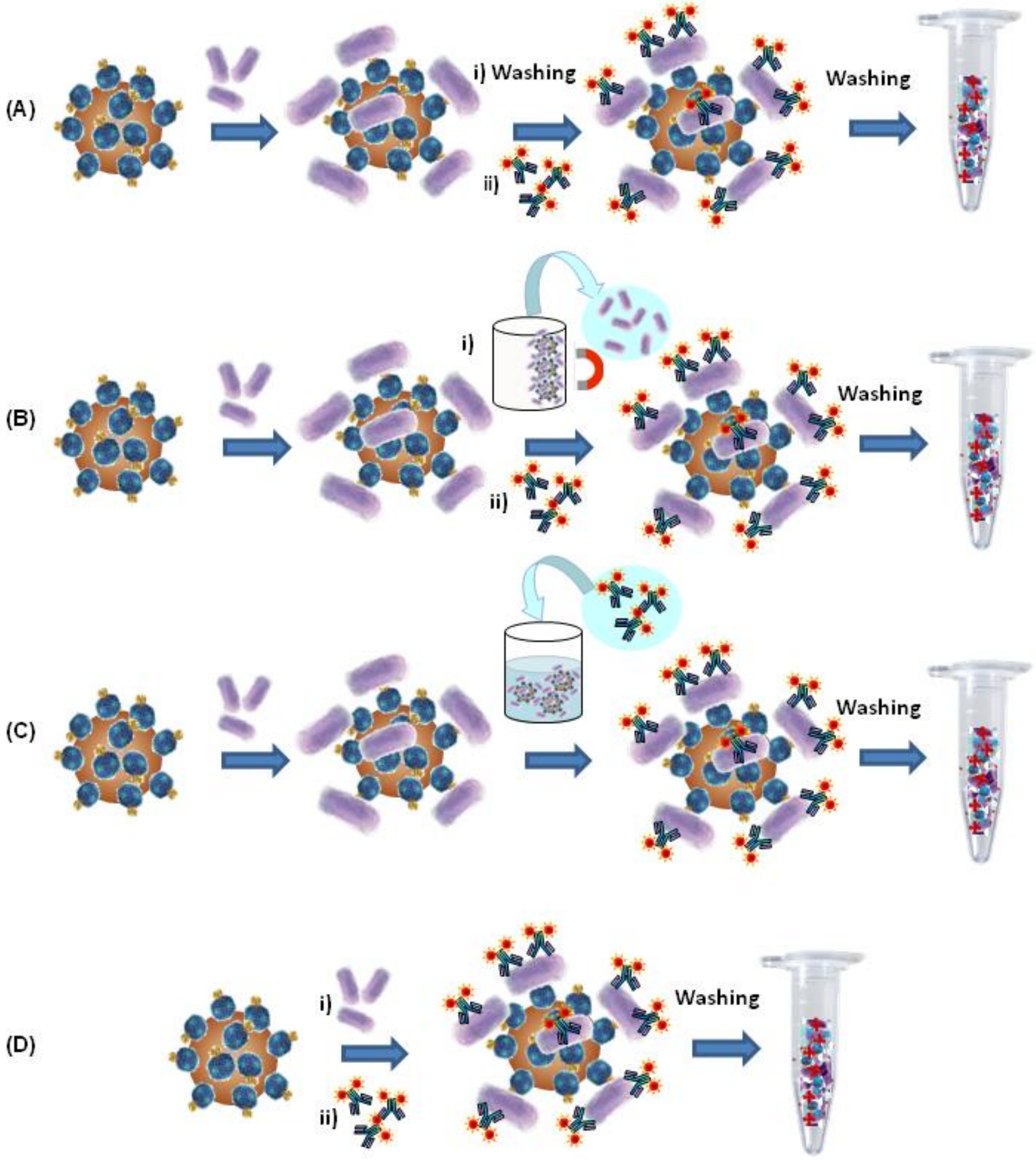
(A)
i) Washing
ii)
Washing
(B)
i)
ii)
Washing
(C)
Washing
(D)
i)
ii)
Washing

Figure 8.7 Schematic representation of the different procedures applied for the optimization of the phagotamagnetic immunoassay protocol. The four tested strategies are detailed in Table 8.1: (A) stepwise protocol; (B) procedure without washing between incubation steps; (C) antibody addition without supernatant discard; and (D) addition of all reagents in one step.

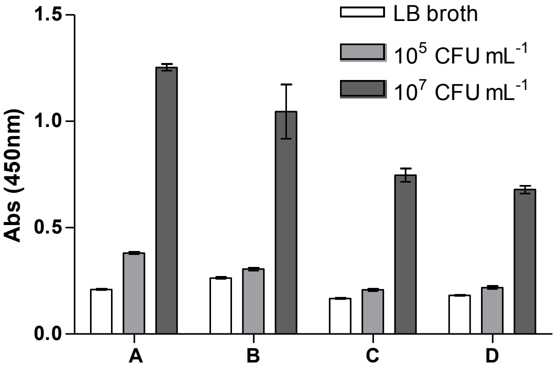

Figure 8.8 Results obtained with the P22-MP following four different procedures and (B) the corresponding signal to background (S/B) ratios below. The reagents were P22-MP 0.05 mg mL^{-1} and Ab-HRP diluted 1/1000. In all cases n=3.

Although in all cases the bacteria were clearly detected, improved results were obtained with the strategy A, by performing the two incubation steps separately with washings in between, showing lower background values and higher positive signals and, as a result, better signal to background ratio at both assayed bacteria concentrations, as detailed in Table 8.5.

Table 8.5 Signal to nonspecific adsorption ratios for the four different strategies tested.

Signal to background ratio	**Strategy**			
[*Salmonella*] CFU mL^{-1}	**A**	**B**	**C**	**D**
10^5	1.86	1.16	1.25	1.20
10^7	5.99	3.96	4.47	3.73

The phagomagnetic immunoassay was evaluated for artificially inoculated *Salmonella* (ranged from 10^1 to 10^8 CFU mL^{-1}) in LB broth and in milk diluted 1/10 in LB for both magnetic carriers, P22-MP and P22-nMP. As shown in Figure 8.9, a slight matrix effect was observed throughout the whole calibration curve, showing a decrease in the signals in the presence of the milk, which became more visible at a high bacteria concentration. Moreover, the effect was more evident in the case of the P22-nMP. This could probably be explained by the fact that the higher surface area per volume ratio given by the smaller size of the particles could go against by increasing the nonspecific adsorption and the influence of the matrix components during the assay.

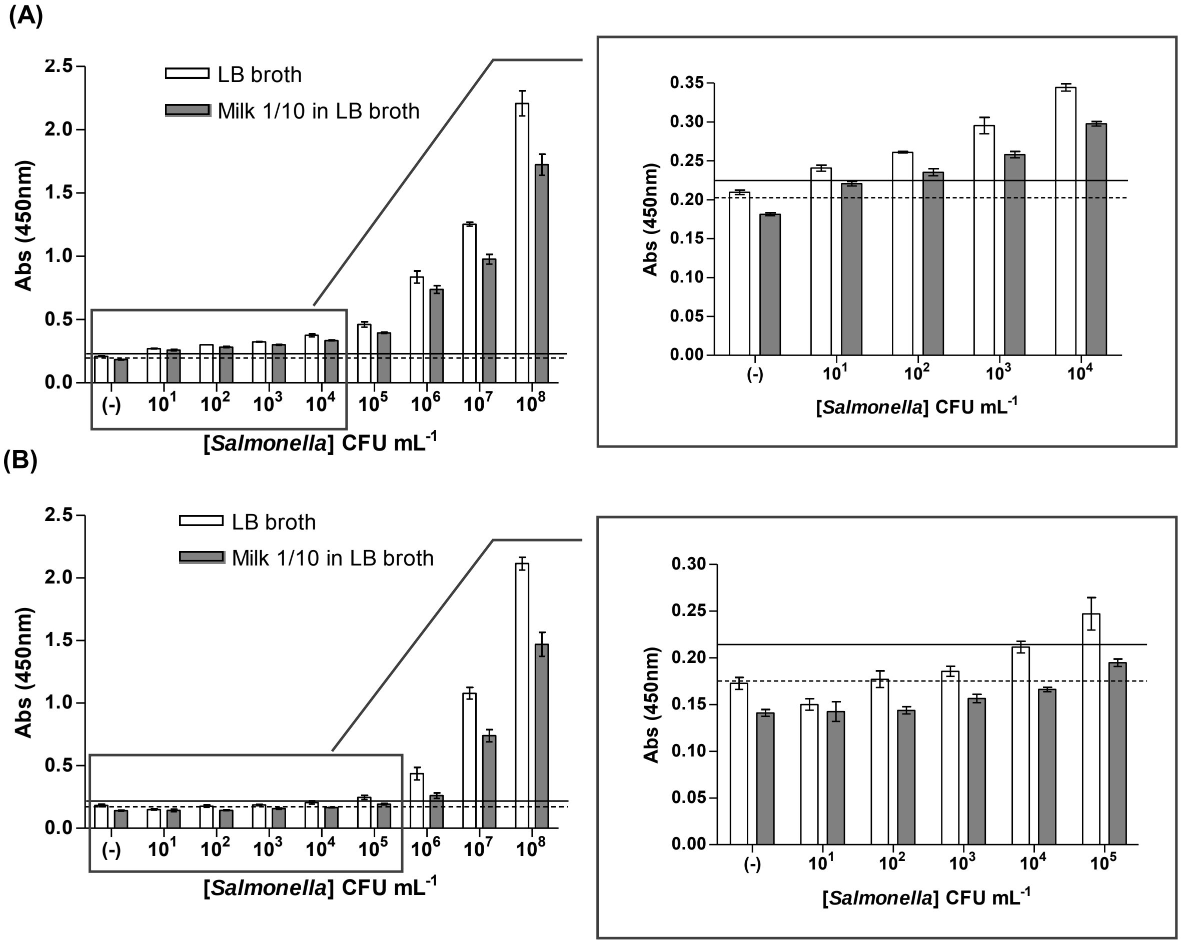

Figure 8.9 Phagomagnetic immunoassay performed with the P22-MPs (A) and P22-nMP (B) by increasing the amount of *Salmonella* from 2.5 x 10^1 to 2.5 x 10^8 CFU mL^{-1}, artificially inoculated in LB broth and in milk diluted 1/10 in LB. The bars on the right side show a zoom shot detailing the signals at the lower bacteria concentration range. The cut-off values for LB broth and milk diluted 1/10 are represented with a solid and dotted line, respectively. In all cases, n = 3, except for the 0 CFU mL^{-1} negative control in which n=10. The reagents concentration was: 0.05 mg mL^{-1} P22-MP or P22-nMP and Ab-HRP diluted 1/1000.

Ten negative samples (0 CFU mL^{-1}) were processed obtaining in the case of the P22-MP a mean value of 0.2042 and 0.1838 absorbance units (a.u.) with a standard deviation of 0.0071 and 0.0070 for the assay performed in LB broth and in milk diluted 1/10 in LB, respectively. The signals corresponding to the LOD, or cut-off values, were then extracted with a one-tailed *t* test at a 99 % confidence level as already explained in Chapter 6 (§ 6.4.4) obtaining a result of 0.224 (solid line) and 0.203 a.u (dotted line) in LB and in milk respectively. As a result, the system was able to give a positive signal already for the first point of the curve in both matrixes (Figure 8.9, A), which corresponds to a concentration of 25 CFU mL^{-1} of *Salmonella*. The LOD values were finally calculated by interpolation of the cut-off signals in the sigmoidal dose response curve (Figure 8.10, A and Table 8.6, A), obtaining a result of 10 CFU mL^{-1} in LB broth and 19 CFU mL^{-1} in milk.

On the other hand, the mean values of the negative samples (0 CFU mL^{-1}) for the P22-nMP obtained in LB broth and milk diluted 1/10 were 0.1726 and 0.1442 a.u. with standard deviations of 0.0143 and 0.0106, respectively. When comparing these results with the values obtained with the P22-MP, higher coefficients of variation were obtained with the nanoparticles (8.3 % in LB and 7.4 % in milk) than with the P22-MP (3.5 % in LB and 3.8 % in milk). Regarding the cut-off values for the phagomagnetic immunoassay performed on P22-nMP, the results were 0.215 and 0.176 a.u. for LB and milk, respectively (Figure 8.9, B), indicating that the system was able to detect the bacteria at a concentration up to 10^5 CFU mL^{-1}.

When the absorbance was plotted *vs.* the logarithm of *Salmonella* concentration and the responses were adjusted to sigmoidal dose response curves (Figure 8.10, B), the obtained parameters (Table 8.6, B) showed higher r^2 values as well as superior slopes in the case of the P22 nMP, indicating a better fitting as well as a higher sensitivity than the P22-MP, as could be expected due to the improved reactivity given by the smaller size of the particles. However, when interpolating the cut-off signals in the sigmoidal dose response curves, the obtained LODs were much the worse than the results obtained with the P22-MP, giving values of 1.09 x 10^5 CFU mL^{-1} in LB and 3.35 x 10^5 CFU mL^{-1} in milk. These results can be related with the high agglomeration observed that could be hindering the biorecognition of the bacteria by the P22-nMP as well as the further labeling step by the Ab-HRP.

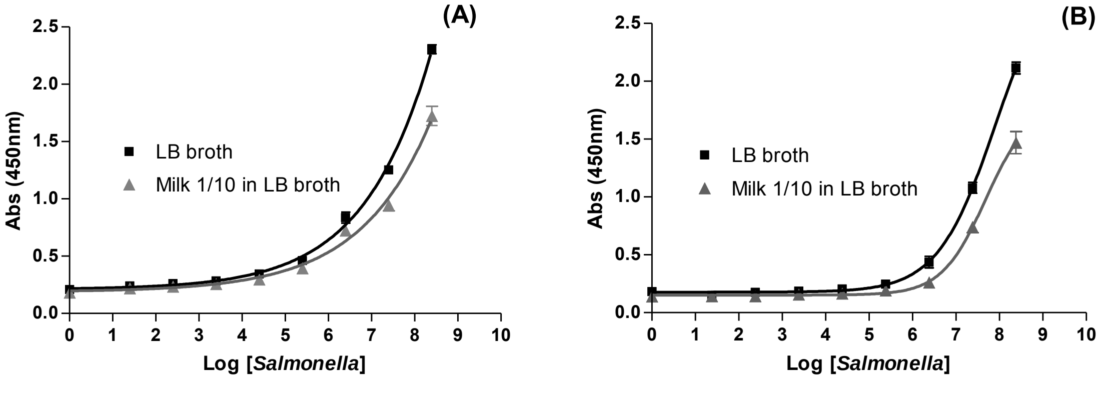

Figure 8.10 Sigmoidal dose response curves obtained in LB and milk after plotting Abs *vs.* logarithm of *Salmonella* concentration for both the P22-MP (A) and P22-nMP (B).

Table 8.6 Parameters of the sigmoidal dose-response curves obtained with the P22-MP (A) and P22-nMP (B) when applying the phagotagging magneto-immunoassay in LB broth and milk.

(A) P22-MP	CV (%) for (-) control	CV (%) at 10^8 CFU mL^{-1}	R^2	Slope	Cut-off	LOD (CFU mL^{-1})
LB broth	3.5	7.8	0,9948	0,29	0,224	10
Milk 1/10 in LB broth	3.8	8.9	0,9841	0,27	0,203	19

(B) P22-nMP	CV (%) for (-) control	CV (%) for 10^8 CFU mL^{-1}	R^2	Slope	Cut-off	LOD (CFU mL^{-1})
LB broth	8.3	7.7	0,9951	0,64	0,215	1.09×10^5
Milk 1/10 in LB broth	7.4	11.5	0,9947	0,83	0,176	3.35×10^5

8.4.3.2 Specificity study

The specificity of the system was evaluated by performing the phagomagnetic immunoassay in milk diluted 1/10 artificially inoculated with 10^6 and 10^7 CFU mL^{-1} of both *Escherichia coli* and *Salmonella*, as well as a negative control as a background reference signal (Figure 8.11). In the case of the P22-MP (Figure 8.11, A) the signals obtained for the *E.coli* samples are almost identical to the blank, regardless the concentration, indicating a high specificity of the assay as well as a low nonspecific adsorption. However, further specificity studies with other accompanying microflora according to the food sample should be done for each case.

However, in the case of the P22-nMP (Figure 8.11, B), although the signals obtained with the non-target gram negative bacteria were quite close to the background adsorption, the results were above the cut-off value at both assayed concentrations, which could cause false positive results. Moreover, a slight raise in the signal was observed when increasing the *E.coli* concentration, suggesting the presence of some degree of cross reaction and thus, a poorer specificity. This behavior could be explained, as in the case of the matrix effect, by the higher surface per mass unit of the nanoparticles leading also to a higher non-specific adsorption. Another possible reason could be that the trapping of the non-target bacteria in the particles conglomerates in addition to some extent of cross-reactivity by the polyclonal antibody used in the labeling step gave place to this nonspecific response.

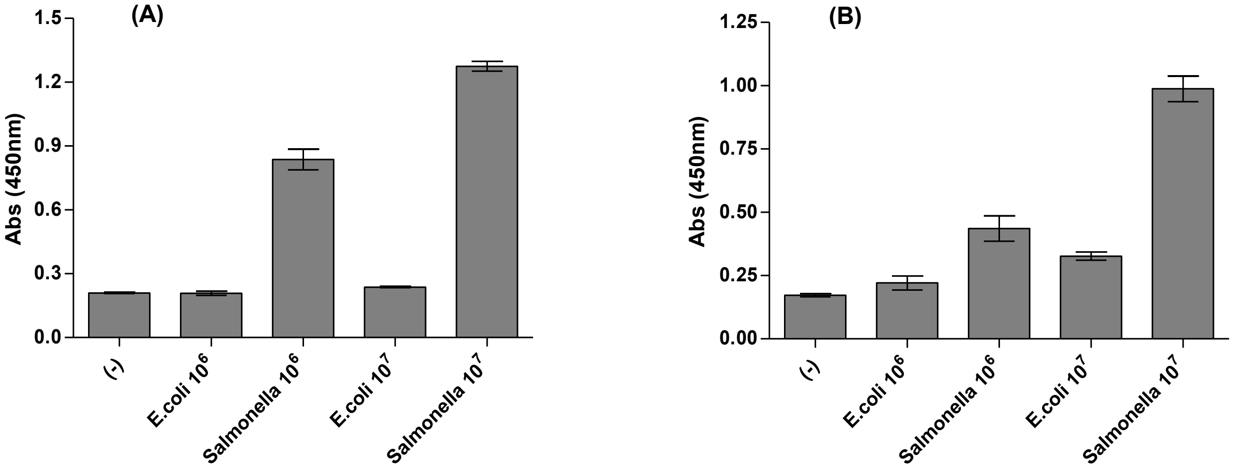

Figure 8.11 Specificity study for the phagomagnetic immunoassay performed with both magnetic carriers, (A) P22-MP and (B) P22-nMP, in diluted milk artificially inoculated, respectively, with: 0 CFU mL^{-1} (negative control), 1.9 × 10^6 CFU mL^{-1} *E. coli*, 2.5 × 10^6 CFU mL^{-1} *Salmonella*, 2.3 × 10^7 CFU mL^{-1} *E. coli* and 3.2 × 10^7 CFU mL^{-1} of *Salmonella*.

For the phagomagnetic immunoassay based on the P22-MPs, the specificity of the system can be ascribed to the phagomagnetic separation step with the highly specific interaction between the membrane receptor of the bacteria and the tailspike of the P22 bacteriophage immobilized on the magnetic carrier, coupled to the low non-specific adsorption of the magnetic microparticles and the second biorecognition, involving the immunological labeling with the Ab-HRP.

8.4.4 Evaluation of the phagomagnetic separation (PMS) of *Salmonella* by conventional culture methods and confocal microscopy

Since better results in terms of sensitivity as well as specificity were obtained with the P22-MP, this system was more deeply studied, analyzing the *Salmonella* capturing capability by conventional culturing and fluorescence microscopy.

The capture efficiency was evaluated by performing the PMS of the bacteria and comparing the initial bacteria amount added to the particles with the counting in the supernatants after the capture. The exact concentration of the initial inoculum coming from the overnight culture in LB broth was found by dilution and plating in LB agar. Three different bacterial dilutions were prepared in LB broth, 2.9 x 10^3, 2.9 x 10^5 and 2.9 x 10^7 CFU mL^{-1}, and a negative control was also processed. The PMS of *Salmonella* Typhimurium LT2 in these samples was performed as described in § 8.3.2

and colony counting was carried out after plating 50 μL of the corresponding supernatants in LB for 18-24 h at 37°C, obtaining the results detailed in Table 8.7. Bacterial cells were enumerated in the initial suspension and the supernatant by plate counting, and the number of captured cells was estimated by subtraction for the efficiency calculations.

Table 8.7 Counted colony number of the initial bacteria related to the amount after plating the supernatants and corresponding PMS efficiencies.

Initial cell number added (CFU)	Cell number in the supernatants (CFU)	PMS efficiency (%)
1.45×10^7	9.0×10^5	95.3 (*)
1.45×10^5	9.6×10^3	95.0 (*)
1.43×10^3	6.0×10^2	68.8 (*)
0 (negative control)	0	/

(*) PMS efficiency= [(initial cell number - cell number in supernatant)/ initial cell number] x 100

Excellent bacteria recoveries were obtained at all tested concentrations, showing better capturing efficiencies than previously reported systems based on immunomagnetic separation [16] using commercial antibody-modified magnetic particles or PMS using inactivated P22 bacteriophages [14]. Higher capture efficiencies were also obtained compared to a previous study using wild type P22 phages covalently bounded to glass substrates for capturing 10^6- 10^7 CFU mL^{-1} of *Salmonella*.[6] Finally, when the results were compared to another work which reported the use of T4 phages with specific binding ligands introduced by phage display techniques for their immobilization on magnetic particles, similar capturing efficiency was obtained at 10^3 CFU mL^{-1}, while better recoveries were also achieved at higher bacteria concentrations. Furthermore the developed strategy is simpler since the native phage didn't require complex engineering steps.[10]

Confocal microscopy was used to study the bacterial recognition capability of the immobilized bacteriophages. The images in Figure 8.12 show a blank without the immobilized phages (A) and the PMS of the bacteria through the P22-MPs with further antibody labeling using primary monoclonal antibodies and anti IgG-Cy5 secondary antibodies as fluorescence reporter (B). The autofluorescence presented by the magnetic particles coating polymer was exploited for their visualization. No bacteria capture was observed in the absence of immobilized phages on the magnetic particles as well as any nonspecific adsorption of the fluorescent label was obtained when no bacteria were present in the sample, as can be seen in Figure 8.12, A.

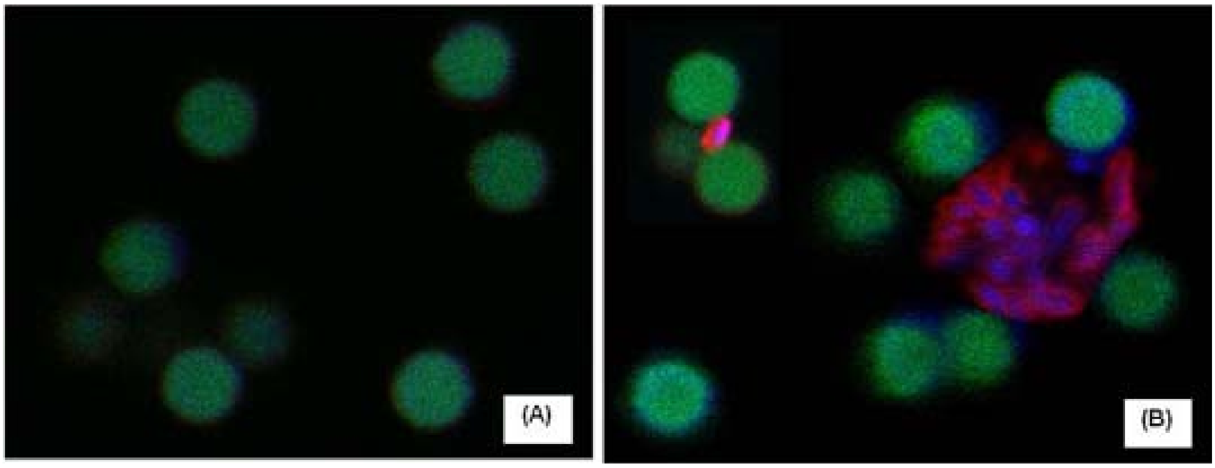

Figure 8.12 Confocal microscopy images of the negative control without immobilized bacteriophages (A) and the captured bacteria on the P22-MPs labeled with a monoclonal primary antibody and a secondary anti IgG-Cy5 (B) In green the magnetic particles (autofluorescent), in blue the bacteria stained with Hoechst 33342 and in red the attached specific antibodies labeled with anti IgG-Cy5.

8.4.5 Phagomagnetic electrochemical immunosensor for the detection of *Salmonella* in milk

Due to the better analytical performance of phagomagnetic immunoassay with optical detection performed on the P22-MP already explained in the previous sections, a similar approach based on a phagomagnetic electrochemical immunosensor using this modified microparticles was studied.

The first step was to optimize the reagents concentration, that is the amount of P22-MPs and labeled antibodies (Ab-HRP) used in this case as electrochemical reporter. Three different P22-MPs concentrations (0.05, 0.1 and 0.2 mg mL^{-1}) and Ab-HRP dilutions (1/200, 1/400 and 1/800) were tested in order to establish the most advantageous conditions to obtain the highest positive signals related to the lowest background values as shown in Figure 8.13. For evaluating the optimal concentration of the electrochemical reporter, the P22-MP concentration was set at 0.1 mg mL^{-1} and the better results were obtained at a dilution 1/400, as shown in Figure 8.13, A. Once the dilution was established at 1/400, the P22-MP concentration was modified. Although a lower signal was obtained at 10^7 CFU mL^{-1} of *Salmonella* for the concentration of 0.05 mg mL^{-1}, the highest signal to nonspecific adsorption ratio was achieved in this case. Moreover, improved signal differentiation was also achieved at

10^5 CFU mL^{-1}, suggesting a better sensitivity of this approach at the lower P22-MP concentration (Figure 8.13, B).

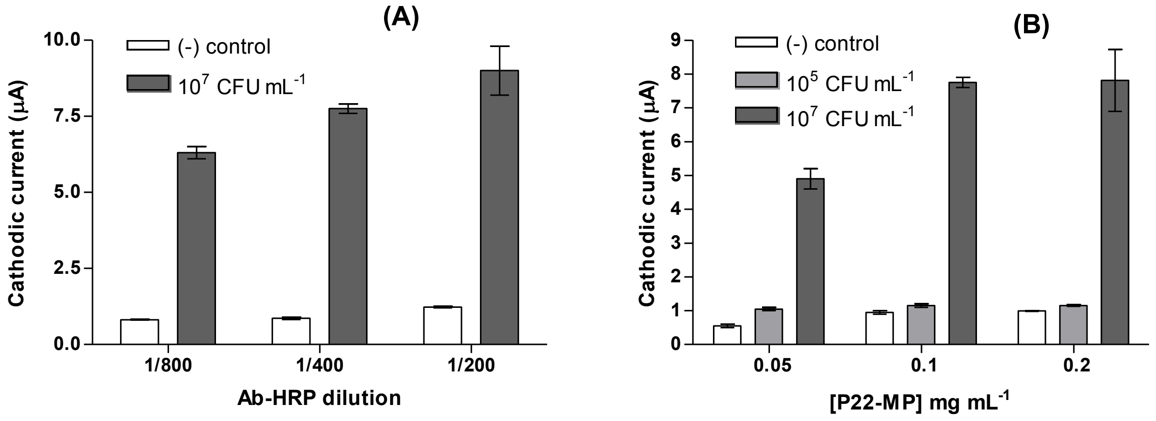

Ab-HRP dilution	**1/800**	**1/400**	**1/200**
CFU mL^{-1}	**10^7**	**10^7**	**10^7**
S/B ratio	7.73	9.01	7.35

P22-MP (mg mL^{-1})	**0.05**		**0.1**		**0.2**	
CFU mL^{-1}	**10^5**	**10^7**	**10^5**	**10^7**	**10^5**	**10^7**
S/B ratio	1.91	8.90	1.21	8.16	1.17	7.89

Figure 8.13 (A) Electrochemical signals obtained at three different Ab-HRP dilutions, with the magnetic particles concentration set at 0.1 mg mL^{-1}, and (B) at three P22-MP concentrations after the label dilution was optimized at 1/400. The tables below the graphs show the signal to background (S/B) ratio for each situation.

Afterwards, the phagomagnetic electrochemical immunosensing approach was evaluated for *Salmonella* artificially inoculated in milk diluted 1/10 in LB preparing a calibration curve ranging from 10^1 to 10^8 CFU mL^{-1} as shown in Figure 8.14. Ten negative samples (0 CFU mL^{-1}) were processed in order to set the cut-off value of the assay, obtaining a mean value of 0.494 μA with a standard deviation of 0.043. The signals corresponding to the LOD values were then calculated, obtaining a cut-off value of 0.614 μA (dotted line).

The amperometric signal was also plotted *vs*. the logarithm of *Salmonella* concentration and adjusted to a sigmoidal dose response curve (Figure 8.15), obtaining a good fit as shown in Table 8.8 (with a R^2 = 0.09925). The LOD value was finally calculated by interpolating the cut-off signal in the aforementioned graph, being the sensor able to detect 48 CFU mL^{-1} of *Salmonella*.

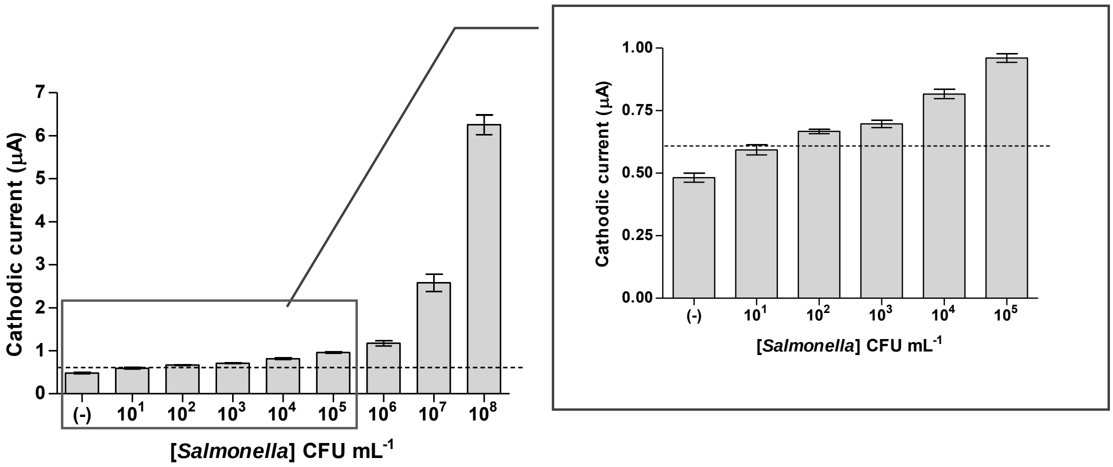

Figure 8.14 Electrochemical signals for the phagomagnetic immunosensing approach by increasing the amount of *Salmonella* artificially inoculated in milk diluted 1/10 in LB broth from 2.3 x 10^1 to 2.3 x 10^8 CFU mL^{-1}. The inset in the right panel show a zoom in the lower bacterial range. The cut-off value is represented through a dotted line in both graphs. The reagents concentration was: 0.05 mg mL^{-1} of the P22-MPs and a 1/400 dilution of the Ab-HRP. Medium: phosphate buffer 0.1 M, KCl 0.1 M, pH 7.0. Mediator: hydroquinone 1.81 mM. Substrate: H_2O_2 4.90 mM. Applied potential= -0.150 V (*vs*. Ag/AgCl). In all cases, n=3, except for the 0 CFU mL^{-1} negative control (n=10).

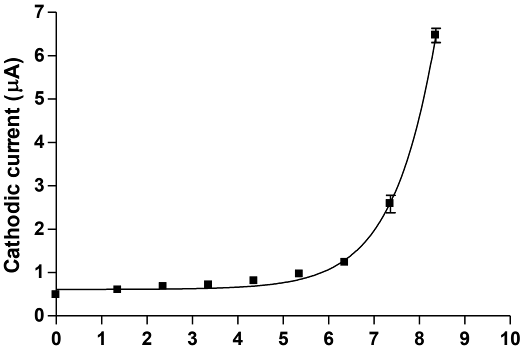

Figure 8.15 Cathodic current *vs*. log of *Salmonella* concentration, showing the fitting to a sigmoidal dose response curve.

Table 8.8 Parameters of the sigmoidal dose-response curve obtained when applying the phagotagging magneto-immunosensing approach in milk diluted 1/10 in LB.

	CV (%) for (-) control	CV (%) for 10^8 CFU mL^{-1}	R^2	Slope	Cut-off	LOD (CFU mL^{-1})
Milk 1/10 in LB broth	7.6	6.4	0,9925	0,47	0,614	48

The achieved limit of detection was similar than the obtained by the phagomagnetic immunoassay with optical detection. Anyway, the electrochemical system showed better fit to the sigmoidal dose response curve (with a r^2 value of 0.9925 in contrast to 0.9841 obtained for the optical detection in milk) and also a higher slope (0.47 in contrast to 0.27) indicating a better sensitivity.

8.4.6 Pre-enrichment studies for the detection of *Salmonella* in contaminated milk

The pre-enrichment step was carried out with a nonselective broth medium, in this case LB broth, using the P22-MP coupled to both optical and electrochemical detection. The procedure followed to perform this study is schematized in Figure 8.16.

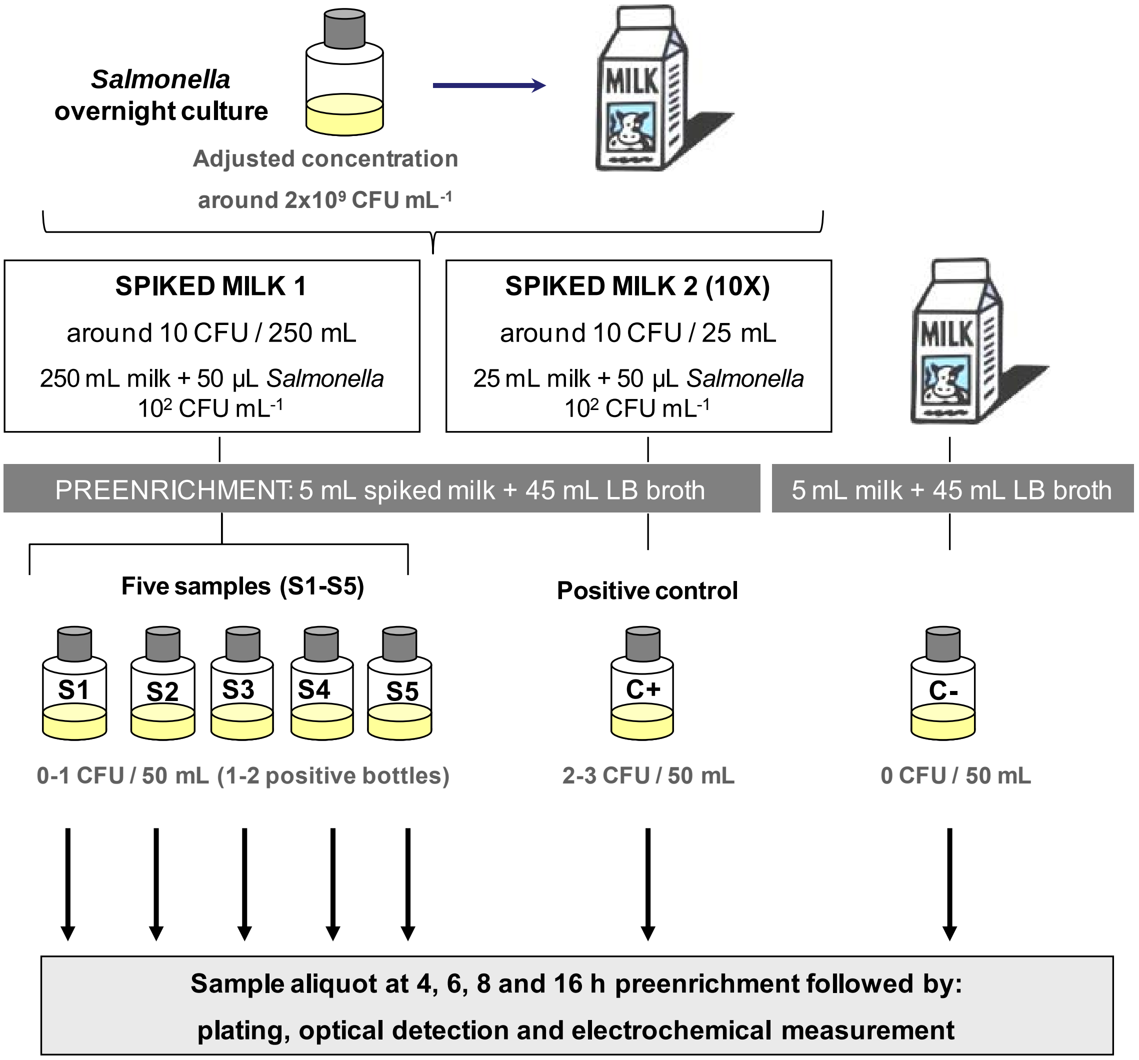
Salmonella overnight culture
Adjusted concentration around $2x10^9$ CFU mL^{-1}
MILK
SPIKED MILK 1
around 10 CFU / 250 mL
250 mL milk + 50 µL *Salmonella* 10^2 CFU mL^{-1}
SPIKED MILK 2 (10X)
around 10 CFU / 25 mL
25 mL milk + 50 µL *Salmonella* 10^2 CFU mL^{-1}
MILK
PREENRICHMENT: 5 mL spiked milk + 45 mL LB broth
5 mL milk + 45 mL LB broth
Five samples (S1-S5)
Positive control
S1
S2
S3
S4
S5
C+
C-
0-1 CFU / 50 mL (1-2 positive bottles)
2-3 CFU / 50 mL
0 CFU / 50 mL
Sample aliquot at 4, 6, 8 and 16 h preenrichment followed by:
plating, optical detection and electrochemical measurement

Figure 8.16 Schematic representation of the steps followed for the pre-enrichment studies. After 250 mL of milk were spiked with around 10 CFU, five portions of 5 mL were taken and preenriched in 45 mL of LB broth at 37 ºC. A positive control (10X of Salmonella) and a negative control were also processed. The samples (S1-S5) and controls were assayed after 4,6, 8 and 16 h pre-enrichment.

In order to contaminate a milk sample with a proportion of around 1 CFU of *Salmonella* in 25 mL and be able to test the capability of our system to fulfill the established regulations, 250 mL of milk were spiked with around 10 CFUs. To achieve this, 50 µL of a *Salmonella* solution with a concentration in the order of 10^2 CFU mL^{-1} were added to the milk. From there, five portions of 5 mL were taken and preenriched in 45 mL LB broth at 37 ºC (samples S1-S5). A positive control containing 10X *Salmonella* concentration was also evaluated, as well as a negative control (0 $CFUmL^{-1}$) following the same procedure. Finally aliquots were taken at 4, 6, 8 and 16 h to test each sample by the optical and electrochemical method. To control the amount of bacteria at the different pre-enrichment times, each sample was also plated in LB agar in order to perform the corresponding bacteria counting through the classical culture method.

Regarding the optical detection, the samples were assayed at the four aforementioned pre-enrichment times. As shown in Figure 8.17, the system was not able to detect the bacteria after just 4 h pre-enrichment. This result was in agreement with the colony counting, in which not even the positive control reached a bacteria concentration above 10 CFU mL^{-1}, being thus below the detection limit of the method in milk (19 CFU mL^{-1}). However, after 6 h of pre-enrichment, 1 of the 5 milk samples was clearly positive (S1) and another, was around the cut-off value (S4), as shown in Figure 8.17, A. Nevertheless after 8 h, S1 was the only positive sample which continued increasing accordingly, while the other suspicious sample (S4) did not show further signal increase. The evolution over the time of the negative control, the sample S1 and the positive control are detailed in Figure 8.17, B.

On the other hand, the electrochemical detection was assayed at 6, 8 and 16 h due to the low growth obtained at 4 h pre-enrichment and the slight higher limit of detection of this method, which needs at least 48 CFU mL^{-1} to be able to give a positive signal. Again the results obtained in this case showed that after 6 h of pre-enrichment 1 of the 5 milk samples (S1) was already positive and the positive control was also clearly above the cut-off value, as shown in Figure 8.17, C. These results were in agreement with the previous optical method. The evolution over the time of the negative control, the sample S1 and the positive control are detailed in Figure 8.17, D.

The exact initial inoculum was found by classical culture method obtaining that the overnight culture used to contaminate the milk had a concentration of 2.8 x 10^9 CFU mL^{-1}, and in fact the milk sample was spiked with around 14 CFUs in 250 mL. As a result the bacteria in both the S1 positive sample (containing 1.4 CFU in 25 mL) and the positive control (with 14 CFU in 25 mL) were able to be detected after a pre-enrichment of 6 h using optical as well as electrochemical detection, showing exponential growth over the time, while the negative control showed as expected no growing at all. Although both methods were able to detect 0.056 CFU mL^{-1} in milk (1.4 CFUs in 25 mL) according to the legislation after 6h pre-enrichment in LB, remarkable improvement of the signals were achieved between 8 and 16 h of pre-enrichment, as can be seen in Figure 8.17, B and D.

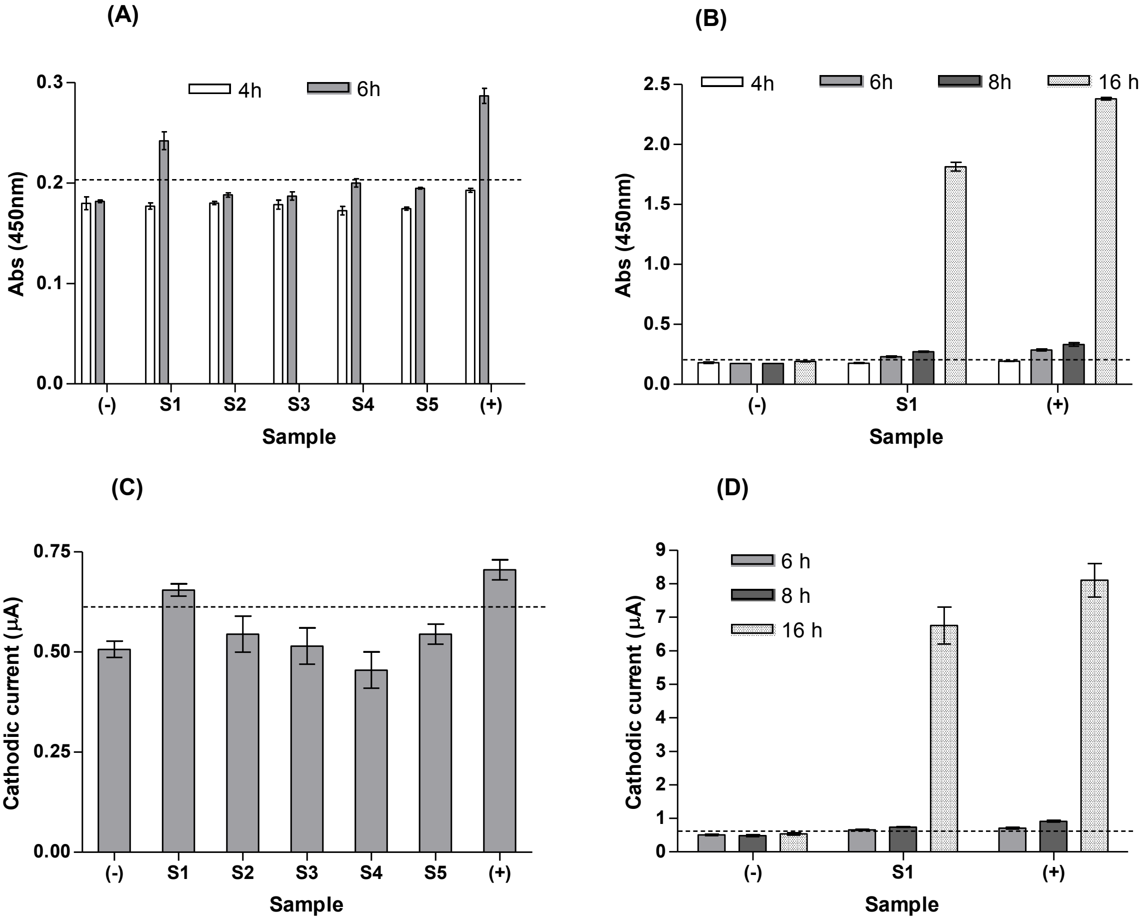

Figure 8.17 Results obtained after different pre-enrichment times of artificially inoculated milk containing 1.4 CFUs in 25 mL (0.056 CFU mL^{-1}) with optical (A and B) and electrochemical (C and D) detection. Five portions (S1 to S5) of the sample, a negative control (0 CFU mL^{-1}), and a 10 X positive control (0.56 CFU mL^{-1}) were assayed at 4 and 6 h for the optical (A) and just 6 h pre-enrichment for the electrochemical method (C). The evolution over the time until 16 h of the S1 positive sample, the negative control and positive control are detailed in C and D. In all cases, n = 3, with exception of the negative control for which n = 16. The dotted lines represent the cut-off values.

8.5 CONCLUSIONS

The sensitive detection of *Salmonella* was demonstrated using two magnetic carriers modified with the bacteriophage P22, applying a phagomagnetic immunoassay with optical detection. The covalent immobilization of P22 bacteriophages was successfully performed on both magnetic micro and nanoparticles, achieving excellent coupling efficiencies. However, magnetic microparticles showed improved performance in terms of sensitivity and specificity, as well as lower matrix effect. These results could possibly be related with the fact that the magnetic nanoparticles showed agglomeration that could hinder the biorecognition event between the phage and the specific receptors in the bacteria and also with the specific antibodies. Moreover, the higher surface area per volume ratio given by their smaller size could also increase the nonspecific adsorption. Nevertheless, the tagging pattern of the nanoparticles, showing a distribution all along the surface of the bacteria could be promising for the specific magnetic tagging of pathogenic bacteria, or for instance, for the removal of bacterial contamination in food or environmental samples. As a result, these could be other potentially applications for further studies.

The phagomagnetic separation followed by the immunological detection with a specific labeled antibody coupled to both optical and electrochemical detection, can be considered as good alternative candidates to the `gold standard' tandem, differential plating and the biochemical/serological assays, reducing considerably the time of the assay from 3–5 days to between 2 and 3 h.

Moreover, it should be also highlighted that a very specific approach was achieved. The method is able to clearly distinguish between pathogenic bacteria such as *Salmonella* and *Escherichia coli*, due to the combined specificity of the different biorecognition events, the P22 bacteriophage used in the phagomagnetic separation step, and the antibody towards the H or flagellar antigen and the O or somatic antigen (part of the LPS moiety) used as optical or electrochemical reporter.

Low matrix effect and outstanding sensitivity were achieved using the P22-MP for the phagomagnetic separation in milk, being able to detect as low as 19 CFU mL^{-1} and 48 CFU mL^{-1} by optical and amperometric detection respectively, without any pre-enrichment step. Comparing the result with other biosensing methods based on bacteriophage biorecognition excellent sensitivity was achieved with these strategies, since previous works reported detection limits of around 10^2 CFU mL^{-1} [11,13], or in the case of reaching lower values longer assay times [17] or more labor-intensive PCR dependent or phage engineering techniques were required. To the best of our knowledge, the achieved limits of detections were only obtained with genetic-based assays coupled with amplification by PCR.[14] Nevertheless, the presented method has the advantage of being more rapid and simple, avoiding the previous labor-intensive DNA extraction and amplification steps. In addition, if the milk sample was pre-enriched for 6 h in LB, as low as 0.056 CFU mL^{-1} of *Salmonella* could be detected using both detection methods, according to the legislation.

Although when the developed phagomagnetic strategy was coupled to optical detection, a slight better detection limit was achieved, higher sensitivity was obtained with the electrochemical method. Additionally, the use of a biosensor is more promising to cover the demand of rapid and on-site testing required for the implementation in HACCP for food safety and the coupling to magnetic particles shows high potential for miniaturization and integration in microfluidic devices and cartridges.

8.6 REFERENCES

(1) Nanduri, V.; Sorokulova, I.; Samoylov, A.; Simonian, A.; Petrenko, V.; Vodyanoy, V. *Biosens Bioelectron* **2007**, *22*, 986–992.

(2) Mejri, M. B.; Baccar, H.; Baldrich, E.; Del Campo, F. J.; Helali, S.; Ktari, T.; Simonian, a; Aouni, M.; Abdelghani, a *Biosensors & bioelectronics* **2010**, *26*, 1261–7.

(3) Olsen, E. V; Sorokulova, I. B.; Petrenko, V. a; Chen, I.-H.; Barbaree, J. M.; Vodyanoy, V. J. *Biosensors & bioelectronics* **2006**, *21*, 1434–42.

(4) Cademartiri, R.; Anany, H.; Gross, I.; Bhayani, R.; Griffiths, M.; Brook, M. a *Biomaterials* **2010**, *31*, 1904–10.

(5) Shabani, A.; Zourob, M.; Allain, B.; Marquette, C. a; Lawrence, M. F.; Mandeville, R. *Analytical Chemistry* **2008**, *80*, 9475–82.

(6) Handa, H.; Gurczynski, S.; Jackson, M. P.; Auner, G.; Mao, G. *Surface Science* **2008**, *602*, 1392–1400.

(7) Handa, H.; Gurczynski, S.; Jackson, M. P.; Mao, G. *Langmuir* **2010**, *26*, 12095–103.

(8) Arya, S. K.; Singh, A.; Naidoo, R.; Wu, P.; McDermott, M. T.; Evoy, S. *The Analyst* **2011**, *136*, 486–92.

(9) Gervais, L.; Gel, M.; Allain, B.; Tolba, M.; Brovko, L.; Zourob, M.; Mandeville, R.; Griffiths, M.; Evoy, S. *Sensors and Actuators B: Chemical* **2007**, *125*, 615–621.

(10) Tolba, M.; Minikh, O.; Brovko, L. Y.; Evoy, S.; Griffiths, M. W. *Applied and Environmental Microbiology* **2010**, *76*, 528–35.

(11) Smartt, A. E.; Ripp, S. *Analytical and Bioanalytical Chemistry* **2011**, *400*, 991–1007.

(12) Smartt, A. E.; Xu, T.; Jegier, P.; Carswell, J. J.; Blount, S. a; Sayler, G. S.; Ripp, S. *Analytical and Bioanalytical Chemistry* **2012**, *402*, 3127–46.

(13) Singh, A.; Poshtiban, S.; Evoy, S. *Sensors* **2013**, *13*, 1763–86.

(14) Liébana, S.; Spricigo, D. A.; Cortés, M. P.; Barbe, J.; Alegret, S.; Pividori, M. I. *Analytical Chemistry* **2013**, *85*, 3079–3086.

(15) Thouand, G.; Vachon, P.; Liu, S.; Dayre, M.; Griffiths, M. W. *Journal of Food Protection* **2008**, *71*, 380–5.

(16) Liébana, S.; Lermo, A.; Campoy, S.; Barbé, J.; Alegret, S.; Pividori, M. I. *Analytical Chemistry* **2009**, *81*, 5812–20.

(17) Yemini, M.; Levi, Y.; Yagil, E.; Rishpon, J. *Bioelectrochemistry* **2007**, *70*, 180–4.

CHAPTER 9

GENERAL CONCLUSIONS AND FUTURE PERSPECTIVES

The detection of food contaminants and food allergens are both important public health issues worldwide. Tracking and tracing for allergen-free food production chains has become important due to consumer-safety concerns and to fulfill international labeling regulations. On the other hand, the detection of contaminants as pathogenic bacteria is an area of prime interest for food safety since infectious diseases spreading every day through food are a life-threatening problem for millions of people around the world. Food safety can only be ensured through the enforcement of quality-control systems throughout the entire food chain from the incoming raw materials until the final consumer, and in this context the availability of rapid, reliable and highly sensitive methods is mandatory. Therefore, great efforts are directed towards the development of simple, selective and cost-efficient methodologies for the on-site detection of different analytes in complex food samples.

As mentioned in Chapter 2, the general aim of this dissertation was to integrate micro and nanoparticles as well as hybrid bionanomaterials on immunoassays and immunosensing devices and to develop alternative methods for the rapid detection of targets of interest in food safety. Gliadin, a food allergen, and *Salmonella*, a food-borne contaminant, were selected as model targets. In all cases, magnetic micro and nanocarriers were used as solid support and integrated in different immunoassay formats, including direct and indirect competitive and sandwich formats. The integration of the magnetic carriers greatly improved the performance of the immunological reactions, due to the increased surface area and the fact that the particles are in suspension. Moreover, magnetic carriers also helped to simplify the analytical procedure, due to the easier and improved washing and separation steps that minimized the matrix effect in complex samples. Furthermore, the magnetic particles can be easily manipulated using a magnetic field, simplifying the handling requirements in the analytical procedures. Finally, the magnetic particles can be integrated into microfluidic devices and cartridges allowing thus further automation and miniaturization.

Excellent coupling efficiencies were obtained in the covalent coupling of proteins of different sizes, including the small gliadin molecules as well as the nanostructured bacteriophages, on tosylactivated magnetic microparticles, as well as carboxyl magnetic nanoparticles, achieving values of around 90 %, and demonstrating thus the robustness and efficient binding capabilities of the magnetic carriers. Moreover, the oriented immobilization was successfully achieved and the stability of the modified magnetic particles was also kept for several months.

Hybrid bionanomaterials, combining nanomaterials with different properties, were successfully integrated into bioanalytical procedures. The coupling of magnetic and metallic nanoparticles with the nanostructured bacteriophages was also demonstrated for bioimaging and biosensing applications.

The highly efficient biotinylation of the P22 bacteriophage was achieved and comprehensively studied during this dissertation. A versatile bionanoparticle for bacterial tagging, namely biotin-P22, was thus assessed for the sensitive detection of bacteria when coupling with fluorescent, optical or electrochemical streptavidin-conjugated reporters. The properties of the biotin-P22 were also explored for bacteria capturing when the biotinylated phage nanoparticles were coupled to magnetic microparticles. These novel hybrid bionanoparticles were extensively characterized through a wide range of techniques, such as electrophoresis, confocal fluorescence microscopy, SEM and TEM. The microscopy images demonstrated the bacteria phagotagging, while the biotinylation was confirmed by the binding to fluorescent streptavidin conjugates as well as streptavidin modified gold nanoparticles. An extensive assessment of this phagic bionanoparticles was performed, including the number of biotin moieties decorating each phage unit. A fluorometric assay was thus performed, obtaining a value of approximately 2000 biotin molecules attached on each phage capsid, being then able to bind (strept)avidin to assemble bottom-up hybrid bionanoparticles while retaining the tailspike capability to biorecognize the bacteria target.

On the other hand, the bacteriophage P22 was also coupled to magnetic particles (P22-MP), as previously explained, achieving a robust hybrid biomaterial consisting of around 1600 phages per particle, which showed outstanding bacteria capturing efficiencies. The developed P22-MP conjugate was characterized by microbiological methods as well as by microscopy techniques, as SEM and confocal fluorescence, which confirm its outstanding ability to capture bacteria.

When assessing the analytical performance of the developed strategies, excellent results were acquired in all the applications for competitive as well as non-competitive magneto-immunoassays coupled to both optical and electrochemical readouts. Therefore, highly sensitive and selective procedures were achieved in all cases, which improved significantly the detection limits reported so far by other currently developed methods and/or provided a methodological simplification.

As a result, the integration of magnetic micro and nanoparticles as well as hybrid bionanomaterials in optical magneto immunoassays and electrochemical magneto immunosensing approaches greatly improved the analytical performance obtaining low LOD values. However, although similar analytical performance were obtained in the presence of the food matrixes when compared to the results in PBST buffer, the matrix effect was not totally overcome, which lead to suggest to preferably perform the calibration curves in the same diluted matrix than the samples to be tested. Moreover, in the case of a competitive approach, this recommendation gathers even more strength, since the matrix effect was more evident as could be observed through the sensitivity reduction (slope decrease), extension of the linear range and IC50 increase obtained in the presence of both tested food matrixes (beer and milk) when compared to the results in PBST buffer.

Regarding the integration of magnetic nanoparticles, it was initially expected that they supply some improvement in the results due to faster assay kinetics given by their smaller size and consequently higher surface to volume ratios. Nevertheless, although obtaining very efficient coupling capability and higher sensitivity than the microparticles, indicated by the larger slopes in the calibration curves, their higher reactivity also played against in the fact of causing higher nonspecific adsorption values and also more significant matrix effects in both the competitive and sandwich assays for detecting gliadin and bacteria, respectively. Interestingly, when comparing the phagomagnetic separation of bacteria performed with magnetic micro and nanoparticles, the pattern of interaction was completely different. Since the bacteria are micro-sized, the reaction with magnetic nanoparticles showed almost a full coverage of the bacterial surface with many magnetic nanoparticles, while this effect was not observed, as expected, for magnetic microparticles, leaving almost the whole bacterial surface bare for further immunological reaction with electrochemical or optical reporters. The aforementioned pattern observed with the magnetic nanoparticles could play a negative role, since they could hinder the further reaction with the antibodies used to provide the optical or electrochemical readout, reducing thus the expected sensitivity of this approach. Moreover, a slight cross-reaction with *E.coli* was also observed when using magnetic nanoparticles, giving thus a poorer specificity than the microparticles system for phagomagnetic separation. However, their high bacteria tagging capability demonstrated through the SEM images suggested a great potential for other applications based on magnetic tagging that could lead to the development of further strategies.

Concerning the integration of magnetic particles in the detection of food allergens such as gliadin, a competitive approach was developed to detect not only the native protein, but also the small gliadin fragments, being thus valid for both non-treated and hydrolyzed foodstuff. The competitive assay format (direct or indirect) was optimized using a magneto immunoassay with optical detection, obtaining improved results with the direct competitive format, which had also the added benefit of being simpler and faster. After optimizing the extraction protocol, the quantification of gliadin in spiked liquid samples, as milk and beer, was successfully achieved, obtaining excellent recovery values, of almost 100 %, for both the optical magneto immunoassay and the electrochemical magneto immunosensor. It should be pointed out that the allergen could be detected at a level of 20 μg kg^{-1} of food, which is thousand times lower than the EC-specified 20 mg kg^{-1} limit for gluten-free food, and besides food samples could be diluted 400 times, reducing food matrix effects. Although similar LODs were obtained in a previous reported electrochemical immunosensor, the magneto immunosensor developed in this work showed a wider linear range and the advantage of being able to detect, due to the competitive format, small gluten fragments that would be underestimated with the sandwich format already reported. Although the magnetic particles bring a lot of advantages when integrated in a competitive immunoassay, one of the main improving issues, which is the pre-concentration of the analyte, is missed in this case since it acts as a limited reagent competing with the analyte for the labeled antibody. However, this advantage of magnetic particles and nanoparticles was exploited in both the immunomagnetic and phagomagnetic separation of bacteria, step that was integrated in non-competitive (or sandwich) immunoassays with electrochemical and optical readouts.

The non-competitive approaches developed for *Salmonella* Thyphimurium detection integrated bacteriophages both as biorecognition element, when immobilized on magnetic carriers, as well as tagging reagent, when conjugated with a signal reporter. Both approaches were able to considerably reduce the time of the bacteria detection from the 3-5 days required in the conventional microbiology methods, to as low as 2-4 h in the studied strategies. It should be pointed out that the P22 bacteriophage was selected in all cases as a model to detect *Salmonella*, but all the strategies can be also extended to other bacteriophages of different sizes and shapes to other bacterial targets.

Novel procedures were design throughout the integration of the bacteriophages, in all cases taking advantages of the remarkable properties of the bionanomaterials previously developed (biotin-P22 and P22-MPs). The first one was a phagotagging magneto immunoassay with optical detection, as well as an electrochemical magneto immunosensing approach based on phage tagging, as extensively described in Chapter 6. Moreover, phagomagnetic immunoassays with optical detection, as well as electrochemical phagomagnetic immunosensors, were described and compared for the first time in the Chapters 7 and 8 of this dissertation. The phagomagnetic separation step was performed by means of a hybrid material based on the conjugation of the bacteriophages on magnetic micro and nanoparticles, in different ways. Chapter 7 describes a biotin-P22/MP conjugate developed by coupling the biotinylated phages to streptavidin-modified magnetic particles, while Chapter 8 is based on the phage covalently coupled to tosylactivated magnetic particles.

The results obtained with the biotin-P22/MP conjugate, showed a poor phage attachment on the magnetic particles (only 20 biotinylated phages per magnetic particle) and a subsequent low efficiency for bacteria capturing in comparison to the phagomagnetic approaches based on phages covalently linked to magnetic carriers. As a result, also worse limits of detection were obtained in this case, with values between 10^3 and 10^4 CFU mL^{-1}. Furthermore, a slight cross-reaction with *E.coli* was observed at high bacteria concentrations (above 10^7 CFU mL^{-1}).

On the contrary, outstanding results were obtained in terms of analytical performance as well as selectivity with both the phagotagging as well as the phagomagnetic based methods using P22-MP. After analyzing in more detail, better sensitivity was obtained with the optical magneto immunoassay and electrochemical magneto immunosensor based on phage tagging when compared to the phagomagnetic immunoassay with optical detection and the phagomagnetic electrochemical immunosensor, as indicated by the higher slopes obtained in the calibration curves. However, better limits of detection were obtained with the phagomagnetic than with the phagotagging strategies, with results in the order of 10^1 and 10^2 CFU mL^{-1}, respectively. Thus, the phagomagnetic based approaches were applied to perform further pre-enrichment studies in milk samples (as explained in Chapter 8) to evaluate the capability of the system to fulfill the required food regulations, which establish that the absence of *Salmonella* in 25 g should be guaranteed at food control points. After performing the corresponding studies, by spiking a milk sample accordingly (approximating to 1 CFU in 25 mL) and monitoring the detection capability of the developed system at different times (4, 6, 8 and 12 h), it is concluded that the bacteria contamination was detected after 6 h pre-enrichment in LB, being thus the LOD as low as 0.056 CFU mL^{-1}.

Finally, when comparing the performance of both detection methods, the optical and the electrochemical readouts, it can be observed that although similar detection limits were obtained in all the strategies studied, better sensitivity and lower matrix effect were achieved with the electrochemical readout. The high sensitivity, selectivity and robustness obtained with the electrochemical magneto immunosensors can be ascribed to the advantageous features provided by the use of magnetic particles coupled to the improved electrochemical properties of the graphite-epoxy composite electrodes developed and highly studied in our research group. Moreover, between the two detection strategies, optical and electrochemical, the second one is the most promising for food safety applications due to their rapid, high sample throughput and on-site testing capability as well as the compatibility with miniaturization and mass fabrication technologies.

As a result, it can be concluded that the novel immunoanalytical strategies using magnetic carriers developed in the present dissertation could provide new tools for the development of low cost and user-friendly biosensor devices that would allow manufacturers to perform a rapid screen-out for contaminants or allergens throughout the food chain, enabling the implementation in HACCP at different stages of the production process.

Future work could be focused in the implementation of the developed immunoanalytical strategies based on magnetic particles in detection kits for decentralized analysis. However, some aspects require further study, as for example the simplification of the analytical procedures by shorting or eliminating pipetting and washing steps as well as the design of miniaturized devices or cartridges. Moreover, the validation in a wider range of food matrixes should be also carefully assessed.

Regarding the bacteria detection, the promising results obtained using the phages could open many gates to further studies. Some examples are the development of other tagging strategies through the conjugation to different kinds of tags such as fluorophores, quantum dots or magnetic labels, or the use of phage based strategies applying them simultaneously for both capturing and tagging in order to achieve antibody-free techniques. Furthermore, novel methods based on phage propagation in their hosts could be used for the even higher signal amplification; and finally different labeled phages could be applied for the development of multiplex detection techniques, allowing the simultaneous detection of multiple pathogens.

PUBLICATIONS

SCIENTIFIC ARTICLES

The following scientific papers have been published during this dissertation, directly related to the content of this research, or related with collaborative projects.

- Laube, T., Kergaravat, S.V., Fabiano, S.N., Hernández, S.R., Alegret, S., Pividori, M.I. Magneto immunosensor for gliadin detection in gluten-free foodstuff: Towards food safety for celiac patients. *Biosensors and Bioelectronics*, **2011**, *27*, 46-52.
- De Souza Castilho, M., Laube, T., Yamanaka, H., Alegret, S., Pividori, M.I. Magneto immunoassays for *Plasmodium falciparum* Histidine-Rich Protein 2 related with Malaria based on magnetic nanoparticles. *Anal. Chem.*, **2011**, *83*, 5570-5577.
- Kergaravat, S.V., Gómez, G.A., Fabiano, S.N., Laube Chávez, T., Pividori, M.I., Hernández, S.R. Biotin determination in food supplements by an electrochemical magneto biosensor. *Talanta*, **2012**, *97*, 484-490.
- Laube, T., Cortés, P., Llagostera, M., Alegret, S., Pividori, M.I. Phagomagnetic immunoassay for the rapid detection of *Salmonella*. *Applied Microbiology and Biotechnology, in revision.*
- Laube, T., Cortés, P., Llagostera, M., Alegret, S., Pividori, M.I. Tagging of bacteria with P22 phage hybrid nanoparticles for bioimaging and biosensing. *Submitted.*
- Laube, T., Cortés, P., Llagostera, M., Alegret, S., Pividori, M.I. Biotinylated bacteriophages on streptavidin magnetic particles for the detection of pathogenic bacteria. *In revision.*
- Laube, T., Cortés, P., Llagostera, M., Alegret, S., Pividori, M.I. Phagomagnetic electrochemical immunosensor for the rapid detection of pathogenic bacteria in milk. *In revision*.
- Laube, T., Cortés, P., Llagostera, M., Alegret, S., Pividori, M.I. Biotinylated bacteriophages as nanotags for the sensitive optical detection of pathogenic bacteria. *In preparation.*

- Laube, T., Cortés, P., Llagostera, M., Alegret, S., Pividori, M.I. Magneto immunosensing of bacteria based on phage tagging. *In preparation.*

On the other hand, the following non-indexed publications also resulted from this dissertation:

- A real winner for celiac patients. *Tecan Journal*, **2012**, *2*, 20-21. (Tecan Award).
- Pividori, M.I., Laube, T. Un método nuevo para la comprobación de productos sin gluten. *Alimentaria*, **2013**, *445*, 82-83.

CONFERENCES AND CONGRESSES

The work carried out during this dissertation was also presented in numerous congresses and conferences, both national and international.

- 3rd International Conference on Bio-sensing Technology, 12 - 15th May 2013, Sitges (Spain).

- *XXIV Congreso de Microbiología de la Sociedad Española de Microbiología*, 10 - 13th July 2013, L'Hospitalet de Llobregat, Barcelona (Spain).

- Ibersensor, 8th Ibero-American Congress on Sensors, 16 - 19th October 2012, Carolina (Puerto Rico).

- XVII Transfrontier Meeting of Sensors and Biosensors, Tarragona, 20 - 21th September 2012, Tarragona (Spain).

- *Segona Edició de Jornades Doctorals del Departament de Química de la Universitat Autònoma de Barcelona*, 6 – 8th June 2012, Bellaterra (Spain).

- First Workshop on Nanomedicine UAB^{CEI}, 5th June 2012, Bellaterra (Spain).

- Biosensors 2012. 22nd Anniversary World Congress on Biosensors, 15 - 18th May 2012, Cancún (Mexico).

- *13as Jornadas de Análisis Instrumental*, 14 - 16th November 2011, Barcelona (Spain).

- *XVI Rencontres Transfrontalières «Capteurs et Biocapteurs»*, 29 - 30th September 2011, Toulousse (France).

- Ibersensor, 7th Ibero-American Congress on Sensors, 9 – 10th November 2010, Lisboa (Portugal).

- *XV Trobada Transfronterera sobre Sensors i Biosensors*, 16 – 17th September 2010, Sant Carles de la Ràpita (Spain).

- IC-ANMBES, First International Conference on Analytical and Nanoanalytical Methods for Biomedical and Environmental Sciences, 18 – 20th June 2010, Brasov (Rumania).

- II International Workshop on Analytical Miniaturization, 7 – 8th June 2010, Oviedo (Spain).

- 8th International Conference on the Scientific and Clinical Applications of Magnetic Carriers, 25 – 29th May 2010, Rostock (Germany).

- Biosensors, 20nd Anniversary World Congress on Biosensors, 26 - 28th May, 2010. Glasgow (UK).

- *XIV Trobada Transfronterera Sobre Sensors i Biosensors*, 24 – 25th September 2009, Banyuls Sur Mer (France).

- *III Workshop Nanociencia y Nanotecnologías Analíticas*, 16 – 18th September 2009, Oviedo (Spain).

- *XIII Trobada Transfronterera Sobre Sensors i Biosensors*, 18 – 19th September 2008, Andorra.

WORKSHOPS AND COURSES

The following workshops and courses were organized during this PhD Thesis, including parts of the work and techniques developed in this dissertation.

- Bioanalytical Nanotechnology School:
    - University of Santo Tomas, 31th January – 4th February 2011, Manila (Philippines).
    - *Universidad Autónoma Metropolitana*, *Unidad Azcapotzalco*, 3 – 6th October 2011, Mexico City (Mexico)
- Workshop "Electrochemical immunosensors for pathogenic bacteria detection", at *Universitat Autònoma de Barcelona*
    - IX Workshop *Métodos Rápidos y Automatización en Microbiología Alimentaria* (MRAMA), 26th November 2010
    - X Workshop *Métodos Rápidos y Automatización en Microbiología Alimentaria,* 25th November 2011.